AD NUMBER

AD449504

LIMITATION CHANGES

TO:

Approved for public release; distribution is unlimited.

FROM:

**Distribution authorized to U.S. Gov't. agencies and their contractors;
Administrative/Operational Use; 30 JUN 1964.
Other requests shall be referred to Army Electronics Labs., Fort Monmouth, NJ.**

AUTHORITY

USAEC ltr 1 May 1968

AD 449504

HYDROCARBON-AIR FUEL CELL

Report No. 5

Contract No. DA 36-039 AMC-03743(E)

ARPA Order No. 247

Task No. 7900.21.903.01.00.

First Semi-Annual Report, 1 Jan. 1964 - 30 June 1964

U.S. Army Electronics Laboratories

Fort Monmouth, New Jersey

ESSO RESEARCH AND ENGINEERING COMPANY
PROCESS RESEARCH DIVISION
LINDEN, NEW JERSEY

PcRD-4M-64

NOTICE

Qualified requestors may obtain copies of this report from DDC.

DDC release to OTS not authorized.

HYDROCARBON-AIR FUEL CELL

REPORT NO. 5

CONTRACT NO. DA 36-039 AMC-03743(E)
ARPA ORDER NO. 247
TASK NO. 7900.21.903.01.00.

FIRST SEMI-ANNUAL REPORT, 1 JAN. 1964-30 JUNE 1964

OBJECT: CONDUCT INVESTIGATIONS LEADING TO THE DEVELOPMENT OF HYDROCARBON AND METHANOL FUEL CELLS

Authored by:

Carl E. Heath
Eugene L. Holt
Hugh H. Horowitz
Duane G. Levine
Charles E. Morrell
Barry L. Tarmy
James A. Wilson
John S. Batzold
Morton Beltzer
George Ciprios
I-Ming Feng
Donald E. LeClair
John M. Matsen
Gershon Metzger
Andreas W. Moerikofer
Eugene H. Okrent
Joseph A. Shropshire
William F. Taylor
Charles E. Thompson
Charles H. Worsham

The work performed under this contract was made possible by the support of the Advanced Research Projects Agency under Order No. 247, through the U.S. Army Electronics Laboratories.

Esso Research and Engineering Company
Process Research Division
Linden, New Jersey

CONTENTS

CONTENTS

Appendix (Cont'd)

Appendix (Cont'd)

ILLUSTRATIONS

TABLES

APPENDIX ILLUSTRATIONS

APPENDIX TABLES

SECTION 1

PURPOSE

The purpose of these investigations is to perform research on the basic components of fuel cells using electrolyte-soluble carbonaceous fuels and fuel cells using hydrocarbon fuels. One objective, which is a continuation of the work carried out under contracts DA36-039 SC-89156 and DA36-039 AMC-00134(E), is to improve the performance of methanol-air fuel cells and to incorporate improved components into multicell batteries to study the engineering problems of multicell operation. A second objective is to determine the feasibility of hydrocarbon-air fuel cells.

The major emphasis of the program is on the simultaneous research and development on all basic aspects of the cells to optimize performance of the entire cell and to take into account interactions between components.

This work is aimed toward the development of practical fuel cells using hydrocarbons or their partially oxygenated derivatives as fuels and air as oxidant. The fuels must be capable of reacting to carbon dioxide, be reasonably available, and pose no unusual corrosion, toxicity or handling problems. Also, the cell must use a CO_2-rejecting electrolyte and operate at temperatures and pressures below 200°C and 75 psig. Other desired requirements include high electrical output per unit volume and weight, high efficiency, long life, high reliability, reasonable cost, particularly catalyst cost, and ruggedness.

The program is divided into seven parts. These are referred to as Tasks A through G in this report. Tasks A and D describe studies on the hydrocarbon and methanol electrodes, respectively. Air electrode research is primarily discussed in Task E, although that air electrode research which is peculiar to the hydrocarbon fuel cell is detailed in Task B. This Task includes work carried out on establishing the basic hydrocarbon cell design, especially with regard to the operation of all components in a single cell. A similar Task, F, is included for the methanol cell. Task G is concerned with work on the development of methanol multicell systems. Finally, Task C describes exploratory studies aimed at new approaches to fuel cells.

SECTION 2

ABSTRACT

Research on both the hydrocarbon and methanol fuel cells has concentrated on improving the performance of individual cell components and translating these results into compatible electrode-electrolyte systems. These efforts encompass work carried out in the following seven categories: the hydrocarbon electrode and the hydrocarbon fuel cell, new systems, methanol and air electrodes, the methanol fuel cell, and prototype development.

2.1 Task A, Hydrocarbon Electrode

Work on the development of a hydrocarbon electrode has concentrated on the use of liquid hydrocarbons directly at the anode, with operating temperatures in the range of 100°C. These conditions could reduce the problems in engineering a fuel cell. Initial results with decane as a model fuel showed that performance was limited by two factors. First, the accumulation of electrochemically active species on the electrode surface appeared to be slow, not because of transport limitation, but apparently because of a slow chemical reaction such as chemisorption of the fuel. Secondly, the liquid fuel tended to flood the Teflon bonded structure, physically blocking up to 95% of the available surface area.

Two potentially promising approaches were taken to the flooding problem. One involved the use of porous Teflon barriers on the fuel side which could control fuel flow by capillarity. The second involved the use of perfluoroacid electrolytes which have a greater tendency to wet Teflon than sulfuric acid solutions. Both approaches doubled the efficiency of catalyst utilization. Attempts were made to improve performance by using various noble metals and alloys as catalysts. It was found that the means of preparation of the catalyst had as great an effect on catalysis as the nature of the element. Emphasis was also placed on maximizing the catalyst surface area, particularly by coprecipitating the noble metal with other materials, such as aluminum hydroxide, which modify the surface properties and are later removed. This approach resulted in platinum catalysts with 60 percent greater surface area and twice the activity of commercial platinum black.

Part of the program has also been concerned with a search for non-noble catalysts. Low temperature steam reforming catalysts with costs of about $2 per pound were considered both as anode catalysts and as components of a separate steam reforming reactor. Preliminary experiments in a chemical reactor showed that these catalysts were active on gaseous decane and steam mixtures at temperatures as low as 260°C, as compared to conventional steam reformer temperatures of 700 to 800°C. Provided the conversion per pass was kept low, excellent yields of hydrogen could be obtained with little methane formation. The product gas could be reacted at over 200 ma/cm^2 at a fuel cell anode without purification. In addition, the decane and water could be reacted slowly even in the liquid phase over these catalysts.

2.2 Task B, Hydrocarbon Fuel Cell

A total cell for testing hydrocarbon-air fuel cell components was constructed and used in the evaluation of a liquid decane-oxygen fuel cell, operating at about 100°C in sulfuric acid electrolyte. Power outputs of 8.2 mwatts/cm^2 at cell voltages of 0.44 volts were obtained. The cell components, particularly the liquid decane electrodes, performed as expected based on previous half cell data.

2.3 Task C, New Systems

Studies have been carried out on new approaches to overcoming problems limiting fuel cell performance. Thus buffer electrolytes were found able to support high current densities. Methanol performance with present catalysts was comparable to that in acid and carbon dioxide was rejected. However, at the oxygen electrode, the necessity for maintaining a gas-liquid interface resulted in relatively high ionic concentration polarization within the porous structure. As a result, performance was inferior to that in acid. In a total methanol-air cell employing a buffer electrolyte, power outputs of over 10 mwatts/cm^2 were obtained. Experiments with slurried platinum black catalyst, using a rotating platinum foil electrode as current collector and stirrer, showed that methanol and decane activities comparable to static systems could be achieved if turbulent flow was maintained. However, greater catalyst quantities were required with the slurry system. The use of supported platinum was not successful. Anomalous catalyst wetting effects were observed with decane.

Other areas examined included redox reactions, where it was found that rhenium heptoxide could oxidize decane to carbon dioxide but the reduced rhenium oxide could not be electrochemically reoxidized. Tests with a flowing fuel system showed that neither decane preheating, electrical heating of the electrode nor open circuit pulsing improved the performance of a platinum-Teflon hydrocarbon electrode. An investigation of the stability of passivating metals under anodic conditions in sulfuric acid resulted in the choice of nuclear-grade zirconium, boron carbide, and boron nitride for further testing. Finally, the phthalocyanine compounds of a number of base metals were found to have little catalytic activity towards oxygen or hydrocarbons in sulfuric and phosphoric acids.

2.4 Task D, Methanol Electrode

Work on the methanol electrode has concentrated on improving the performance and life of the platinum-ruthenium and P-type catalyst systems. Sustained and exceptionally stable performance at levels comparable to those attainable with the P-type catalyst were obtained with the platinum-ruthenium catalyst by activating the catalyst in an alkaline solution. Polarizations at 60°C averaged 0.35 volts at 100 ma/cm^2. The susceptibility of the P-type catalyst to losing activity when overpolarized was overcome by stabilizing the catalyst with potassium ions. However, this stabilization requires the presence of methanol in the electrolyte. Further improvements in this catalyst were made by the controlled addition of ruthenium. The polarization at 60°C amounted to only 0.32 volts at 100 ma/cm^2, with little performance loss resulting from overpolarization. In addition, because the catalyst preparative procedures are slow, a fast procedure, producing slightly less active catalysts, was developed.

Several new methods for preparing methanol catalysts were developed. One method employed the radical anion formed by reacting metallic sodium with certain organic compounds such as napthalene as the reducing agent. This technique produced catalysts with comparable activity to other methods and hence showed no particular advantage. A second technique used the co-reduction and subsequent removal of silver

to prepare platinum electrodes with about 80 percent more surface area and over three times as much current at a constant polarization per milligram of catalyst. In addition, studies with co-metal catalysts not containing platinum resulted in an iridium-ruthenium catalyst that at 60°C was polarized only 0.36 volts at 100 ma/cm^2. This performance is comparable to that obtained with platinum-ruthenium.

Additional studies were carried out on the Pt-Re_2O_7-CH_3OH interaction. Double layer capacitance measurements were made to determine the effect of Re_2O_7 pre-adsorption on subsequent methanol coverage. It was found that the rhenate ions occupy 60 to 80 percent of the available platinum surface with methanol covering the remaining sites. This confirms previous indications that the pre-adsorbed rhenate layer covers most of the surface.

2.5 Task E, Air Electrode

The performance of thin carbon electrodes was maximized by reimpregnation with additional platinum. It was also found that polarization debits as low as 40 mv at 100 ma/cm^2 were obtained when the catalyst loading was reduced to 1.3 mg/cm^2 if the reduction was carried out by a radical anion method. Application of a porous Teflon layer eliminated the flooding of this structure under hydrostatic pressure. Teflon-coated platinum-Teflon electrode performances were proportional to catalyst loading between 1.5 and 14 mg/cm^2. At the lowest level, activity could be improved by adding gold to enhance conductivity while at high loadings the use of a multi-layer structure allowed fuller use to be made of the catalyst.

Cathodization of a platinum catalyst caused a temporary improvement in performance while anodization resulted in a temporary decrease. The incorporation of gold into platinum did not shift the potential of platinum oxide formation or reduction although, in the case of smooth, melted alloys, oxide formation was repressed. A theoretical oxygen potential of 1.23 volts was measured on gold following severe anodization. However, this was found due to a gold oxide layer rather than a reversible oxygen reaction.

2.6 Task F, Methanol Fuel Cell

A major performance limitation in methanol-air cell operation was found to be poor contact between the cathode and membrane. A technique was developed for pressing the membrane and cathode together without adversely effecting the membrane porosity. Use of these clad cathodes in 4" x 4" cells resulted in lower cell resistance, better utilization of the cathode surface for O_2 reduction, and improved compatibility. Improved fuel and air distribution in these cells had no effect on performance.

Three new catalysts were tested in single cell operation. The ruthenium modified P-type catalyst was the most stable of the three and gave substantially improved performance when combined with a clad cathode. Maximum power reached 45 mwatts/cm^2. Scale-up of these components to 9" x 5-3/4" was satisfactory. However, higher resistance due to the design of the larger cell remains a problem.

2.7 Task G, Prototype Development

Engineering research has aimed at extending consideration of problems in a methanol-air power unit. Improved fuel cell efficiency has been shown to result in considerable improvement in electronic control of such a unit. Air distribution studies in the 9" x 5-3/4" multicell stack, selected in the design, have shown that at least five times stoichiometric air flow is required for uniform cell performance.

Finally, chemical oxidation of methanol at the cathode, which must be suppressed during cell operation to minimize compatibility losses, has been found to be useful in start-up. By promoting this reaction, operating temperatures of 60°C were achieved within 12 minutes.

Studies in multicell units highlighted two general problems: deactivation of the P-type anode because of its sensitivity to oxidation and increased ohmic polarization at the cathode due to poor contact with the membrane. Because of this, tests have been initiated with new components from single cell work, ruthenium modified P-type anodes, and clad cathodes.

SECTION 3

PUBLICATIONS, LECTURES, REPORTS, AND CONFERENCES

3.1 Lectures

Tarmy, B. L. - Methanol Fuel Cells - Second ARPA Fuel Cell Conference, Linden, New Jersey, February 6, 1964.

Heath, C. E. - Methanol Fuel Cells - 18th Annual Power Sources Conference, Atlantic City, New Jersey, May 19, 1964.

3.2 Conferences

January 28, 1964 - Linden, New Jersey

Organizations Represented: United States Army Electronics Research and Development Laboratories
United States Army Engineer Research and Development Laboratories
Esso Research and Engineering Company

The meeting was held to review the status and future plans for the Hydrocarbon-Air Fuel Cell program.

January 31, 1964 - Fort Monmouth, New Jersey

Organizations Represented: United States Army Electronics Research and Development Laboratories
Mr. C. Daniel, Consultant to USAELRDL
Esso Research and Engineering Company

This meeting was held to review the research program from the aspect of statistical evaluation of data and designed experimental programs. It was agreed to compare several strategies in several projects currently underway.

February 4, 1964 - Princeton, New Jersey

Organizations Represented: Prof. John Tukey, Consultant to Esso Research and Engineering Company
Esso Research and Engineering Company

The use of statistics in designing catalyst research programs was discussed.

March 13, 1964 - Linden, New Jersey

Organizations Represented: United States Army Electronics Research and Development Laboratories
Mr. C. Daniel, Consultant to USAELRDL
Esso Research and Engineering Company

The meeting was held to discuss the studies in the application of designed experiments to catalyst research.

April 28, 1964 - Linden, New Jersey

Organizations Represented: Advanced Research Projects Agency
United States Army Electronics Research and Development Laboratories
United States Army Engineer Research and Development Laboratories
Esso Research and Engineering Company

The meeting was a review of progress and plans for the methanol-air and hydrocarbon-air fuel cells.

3.3 Reports

This report is written in conformance with the detailed reporting requirements as presented in the Signal Corps Technical Requirement on Technical Reports (SCL-2101P, 18 February 1963) under the terms of our contract; these requirements differ from the usual requirements for reports issued within Esso Research and Engineering Company.

SECTION 4

FACTUAL DATA

4.1 Task A - Hydrocarbon Electrode

During the year 1963, prior to the inception of this contract, some effort was expended determining whether it would be possible to oxidize a liquid hydrocarbon in the kerosene or jet fuel boiling range directly at a fuel cell anode. Appreciable activities were achieved using liquid decane on platinum black-Teflon electrodes. Furthermore, the difference in activity between 3.7 M sulfuric acid at 100°C and 14.7 M phosphoric acid at 150°C was not very large (Figure A-1).

Figure A-1

Best Performance Liquid Decane 1963

Pt-Teflon Electrodes
22 mg Pt/cm^2

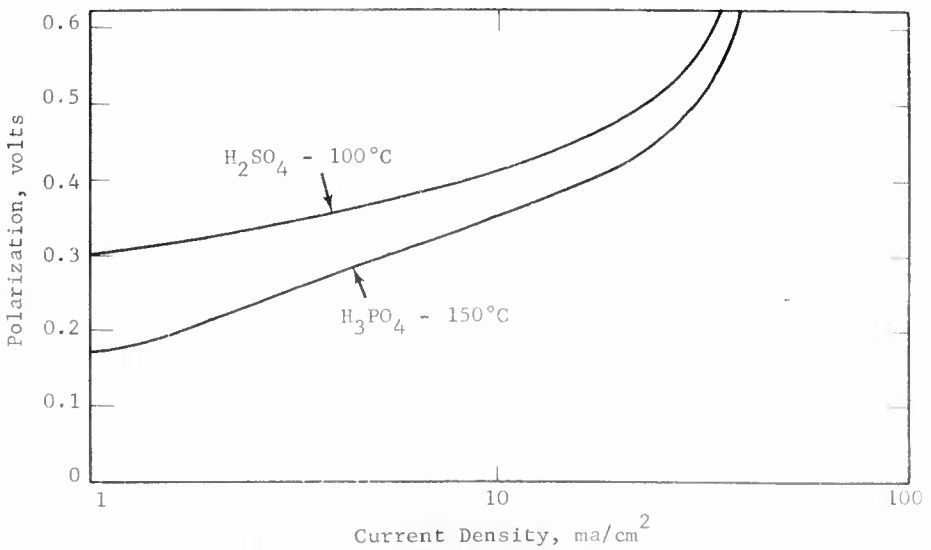

Polarization, unless otherwise noted, is defined here and elsewhere as the difference between observed voltage and the voltage of a reversible electrode operating with the same reactant, temperature, pressure and electrolyte. Measurements have been made using saturated calomel, silver-silver chloride, or direct hydrogen reference electrodes and values have been adjusted for the effects of liquid junction and thermal potentials. Details of this procedure are contained in Appendix A-1.

Because there was appreciable activity and the system would have ideal utility for a practical fuel cell, it was decided to concentrate research on a liquid decane electrode at or near 100°C. A final fuel cell was envisioned into which a liquid fuel similar to JP-4 could be poured directly, which would operate on relatively dilute electrolyte at temperatures at which heat and water balance problems would be relatively easy to solve, and which could achieve relatively high fuel conversion levels, since the product carbon dioxide separates readily from the liquid fuel and electrolyte.

It was known that specific electrodes and operating conditions existed under which gaseous hydrocarbons could be operated at hundreds of ma/cm^2 at relatively low polarizations. Such operation is, in fact, discussed in this report. However, due to the difficulties involved in obtaining a gaseous feed with kerosene-like hydrocarbons and of maintaining such a system at the necessary 150°C, it was felt that the liquid fuel-100°C system should be the goal. Furthermore, the type of electrodes required for the high temperature gas operation were of no advantage or actually inferior for the liquid fuel performance.

Therefore, the present studies were concerned with the means of fabricating optimum platinum based electrodes, determinations of the factors presently limiting performance, and improvements of catalysts to be used in the target system.

In addition, two longer range projects were undertaken to develop non-noble hydrocarbon fuel cell catalysts. One involved the adaptation of active low temperature steam reforming catalysts to fuel cell use. The other was concerned with the stabilization of catalytic non-noble metals toward acid by incorporating them into phthalocyanines. The latter is reported under Task C.

Phase 1 - Study of Decane Reaction on Pt-Teflon Electrodes

In order to gain some insight into the ultimate feasibility of liquid paraffin fuels for fuel cell use, a series of studies was carried out to establish the performance of a typical hydrocarbon fuel and the effect of operating parameters on this performance. It was hoped in this manner to obtain mechanistic criteria useful in the ultimate development of a liquid hydrocarbon fuel cell. Initial studies were carried out using n-decane ($C_{10}H_{22}$), and variables were studied both in steady state performance runs and, later, by voltage scanning techniques. Later studies were directed to butane fuel in order to establish points of similarity in the reaction of paraffin fuels having different molecular weights and physical states. Emphasis was placed on internal consistency of results rather than on optimization of the electrode system.

Part a - Experimental Technique

Initial performance tests on decane were carried out using liquid fuel feed in combination with aqueous sulfuric acid electrolyte. Electrodes chosen for the study were composed of two parts by weight of commercial platinum black mixed with one part Teflon powder (duPont), pressed into a 52 mesh platinum screen for current collection and mechanical support. They contained 30-35 mg Pt/cm^2.

The basic electrode was held between two Teflon gasket members with electrode area of either 1 or 5 cm^2. For operation, the electrode was placed in a special flange cell (Diagram, Appendix A-2) which permitted either gaseous or liquid fuel feed, and operated against a driven platinum screen counterelectrode. Both steady state and potential scan measurements were made with this apparatus, primarily in 3.7 M sulfuric acid at 100°C.

Part b - Steady State Performance of Liquid Decane Fuel

Initial performance tests were carried out using liquid decane and 3.7 M sulfuric acid electrolyte at 100°C. Performance was found to be somewhat sluggish with open circuit polarizations of 0.1-0.2 volts and limiting currents in the range 5-10 ma/cm^2 (Appendix A-3). Performance near limiting current conditions deteriorated somewhat with time in most cases. No evidence of a defined Tafel behavior was present for any of the electrodes tested. Thus, the liquid decane electrode was not well suited for mechanism studies.

A few runs were carried out to determine if benefits could be obtained by feeding decane as a steam distillate. For this purpose, vapor feed was taken from a boiling vessel containing decane and water. Decane partial pressure under these conditions is about 95 mm Hg. It was found that performance under these conditions was similar to that in the liquid feed system with the possible advantage of somewhat more stable performance in the steam distillation case. A short Tafel slope corresponding to 0.14 volts/decade was found (Appendix A-3). This value corresponds to $\alpha = 1/2$ in the Tafel expression and suggests the existence of an electron discharge limited rate in this region. However, the activity levels were still too low on this system to warrant its extensive further use.

Brief tests were carried out to determine the performance of decane fuel on catalyzed carbon electrodes similar to those described previously (4). Decane fuel was carried to the feed chamber on a stream of argon from a preheat vessel at 150°C. Electrolyte was 14.7 M phosphoric acid at 140°C. Performance of this system was similar to that observed on platinum-Teflon electrodes, with 5 ma/cm^2 at 0.25 volts polarization and limiting current of about 10-15 ma/cm^2 (Appendix A-3). A brief comparison with argon-n-heptane feed from a preheat vessel at 75°C indicated even somewhat lower performance. No evidence of Tafel behavior was observed in either case. Thus, there was no advantage for the hot phosphoric acid over 100°C sulfuric acid electrolyte for liquid decane fuel.

Part c - Slow Accumulation of Adsorbed Fuel

To augment the steady state measurements, the limitations on decane reactivity were further examined by the voltage scan technique. This technique is capable of breaking the electrochemical process into two parts, the accumulation of electrochemically active species on the electrode, and the anodic oxidation of these species. Platinum-Teflon electrodes were tested in the flange cell previously described, with the potentiostatted triangular signal supplied by a Duffers Model 600 Potentiostat in combination with a Servomex Low Frequency Wave Form Generator (Type LF-51). Current voltage diagrams, generally over a one volt range, were recorded on a Moseley Model 135 X-Y Plotter. A typical diagram for oxidation of decane in 3.7 M sulfuric acid is shown in Appendix A-4. The quantity of coulombs consumed in the oxidation of fuel was determined by multiplying the area under the fuel peak by a scale factor appropriate to the given scan rate and current sensitivity.

It was found that accumulation of oxidizable material at this type of electrode was very slow. That is, the number of coulombs in the decane peak increased significantly with the delay time between scans (Figure A-2 and also Appendix A-5). Furthermore, the initial slope of the coulombs-delay time curve corresponded to roughly 6-7 ma/cm^2, a value similar to the observed limiting currents in the steady state performance curves with this type of electrode. It was, therefore, concluded that the decane activity was not limited by the electrochemical steps involved in the

oxidation of chemisorbed decane or its fragments, but was limited by the rate of accumulation of the chemisorbed species. The next step was to determine whether the latter process was being restrained by slow mass transport or by slow chemical reactions.

Figure A-2

Accumulation of Coulombs in Decane
Peak with Delay Time between Scans

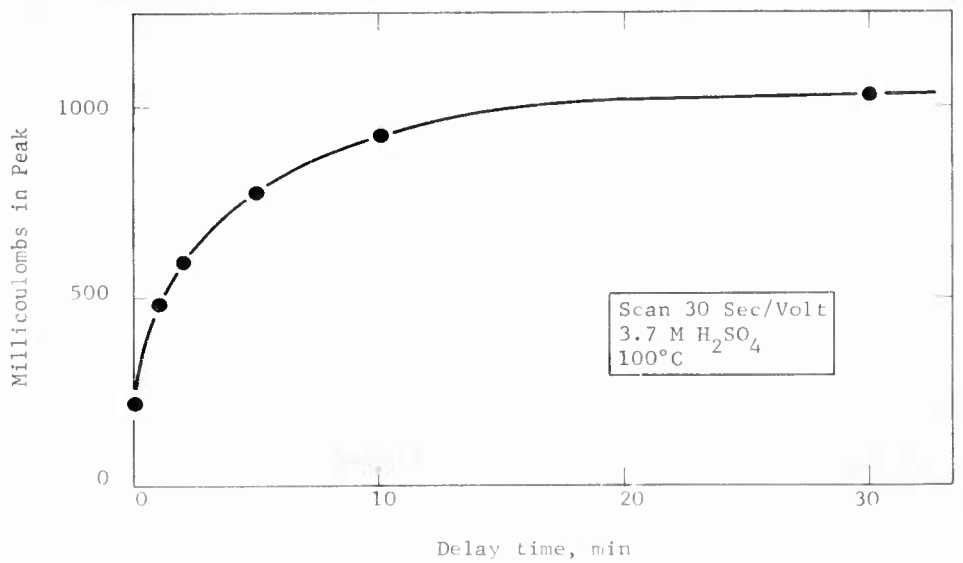

Part d - Evidence for Chemical Reaction Rate Limitation

Two criteria were used to distinguish between the mass transport and chemical reaction rate limitations. One was the nature of the relation between the coulombs accumulated and the scan time and the other was the energy of activation of the process. A series of continuous triangular voltage scans were obtained at 10, 20, 30 and 40 seconds per volt scan speed at 60, 80 and 100°C. For all three temperatures, the total coulombs accumulated in the decane peak was shown to vary linearly with reciprocal rate of scan (Figure A-3). This behavior should not result if the overall process of accumulation is diffusion controlled. For that case a reciprocal square root relationship is expected (5).

Figure A-3

Dependence of Peak Coulombs on Scan Rate

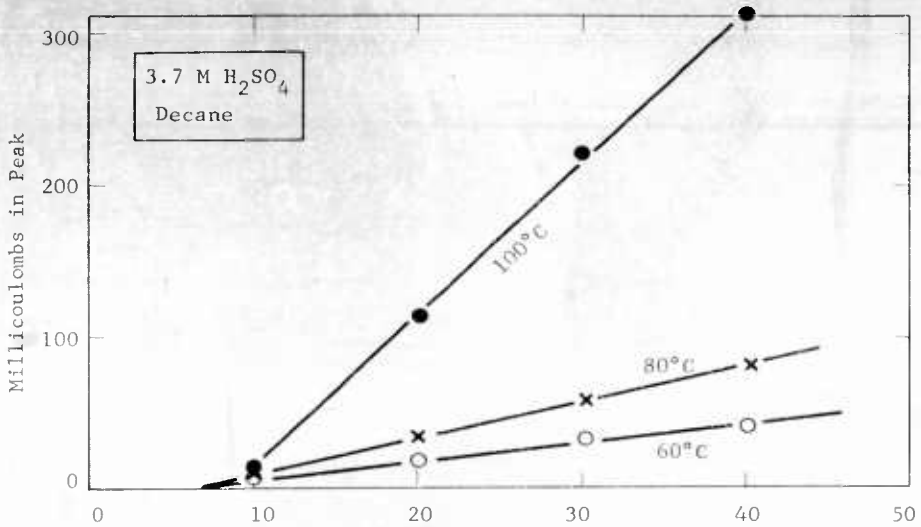

Further evidence of the non-diffusional nature of this limitation was gathered from an analysis of the temperature effect on total coulombs, Q_d. For this purpose, an Arrhenius plot was constructed using the quantity of coulombs observed in the peak at a fixed rate of scan as a measure of rate at the given temperature. A second plot was made using the difference in coulombs between two fixed rates of scan. The data for both cases, Figure A-4, indicate an activation energy for the rate limiting process of about 14 kcal/mole. Since this value is too high to be associated with diffusional effects, it is presumed that the rate limiting step involves a slow adsorption or similar phenomenon of a chemical nature.

Figure A-4

Effect of Temperature on Decane Peak Coulombs

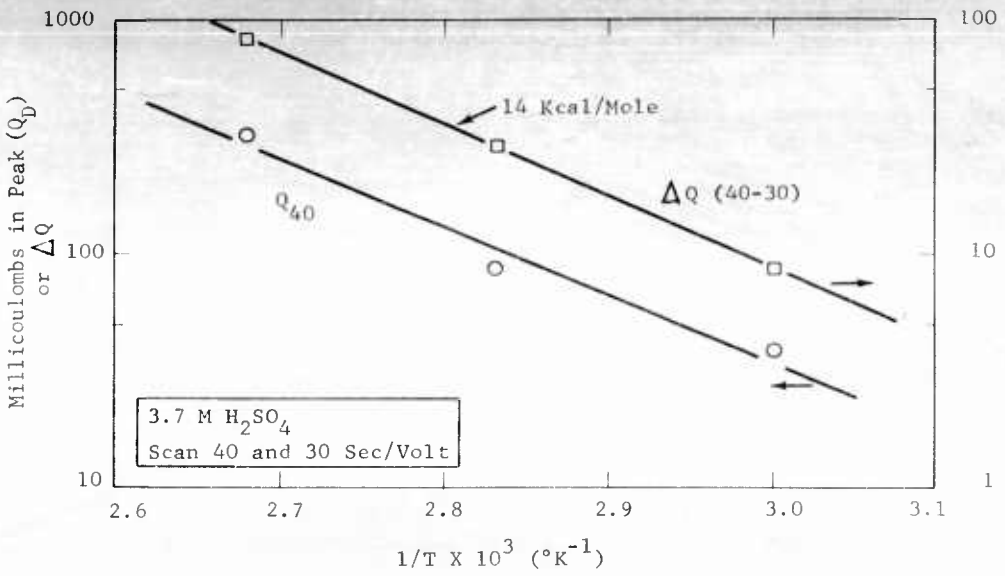

In addition to the above data it was determined that a sharp effect of acid concentration on the rate of accumulation of decane coulombs existed (Appendix A-5). This also precludes a transport limitation. Finally the rate above was observed to be nearly linearly proportional to decane concentration when cetane was used as a virtually inert diluent (Appendix A-5). This fact will be contrasted with the behavior of butane fuel to be discussed later.

In summary, the observed limiting rate in the decane-sulfuric acid system at 100°C seems to be controlled by some type of chemical step, possibly adsorption or initial surface dehydrogenation prior to electron transfer. It seems doubtful that a true electron transfer limited region is ever observed under these reaction conditions. The argument for the existence of the "chemical" limitation is supported particularly by the slow accumulation of reactive species, the high energy of activation and the strong dependence on sulfuric acid activity.

Phase 2 - Comparative Performance of Butane Feed

Due to difficulties in establishing reproducible steady state performance of liquid fuels such as decane, an effort was made to find a more suitable gaseous fuel. Due to its position as the highest carbon number paraffin fuel gaseous at room temperature, butane was chosen. Performance was studied in the flange cell previously described with the fuel chamber adapted for preheating and equilibration of gaseous fuel and electrolyte.

Studies encompassed temperature and concentration variables and state of fuel presaturation with water vapor. The study was aimed at obtaining consistent comparisons in the electrode-electrolyte system that was optimum for decane rather than optimization of butane performance. The electrode used was the platinum-Teflon mixture described previously.

The final exposed surface area in the electrode holder was 1 cm^2, containing 30-35 mg platinum. Butane fuel was Instrument Grade (Matheson) in most cases. No effect was observed on changing to C.P. Grade.

Part a - Steady State Performance

Steady state performance of butane was initially determined in 3.7 M sulfuric acid at 95-100°C. Performance showed excellent open circuit polarizations, often negative to the calculated theoretical value for the equilibrium butane-CO_2 reaction, reasonably stable Tafel slopes of 0.10-0.14 volts, and limiting currents of 15-25 ma/cm^2, (Appendix A-6 and Figure A-5). Use of pre-equilibrated versus dry butane feed was shown to result in no change in performance. It is presumed that 3.7 M sulfuric acid at these temperatures is easily able to supply the water requirements of the fuel reaction at this electrode.

Figure A-5

Performance of Butane
Fuel on Pt-Teflon Electrode

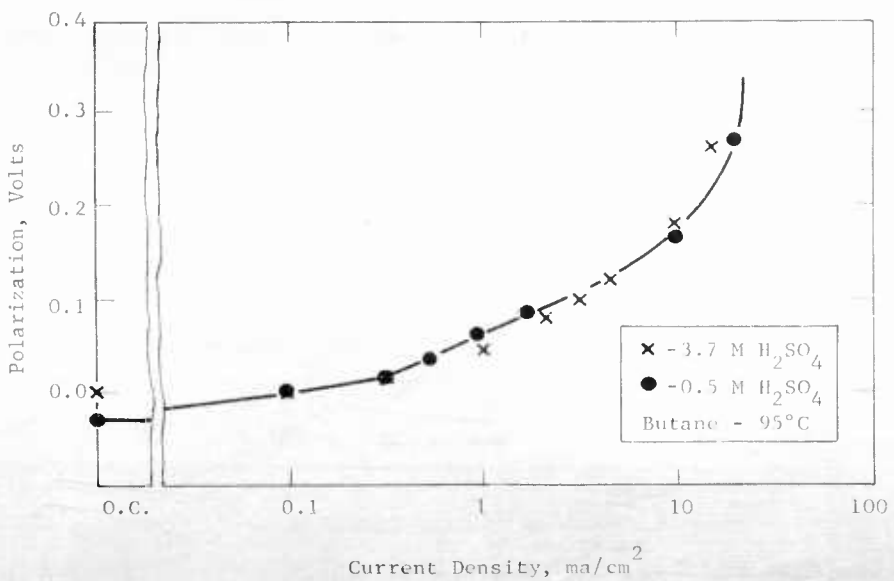

Part b - Rate Limiting Steps

While the anodic activity of butane is about five times that of decane, the rate limiting step appears to be the same, as evidenced by the similarity of the diagnostic criteria. As in the case of decane the voltage scan technique was used to measure the accumulation of an electrochemically reactive species. Voltage scan data at various scan speeds and temperatures were obtained to augment the steady state performance curves. With butane, as with decane, the rate of accumulation of coulombs due to hydrocarbon was slow (Appendix A-7) and the limiting slope was of the same order of magnitude as the limiting current. The energy of activation of the limiting process is ten kilocalories per mole, again suggestive of a chemical reaction rate limitation, though not as conclusively as in the case of decane. The Tafel slope corresponds to an electrochemical transfer coefficient of one half just as for gas phase decane (Table A-1).

Table A-1

Summary of Butane-Decane Comparison

	Liquid Decane		Gaseous Butane	
	Voltage Scan	Steady State	Voltage Scan	Steady State
Open Circuit Polarization (volts)	--	0.1-0.2	--	$\sim$0.0
Approximate Limiting Current (ma/cm^2)	7	10	37	25
Activation Energy (kcal/mole)	14	--	10	(20*)
Scan Time Dependency	linear	--	nearly linear	--
Tafel Slope (volts/decade)	--	(0.12**)	--	0.10-0.14
Acid Conc Dependency	sharp minimum	slight	slight	none
Fuel Conc Dependency (d log I/d log c)	1	--	$<\frac{1}{2}$	$<\frac{1}{2}$

* In the Tafel region only.
** Observable with a gaseous feed.

A brief comparison was made of the effect of 14.7 M phosphoric acid electrolyte on butane performance at 150°C on the Pt-Teflon electrode. Butane feed was used in both pre-equilibrated and dry state. Just as with decane, it was found that little difference existed between dry and vapor equilibrated feed and, surprisingly, that butane performance at 150°C in this electrolyte was no better than performance at 100°C in 3.7 M sulfuric acid. This behavior must in some way be related to the particular structure under study here, since it is known that increased temperature (and change in phosphoric acid electrolyte) produces the expected response when applied in conjunction with the sintered Pt-Teflon structure, Phase 6, Part b. No further explanation of this effect is yet available.

There were two differences between the behavior of butane and decane. Changes in sulfuric acid concentration had essentially no effect on butane activity, whereas there was an effect in the decane case. This phenomenon is not yet understood. Secondly, butane limiting currents were not linearly related to fuel concentration, or partial pressure. In contrast to decane, the fuel concentration dependency was less than square root (Appendix A-8). This may merely be a reflection of the higher chemical reactivity of butane, which maintains the surface coverage of reactive species nearer saturation than is the case with decane.

In short, in its general characteristics the butane reaction provides a more active, reliable and reproducible system for catalyst testing than does decane, at the same time involving catalytic limitations similar to those inherent in the oxidation of the heavier fuels. The word "limitation" needs qualification, however. The Tafel slopes and limiting currents observed here apply to a given electrode structure and available catalyst area. There are undoubtedly factors which can change the amount of surface area available for reaction and thereby shift the activity curves to higher or lower current densities. The existence of catalyst limitations therefore does not preclude the simultaneous existence of physical or structure limitations of equal importance. Some of these are discussed below.

Phase 3 - Flooding Measurements

Visual observations indicated that wetting problems are a key factor limiting catalyst utilization with a liquid fuel. The platinum-Teflon electrodes wet readily with decane but do not wet with aqueous electrolyte. Hence, when these electrodes are positioned at a decane-electrolyte interface their pores will be occupied mainly by the decane, which is an electrical insulator. A number of experiments verified this.

In one experiment voltage scans were obtained on an electrode exposed to electrolyte on both sides and then exposed to decane on one side, electrolyte on the other. The total number of coulombs in the hydrogen and oxide peaks and in the electrode capacitance were determined by integration of the scan in each case. The results indicated twenty times as much reactive platinum surface area in the absence of decane as in its presence.

In another experiment an electrode was weighed after exposure to pure electrolyte, pure decane, and both in an operating half cell. From the difference in densities between decane and electrolyte (0.7 versus 1.2, respectively) it was possible to calculate the amount of electrolyte in the electrode. Again, the results showed that an operating electrode is 95% flooded by liquid decane (Table A-2).

Table A-2

Measurements of Decane Flooding

	Voltage Scan		Weighing Measurement	
Electrode Condition	Total Milli-Coulombs	Fraction Filled With Electrolyte	Weight, mg, Minus Solids	Fraction Filled With Electrolyte
Exposed to Electrolyte	59	1.00	103	0.77(1)
Exposed to Decane	--	--	77	0.00
In Cell After 20 Min	--	--	88	0.20
In Cell After > 2 Hrs	3.1	0.05	80	0.055

(1) Some air probably trapped in pores.

In another series of experiments, the extent of decane flooding was determined by adding 2 volume % methanol to the electrolyte and measuring the methanol limiting current before and after operation. Earlier studies had shown that the limiting currents obtained with dissolved methanol fuel were directly proportional to the platinum surface area. Therefore, these limiting currents could be used as a measure of the catalyst surface area exposed to electrolyte or unflooded by decane. As can be seen from Table A-3, about half the surface area was lost when the electrolyte on one side of the porous electrode was replaced by decane, and over 85% was lost after a decane run (with methanol-free electrolyte) of several hours duration. This is in qualitative agreement with the other flooding experiments, since different electrode structures were used. All the measurements indicate that flooding by fuel is a major problem, of the order of 90% of the internal electrode surface area being lost due to it.

Table A-3

Results of Methanol Tests to
Determine Extent of Decane Flooding

When Tested[a]	Chamber Contents[b]		Estimated Limiting Current, ma/cm^2
	Fuel	Electrolyte	
Before	M	M	1100
Before	D	M	520
After	D	M	140

(a) Relative to decane oxidation run.
(b) M = 2 vol % methanol in 30% sulfuric acid, D = decane.

The barrier electrodes, modified electrolytes, and gas phase feeding systems reported below are essentially attempts to overcome this flooding problem.

Phase 4 - Electrode Structure

In view of the large effects of flooding on available catalyst surface area it was felt that structural modifications which could alter the three phase contact region, could produce sizable performance improvements. Therefore, a program was begun to optimize the structure of liquid decane electrodes.

Part a - Fabrication Variables

In preliminary experiments a number of mechanical variables were examined in order to establish an optimum base case. Electrodes were prepared by pressing dry mixtures of commercial Pt-black and binder (Teflon and other hydrophobic plastics) into tantalum or platinum screens. They were evaluated in 3.7 M sulfuric acid at 105°C on liquid decane galvanostatically in a setup similar to that described in Appendix A-2. Due to the occasional occurance of voltage oscillations and other time dependent behavior, performance data is not reported unless the voltage at each current density remained constant for at least two hours with a slope of less than ten millivolts per hour. As the electrode preparation and operation techniques improved, the occurrence of time dependent phenomena became increasingly rare.

It was first found that care in the pressing of electrodes was important. Simply leveling the dry powder in a circular restraining ring prior to pressing doubled the current outputs. Ballmilling the catalyst-Teflon mixtures for more uniform dispersion had no benefit, however (Appendix A-9).

Tests were made to evaluate the effect of platinum catalyst loading in a given electrode structure. Electrodes were prepared having catalyst loadings from 25 to 200 mg platinum/cm^2. Although the current density at 0.4 volts polarization increased steadily as catalyst loading increased, the utilization of this catalyst decreased. As shown in Figure A-6 and Appendix A-9, catalyst utilization at 0.4 volts polarization decreased from 0.12 ma/mg Pt to 0.05 ma/mg Pt as catalyst loading increased from 25 to 200 mg Pt/cm^2.

Figure A-6

Variation of Electrode
Performance with Catalyst Loading

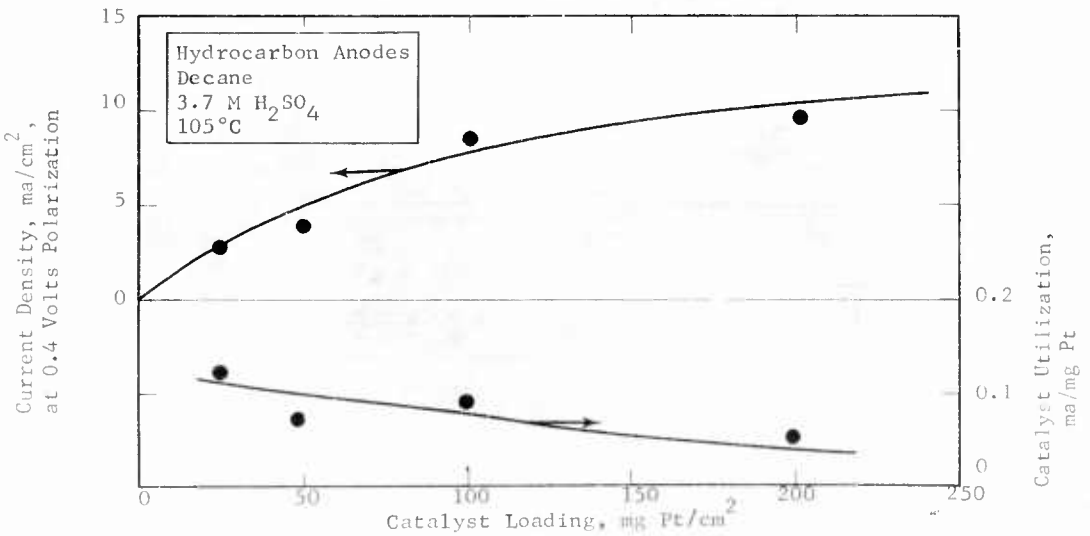

When the amount of plastic binders and the ratio of catalyst to plastic were varied over wide ranges, large variations in decane activity resulted. An attempt was made to establish exact cause and effect relations for these observations. However, the fabrication techniques available did not appear to be capable of adequately controlling the underlying factors, such as the distribution of pore diameters and lengths. A partial correlation of activity was possible with the measured thickness of the catalyst pad. Catalyst utilization appeared to reach an optimum at an electrode thickness near 40 mils. The peak value was 0.14 ma/mg Pt at 0.5 volts polarization, although there was a large variation of this number due to the lack of control over complex factors mentioned above (Figure A-7 and Appendix A-9).

Figure A-7

Effect of Electrode Thickness on Catalyst Utilization

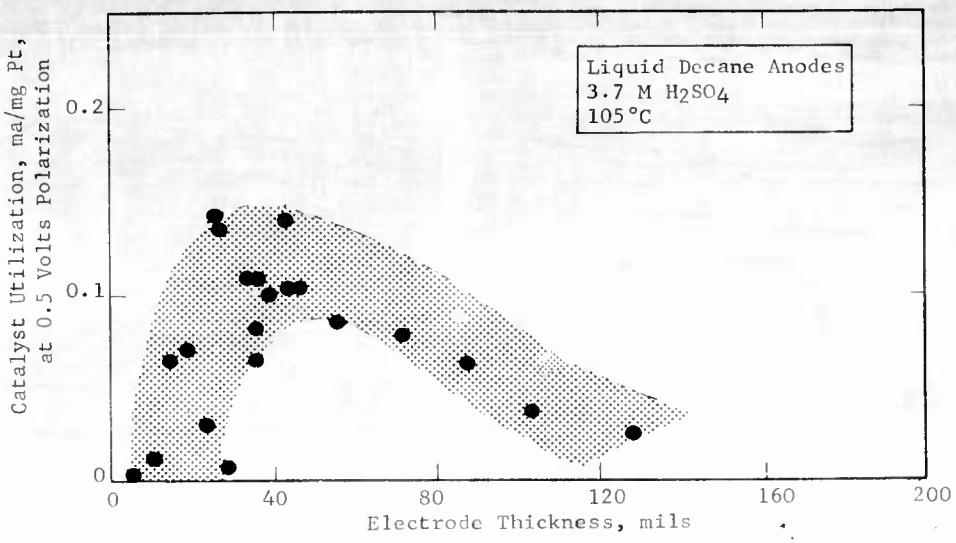

However, since most of the electrodes were made up to a fixed catalyst loading in terms of mg/cm^2, the electrode thickness correlated with the fraction of platinum relative to the total solids on the electrode. Therefore, the platinum utilization could also be plotted against the apparent platinum density in terms of mg/cm^3, again to yield a maximum at 2 mg/cm^3.

The results may be considered as indicative of a diffuse three phase contact area which reaches an optimum thickness or catalyst density. The optimum does not seem to be related to electrolyte or electronic ohmic resistance, as indicated by separate experiments showing these factors to be negligible. Wetting, flooding, and contacting problems appear to be more significant than resistance losses.

Part b - Barrier Electrodes

The fuel flooding of platinum-plastic electrodes could be reduced by inserting a porous plastic barrier on the decane side of the electrode. The first material evaluated as a barrier was a porous Teflon disc of nine micron average pore diameter. The barrier may serve two purposes. On the one hand it may control the feeding of decane to the electrode by preferential wetting and capillarity. It was observed that the porous Teflon would soak up decane readily but would not discharge it into an electrode without an applied hydrostatic head. When half cells were assembled using presoaked barriers the electrodes remained at the platinum oxide potential until a head of liquid decane was applied. The electrodes then attained their open circuit potential instantaneously.

On the other hand the barrier may merely permit the use of lower electrode fabrication pressures, which are generally beneficial to performance. Lower fabrication pressures give electrodes that are more easily penetrated by both phases but which leak and are weak. The barrier strengthens such electrodes and prevents leakage.

Figure A-8 illustrates the twofold current density advantage of a lightly pressed (200 psi) electrode operated with the barrier on the fuel side at 100°C in 3.7 M sulfuric acid over non-barrier electrodes (See Appendix A-10).

Figure A-8

Effect of Porous Teflon Barrier on Decane Performance

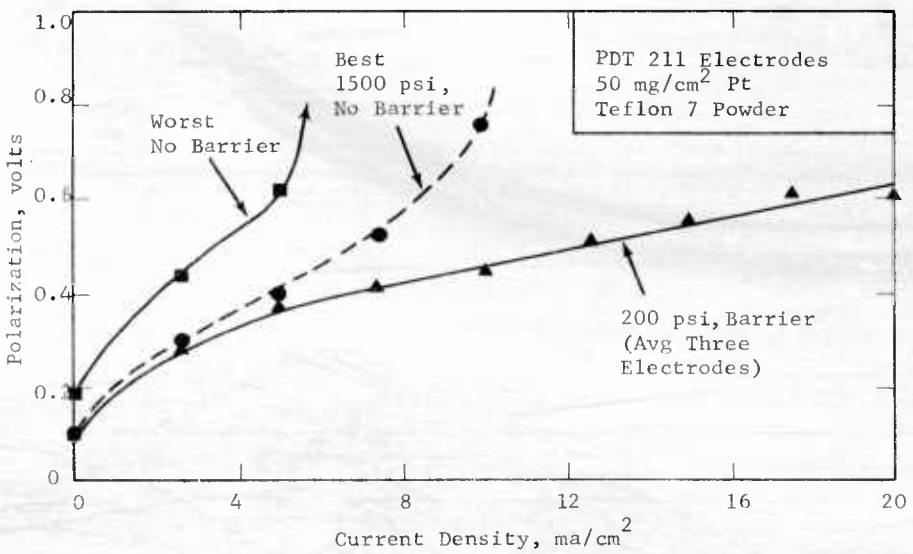

While there was a range of performance for both barrier and non-barrier electrodes, one direct comparison of the operation of an electrode pressed at 1500 psi with and without a barrier indicated that most of the advantage noted above is due to the lower pressing pressure (Table A-4).

Table A-4

Barrier Advantage Small For
1500 psi Fabrication Pressure
(105°C, 3.7 M H_2SO_4, 50 mg Pt/cm^2)

Fabrication Pressure, psi	Barrier	Polarization at Indicated ma/cm^2, volts			
		0	5	10	20
1500	No	0.12	0.44	0.77	--
1500	Yes	0.06	0.39	0.66	--
200	Yes	0.12	0.40	0.46	0.62

Whatever the mechanism of the barrier improvement, it appears that it is not acting merely to control the rate of fuel flow to the anode. Increasing the barrier thickness from 62 to 375 mils had essentially no effect on performance (Appendix A-10).

An improvement in structural stability, which did not affect performance significantly, was made by substituting a Teflon emulsion (DuPont "41BX") for the Teflon 7 powder. The former has a particle size in the 0.1 micron range as compared to the latter's ten or more micron size. Mixing of the emulsion with catalyst yields a homogeneous gel whereas mixtures of the powder with catalyst require considerable agitation or ballmilling to obtain a uniform coating. The finished electrode prepared from the Teflon emulsion has greater strength and homogeneity than the Teflon 7 electrodes.

Overall, both of these types of barrier electrodes gave generally superior catalyst utilization to the electrodes without barriers tested earlier, although the range was wide (Table A-5). A statistical "t" test showed that the difference between the two types of electrodes was significant at greater than 99.9% confidence.

Table A-5

Comparison of Performances of Electrode Structures

Electrode	No. Tested	Catalyst Utilization at 0.5 Volts Polarized, ma/mg Pt	
		Average	Maximum
With Barriers	22	0.16	0.25
Without Barriers	20	0.07	0.14

Attempts to fabricate barriers from Teflon 7 powder have not as yet been successful. Performance improvements over the non-barrier system have been obtained but the commercial porous Teflon barrier gives the best performance so far. Failure of the fabricated barriers appears visually to be due to fuel starvation rather than flooding (Appendix A-10).

A number of other barrier systems have also shown promise in fuel flooding control. For example, the carbon membrane structures described in Report 4 improved the performance of platinum Teflon electrodes (Appendix A-10).

In short, porous Teflon barriers appear to be able to control fuel flooding to some extent, probably by permitting lightly pressed, more porous structures to be used. Electrodes equipped with them have given the best stable liquid decane performance yet obtained at 100°C. Further improvement is still required, however. Other means to control flooding were therefore examined as explained below.

Phase 5 - Electrolyte Variations

A number of electrolyte modifications were made, primarily to alter the wetting properties of the electrolyte in its competition with the fuel for the catalyst surface, but also to permit raising the temperature and testing for any harmful influence of sulfate ions.

Part a - Fluorinated Acids

The first substance examined in this study, perfluorobutyric acid, was selected because its solutions wet Teflon, having a Teflon-like group at one end of the molecule and a carboxylic acid group at the other. It was expected to be able to compete with decane more successfully than sulfuric acid could for the surface of the Teflon. It would permit the electrolyte to penetrate the electrode structure more easily and thereby eliminate some of the area loss due to fuel flooding encountered with sulfuric acid. The perfluoroacids are also stable to oxidation and hydrolysis. They are highly ionized and therefore highly conductive. Subsequently perfluoroglutaric acid was examined because of its higher boiling point and lower equivalent weight, despite the fact that its solutions do not wet Teflon as well.

Initial tests with perfluorobutyric acid on a platinum-Teflon electrode indicated that the improved wetting properties of the electrolyte were beneficial to liquid decane performance but harmful to the performance of a gaseous fuel, ethane, as would be expected from the improved electrolyte wetting properties (Table A-6).

Table A-6

Comparative Performance of Perfluorobutyric and Sulfuric Acids

30 wt % solutions, 100°C, PDT electrodes

	Approximate Limiting Currents, ma/cm^2	
	H_2SO_4	C_3F_7COOH
Ethane Gas	25	5
Liquid Decane	3.5	12

Of particular interest was the observation that with a thin carbon electrode, where fuel flooding is normally very severe, the new electrolyte permitted some current to be drawn. Since the carbon based electrodes have catalyst loadings significantly less than that of the usual platinum-Teflon electrodes (1-3 mg/cm^2 versus 20-100 mg/cm^2), the new electrolyte may permit improvements in catalyst utilization (Table A-7 and Appendix A-11).

Table A-7

Catalyzed Carbon and Pt-Teflon Electrodes
In 1.4 M Heptafluorobutyric Acid at 95°C

Electrode Type	Catalyst Loading, mg/cm^2	Current Density at 0.5 Volts Polarization, ma/cm^2	Specific Current Density, ma/mg
Catalyzed Carbon	3	4	1.3
Pt-Teflon	50	8	0.16

Preliminary work was also carried out on hexafluoroglutaric acid because of its higher boiling point. The maximum operating temperature range of hexafluoroglutaric acid solutions was determined from boiling point measurements of solutions of various concentrations. Its solutions were far more ideal than those of sulfuric or phosphoric acids, reaching a boiling point of only 120.5°C at 80 wt % concentration. From the boiling point elevation it was possible to estimate that the solutions were nearly totally ionized up to at least 40% concentration (2.8 Molar).

Using decane as the fuel and a PDT electrode, a 1.25 M hexafluoroglutaric acid solution was evaluated at 100-105°C. It gave about the same limiting current density as 3.7 M sulfuric acid (10.5 ma/cm^2 at 0.5 volts polarized as compared to 12.5 ma/cm^2 for sulfuric acid). However, at lower polarizations the fluoro acid gave somewhat higher current densities. As indicated in Figure A-9, increased fluoro acid concentration results in markedly lower performance. An electrolyte additive to be discussed below, improved its performance.

Figure A-9

Performance of Hexafluoroglutaric Acid Electrolytes

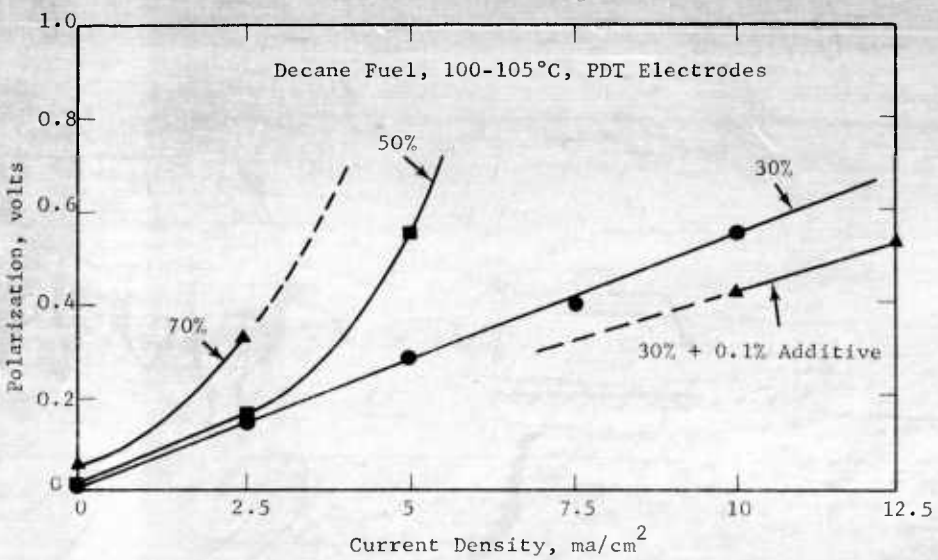

These results are quite promising in view of the fact that no attempt was made to optimize the electrode for this electrolyte. Physical limitations may be the reason for the linear polarization-current density curve. The results show incidentally that sulfate ions are not having any specific harmful effect. The new acids offer another "degree of freedom" in the optimization of the structural and wetting properties of liquid fuel electrodes.

Part b - Electrolyte Additives

Studies carried out prior to the inception of this contract have shown that certain electrolyte additives, stable to oxidation, could give factors of two to three improvement in current density with liquid decane. One of these was tested with the new barrier electrodes and still found to be effective (Table A-8).

Table A-8

Effect of Electrolyte Additive

Barrier Electrode, 3.7 M H_2SO_4, 105°C, Decane Fuel

Additive Conc, wt %	Current Density, ma/cm^2 at 0.5 Volts Polarization
None	6.6
0.1	12.5

Such additives continue to appear promising and are being used frequently for electrode structure optimization studies (Appendix A-10).

Part c - Phosphoric Acid Electrolytes

Phosphoric acid electrolytes were also examined using liquid decane fuel with two types of electrode structures. In both cases, the use of 14.7 M phosphoric acid at 150°C gave only minor performance improvements over 3.7 M sulfuric acid at 105°C despite the 45°C rise in temperature (Table A- 9).

Table A-9

Phosphoric Acid Performance

(50 mg Pt/cm^2)

Electrode	Acid	Temp, °C	Current Density, ma/cm^2 at 0.5 Volts Polarization
Carbon	3.7 M H_2SO_4	105	6.5
Barrier	14.7 M H_3PO_4	150	7.4
Pt 8515	3.7 M H_2SO_4	105	9.0
Pt 8515	14.7 M H_3PO_4	150	10.0

The best liquid decane performance at 150°C in phosphoric acid was inferior to the best obtained in sulfuric acid at 105°C. Physical factors limiting the reactivity of the liquid fuel may be over-riding the possible benefits of higher temperatures.

A brief examination of the conductivity of mixed sulfuric acid and phosphoric acid electrolytes at room temperature was made to determine whether the protonation of one acid by the other might produce an increase in conductivity at low water contents. Such a finding could be useful in overcoming the startup problem with concentrated phosphoric acid electrolytes and could also provide a lower temperature electrolyte of simpler water balancing problems.

The conductivity measurements indicated small conductivity maxima at fixed water contents, the optimum conductivity being slightly higher than in solutions of sulfuric acid alone (Appendix A-12). Such acid mixtures are to be tested with decane.

Phase 6 - Gas Phase Testing

To determine how much of an improvement in decane performance could be achieved by structure optimization, decane was fed as a gas to an electrode system known from other studies to be optimum for gaseous fuels. The gaseous feed was expected to eliminate fuel flooding problems.

Part a - Electrode Preparation

Sintered platinum-Teflon electrodes were prepared using emulsified Teflon (Dupont-41BX). The electrode consisted of 85% commercial platinum, 15% Teflon (skimmed) emulsion (by weight), cold pressed at 500 psi(to reject water) and sintered for one minute at 343°C and 1100 psi (Dixon Graph-Air was used as the mold release). The performance of this class of electrodes was evaluated in 14.7 M phosphoric acid electrolyte at 150°C.

Part b - Butane Performance

These electrodes were first checked with butane gas. Performance was excellent, with 200 ma/cm^2 available at 0.28 volts polarization, and a limiting current of about 400 ma/cm^2 (Figure A-10 and Appendix A-13).

Figure A-10

Performance of Butane on Sintered Pt-Teflon Emulsion Electrode

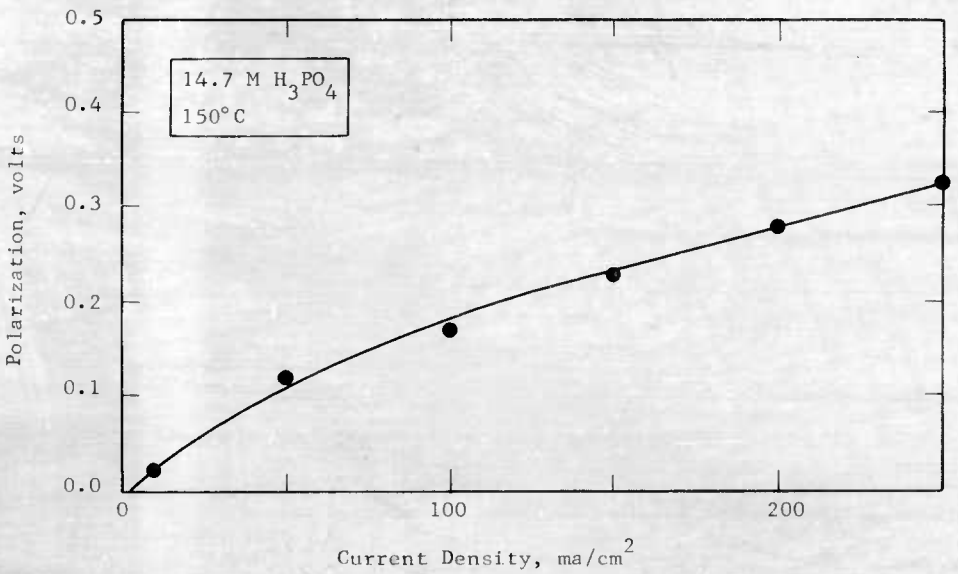

Operation was found to be essentially identical using either dry or pre-equilibrated fuel. The excellent performance of this electrode structure is highly specific to the particular electrolyte and temperature. When operated in 3.7 M sulfuric acid at 100°C, performance was markedly impaired, giving a limiting current of 25 ma/cm^2 with 10 ma/cm^2 available at 0.12 volts polarization.

Part c - Decane Performance

Two modes of delivery of gaseous decane were examined, steam distillation and vaporization into a carrier gas. In the steam distillation experiments, decane vapor was carried to the electrode by a boiler vessel containing 65% sulfuric acid. The steam-decane mixtures were supplied to the fuel chamber at 140°C. In the carrier gas experiments decane was evaporated into a stream of flowing argon from a boiler held at 150°C. Fuel partial pressure was checked by dewpoint measurements.

The current densities achieved with either type of gaseous feed were of the order of ten times higher at a given polarization than those obtained with liquid decane or with gaseous decane using a Pt-powdered Teflon electrode (Figure A-11 and Appendix A-13).

Figure A-11

Performance of Decane on
Sintered Pt-Teflon Emulsion Electrode

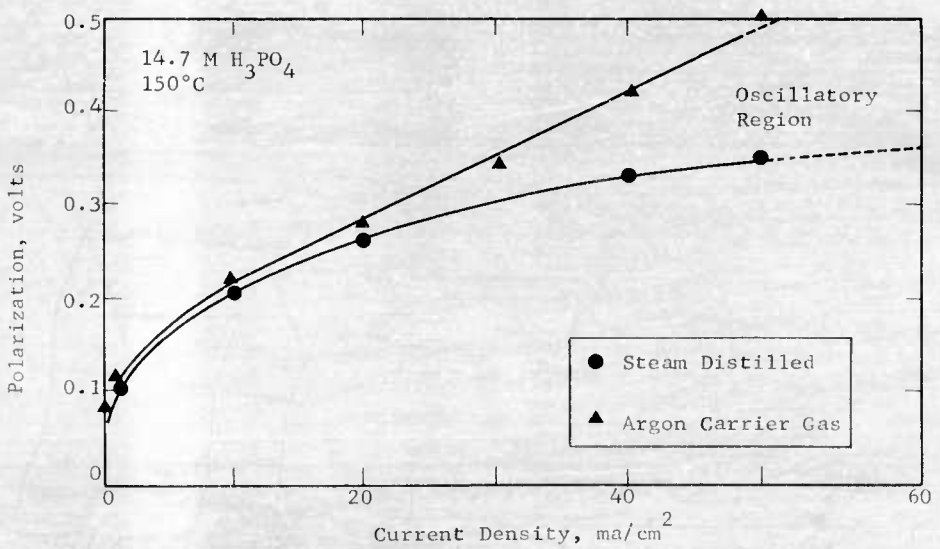

Performance with the steam carrier gas appeared to be superior to the argon, with 50 ma/cm^2 available at 0.35 volts polarization as opposed to 30 ma/cm^2 for argon carrier gas. Limiting currents of about 100 ma/cm^2 were reached. However, considerable voltage oscillation was observed between 50 and 100 ma/cm^2. These appeared to be associated with temperature fluctuations.

This electrode system, as is, is unstable for practical use because it appears to be attacked at 150°C in 14.7 M phosphoric acid. Small pinhole cracks appear due to either temperature or acid attack which eventually cause leakage of fuel and electrolyte. One solution is to provide auxiliary interface maintaining components such as a barrier. The use of a 9 micron porous Teflon barrier as an interface holder has been beneficial. As indicated in Figure A-12, the barrier electrode performance was excellent, with 80 ma/cm^2 available at 0.5 volts polarized and a limiting current of about 140 ma/cm^2.

Figure A-12

Performance of Gaseous
Decane on Barrier Electrode

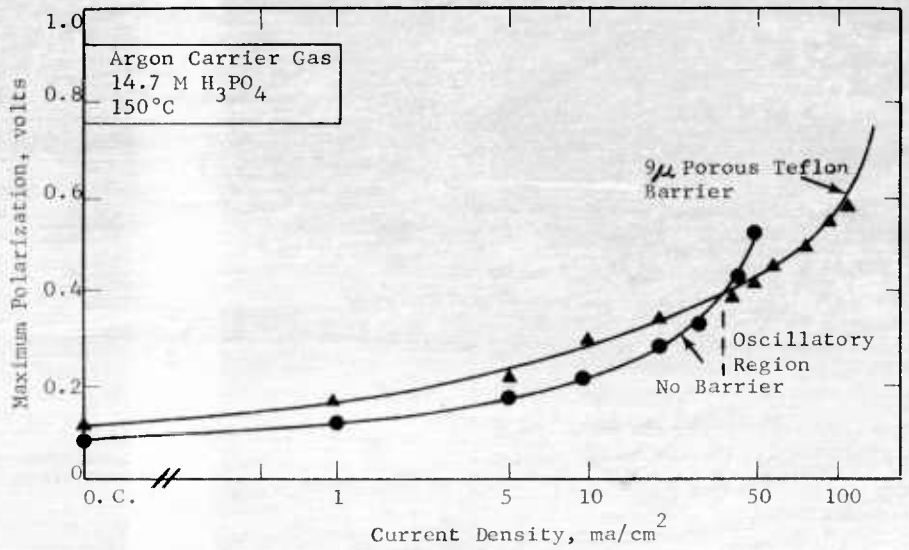

As with the non-barrier systems, oscillations were observed above 40-50 ma/cm^2. However, the maximum polarization at each current was plotted in Figure A-12.

The performance of these electrodes with gaseous fuels offers a promising means of utilizing hydrocarbons in a fuel cell provided the problems associated with operating at 150°C with phosphoric acid can be solved. These problems include corrosion, electrode structural stability and cell heat and water balance. In terms of the objective of using a liquid hydrocarbon, these results do no more than confirm the importance of structural effects and their extreme specificity, and reinforce the hope that relatively small adjustments in electrode wetting properties can produce large performance improvements. This type of electrode shows no advantage at 100°C in 3.7 M sulfuric acid with butane fuel over the cold pressed electrodes made with powdered Teflon. In fact, with liquid decane at 100°C this present electrode is distinctly inferior to the powdered Teflon type.

Phase 7 - Noble Metal Catalysts

Several noble metal catalysts, particularly those that had shown promise in the methanol work, were evaluated on saturated hydrocarbon fuels. The results obtained were not considered as the final verdict on the "true" catalytic properties in view of the large effects of electrode structure and wetting properties on performance that had been detected earlier. Changes in grain size and density and hydrophobicity might well mask variations in catalytic ability. Nevertheless significant comparisons could be obtained.

Part a - Catalytic Activity of Several Noble Metals with Liquid Decane

The catalytic activity of selected noble metals as fuel cell electrodes was examined in order to discern whether catalytic activity could be simply related to some basic property of the metal. A recent article (6) suggests that for a large number of processes the catalytic effectiveness of various metals is linearly related to their surface tensions.

Metallic rhodium, iridium and platinum were prepared by reduction of appropriate salts by each of two methods, sodium borohydride reduction and a special high temperature reduction technique. Attempts to reduce zirconium salts to the free metal were unsuccessful. A white oxide of zirconium was the product of this reaction.

The examination of the data obtained from evaluation of these materials (Appendix A-14) failed to suggest any obvious relationship between basic metal properties and their effectiveness as fuel cell catalysts. In fact the factor that tended to exert the greatest influence on performance was the manner in which the catalyst was prepared. Thus, commercial platinum black demonstrated performance obviously superior to those of the two platinum blacks prepared by $NaBH_4$ and high temperature reduction respectively. These results, plus the observation that neither platinum-ruthenium (40%) nor platinum-rhodium prepared by similar methods possesses any distinctive performance advantage over ordinary commercial platinum served to strengthen the impression that the method of catalyst preparation is a variable deserving specific and detailed attention in current fuel cell studies. This factor, in addition to the electrode structural factors mentioned earlier, makes general comparisons between different metals difficult but on the other hand greatly increases the number of catalyst possibilities.

Part b - The Preparation of High Surface Area Platinum Black

The most obvious way of improving the catalytic activity of platinum black is to increase its surface area. This was achieved quite simply by co-precipitating platinum and aluminium hydroxide in a procedure that takes advantage of the fact that the aluminate ion is precipitated as a high surface area gel by acid. The acidity can be furnished either by the noble metal compounds themselves e.g. H_2PtCl_6 or by the addition of excess mineral acid and finally by the acid that is invariably produced by reducing agents which do not liberate hydrogen from the solvent. For example

$$2\ HCOOH + PtCl_6^{=} \longrightarrow Pt^{\circ} + 2\ CO_2 + 6\ Cl^{-} + 4\ H^{+}$$

$$4\ H^{+} + 4\ Al(OH)^{-}_4 \longrightarrow 4\ H_2O + 4\ Al(OH)_3$$

The noble metal is then adsorbed and reduced simultaneously or sequentially on the alumina surface. The alumina is readily redissolved in either acid or base resulting in a high surface area catalyst. The surface area of a particular reduction can be varied by varying the ratio of aluminum hydroxide precipitated to metal reduced.

Although this procedure has not as yet been optimized with regard to reaction conditions, initial experimental results using formaldehyde as the reducing agent have been encouraging. In a typical preparation a 2 M sodium aluminate solution was titrated with 3.7 M H_2SO_4 until precipitation began. An equal volume of U.S.P. Formalin was added along with half the volume of 0.073 M chloroplatinic acid. After standing 16 hours the precipitate was centrifuged and the aluminum hydroxide dissolved in 6 M KOH overnight. The remaining platinum was washed with water. In different runs platinum blacks with surface area 50-90% greater than that of commercially available products have been obtained (Table A-10). The fuel cell performance of these materials on decane (Appendix A-14) and on methanol is likewise improved.

Table A-10

Comparison of Platinum Catalysts

	Commercial	Formaldehyde-Aluminate
Surface Area (% Theoretical Monolayer)	10	16
Decane Current Density (ma/cm^2) 100°C, 0.34 volts polarized	3.5	7
Methanol Current Density (ma/cm^2) 60°C, 0.45 volts polarized	20	60

Surface area measurement studies have also led to the conclusions that little if any platinum is buried in pressing techniques employed to make electrodes, and that little if any platinum surface area is lost during its use in a decane anode (Table A-11).

Table A-11

B.E.T. Argon Surface Area
of Platinum Black Electrode

Material	Surface Area m^2/gm
Commercial Pt Black	20.2
Powdered Binders	2.5
Electrode Scrapings*	
Pressed 1:1 Mixture of Pt + Binders	
Actual	11.1
Calculated	11.4

* After use in a decane half cell at 100°C in 3.7 M sulfuric acid.

The general approach of using various reducing agents and additives to modify the crystal structure and surface area of platinum or other noble metal catalysts appears to offer promise as a means of improving activity.

Part c - Use of P-type Catalyst with Liquid Decane

Two types of experiments were run to determine whether P-type catalyst would show activity on liquid decane in "non-static" systems. In one procedure, the catalyst, mounted in a Pt screen, was first boiled for one-half hour in decane and then placed in 3.7 M sulfuric acid at 95°C. It was found, as shown in Figure A-13, that current densities as high as 100 ma/cm^2 could be achieved. However, these performance levels were of temporary duration, although at 10 ma/cm^2 the activity was maintained for up to several hours. At the highest currents, constant polarization performance could be achieved for only several minutes, followed by a rapid increase. There was, however, no coulombic correlation between the various current densities. A blank was run with a P-type electrode which was not reacted with decane and essentially no activity was obtained.

Figure A-13

Initial Performance of P-type Catalyst

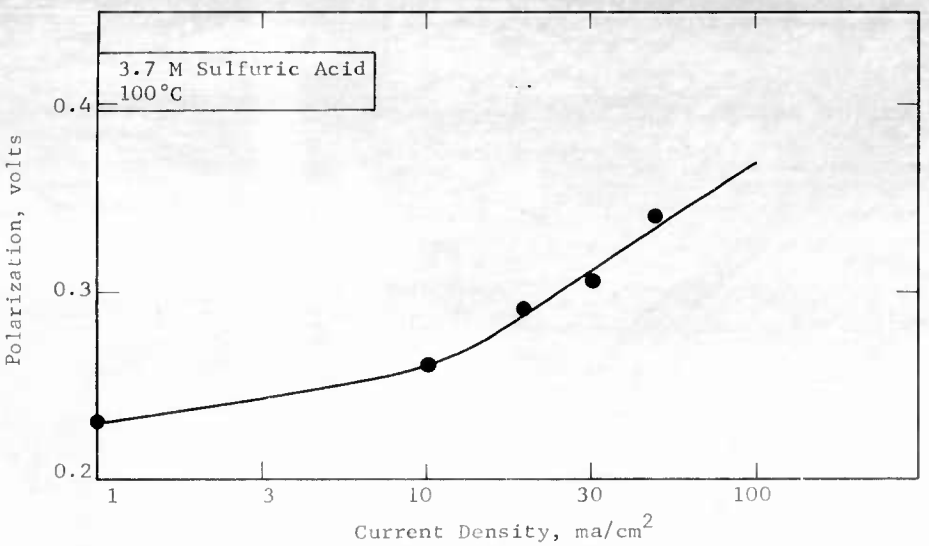

In the second method, a fresh P-type electrode was simply positioned at a decane--3.7 M sulfuric acid interface at 100°C. Up to about 30 ma/cm^2, similar performance to the above was found, but it failed at higher levels. In both cases, the initial activities shown in Figure A-13 could not be regained by treating again in decane. Thus, although the P-type catalyst appears to have activity toward decane, it is irreversibly deactivated with use. Further work will be necessary to define and prevent this deactivation.

Part d - Performance of Butane on Methanol Type Catalysts

A few experiments were carried out to test the performance of typical active methanol catalysts on hydrocarbon fuel. Catalysts tested included Pt-Ru, Ir-Ru and a ruthenium modified P-type catalyst. Tests were conducted in 3.7 M sulfuric acid at 100°C using pre-equilibrated butane fuel, on cold pressed catalyst-Teflon 7 electrodes.

Of the three catalysts tested only the Ru-modified P-type catalyst showed any activity for butane oxidation and this activity was inferior to commercial platinum black (Appendix A-6). The negative result means either that the rate controlling step in hydrocarbon oxidation is different than that in methanol oxidation, or that adverse effects of the catalysts on the electrode pore structure and wetting properties are masking their true catalytic activity.

Phase 8 - Non-noble Steam Reforming Catalysts

To avoid the use of expensive noble metal catalysts of limited availability, an investigation was begun into the possible use of low cost steam reforming catalysts in hydrocarbon fuel cells. These catalysts are known to be able to convert hydrocarbons to hydrogen and carbon dioxide in the presence of water vapor at high temperatures and pressures. The present studies were undertaken to determine whether they would be reactive under atmospheric pressure and low temperature conditions, and, if so, whether the selectivity to hydrogen and the rates would be appropriate to fuel cell use. In the beginning of this program no attempt was made to decide whether the catalyst would be used in a separate chamber or whether it would be incorporated into a fuel cell anode. Therefore, the exploratory phase of this program was arbitrarily carried out in a gas phase reactor.

Part a - Catalyst Activity at Low Temperatures

The chemical activity of catalysts for the conversion of decane in the presence of water was measured in a bench scale laboratory reactor shown in Appendix A- 15. In this apparatus water and decane were fed at a controlled rate to the vaporization zone of a tubular reactor. The gases then passed over the heated catalyst, where the conversion occurred, and out through a water cooled condenser, which liquified the unreacted decane and water. The rate of formation of non-condensible gases was measured using a wet test meter. The effluent from this meter went into sample bombs for mass spectrometer analysis. The reaction rates were calculated from the wet test meter readings and the gas analysis.

The activity of the catalyst was determined at various temperatures. An Arrhenius plot did not give a straight line, but the average activation energy was in the range of 16 kcal per mole (Figure A-14).(See Appendix A-16.)

Figure A-14

Temperature Dependence of Decane Steam Reforming Rate

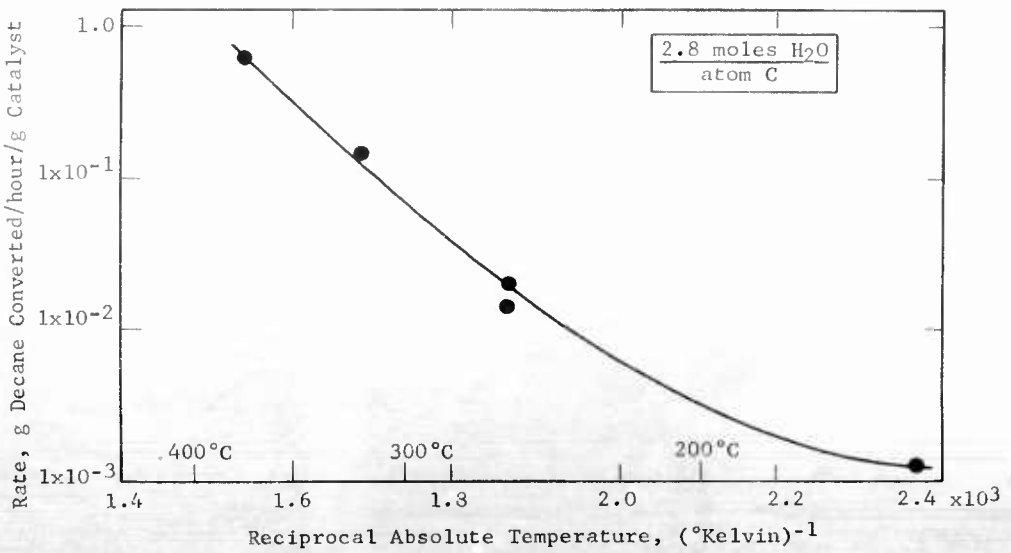

From the above rates catalyst requirements to produce a KW of power were then calculated and are shown in Table A- 12.

Table A-12

Catalyst Requirement Versus Temperature

Temperature, °C	Catalyst Requirement, lbs/KW(1)
370	0.47
315	2.5
260	12.8
205	63
150	200
Maximum Permissible(2)	7

(1) Assumes 4 ft^3/hr of H_2 is equivalent to 200 watts and stoichiometry $C_{10}H_{22} + 20\ H_2O \longrightarrow 10\ CO_2 + 31\ H_2$. Based on activity of standard catalyst T-1.

(2) Assuming the catalyst is applied to electrodes operating at no less than 35 mwatts/cm^2 and a maximum loading of 100 mg/cm^2.

In a vapor phase chemical system the catalyst has sufficient activity at temperatures above 250°C for a practical system. Reaction rates here at 370°C are comparable to conventional systems operating at 700-800°C. Under the assumption that the same rates of decane conversion that were obtained in a vapor phase chemical system will be obtained in an electrochemical system, the catalyst would not have sufficient activity at 100°C to be attractive at reasonable loadings. However, an electrochemical potential, which would remove product hydrogen as it forms, might accelerate the reaction considerably.

Part b - Reaction Products

The composition of the dry product gas, as determined by mass spectrometer analysis, is shown in Figure A-15.

Figure A-15

Product Analysis-Decane Steam Reforming Runs

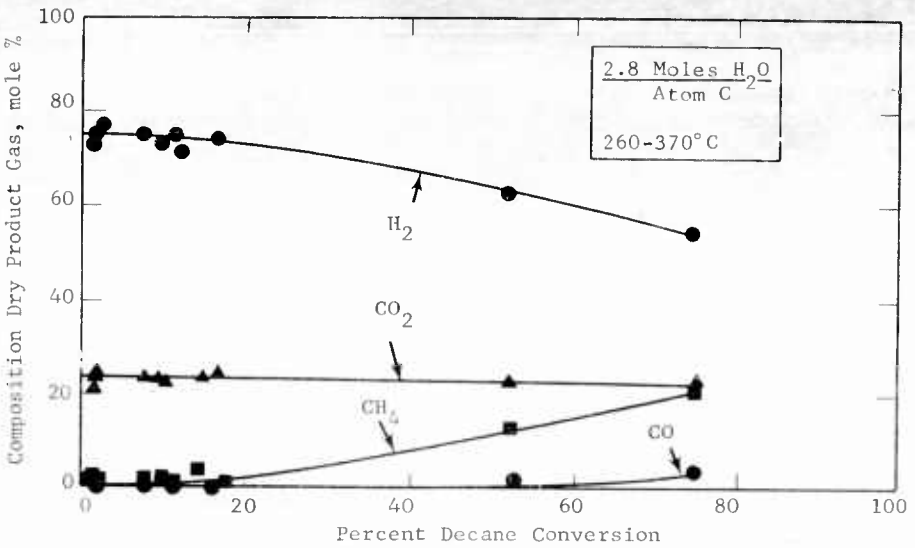

It can be seen that a high concentration of hydrogen is produced, particularly at low conversion levels. Carbon dioxide and carbon monoxide content remain relatively constant. The methane content rises as the hydrocarbon conversion level rises. Thus, despite temperatures which thermodynamically favor methane production, virtually theoretical yields of hydrogen can be obtained, provided the conversion per pass is kept low.

Part c - Electrochemical Activity of Product Gas

The electrochemical activity of the decane steam-reformate was demonstrated by using the effluent gas from the laboratory reactor running at 260°C to run an anode half cell of the type described in Appendix A-2 . For comparison purposes a test was made on the same anode using pure hydrogen. The steam reformer product was inferior to pure hydrogen in performance but did yield over 200 ma/cm^2, with decane as the original fuel (Table A-13).

Table A-13

Demonstration of Electrochemical Activity of Decane Steam Reformate(1)

Current Density, ma/cm^2	Volts Polarized from Theoretical H_2	
	Pure H_2	Product Gas
0	0	0
10	.005	.003
20	.006	.008
50	.017	.035
100	.037	.117
150	.057	.227
200	.075	.330

(1) Vapor Phase chemical system: 40 grams catalyst T-1, 260°C, 29 cc decane/hr, 82 cc H_2O/hour.
Electrochemical System: 3.7 M sulfuric acid, 60°C, catalyzed carbon anode.

The run described above represents a steam reformer-fuel cell system which has a number of advantages over other systems of this type: The product gas is used without purification, that is, no palladium diffuser is involved. The steam reforming catalyst is non-noble and low in cost. In addition, the reformer operating temperature is 260°, rather than the 700 to 800°C ordinarily employed.

Part d - Catalyst Modification Studies

A catalyst modification program was undertaken to develop a catalyst more compatible for use in an electrode and to increase catalyst activity. This data is tabulated in Appendix A-16. As a result of this work a catalyst 50% more active than the standard catalyst was developed, which in addition should be more compatible with an anode system. However, since factors of improvement greater than twenty are required to operate at 150°C or less, improvements of this order of magnitude will not affect the utility of these catalysts. In their present activity ranges they must succeed or fail depending upon their ability to be used in a separate chamber at a higher temperature, or to be accelerated by electrochemical polarization. Therefore, further small magnitude improvements will no longer be sought, until the usefulness questions are answered.

Part e - Liquid Phase Study

An experiment was made to investigate the use of catalyst type T-1 in a liquid phase reactor. Activity with liquid phase water and hydrocarbon is a necessary preliminary to the use of these catalysts as anode ingredients. It could also provide a lead to a separate liquid phase hydrogen generator which could avoid the excessive heat of vaporization efficiency losses inherent in vapor phase steam reforming systems. The layout of experimental equipment is shown in Appendix A-17.

The catalyst was activated by treatment with lithium biphenyl radical anion solution. It was treated with a 4/1 water/decane emulsion at 60°C. As the emulsion slowly separated, product gas was evolved at a gradually declining rate in the range of 0.5 liters per hour per 480 grams of catalyst. Due to the low gas evolution rate it was not possible to obtain mass spectrometer samples that were free of nitrogen and air. However, analyses corrected to a contaminant free basis showed good selectivity to hydrogen (Table A-14).

Table A-14

Analysis of Liquid Phase Steam Reformate

	Sample 3	Sample 4
H_2	58.1	66.0
CH_4	6.1	2.2
Total C_2	5.3	3.3
Total C_3	--	--
Total C_4	0.8	--
Total C_5	1.0	1.5
Total C_6	0.1	--
CO_2	28.6	27.0
	100.0	100.0

Thus, these preliminary results indicate that liquid phase steam reforming of decane may be possible. They also indicate that the electrochemical activity of these catalysts is not precluded by the existence of the reactants in the liquid state.

Part f - Attempted Anode Preparation

A number of preliminary attempts were made to prepare fuel cell anodes from the low temperature steam reforming catalysts for use in buffer electrolytes. Activation procedures tried were lithium biphenyl radical anion treatment, cathodization in 15 M KOH electrolyte, and sodium hypophosphite solution treatment followed by cathodization in 3 M KOH. Anodic tests with hydrogen using 3 M KOH electrolyte indicated that the anodes were essentially inactive electrochemically. It is believed that the poor conductivity of the catalyst mixture is the chief problem to be overcome before electrochemical activity can be achieved.

4.2 Task B, Hydrocarbon Fuel Cell

The goal of this engineering research program is to assess the feasibility of the hydrocarbon-air fuel cell components in a complete power source. Since several fuel cell systems exist, each presenting unique system requirements, early analysis of these components in a total cell assembly under actual operating conditions is required. Therefore, a total cell test facility with sufficient flexibility for use with a variety of electrode structures was constructed. Testing of potential systems is in progress. The details of the construction of this unit are presented in Appendix B-1.

Phase 1 - Liquid Hydrocarbon-Air Fuel Cell

The first system examined employed decane in the liquid state as the fuel and oxygen as the oxidant. The fuel cell was operated at temperatures of about 100°C. The fuel electrodes were the interface maintaining electrodes discussed in Task A. The Cyanamid AA-1 electrodes, backed with Permion 1010 membranes, were used as the oxygen electrodes.

Part a - Cell Performance

The initial studies were carried out to determine whether the concept of using interface maintaining electrodes for liquid hydrocarbon fuels was practical. In the first set of experiments, the operating conditions were adjusted to produce a temperature gradient across the cell between the fuel and electrolyte chambers. The fuel was maintained at 126°C, while the electrolyte and air chambers were held at approximately 100°C. Power outputs of 3.8 mwatts/cm^2 at a cell voltage of 0.31 volts were obtained with liquid decane. However, it was found that mechanically mixing electrolyte into the circulating fuel increased the power output to 8.2 mwatts/cm^2 and the cell voltage to 0.44 volts. These results are shown in Figure B-1. .

In another series of runs, the temperature throughout the cell was maintained at 103°C. Under these conditions, power outputs of 4 to 6 mwatts/cm^2 at cell voltages of 0.50 volts were obtained. However, current densities only as high as 12.5 ma/cm^2 were used. Consequently, the maximum power capability of the system was not established. The performance under these conditions is illustrated in Figure B-2 . Appendix B-2 details the results of all these tests.

Figure B-1

Performance of Decane-Oxygen
Cell Having a Temperature Gradient

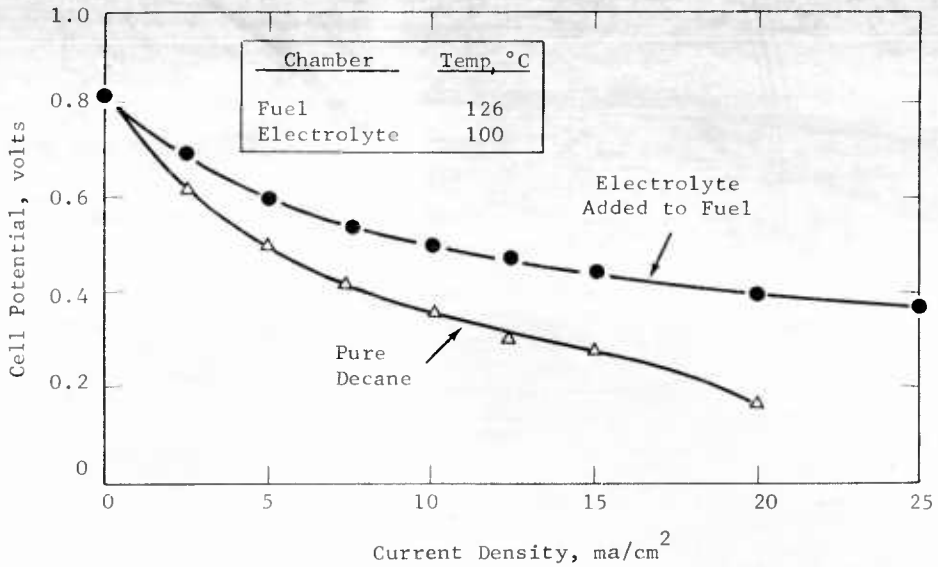

Figure B-2

Performance of Decane-Oxygen Cell
Maintained at a Uniform Temperature

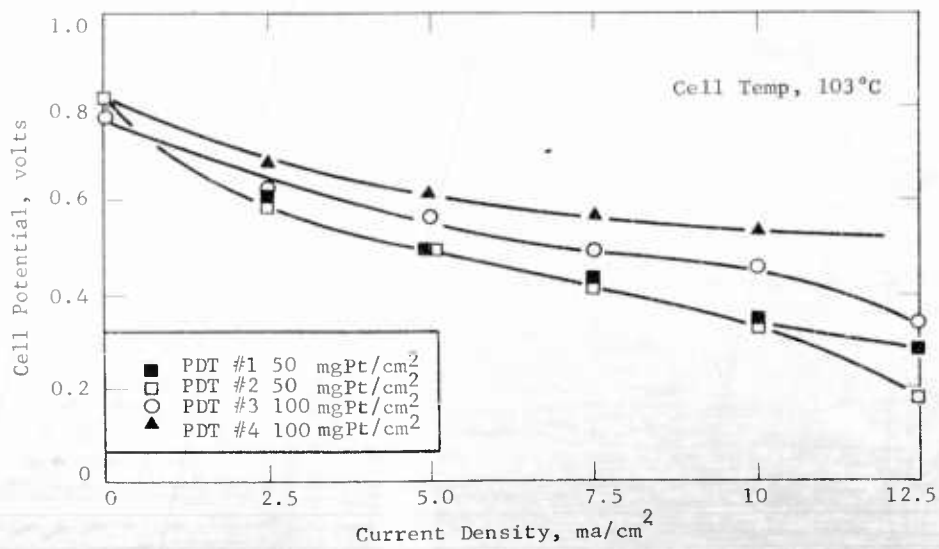

Measurements were also made of the polarizations of the individual electrodes in the cell using hydrogen reference electrodes. As can be seen in Figure B-3 , the major source of voltage loss was the polarization at the fuel electrodes. The polarization at this electrode was 0.26 volts at open circuit, increasing to 0.40 volts at 7.5 ma/cm^2. In contrast the observed oxygen electrode polarization was independent of current density in the range of current densities used, amounting to about 0.23 volts. These data are in agreement with comparable half cell data obtained in Task A. Although the performance levels are somewhat lower than those expected from the data obtained prior to the inception of the contract, they do demonstrate the feasibility of translating the results obtained in half cells into total cells.

Figure B-3

Performance of Individual Electrodes

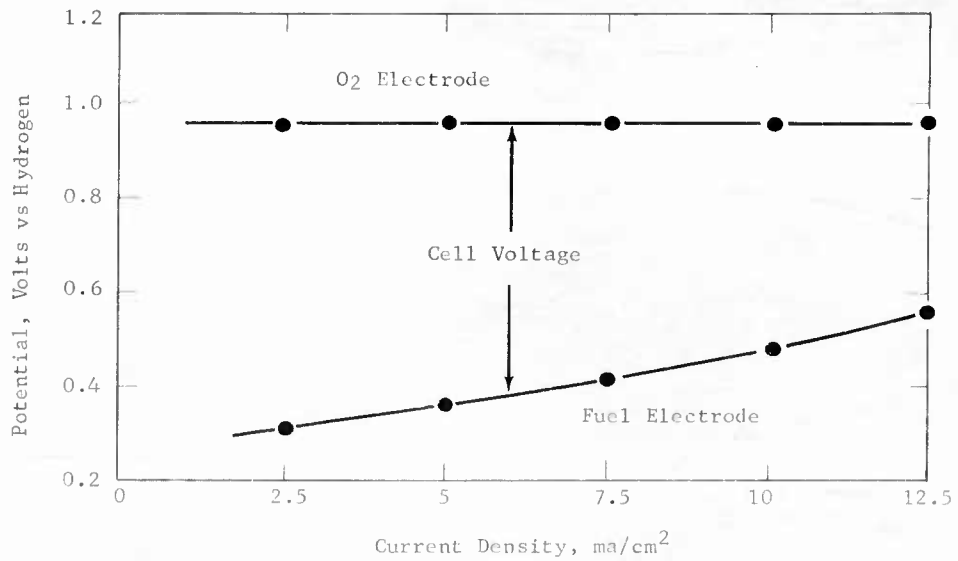

Part b - Cell Instability

In all the cells tested, performance of both the fuel and air electrodes was unstable. The oxygen electrode showed a decay in activity over the course of a few days of operation. However, this was caused by the separation of the cathode from the Permion membrane and the consequent formation of gas pockets. Pressing the membrane to the electrode at 1000 psi corrected this problem.

The fuel electrode showed some of the instabilities previously discussed in Task A. As indicated in Figure B-4 , the anode performance decreased with time and the response to changes in current density was very slow. In addition, the performance deteriorated after cell operation at high current densities.

Figure B-4

Time Dependence of Anode Performance

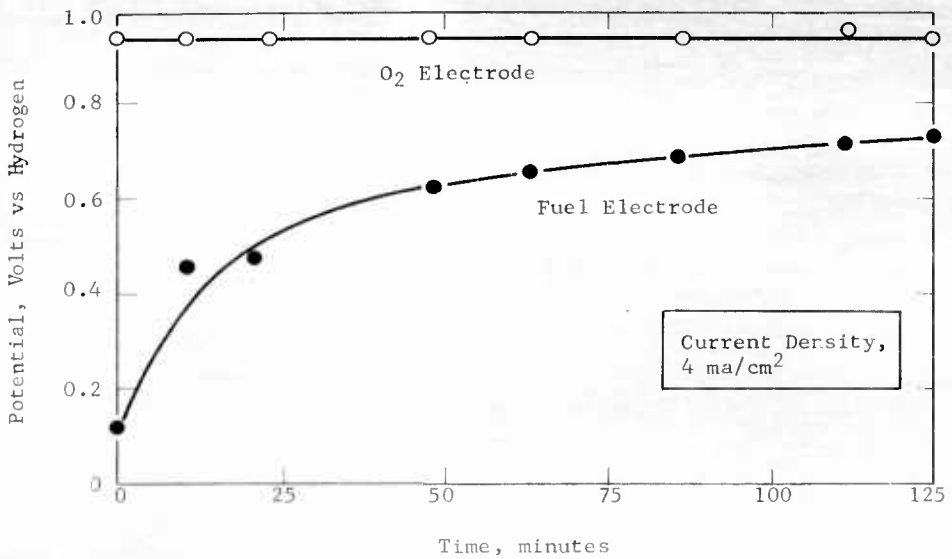

Part c - The Effect of Acid Concentration

A preliminary evaluation was also made of the effect of sulfuric acid concentration on cell performance. The acid concentration was varied from 3.7 M to 10.3 M. These data indicated that increasing the sulfuric acid strength above 3.7 M impairs cell performance at both the open circuit and under load. This is shown in Table B-1 .

Table B-1

Effect of Acid Strength on
Total Cell Performance

Partially Deactivated Electrodes
Cell Temperature 126°C

Sulfuric Acid Concentration, M	Cell Potential at Indicated ma/cm^2, volts		
	0	2.5	5.0
3.7*	0.81	0.48	0.30
8.1	0.71	0.40	0.20
10.3	0.58	0.16	--

* Cell temperature - 100°C.

Part of this loss is probably due to the direct chemical attack on the electrodes. The electrolyte darkened in color after operation and, upon disassembly, both the anode and the Permion 1010 membrane appeared to have been attacked. These results are consistent with the half-cell data reported in Task A.

4.3 Task C, New Systems

Fuel cell research often falls within fairly restricted, well-defined limits. The New Systems work has been instituted to investigate approaches outside of these areas which might offer advantages for fuel cell performance. Thus, new electrolytes in the form of buffer solutions have been studied. The use of a flowing fuel system has also been examined. In addition, several slurried catalysts suspended in the electrolyte have been investigated. Other studies have looked at possible redox systems for the fuel electrode, as well as phthalocyanine complexed catalysts for anode and cathode use. A number of possible new materials for fuel cell component use were also screened.

Phase 1 - Buffer Electrolytes

One alternative to corrosive strong acids or non-carbon dioxide rejecting strong bases is a buffer electrolyte. It must be demonstrated, however, that this type of system is capable of supporting practical current densities. Therefore, the activity of methanol and of air were investigated in buffers, with emphasis on the performance of various catalysts and electrode structures. In addition to this half-cell work total cell performance was measured to define compatibility and transport problems.

Part a - Methanol Catalysts in Buffer Electrolytes

A number of catalysts were tested for activity with methanol in solutions consisting of, in addition to 1M methanol, 1M each carbonate and bicarbonate or dibasic and monobasic phosphate salts. These electrolytes had measured pH values of 10.7 and 6.6 respectively at 25°C, although the tests themselves were run at 60°C. However, only a small pH shift occurs in this temperature interval. The catalysts were reduced from their salt solutions by potassium borohydride and pressed into platinum gauze electrodes. They included the P-type catalyst, platinum, platinum with molybdenum or ruthenium, several types of nickel, nickel with rhenium, and cobalt with molybdenum or rhenium. Complete performance details are found in Appendix C-1.

The catalysts could be divided into two groups. The P-type, platinum, and platinum-ruthenium samples were active while the remainder had poor to negligible activity. Within the first group, the same relative activities were obtained in both electrolytes, although overall performances were better in the carbonate-bicarbonate system. Thus, as shown in Figures C-1 and C-2, the P-type catalyst was most active, being polarized 0.32 and 0.35 volts at 100 ma/cm^2 in carbonate-bicarbonate and phosphate buffers respectively. The platinum-ruthenium and platinum catalysts were less active, with platinum having polarizations of 0.53 and 0.55 volts in the two solutions. Platinum-ruthenium activity was intermediate to the other two. Carbon dioxide evolution was readily observed in all these tests with the exception of the P-type electrode in the carbonate-bicarbonate electrolyte. This system did not produce gas until a current density of almost 2000 ma/cm^2 was reached.

Of the nickel catalysts, only certain samples exhibited any activity, and then only in phosphate buffer. Thus, a number of types of nickel including a sintered powder electrode and commercial and sodium borohydride reduced powders were tested but only the sintered and borohydride reduced electrodes could support any current. They both evolved carbon dioxide, but also decayed rapidly under load. In both of these electrolytes nickel dissolution was detected visually and with dimethylglyoxime.

Figure C-1

Methanol Performance in Phosphate Buffer

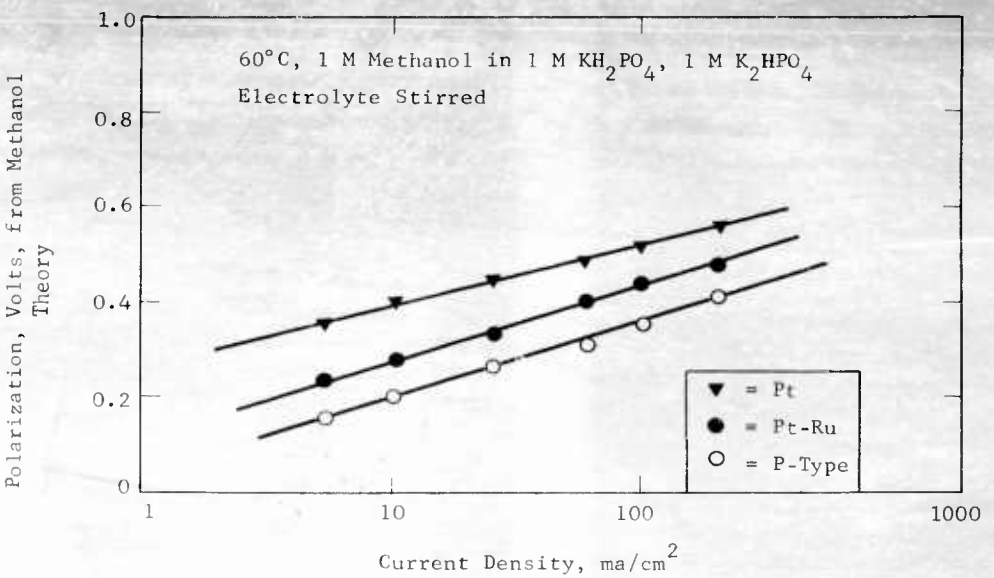

Figure C-2

Methanol Performance in Carbonate Buffer

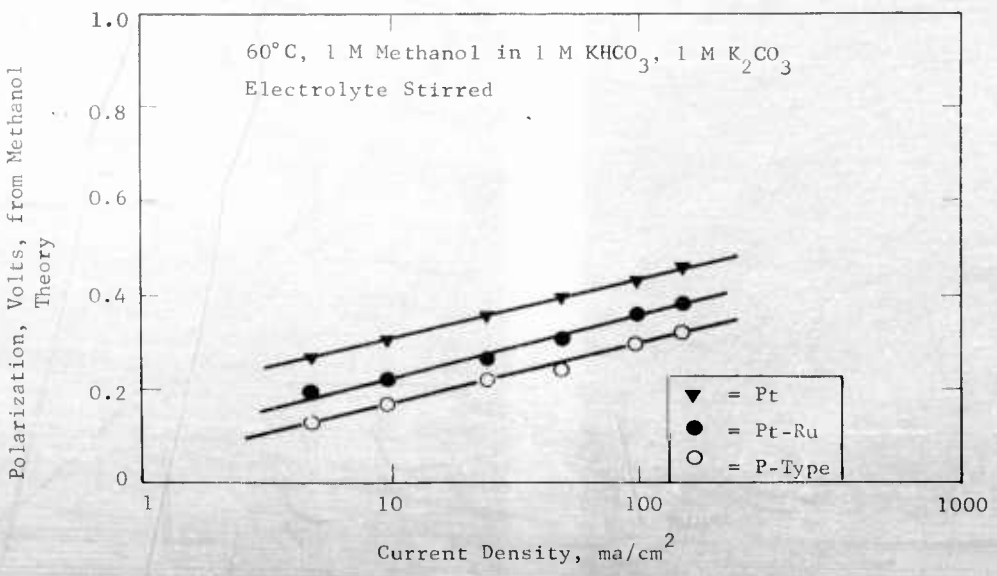

The remaining catalysts were all inactive with the exception of platinum-molybdenum. This catalyst, prepared in the presence of barium ions which could possibly stabilize the molybdenum, was polarized only 0.15 volts in phosphate buffer at 2 ma/cm^2. However, at higher current densities it deactivated irreversibly to the performance of plain platinum. A similar catalyst was checked in 3.7M sulfuric acid and behaved in the same manner. It appears then that operation in buffer or with added barium does not benefit the platinum-molybdenum catalyst.

It has been demonstrated that buffer electrolytes are suitable for use at methanol electrodes. They allow high performance levels to be reached with present active catalysts and, in most cases, lead to the production of carbon dioxide. Thus, an alternative to strong acid or base electrolytes may be possible, permitting the use of less expensive catalysts and other fuel cell components.

Part b - Concentration and Stirring Effects at the Methanol Electrode

In the previous section the performances of methanol electrodes were described in stirred solutions. Stirring was used to suppress ionic concentration polarization which can arise in buffer electrolytes and mask the true catalytic activity. Further studies of concentration polarization were carried out in unstirred solutions and at higher concentrations to determine if the high performance observed on certain catalysts could be supported by buffer electrolytes unaided by stirring.

Tests on platinum electrodes in 1 M each potassium mono-dibasic phosphate and in 2 M each rubidium mono-dibasic phosphate* solutions at 60°C showed that adequate performance is maintained even in the least favorable case. Thus, the lowest concentration solution, unstirred, had only a 50 mv debit at 100 ma/cm^2 compared to the stirred activity reported in Part a. Table C-1 shows this as well as results in the more concentrated solution, where the effect of stirring was much less, amounting to only 15 mv at 100 ma/cm^2.

Table C-1

Effect of Stirring and Buffer Concentration on Anode Performance

Current Density, ma/cm^2	Improvement in Methanol Performance, Volts, Effected by Stirring	
	Electrolyte	
	1M KH_2PO_4 1M K_2HPO_4	2M RbH_2PO_4 2M Rb_2HPO_4
25	0.020	0.010
50	0.040	0.010
100	0.050	0.015
150	0.050	0.015

* The rubidium salts were used because of their greater solubility.

The performance in the more concentrated solution, unstirred, was similar to the more dilute electrolyte with stirring. These results show that methanol electrodes can operate in buffer electrolytes at high performance levels without the need for stirring or other techniques for minimizing ionic concentration polarization.

Part c - Effect of Structure on Cathode Performance

The feasibility of buffer electrolytes has been shown at the methanol electrode. Since this anode utilizes a relatively non-porous structure, ionic concentration polarization is not a severe problem. However, in the case of gaseous reactants, where an interface must be maintained, considerable concentration polarization might occur within the porous electrode. To study this effect, a number of cathode structures were tested with air and oxygen in 1M each carbonate-bicarbonate or mono-dibasic phosphate buffers at 60°C. Full details are found in Appendix C-2.

The cathodes contained, in all cases, an American Cyanamid Type AA-1 electrode. Since this structure could not by itself hold an interface, it was clad with a variety of interface maintainers to form the total electrode. These were a Nalfilm D-30 membrane, a Gelman SA membrane, a Dacron felt pad, and simply a second AA-1 electrode. Tests were made with oxygen on the first three structures. As shown in Figures C-3 and C-4, the most active cathode was the one backed by the Dacron felt.

Figure C-3

Effect of Structure on Oxygen Performance in Phosphate Buffer

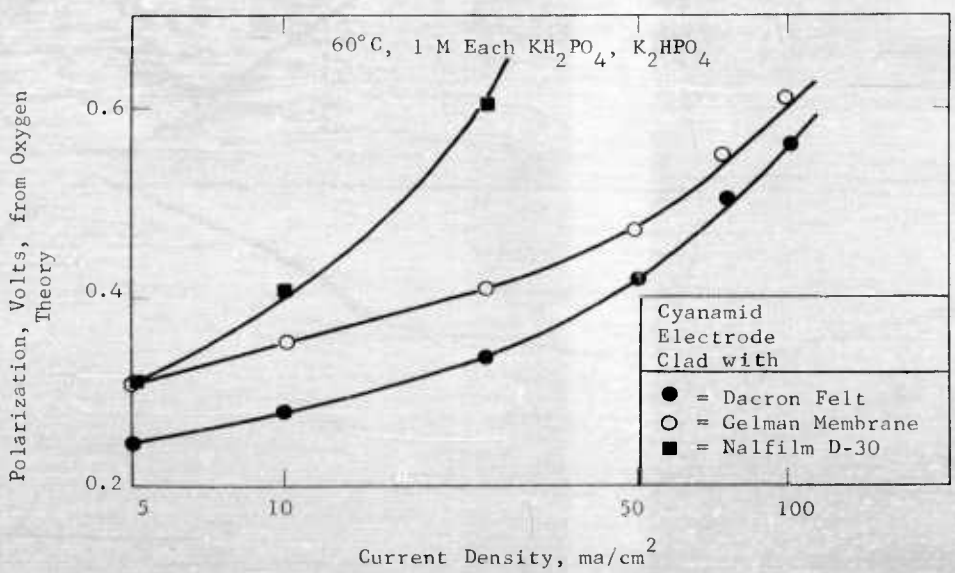

It was polarized 0.42 volts from the theoretical oxygen potential at 50 ma/cm^2. In comparison, the Nalfilm D-30 backed structure had a limiting current of less than 50 ma/cm^2 and was already polarized 0.60 volts at 25 ma/cm^2. In the two cases tested in both electrolytes, almost similar results were obtained. The order of reactivity of these electrodes was the same as the amount of bulk flow permitted by each. Thus, the Nalfilm D-30 clad structure allowed no bulk flow through it, while the Dacron felt electrode was relatively open to electrolyte flow.

Figure C-4

Effect of Structure on Oxygen Performance in Carbonate Buffer

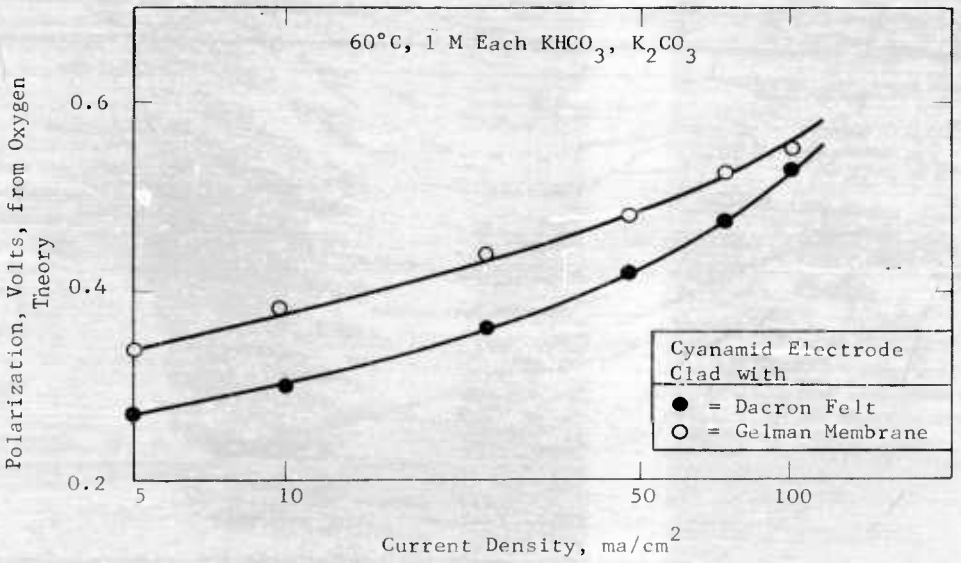

These results illustrate the importance of ionic concentration polarization in the performance of these porous structures. This is further exemplified by the fact that all three electrodes had essentially similar activity in 3.7M sulfuric acid, where concentration polarization is not a problem. Another experiment, designed to measure the concentration polarization effect directly, consisted of using hydrogen as reactant. Since this fuel has practically no activation polarization, only the ionic concentration polarization will be measured. As shown in Figure C-5, the Gelman clad electrode is considerably less polarized than the Nalfilm clad electrode. In fact, the difference in concentration polarization is approximately equal to the actual performance differences with oxygen.

Figure C-5

Hydrogen Performance in Buffer Electrolyte

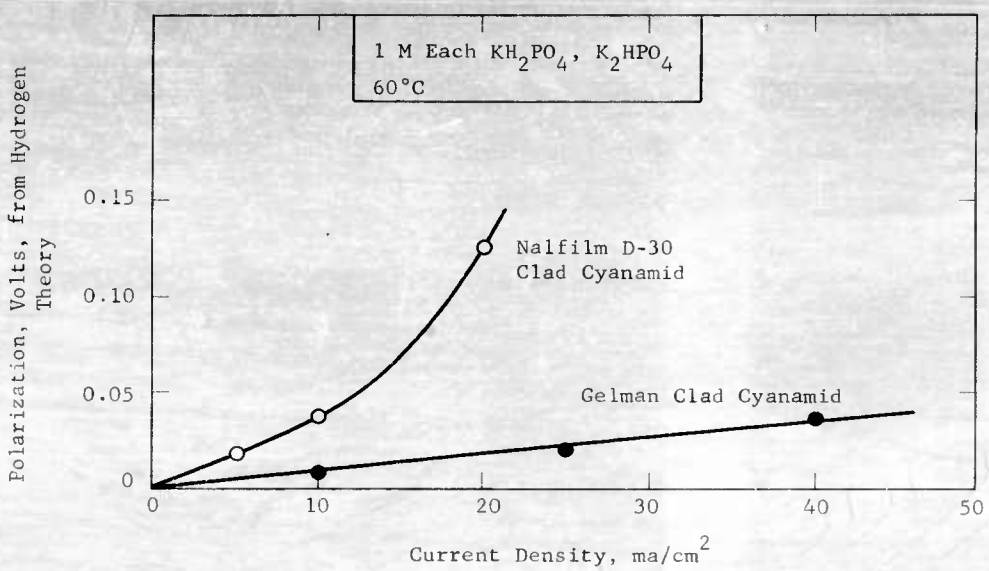

A final aspect investigated was the substitution of air for oxygen. As shown in Figure C-6, a performance loss of 40 to about 200 mv occurred with a Gelman clad electrode over the current density range of 10 to 50 ma/cm^2. In addition, the cathode had a limiting current of less than 100 ma/cm^2 with air. However, a cathode consisting of two Type AA-1 electrodes performed as well on air as the Gelman clad electrode with oxygen, although it allowed much less electrolyte bulk flow. These results indicate that oxygen or air cathodes can be operated at satisfactory performance levels in buffer electrolytes provided suitable structures are used which minimize ionic concentration polarization.

Figure C-6

Comparative Activity of Oxygen and Air

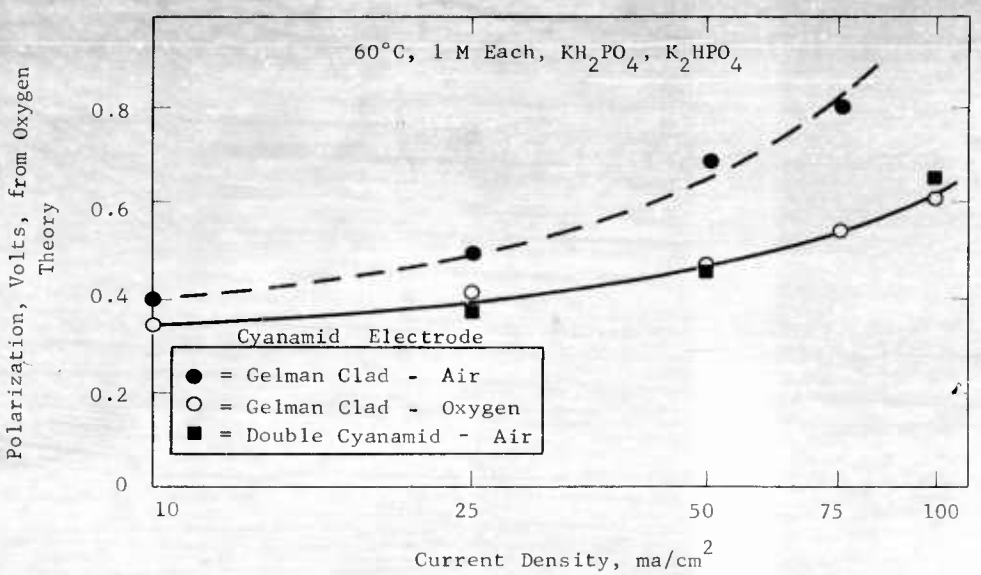

Part d - Effect on Cathode Performance of Buffer Concentration and Ratio

With the very important role of ionic concentration polarization established, the effects of higher buffer concentration and also of altering the buffer ratio in the direction of the more acidic compcnent were investigated. The performance of a Gelman clad electrode in 1 M each potassium mono-dibasic phosphate with oxygen was compared with its activity in 1.5 M mono- and 0.5 M dibasic potassium phosphate, and 2 M each rubidium mono-dibasic phosphate at 60°C.

The performances in these solutions were essentially similar at current densities up to about 50 ma/cm^2. At higher levels, where concentration polarization is more important, the use of 1.5 M mono- and 0.5 M dibasic phosphate and of 2 M each mono-dibasic phosphate buffers benefited performance. Thus, as shown in Table C-2, these electrolytes were each polarized 50 mv less than in the 1 M each system at 100 ma/cm^2.

Table C-2

Effect of Buffer Composition on Performance

Current Density, ma/cm^2	Polarization, Volts, from Oxygen Theory		
	Electrolyte		
	1M KH_2PO_4 1M K_2HPO_4	1.5M KH_2PO_4 0.5M K_2HPO_4	2M RbH_2PO_4 2M Rb_2HPO_4
10	0.35	0.35	0.34
25	0.41	0.40	0.38
50	0.47	0.47	0.46
75	0.55	0.51	0.52
100	0.61	0.56	0.56
150	--	0.68	0.66
200	--	0.78	0.72

In addition, the limiting current was extended beyond 100 ma/cm^2. The methanol anode was also tested in the 1.5/0.5 buffer and found to suffer a 25 mv loss at 100 ma/cm^2, not enough, however, to offset the cathode gain. Thus, further benefits in cathode performance in buffer electrolytes, over and above structure improvements, should be obtainable by proper adjustment of solution composition.

Part e - Total Cell Performance

The results obtained with anode and cathode half cells in buffer electrolytes suggested that complete cells might be feasible. Studies were therefore begun aimed at defining more fully the possibilities and problems of a total cell. A standard 4" x 4" Teflon cell (2) was assembled with a P-type anode and a Gelman SA membrane backed Type AA-1 electrode as oxygen cathode. The electrolyte was 1M each in potassium mono-and dibasic phosphate. Complete performance data are shown in Appendices C-3 to C-8.

Operated in the simplest manner, with methanol-containing electrolyte circulating between the electrodes, only negligible power could be drawn from the cell. Thus, both at ambient temperature and at 60°C, a maximum of 0.75 mwatts/cm^2 was obtained at 5 ma/cm^2 with 0.5M methanol. Using 0.05M fuel, the performance improved to 1.4 mwatts/cm^2, indicating fuel incompatibility at the cathode to be the cause of the low activity. Accordingly, the cell was modified to allow a dual flow of electrolyte. One path, directly between the two electrodes, contained electrolyte free of fuel. The second stream was directed to the far side of the anode and contained the fuel. In this way peak power was raised to 2.8 mwatts/cm^2 at 12 ma/cm^2, using 0.125M methanol at 60°C. However, the largest improvement resulted from the addition of a Gelman SA membrane between the two electrodes to further retard electrolyte mixing. The cell configuration following this change is shown in Figure C-7.

Figure C-7

Buffer Total Cell with Additional Membrane Separator

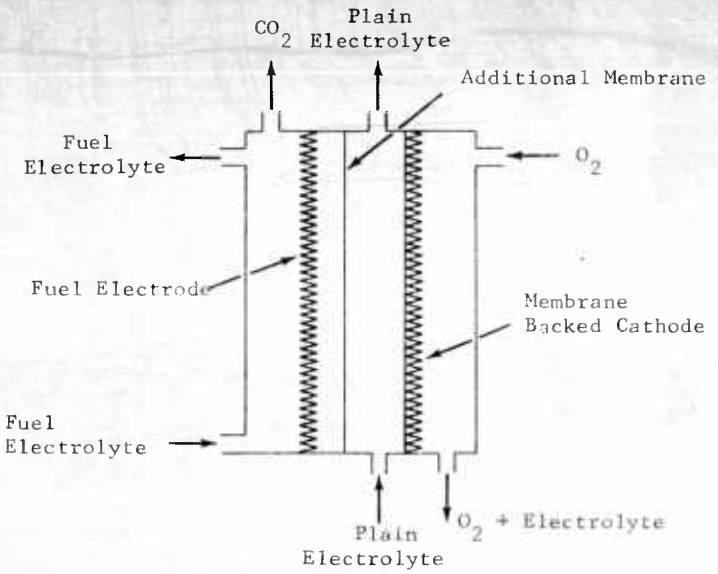

With this new arrangement higher methanol concentrations could be tolerated. In addition, pre-heating the electrolyte was also of benefit. The power output was thus raised to over 11 mwatts/cm^2 at 60°C and 2.0M methanol. Table C-3 shows these results obtained with oxygen.

Table C-3

Effect of Operating Variables on Total Cell Power Output			
Fuel Conc, M	0.5	1.5	2.0
Electrolyte Preheating	no	yes	yes
Cell Temp, °C	60	60	76
Peak Power Output, mwatts/cm^2	3.9	11.4	14.2

A run was also made at 76°C with air as the oxidant. The performance of this cell, as well as one employing the double Type AA-1 cathode described in Part c is shown in Figure C-8, where it is seen that peak power outputs of 9 and 12.6 mwatts/cm^2 were obtained respectively.

Figure C-8

Buffer Cell Performance with Double Type AA-1 Air Electrode

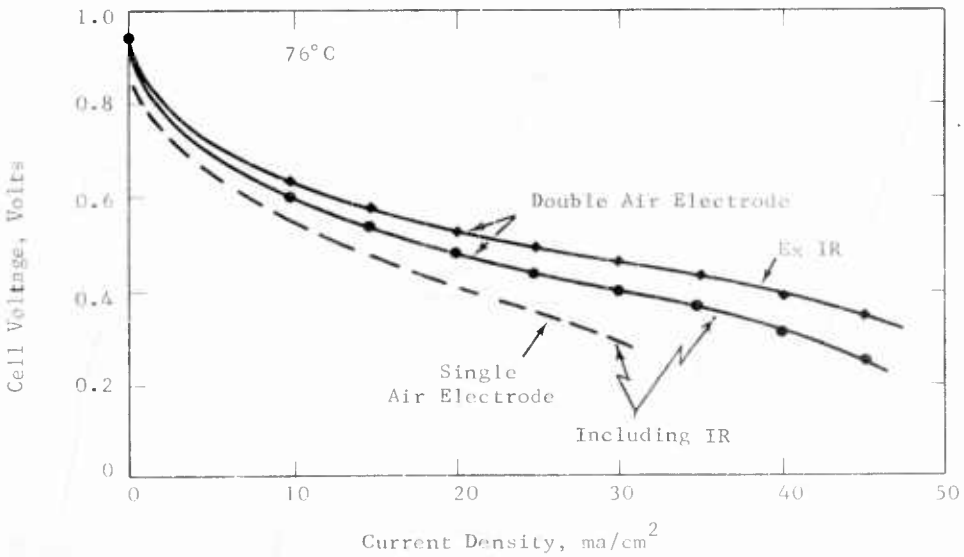

The feasibility of buffer electrolyte fuel cells has been demonstrated by these experiments. However, they have utilized rapid, once-through electrolyte flows to minimize methanol incompatibility at the cathodes. Incompatibility is a more severe problem in buffer electrolytes because of the necessity for bulk flow to reduce ionic concentration polarization. More practical means of overcoming the effect of methanol, either by development of new catalysts or structures, will be necessary before the advantages inherent in the buffer system can be realized.

Phase 2 - Hydrocarbon Redox Systems

The direct electrochemical oxidation of hydrocarbon fuels is difficult to achieve efficiently. The inertness of these compounds, coupled with their insolubility, causes problems which have thus far limited performance. One approach to overcoming these disadvantages is the use of an indirect "redox cycle" where the fuel is chemically reacted. The resulting reduced form of an oxidizing agent is then electrochemically reoxidized at the fuel electrode to complete the cycle. Studies were carried out to test the chemical and electrochemical reactivity of a number of such systems.

Part a - Chemical Reactivity

Several possible redox compounds were tested for their chemical reactivity towards decane and methanol by refluxing their slurries in these fuels. Sodium molybdate, molybdic acid, cupric oxide, ammonium metatungstate, and potassium perrhenate showed no activity under these conditions. The only compound reduced was rhenium heptoxide, which was converted to the trioxide in both decane and methanol. The reaction with decane resulted in the formation of carbon dioxide, while in the case of methanol no carbon dioxide was found. Rhenium heptoxide was also dissolved in 9M sulfuric acid and tested with decane at 106°C. In this system reduction of the oxide occurred but no carbon dioxide was formed.

Part b - Carbon Dioxide Formation

Having established the reduction by decane of rhenium heptoxide and the accompanying oxidation of decane to carbon dioxide, a quantitative study was made of the completeness of reaction. As part of this work the effect of various catalysts was also looked at. In all cases, a slurry of rhenium heptoxide with, in some cases, added catalyst, was refluxed in decane at 172°C. Nitrogen was used to blanket the reaction and also to carry the product gas through Drierite and Ascarite tubes.

It was found, as shown in Table C-4, that simply boiling a slurry of rhenium heptoxide in decane gave 30-40% of the carbon dioxide expected from the following reaction:

$$31\ Re_2O_7 + C_{10}H_{22} \longrightarrow 62\ ReO_3 + 10\ CO_2 + 11\ H_2O.$$

Adding the heptoxide directly to boiling decane rather than heating the mixture together from room temperature as normally done resulted in an 80% carbon dioxide yield. Platinum and, to a lesser extent, gold, catalyzed the reduction. At its highest ratio, platinum caused, in one case, partial conversion to rhenium dioxide and an increase in the carbon dioxide yield to over 200% of that expected from the above reaction. However, in a repeat test only 80% yield was obtained. These results show that decane oxidation does not go only to carbon dioxide, but is probably accompanied by side reactions leading to partially oxidized products. No attempt has been made as yet to identify these products. However, the chemical half of this redox cycle has been demonstrated to be possible.

Table C-4

Rhenium Heptoxide Reaction with Decane

Catalyst	Ratio, Catalyst/ Rhenium Heptoxide	Carbon Dioxide Yield, wt %
None	--	30-40
Pt	0.005	30-40
	0.025	63
	0.050	80-200
Au	0.005	30-40
	0.050	60
Ni	0.005	30-40
	2.50	30-40
W	0.005	30-40
	0.05	30-40
None	--	80*

* Rhenium heptoxide added directly to boiling decane.

Part c - Electrochemical Reoxidation of Reduced Rhenium Oxide

To complete the redox cycle between rhenium heptoxide and decane, it is necessary to oxidize the reduced product at suitable potentials. Estimates of the rate of the chemical reduction indicate that a reaction rate equivalent to at least 50 ma/cm^2 was attained. Therefore, the chemical half of the redox cycle should not be the limiting part. Tests of the electrochemical activity of rhenium trioxide were carried out in 3.7M sulfuric acid. It was found that although open circuit potentials of 0.3 to 0.4 volts from the theoretical decane potential were achieved, no current could be drawn from the rhenium trioxide, either by itself or mixed with powdered platinum or gold to enhance conductivity. Apparently, there is still insufficient conductivity in the system, even with added metal powder, to allow reoxidation of the oxide. In an effort to avoid this problem, attempts were made to dissolve the rhenium trioxide to give the rhenate ion, which should be easily oxidizable. However, the oxide was insoluble in 3.7M sulfuric acid and 3 and 9M sodium hydroxide.

Phase 3 - Dynamic Electrode Studies

A major problem in achieving efficient hydrocarbon reaction is establishing and maintaining a suitable three phase interface. One approach to this difficulty has been the use of a "flowing fuel system," in which a liquid hydrocarbon is bubbled from a sprayer into the electrolyte. In rising through the aqueous phase, the fuel contacts and passes through and around an electrode maintained in the electrolyte. By this means, problems associated with static systems, such as electrode flooding, are minimized. Using the flowing fuel system, studies have been carried out on the effects of fuel and electrode heating, open circuit pulsing, and of several electrode structures.

Part a - Heating Experiments

The effects of preheating decane prior to its contacting the fuel electrode and of electrically heating the anode itself were studied in 3.7M sulfuric acid at 105°C. The electrodes were platinum gauzes into which were pressed 2:1 weight ratios of commercial platinum black and teflon powder.

In the first experiment, decane was preheated to 160°C before passage through the glass frit sprayer into the electrolyte. Although much finer bubbles were produced, no improvement in performance was obtained and it was necessary to keep the electrolyte boiling to maintain maximum activity. In addition, some decane decomposition occurred even though the system was blanketed with nitrogen.

A preliminary test was also made in which an AC current was used to heat the fuel electrode. No changes in performance were measured as the impressed AC potential was increased until 80 volts was reached. At this level a sharp and partially irreversible polarization increase occurred. The cause of this effect is not clear and additional work will be necessary to clarify it.

Part b - Open Circuit Pulsing

Various types of pulsing have in the past proven beneficial to fuel electrode performance. Therefore, a test was made of the effect of periodically open circuiting the electrode. The experiment was carried out in 3.7M sulfuric acid at 105°C using the platinum-Teflon electrode described in Part a. The anode was alternately polarized at 20 ma/cm^2 and open circuited, allowing equal time to each period until the polarization reached 0.45 volts from the theoretical decane potential. The periods were varied in length from 5 seconds to 2 minutes. As shown in Table C-5, the on-current time necessary to reach 0.45 volts was essentially independent of period length and about twice that needed during continuous current flow. However, since the time average current was only half of that during continuous operation, no net gain in output was achieved. To check on the benefits of longer open circuit periods, the electrode was also run at conditions of one minute on and two minutes off. As before, no net improvement occurred. From these results it appears that open circuit pulsing is of no benefit in improving fuel electrode performance with decane fuel.

Table C-5

Effect of Period Length on Performance

Period Length, Sec	5	30	60	120	∞*	60 on 120 off
Time to Reach 0.45 volts, Sec	420	360	330	360	180	390

* No open circuit pulsing.

Part c - Other Electrode Structures

A sintered platinum-Teflon electrode prepared using emulsified Teflon and a platinized gauze were tested with decane in the flowing fuel system using 3.7 M sulfuric acid at 105°C. The open circuit polarization of the former was initially 0.6 volts from the theoretical decane potential, normally an unstable region for no-load conditions. Upon interrupting the fuel flow, however, the polarization fell to 0.1 volts. The electrode, with fuel flow restored, could maintain 1 ma/cm^2 at only 0.16 volts polarization but failed suddenly at 2 ma/cm^2 after several minutes at 0.3 volts. It appears that this structure was too impermeable for successful operation in this system. The platinized gauze gave no activity at all, neither at open circuit nor under load. Repeated attempts to activate the catalyst with anodic and cathodic pulses were unsuccessful.

Phase 4 - Slurry Catalyst Systems

The conventional fuel cell electrode is a structure which combines the functions of catalyst and current collector. It is possible that such a dual role does not allow maximum efficiency for each function and that overall performance might be improved by separating these tasks. One method of accomplishing this is to utilize the catalyst in the form of a slurry impinging upon a current collector (7,8). Studies were therefore begun aimed at determining the capabilities of slurried catalysts using a rotating electrode as stirrer and current collector. The present work utilized supported and unsupported platinum, as well as other catalysts with methanol and decane. The electrolyte was generally sulfuric acid, although phosphate buffer was briefly examined.

Part a - Effect of Operating Conditions on Slurry Cell Performance

Initial investigations with the slurry catalyst system looked at the effect of physical factors on performance. Thus, cell shape, size, and electrode rotation speed were examined in 1M methanol and 3.7M sulfuric acid at 60°C. The catalyst was platinum black, at 10 to 20 mg/ml concentration. The cell shape was found to be the most important variable. As shown in Table C-6, H-shaped cells were least efficient, due to poor stirring of the catalyst, which tended to collect in the connecting side-arm. Cylindrical round bottom cells showed great improvement, with the addition of vertical wall ribs leading to optimum performance. Incorporating all these elements gave an activity level of only 0.36 volts polarization at 10 ma/cm^2, based upon the collector electrode total surface area. Appendix C-9 describes the final cell in detail. The effect of rotation speed was constant above about 1000 rpm, as was cell volume over the range of 50 to 100 ml, as shown in Figure C-9

Table C-6

Effect of Cell Configuration on Performance

Cell	Electrode	Polarization from Methanol Theory at 10 ma/cm^2
H-shaped	Foil	0.74
H-shaped	Perforated Foil	0.70
Cylindrical	"	0.44
Cylindrical-ribbed	"	0.36

Figure C-9

Influence of Cell Volume on Performance

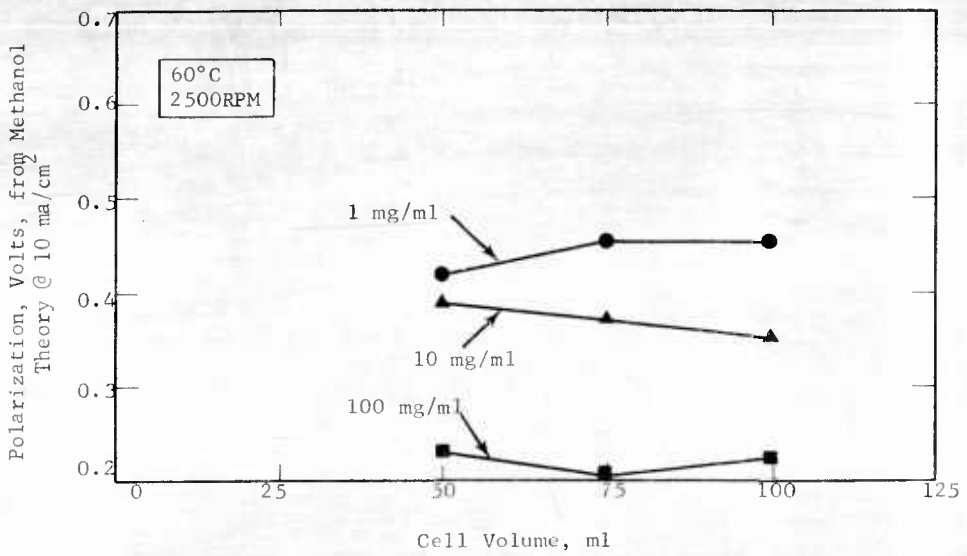

Part b - Effect of Catalyst Concentration on Slurry Cell Performance

Having established suitable operating conditions for the slurry system, the effect of catalyst concentration was studied using platinum black. It was found, as shown in Table C-7, that performance improved with catalyst concentration. Thus, polarization decreased by 150 mv between 1 and 100 mg/ml of catalyst at 50 ma/cm2 in the 75 ml cell. Complete details of these runs are given in Appendix C-10.

Table C-7

Influence of Platinum Concentration on Methanol Performance

Cell Volume 75 ml

Catalyst Conc, mg/ml	Polarization at Indicated ma/cm^2			
	1	10	50	100
1	0.30	0.45	0.57	0.60
10	0.18	0.37	0.48	0.54
100	--	0.20	0.32	0.38

These results indicate that performance levels comparable or superior to static systems can be achieved. However, considerably larger amounts of catalyst are required. In addition some uncertainty exists as to the exact significance of the polarization measurements since preliminary experiments have suggested, particularly at higher catalyst concentrations, that the entire slurry possesses electronic conductivity. This would allow current flow, and hence ohmic polarization, through the whole system. In turn the observed polarization would then be a function of the reference electrode placement. This effect, as well as methods for reducing the total amount of catalyst, must be clarified before firm conclusions concerning the slurry system can be arrived at. In addition, engineering evaluations of the power requirements of such systems are also required.

Part c - Performance of Decane in the Slurry Catalyst System

The activity of decane with slurried platinum catalyst was investigated in 3.7M sulfuric acid at 100°C using the same equipment as described in Part a. Conditions were optimized at 3500 rpm, with 33 and 50 vol % decane. By positioning the rotating anode at the decane-sulfuric acid interface, efficient emulsification was achieved. It was found necessary to wet part of the catalyst with each phase prior to operation. If this was not done the catalyst tended to remain wetted with whichever liquid it first contacted, resulting in poor and unstable performance.

The activity of decane in this system was higher than with static electrodes. For example, as shown in Table C-8, polarizations of 0.15, 0.21, and 0.57 volts polarization from the theoretical decane potential were measured at 1, 10, and 100 ma/cm^2 respectively with a catalyst concentration of 50 mg/ml. Complete details are given in Appendix C-10.

Table C-8

Decane Performance in Slurry Catalyst System
50 vol % Decane - 50 vol % Sulfuric Acid

Catalyst Conc, mg/ml	Polarization at Indicated ma/cm^2		
	1	10	100
1	0.33	--	--
10	--	0.39	--
50	0.15	0.21	0.57
100	0.12	0.15	0.41
270	--	--	0.22

Figure C-10 illustrates that these performances were linear with catalyst concentration over the entire range studied. It was found that these activities were stable with time, at least for periods of up to 4 hours, at which time the experiments were voluntarily halted.

In other studies carried out with this system, it was found that boiling the emulsion caused a severe but reversible loss of performance. The addition of a surfactant, tridecylpolyethoxy alcohol, caused a very slight improvement in activity at 100°C. Pulsing the electrode to a higher current density and then returning it to the original value produced a large but temporary improvement. Thus, at 100 ma/cm^2 and 0.4 volts polarization, a brief period at 200 ma/cm^2 was followed by a new polarization at 100 ma/cm^2 of only 0.26 volts. This decayed back to 0.4 volts over a 2 hour interval.

Figure C-10

Dependence of Decane Performance
on Catalyst Concentration

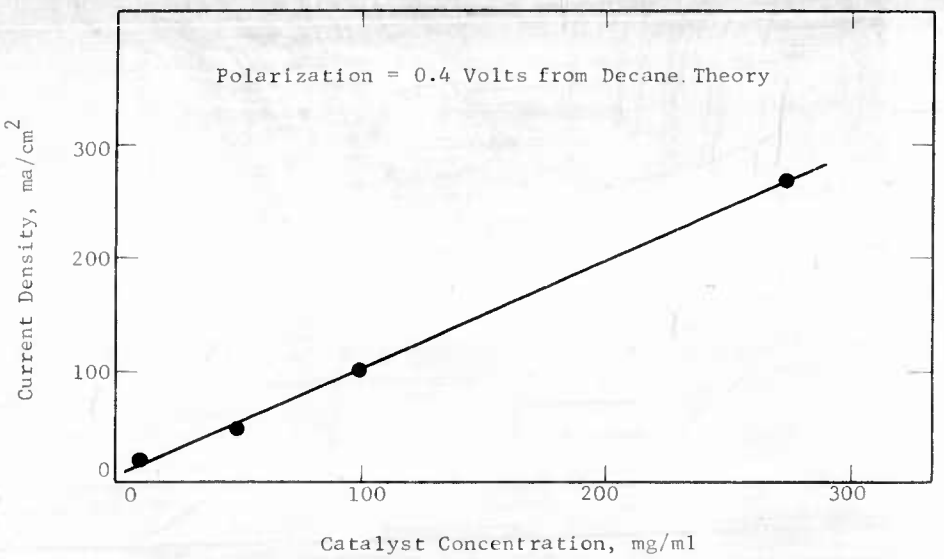

In common with the methanol system, decane performance appears superior to the static system. However, the complications discussed in connection with the former fuel which need further study, are also present with decane. In addition, the wetting effects discussed above must also be looked at more carefully.

Part d - Performance of Other Slurry Catalysts

A number of catalysts other than platinum black were investigated in the slurry cell system. Thus, the P-type catalyst was tested with methanol and the ruthenium-modified P-type with decane. Neither catalyst was as active as platinum, with the P-type showing a polarization of 0.39 and 0.61 volts polarization at 10 and 100 ma/cm^2 and the ruthenium-modified P-type having a limiting current of only 10 ma/cm^2. Both catalysts were tested at a concentration of about 10 mg/ml. Several supported catalysts, prepared by radical anion reduction (9) of platinum on Teflon or by hydrogen or sodium borohydride reduction on sand were also tried with decane. It was hoped that these supported catalysts, because of their lower density, would be slurried more easily than pure platinum. In addition they should afford more efficient catalyst utilization. However, no activity was obtained with these materials. Further experimental data is given in Appendix C-10.

Part e - Slurry Catalyst System with Buffer Electrolyte

Several runs were carried out in which the sulfuric acid electrolyte was replaced by 1M each potassium mono-dibasic phosphate buffer. The catalyst was platinum black, tested with methanol at 60°C and 100 mg/ml concentration, and with decane at 95°C and 50 mg/ml concentration. Complete details are shown in Appendix C-10. In methanol, performances equivalent to those in acid were obtained at the lower current densities. Thus at 10 and 50 ma/cm^2 respectively, the polarizations were 0.22 and 0.38 volts. However, beyond 50 ma/cm^2 the performance became unstable. It was found that the activity did not reach a plateau with stirring rate as in acid, but exhibited a maximum at about 1500 rpm. The same optimum was observed with decane, but activity in this system was comparable to acid only up to about 10 ma/cm^2, the polarization being 0.21 volts. Above this current density an irreversible decay occurred and the catalyst became completely decane wetted. Upon cathodization, the catalyst became completely electrolyte wetted and lost all activity. These results illustrate the importance of wetting effects, already seen with the acid electrolyte, to the performance of the slurry system. Further work will be needed to clarify these observations.

Phase 5 - New Materials

One method of minimizing problems of corrosion in fuel cells has already been discussed, the use of buffer electrolytes. There is also an alternative approach involving the search for materials able to withstand corrosive electrolytes. Previous work has been carried out in highly concentrated phosphoric acid at elevated temperatures (10). However, since the bulk of our work involves 3.7 M sulfuric acid at temperatures of 100°C or less, a program seeking new materials stable under these conditions has been instituted.

Part a - Cyclic Voltammetry of Passivating Metals

A variety of zirconium and zirconium alloy samples, two titanium-palladium alloys, and powdered boron carbide and boron nitride were tested by cyclic voltammetry in 3.7 M sulfuric acid at 100°C. A sweep rate of two minutes was used to cover the range of 0 to 1.2 volts from the standard hydrogen potential. It was found that a nuclear grade hafnium-free zirconium sample had the lowest anodic current, about 2 microamps/cm^2 at 0.8 volts. The others, including two regular grades of zirconium containing 0.05 and 0.2 wt % respectively of chromium and iron, zirconium -5 wt % copper, and zirconium -0.2 wt % Pd, as well as the two titanium -0.15 wt % palladium samples, all had currents about ten times higher. In no case was catalytic activity observed upon addition of methanol.

The nuclear grade zirconium was further tested at 0.6 volts for a period of one week. A steady state current of less than 1 microamp/cm^2 was obtained, but the exact current could not be determined with the equipment used. Only about 1 mg of zirconium was found in the electrolyte, equivalent to a loss of 0.005 wt % from the 20 gm sample.

The powdered boron nitride and boron carbide samples were mixed with Teflon powder and pressed into tantalum screens for testing. Preliminary tests indicate that both may undergo alternate oxidation and reduction of their surfaces, rather than straight corrosion. This will be investigated further to determine if they indeed do not corrode. Neither showed any activity towards methanol.

Phase 6 - Phthalocyanine-Based Catalysts

The development of non-noble metal catalysts would offer a decided economic advantage for fuel cell use. As part of a program aimed towards this end, a number of base metal phthalocyanine compounds were tested for catalytic activity with hydrocarbons and oxygen. In contrast with other work conducted with basic electrolytes (11), these tests were conducted in 3.7 M sulfuric acid in the hope that these compounds would stabilize the metal components in acid electrolyte without interfering with their catalytic properties. Several were also tested for any possible synergistic effects when mixed with platinum.

Part a - Electrode Preparation

Electrodes containing phthalocyanine catalysts were made by mixing carbon powder with a phthalocyanine solution in cold concentrated sulfuric acid. Upon dilution the phthalocyanines precipitated in a very finely divided state. The resulting mixture was collected by settling and washed thoroughly. Teflon powder was then added and the mixture pressed into a platinum gauze at 10,000 psi. Finally the electrode was sintered at 340°C. When it was desired to include platinum as a co-catalyst, platinized carbon was either added prior to pressing, or else the phthalocyanine-impregnated carbon was re-impregnated directly with chloroplatinic acid and reduced.

The phthalocyanine compounds themselves were synthesized by standard techniques (12), and purified by washing in dilute alkali and acid, followed by prolonged Soxhlet extraction with methanol. Chemical analyses for metal contents gave results deviating by no more than 0.1% from theory. The completed electrodes were tested in cells described in Appendix A-2. All gases fed to the electrodes were preheated to the cell temperature.

Part b - Metal Phthalocyanines as Oxygen Catalysts

The phthalocyanines of iron, cobalt, nickel, manganese, zinc, copper, and vanadium were tested for oxygen catalyst activity. Initial studies were carried out in 3.7 M sulfuric acid at 100°C, but parallel work with ethane showed no activity for these catalysts with hydrocarbons at these conditions. All later work was therefore performed in 12.1 M phosphoric acid (75 wt %) at 130°C. Complete details of these studies are shown in Appendix C-11.

The only phthalocyanine to show activity greater than a carbon blank was that of iron. As shown in Table C-9, the initial activity of this compound in sulfuric acid was 0.1 volt better at 10 ma/cm^2 than the carbon blank. In phosphoric acid, a higher phthalocyanine content was necessary, 10 wt % giving an 0.08 volt improvement over the blank at 10 ma/cm^2. For the same electrode tested in both electrolytes, performance deteriorated more rapidly with current density in phosphoric acid, due possibly to a greater tendency to flood the carbon electrode.

Table C-9

Initial Oxygen Performance of Iron Phthalocyanine

Electrode	Electrolyte	Polarization from Oxygen Theory at Indicated ma/cm^2		
		1	10	20
Blank	3.7 M Sulfuric Acid	0.50	0.68	0.75
"	12.1 M Phosphoric Acid	0.49	0.68	0.79
Iron Phthalocyanine, 5 wt %	3.7 M Sulfuric Acid	0.47	0.58	0.63
"	12.1 M Phosphoric Acid	0.53	0.67	0.84
Iron Phthalocyanine, 10 wt %	12.1 M Phosphoric Acid	0.44	0.60	0.72

In all cases these initial activities decayed with time, approaching equilibrium values close to or poorer than the blanks.

The chemical stability of these compounds under cathodic conditions, indicated by lack of color formation in the electrolyte, appeared good in sulfuric acid at 100°C. In phosphoric acid however, some color developed, indicating chemical attack. Anodization under oxygen caused strong color formation and, with the exception of the vanadium compound, further loss of activity. This latter catalyst was slightly improved by brief anodization, but harmed by further treatment. In any event, it does not appear that any of these compounds show promise as cathode catalysts in acid electrolytes.

Part c - Metal Phthalocyanines as Hydrocarbon Catalysts

Most of the phthalocyanines described in Part b were also tested for their activity as anode catalysts, using ethylene or ethane in 12.1 M phosphoric acid at 130°C. Appendix C-12, Group A, describes preliminary screening aimed at determining their approximate activity levels while Group B shows more accurate measurements of the low current density performance of the carbon blank, and zinc and copper phthalocyanines. The copper complex was the only one able to sustain currents for extended periods of time. However, the performance was quite poor and required prolonged cathodization for activation. Runs with nitrogen showed that the activity was due to ethylene oxidation and not oxidation of adsorbed hydrogen or some other species. A comparison of copper phthalocyanine performance with that of the carbon blank using ethylene is given in Table C-10. It is apparent that these metal phthalocyanines are not very active catalysts for hydrocarbon oxidation.

Table C-10

Hydrocarbon Performance of Copper Phthalocyanine

Electrode	Polarization from Ethylene Theory at Indicated ma/cm^2		
	0.05	0.1	0.5
Blank	0.53	0.64	0.78
Copper Phthalocyanine, 10 wt %	0.33	0.42	0.69

Part d - Platinum-Metal Phthalocyanine Mixtures as Oxygen Catalysts

Several physical mixtures of platinized carbon and phthalocyanine-impregnated carbon, prepared as described in Part a, were tested for activity towards oxygen in 12.1 M phosphoric acid at 130°C. In addition, two carbon "blanks", containing only platinum, were also tested. In all cases a platinum concentration of 1.3 mg/cm^2 was used. The activities of these electrodes were found to vary in a complex manner with the way in which they were tested. Thus, the best sample, containing copper phthalocyanine, became progressively better with operation and finally reached a steady performance of 0.53 volts polarization at 100 ma/cm^2. On the other hand, blank "A", identically treated, showed initial improvement with cathodic operation but then decayed badly, especially at higher current densities. This was probably due to gradual flooding of the electrode. These results are shown in Table C-11.

Table C-11

Oxygen Performance of Metal Phthalocyanine-Platinum Mixtures

Electrode	Reading	Polarization from Oxygen Theory at Indicated ma/cm^2			
		1	10	20	100
Blank "A"	Initial	0.32	0.42	0.46	0.61
	Final	0.30	0.38	0.95	--
	Best	0.28	0.63	0.43	0.61
Platinum-Copper Phthalocyanine	Initial	0.53	0.86	1.18	--
	Final	0.27	0.38	0.42	0.56
	Best	0.26	0.37	0.42	0.53

Of the remaining electrodes tested, a blank prepared from carbon which was not treated with concentrated sulfuric acid did not lose activity with prolonged cathodic operation, but did under anodic conditions. Another copper phthalocyanine electrode, which had been tested first as an anode, tended to flood when run cathodically, although its initial performance was comparable to that shown in Table C-11. In addition, iron and vanadyl phthalocyanine electrodes were poorer than the copper samples, as was an electrode made by impregnating copper phthalocyanine-containing

carbon directly with platinum. Complete details of all runs are given in Appendix C-13. From these results, it is difficult to detect any catalytic synergistic effects. However, it does appear, at least in the case of the copper phthalocyanine, that the wetting characteristics of the electrode have been improved.

Part e - Platinum-Metal Phthalocyanine Mixtures as Hydrocarbon Catalysts

The electrodes tested as cathodes in Part d were then also tested as fuel electrodes in 12.1 M phosphoric acid at 130°C with ethylene. In addition, a fresh copper electrode was also checked. Blank "A", prepared from carbon treated with concentrated sulfuric acid, deteriorated with anodic operation, apparently due to flooding. Blank "B", made with untreated carbon, and the aged copper sample both showed stable performance, indicating that cathodic operation had induced stabilization. In contrast the fresh copper electrode actually improved with anodic polarization, but was still inferior to its cathodically aged twin at steady state. The iron sample was stable, but no better than the blanks, while the vanadyl electrode decayed badly with use. The only clear cut performance advantage over the blanks was shown by the copper phthalocyanine-containing electrodes, especially at higher current densities. As shown in Table C-12, the mixed samples could reach 100 ma/cm^2, although at high polarization levels. Complete performance details are given in Appendix C-14.

Table C-12

Hydrocarbon Performance of Metal Phthalocyanine-Platinum Mixtures

Electrode	Polarization from Ethylene Theory at Indicated ma/cm^2			
	1	10	50	100
Blank "B"	0.44	0.57	0.75	--
Copper, aged	0.40	0.55	0.72	0.85
Copper, fresh	0.44	0.62	0.76	0.82

Operation under more severe conditions, in 14.7 M phosphoric acid (85 wt %) at 160°C with ethylene and ethane also showed the copper samples to be more stable. Re-running as cathodes following this also confirmed this conclusion. A clue to the reason for these effects was given by some results with hydrogen at 130°C. The blank electrode "B", containing only platinum, failed at less than 20 ma/cm^2. However, the copper sample was still polarized only 0.09 volts at 100 ma/cm^2. Based on these results, no direct chemical synergism can be established, but an improvement in the wetting properties of the copper phthalocyanine-containing electrode does seem to occur.

4.4 Task D, Methanol Electrode

Work on the development of more active catalysts for the methanol anode has continued. Emphasis has been placed on new preparative procedures for two and three component catalyst systems based on ruthenium, with particular attention both to initial activity and to ability to withstand overpolarization, drying, and severe handling techniques. Other work in this area included attempts to improve the stability of P-type catalysts, the development of a technique to increase the specific surface area of present catalysts, the application of the radical anion technique to catalyst preparation, and an adsorption study with the Pt-Re_2O_7 system to further our understanding of its mechanism.

Phase 1 - Preparation and Performance of Platinum-Ruthenium Catalysts

It was previously reported that platinum-ruthenium catalysts were significantly better than platinum, although not as good as P-type catalysts(3). Problems also existed with the stability of the catalyst, although the addition of other components was reported to improve both the stability and the activity of the catalyst(4). A thorough study of the two component system was made, with the effort concentrated on composition and preparation techniques.

Part a - Performance of Pt-Ru Catalysts as a Function of Composition

A number of catalysts, containing various amounts of ruthenium, were prepared by sodium borohydride reduction. The catalysts were tested in 3.7 M H_2SO_4 containing 1 M methanol at 60°C. The results showed that the activity increased with increasing ruthenium content up to 33 atom %, and then remained essentially constant up to 70 atom %, at a value of about 0.34 volts polarization at 50 ma/cm^2. Tafel slopes of 0.06 volts per decade of current were routinely obtained on these catalysts, the same value usually obtained with platinum alone. These results are outlined in Figure D-1 and in Appendix D-1. Therefore, the platinum-ruthenium system produces a highly active catalyst for methanol oxidation, comparable at 50 ma/cm^2 to the P-type catalyst(4).

Figure D-1

Effect of Ruthenium Content on Methanol Performance

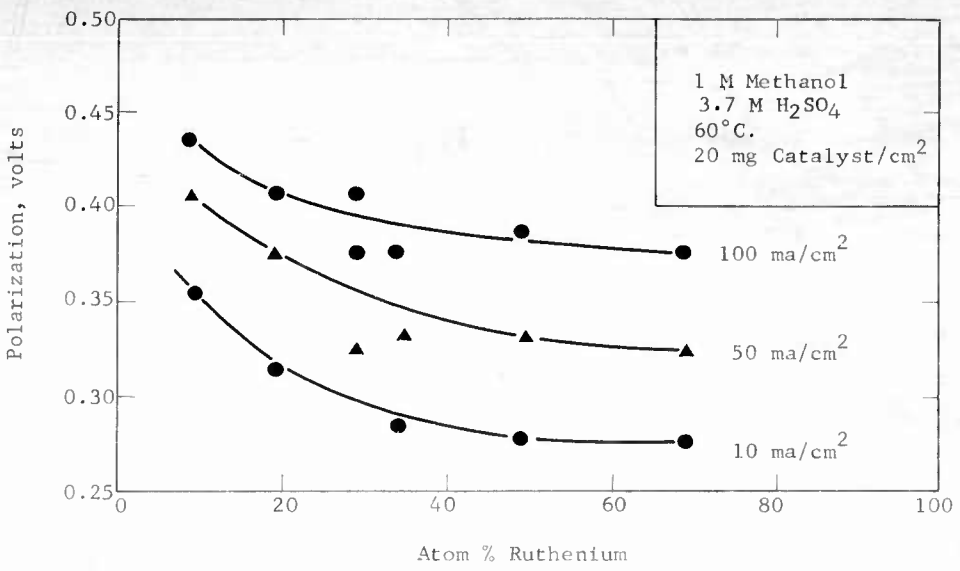

Analytical results indicated that the reduction technique used resulted in complete reduction of the metal salts, H_2PtCl_6 and $RuCl_3$, used in the preparation of the catalyst. The lack of color of the supernatant solution after the reduction step supported this idea. The analytical results are shown in Table D-1.

Table D-1

X-ray Fluorescence Analysis of Platinum-Ruthenium Catalysts

	Composition, Atom % Ruthenium				
Solution Before Reduction	10	20	33	50	70
Recovered Catalyst	6	16	32	53	71

Part b - Performance of Pt-Ru Catalysts as a Function of Preparative Technique

With a fixed composition, the final activity of the catalyst was relatively independent of the technique used for reduction. As an example, Pt-40 Ru catalyst was prepared using sodium borohydride, hydrogen, and formaldehyde as reducing agents. The resulting catalysts, when used as methanol anodes in 3.7 M H_2SO_4 at 60°C, gave polarizations of 0.33, 0.29, and 0.35 volts at 50 ma/cm^2 respectively. These results are listed in Table D-2 and Appendix D-1.

Table D-2

Effect of Reduction Method on Performance

1 M methanol, 3.7M H_2SO_4, 60°C, 20 mg Pt-40 Ru/cm^2

Reductant	Polarization at Indicated ma/cm^2, volts			
	1	10	50	100
$NaBH_4$ (20°C)	0.22	0.28	0.33	0.35
H_2 (180°C)	0.18	0.25	0.29	0.32
CH_2O (70°C)	0.27	0.32	0.35	0.36

Thus, the activity of the platinum-ruthenium system is relatively insensitive to preparation technique.

In order to prepare catalysts with activities such as those listed above, it was found necessary to provide an activation treatment by exposure of the catalyst, or of the electrode after preparation, to a basic solution. The effect of this activation, on an electrode made from a representative batch of Pt-40 Ru catalyst prepared by sodium borohydride, was to decrease the polarization at 50 ma/cm^2 from 0.40 volts to 0.33 volts. These data are listed in Table D-3. Other examples can be found in Appendix D-1.

Table D-3

Effect of Electrode Treatment in KOH on Methanol Activity

Pt-40 Ru, 1 M methanol, 3.7 M H_2SO_4, 60°C

Time in 6 M KOH	Polarization at Indicated ma/cm^2, volts			
	1	10	50	100
None	0.25	0.34	0.40	0.43
1 minute	--	0.31	0.35	0.38
10 minutes	0.23	0.28	0.33	0.36
64 hours(1)	0.22	0.28	0.33	0.35

(1) Catalyst treated prior to electrode fabrication.

Similar effects were found for catalysts prepared by hydrogen reduction. Since formaldehyde reduction was carried out in basic solution, such a treatment was unnecessary and of no value.

With respect to reduction by hydrogen, an investigation of the reduction temperature on catalyst activity was made. The results showed that platinum-ruthenium catalysts, reduced at 260°C and 185°C, gave polarizations at 50 ma/cm^2 of 0.30 and 0.29 volts, respectively. Higher temperature reductions with both hydrogen and carbon monoxide produced less active catalysts, perhaps because of loss of surface area due to sintering. These data are listed in Appendix D-1.

Physical mixtures of finely divided platinum and ruthenium were tested for methanol activity. The initial performance of this catalyst was rather poor, being polarized 0.48 volts at 50 ma/cm^2. However, the activity could be markedly improved by a voltage scanning technique in which the potential of the electrode, in the absence of fuel, is repeatedly driven at a constant rate between incipient hydrogen evolution and incipient oxygen evolution. After ten of these cycles, the polarization at 50 ma/cm^2 decreased 0.08 volts to 0.40 volts polarization. These results are presented in Table D-4.

Table D-4

Effect of Voltage Scanning on Physical Mixture of Pt and Ru

No. of Times Scanned from 0 to 1.5 Volts Polarized	Polarization at Indicated ma/cm^2, volts			
	1	10	50	100
None	0.25	0.43	0.48	0.52
10	0.26	0.34	0.40	0.44

Changes in the scan pattern were observed with successive scans showing less and less contribution from platinum and more closely approaching the type of scan obtained with co-reduced components. These changes are outlined in Appendix D-2. These results indicate the possibility of a redox mechanism involving an oxide of ruthenium.

Phase 2 - Characteristics of Modified P-type Catalysts

A study of the effects on the characteristics of P-type catalysts by modification with controlled amounts of ruthenium was made. This study included preparation variables, initial performance, stability, tolerance to low methanol concentration, and ease of fabrication of large electrodes. These are the most important characteristics needed by a methanol anode catalyst.

Similar but more limited studies were carried out on P-type catalysts stabilized with potassium. The P-type catalyst has the disadvantage of being easily deactivated by overpolarization or improper handling. This disadvantage could be overcome to some extent by changes in the preparation of the catalyst.

Part a - Preparation and Activity of
Ruthenium Modified P-type Catalysts

The preparation and activity of P-type catalysts modified with ruthenium were investigated. The same preparation techniques studied with the platinum-ruthenium system were applied. In one set of experiments, ruthenium modified P-type catalysts were prepared using sodium borohydride and hydrogen as reducing agents. These catalysts were 0.32 and 0.31 volts polarized at 50 ma/cm^2 respectively. Tafel slopes of 0.08 to 0.09 volts per decade were usually obtained, a value intermediate between platinum-ruthenium and the standard P-type materials. Typical performance data for this type of catalyst, compared to platinum-ruthenium, are shown in Figure D-2. Performances of individual catalysts of this type are listed in Appendix D-1.

Figure D-2

Performance Comparison of Active Methanol Catalysts

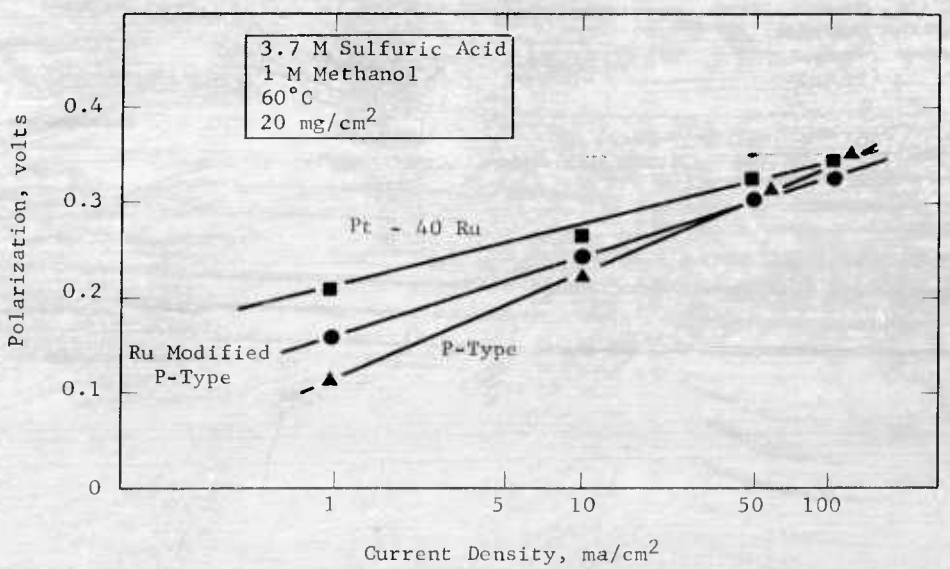

Part b - Assessment of Catalyst Stability

Since the development of a satisfactory methanol anode catalyst necessitates not only good initial activity, but also maintenance of activity after overpolarization, a test of the stability of the three active methanol catalysts to overpolarization was initiated. In the overpolarization test, the catalyst activity was determined in 1 M methanol both before and after the electrode was subjected to two 15 minute periods of operation at a potential of 0.8 volts from methanol theory. The activity was measured in 1 M methanol at 60°C in 3.7M H_2SO_4, and the overpolarizations carried out in 0.05 M methanol to simulate methanol starvation. The platinum-ruthenium cata-

lysts, irrespective of their methods of manufacture, showed no loss of performance when subjected to this overpolarization test. Ruthenium modified P-type catalysts were not completely stable, commonly exhibiting a shift in Tafel slope to values close to 0.06 volts per decade, although the overall performance loss at 50 to 100 ma/cm^2 varied between no change and 30 millivolts. Potassium stabilized P-type catalysts always lost about 60 millivolts following overpolarizations. Representative data are outlined in Table D-5. Complete data are included in Appendix D-1.

Table D-5

Effect of Overpolarization on Methanol Catalysts

1 M methanol, 3.7 M H_2SO_4, 60°C

Catalyst Type	Overpolarized	Polarization at Indicated ma/cm^2, volts			
		1	10	50	100
P-type (K stabilized)	No	0.17	0.26	0.34	0.38
	Yes	0.22	--	0.39	0.43
Ruthenium Modified P-type	No	0.16	0.24	0.30	0.33
	Yes	0.19	0.25	0.31	0.34
Platinum-Ruthenium	No	0.24	0.30	0.34	0.36
	Yes	0.24	0.28	0.32	0.34

Thus, in this test, both the platinum-ruthenium and ruthenium modified P-type are superior to the stabilized P-type.

A separate study of the potassium stabilized P-type catalyst indicated that in 3.7 M H_2SO_4 containing 1 M methanol and 1 M potassium sulfate, no performance loss was found upon overpolarization. However, in 0.05 M methanol, the added salt had no effect. These data are illustrated in Table D-6.

Table D-6

Effect of Overpolarization on P-type Electrodes

Reducing Agent	Methanol Concentration, M	Potassium Sulfate Conc, M	Performance Loss, millivolts
KBH_4	1.0	--	80
$NaBH_4$	1.0	--	150
KBH_4	1.0	1.0	0
KBH_4	0.05	0.01	50
KBH_4	0.05	0.05	60
KBH_4	0.05	0.10	60
KBH_4	0.05	0.50	60

Thus, although the potassium stabilized P-type catalyst has stability to overpolarization greatly superior to P-type, losses in performance are still encountered under conditions of low methanol concentration.

A further indication of the stability of the catalysts containing ruthenium was obtained by observing the effect on performance of representative catalysts before and after complete drying in air. The dried catalyst was fabricated into test electrodes by intermixing with 10 wt % Teflon powder (Dupont #7) before pressing. Methanol activities were measured at 60°C in 3.7 M H_2SO_4 containing 1 M methanol using catalyst from the same batch before and after drying in air. A ruthenium modified P-type catalyst lost only 30 to 40 millivolts on air drying, while platinum-ruthenium was equally active, whether dried or not. These data are shown in Table D-7. Other examples appear in Appendix D-1. This stability of performance when air dried is of particular benefit during the fabrication of large electrodes. It means that fewer precautions are required to prevent the drying out of the catalyst.

Table D-7

Effect of Air Drying on Methanol Performance

1 M methanol, 3.7 M H_2SO_4, 60°C

Catalyst	Dried	Polarization at Indicated ma/cm^2, volts			
		1	10	50	100
Ruthenium Modified P-type	No	0.13	0.22	0.28	0.31
	Yes	0.17	0.26	0.31	0.35
Platinum-Ruthenium	No	0.23	0.29	0.34	0.36
	Yes	0.22	0.28	0.33	0.36

An anode operating in a methanol battery stack could be subjected to severe overpolarization if its supply of methanol was temporarily interrupted. Therefore, an electrode subjected to such a condition must be capable of recovery when the supply of methanol is restored. Two requirements for a satisfactory catalyst exist. There is no permanent loss of activity due to the overpolarization itself, and secondly the catalyst has the ability to recover potential against the current being supplied by the other cells in the battery. Since the platinum-ruthenium system satisfies the first requirement, an experiment was set up to test the second.

In order to simulate the condition existing with methanol starvation in a single cell, a platinum-ruthenium electrode was potentiostatted at a potential of 0.96 volts polarized from methanol theory at 60°C in 3.7 M sulfuric acid. A constant current driver was connected in parallel, delivering 50 ma/cm^2 anodic current. Under these conditions, the net current through the electrode is zero, simulating a situation where the anode and cathode are connected with a diode shunt. Methanol was added stepwise, and the difference in current being supplied by the driver and potentiostat observed. This difference represents the current capabilities of the electrode at the fixed, highly anodic potential. Recovery of the electrode is then indicated by a change in sign of the current supplied by the potentiostat.

For the platinum-ruthenium electrode, recovery was observed at a methanol concentration slightly greater than 0.1 M, indicating no problems would exist with temporary methanol starvation. These data are outlined in Table D-8.

Table D-8

Recovery of a Highly Polarized Platinum-Ruthenium Electrode

Electrode potentiostatted at 0.96 volts polarized, 3.7 M H_2SO_4, 60°C

Methanol Concentration	Anodic Current (Driver), ma/cm^2	Cathodic Current (Potentiostat), ma/cm^2	Current Supplied by Electrode, ma/cm^2
0	50	50	0
0.1 M	50	8	42
0.2 M	50	-50	100

Part c - Catalyst Life Studies

Life testing of P-type catalysts has been concluded, and life tests of platinum-ruthenium and ruthenium modified P-type catalysts begun. Testing is carried out at 50 ma/cm^2 in 3.7 M H_2SO_4 containing 1 M methanol at either 60°C or 82°C. Electrodes are operated in a driven system with a platinum mesh cathode, power being supplied by a constant current source. Cells are routinely open circuited for a few minutes each day.

Test results show that P-type and Pt-Ru catalysts have relatively good stability with performance declines of approximately 10 millivolts per 1000 hours. The ruthenium modified catalyst tests have not progressed sufficiently for certain judgment, although no serious short term deactivation is apparent. Results of these tests appear in Appendix D-3.

Part d - Catalyst Tolerance to Low Methanol Concentration

A study was conducted to compare the three catalysts of interest in terms of their ability to maintain good performance at low methanol concentration. Low concentrations are essential for reducing the transport of methanol to the air electrode and hence minimizing voltage losses at this electrode. The criterion used was the difference in polarization at constant current density in the Tafel region when the methanol concentration was changed from 1 M to 0.05 M. In this test, platinum-ruthenium lost only about 25 millivolts, ruthenium modified P-type lost 45 to 70, and potassium stabilized P-type lost about 90. These data are summarized in Table D-9.

Table D-9

Comparison of Activity Losses Using
0.05 M and 1 M Methanol Concentrations

Catalyst	No. of Tests(1)	Voltage Loss in 0.05 M Methanol Compared with 1 M Methanol, mv
Pt-40 Ru	8	26 ± 8
Ruthenium Modified P-type(2)	7	46 ± 14
Ruthenium Modified P-type(3)	9	73 ± 14
P-type	6	92 ± 5

(1) Different catalyst batches.
(2) RuP-2, RuP-3, RuP-6.
(3) RuP-1, RuP-4, RuP-5.

Thus, platinum-ruthenium, and ruthenium modified P-type have an advantage over potassium stabilized P-type at low methanol concentrations.

In another set of experiments, a direct comparison of a Pt-33 Ru catalyst and a potassium stabilized P-type catalyst was made at different methanol concentrations. The electrolyte was 3.7 M H_2SO_4 at 60°C in both cases with 1 M potassium sulfate added for the P-type evaluation.

With the electrodes potentiostatted at 0.36 volts polarized, the methanol concentration was increased in a stepwise manner from 0.05 M to 1 M. At concentrations below 0.4 M, the platinum-ruthenium catalyst supported significantly more current than the stabilized P-type catalyst. The latter catalyst was similar to the standard P-type catalyst reported earlier[3]. The results of these tests are outlined in Figure D- 3 .

Figure D-3

Effect of Methanol Concentration on Performance

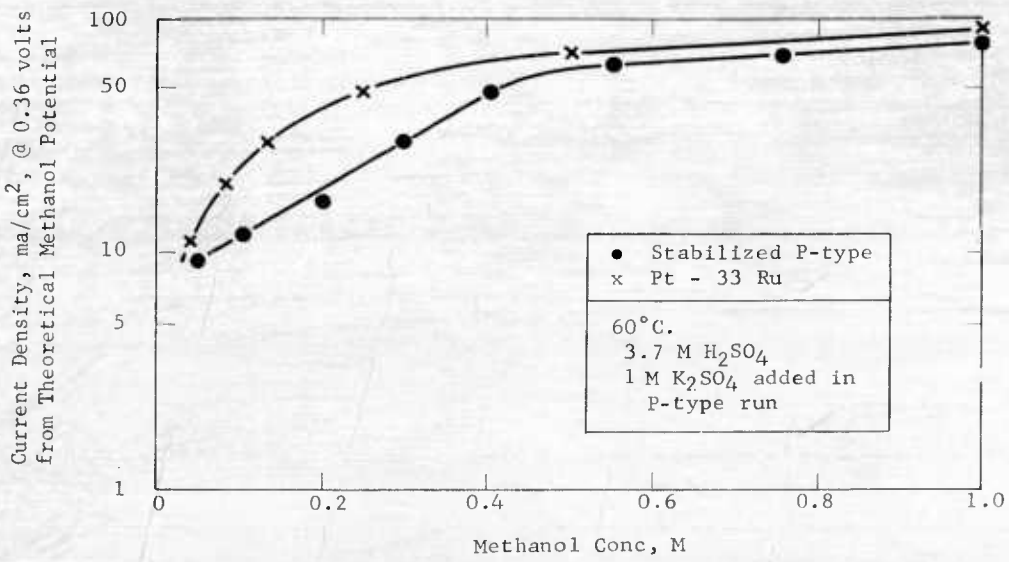

These results support the previous data, showing superiority in tolerance of low methanol concentrations for platinum-ruthenium catalysts.

Part e - Fabrication of Large Electrodes

In order to easily prepare large electrodes certain bulk catalyst properties are required. The most important of these appears to be the easy formation of agglomerates of the fine particles of catalyst after the reduction step. Unless this occurs, washing and recovery of the catalyst by centrifuging can be a tedious procedure. A new simplified procedure was developed for catalyst manufacture which provides catalysts with the bulk properties required for easy application to large electrodes. In this procedure, reductions are carried out in concentrated solutions at room temperature, using slow, quantitative additions of borohydride solution. The catalyst in this form is easily separated without centrifuging. After the electrode is made, the necessary activation step is accomplished by exposure to 6 M KOH.

Data available at this time indicate that catalyst prepared by this procedure may suffer a small activity loss, when compared with catalyst prepared by the more complicated techniques used in much of the work. This activity loss, amounting to 40 millivolts at 50 ma/cm^2, is indicated by the data outlined in Table D-10. Complete data are listed in Appendix D-1. However, this decline is not too important considering the added advantages in making larger electrodes.

Table D-10

Activity Debit of
Simplified Preparation Procedure

Catalyst Preparation Procedure	Volts Polarized at 50 ma/cm^2 *
Simplified	0.33 $\pm$ .02
Standard	0.29 $\pm$ .02

* Based on six tests with each method.

Part f - Effect of Nitric Acid on
Stabilized P-type Electrodes

Earlier work has shown the P-type catalyst to be poisoned by the presence of nitric acid(3). Tests were also made with the potassium stabilized P-type catalyst in 3.7 M sulfuric acid and 1 M methanol with 1 M potassium sulfate added. It was found, as shown in Table D-11, that the stabilized catalyst was also sensitive to nitric acid. Thus at 50 ma/cm^2 it lost 40 mv with 0.1 vol % nitric acid added and 100 mv with 0.5 vol %. These results are essentially similar to the earlier findings.

Table D-11

Performance of Stabilized P-type
Electrode in the Presence of Nitric Acid

Nitric Acid, vol %	0	0.1	0.2	0.3	0.5
Polarization, volts	0.33	0.37	0.39	0.40	0.43

Experiments with ruthenium containing catalysts showed even greater performance loss on nitric acid addition.

Phase 3 - Procedures Aimed at Enhancing Methanol Performances

In addition to the catalyst work already described, which was aimed at producing by simple techniques a platinum-containing catalyst of high activity meeting the requirements of the methanol anode, a number of other studies were carried out which, potentially at least, could provide better catalysts and structures for the methanol anode. These included a study of catalyst preparation in non-aqueous solution by means of radical anion reduction, using both noble and non-noble components, a modified preparation technique aimed at increasing the surface area of catalyst preparations, and attempts to modify the structure of a methanol anode to increase catalyst utilization.

Part a - Radical Anion Reduced Catalysts

In the search for more active methanol catalysts, an evaluation was made of the use of radical anion reduction(9) for preparing catalysts. The reducing agent employed is the radical anion formed from the reaction of metallic sodium or other alkali metals with certain organic compounds, such as naphthalene. The radical anion is stabilized in an ether solvent, such as tetrahydrofuran, and is then able to reduce other metal salts to a high surface area precipitate.

Using this technique, binary and a few ternary catalyst combinations were evaluated as methanol electrodes. These consisted of platinum and a number of noble and base metals. With the exception of Pt-Ru, none of the catalysts proved to be better than platinum. The Pt-Ru electrodes were polarized 0.24 volts at 1 ma/cm^2 and 0.37 volts at 100 ma/cm^2. This catalyst performance was stable with the polarization increasing by only 10 mv during a two week period. Storage had little effect upon performance. These results are presented in Table D-12 and summarized in Appendix D-4, D-5 and D-6.

Table D-12

Performance of Radical
Anion Reduced Pt-Ru Catalysts

3.7 M sulfuric acid, 1 M methanol, 60°C

Catalyst	Polarization at Indicated ma/cm^2, volts			
	1	10	50	100
Pt-20 Ru	0.24	0.31	0.36	0.38
Pt-20 Ru (repeat)	0.28	0.33	0.37	0.38
Pt-33 Ru	0.24	0.29	0.34	0.36
Pt-33 Ru, stored in H_2O for 3 days	0.23	0.30	0.34	0.37

These results indicate that this technique has no special advantage over the other reduction methods used for preparing these catalysts.

Part b - Preparation of Platinum
with Increased Surface Area

Commercial platinum black has been extensively used as a catalyst for fuel cell anodes. Its superior activity may be related to a higher specific surface area than many other forms of platinum. A technique designed to produce platinum having increased specific surface area was tried. This technique consisted of preparing a finely divided platinum silver mixture by reduction at elevated temperature using hydrogen, followed by a leaching of silver from the mixture. Two leaching techniques were tried, one consisting of anodization to potentials where silver is dissolved, and a simple nitric acid treatment of the mixture.

Surface area measurements were carried out on samples of the catalyst using an electrochemical technique. This consisted of measurement of the coulombs required to reduce the layer of oxide formed by polarizing the catalyst to incipient oxygen evolution in sulfuric acid. In addition methanol performance was measured and correlated with the surface area measurements.

Electrochemical measurements showed that platinum prepared in this manner had surface areas at least 1.5 times that of commercial platinum black. In addition, more than proportionate increases in methanol activity resulted, the specific methanol activity of the highest surface area sample being about three times that of commercial platinum black. This observation may be explained by the assumption that increases in surface area result in a higher proportion of more active dislocations. Data from which these conclusions were drawn are outlined in Table D-13.

Table D-13

Use of Silver for Increasing Platinum Surface Area

Source of Platinum	Surface Area millicoul/mg	Specific Methanol Activity ma/mg at 0.45 volts Polarization
Commercial (Engelhard)	100	1.2
Pt-25 Ag (Anodized)	160	2.0
Pt-25 Ag, HNO_3(1)	177	4.0

(1) Yield indicated complete removal of silver.

Conventional performance runs using 1 M methanol in 3.7 M sulfuric acid at 60°C confirmed the conclusion that this preparative technique produces platinum of enhanced activity. These data are listed in Table D-14.

Table D-14

Performance of Platinum as Methanol Catalyst

Preparative Technique	Polarization at Indicated ma/cm^2, volts			
	1	10	50	100
$NaBH_4$	0.40	0.46	0.50	0.55
Radical Anion	0.27	0.43	0.47	0.50
Commercial	0.37	0.43	0.47	0.51
Pt-Ag-Anodized(1)	0.37	0.42	0.46	0.49
Pt-Ag-HNO_3	0.35	0.41	0.44	0.46

(1) Lower catalyst loading due to loss of silver.

This preparative technique has not yet been applied successfully to more active catalyst combinations.

Part c - Studies of Methanol Electrode Structure

Since performance of fuel cell electrodes can be influenced by structure, a study was undertaken to find out if structural variations could lead to improvement in the methanol electrode. The objective was to increase the available catalyst surface and/or improve mass transport of fuel in and carbon dioxide away from the active sites.

The catalyst used in this study was a commercial Engelhard platinum black. This was mixed with various combinations of Teflon, and carbon black, and spread on one-square-inch electrode screens, always keeping the platinum density at 20 mg/cm^2. Electrodes were pressed at various pressures up to 8000 psi and were tested in a glass half cell previously described.

None of the structural variations tested gave significantly better performance than the standard electrode of pure platinum black pressed at 8000 psi. Some of the variants apparently entered into a limiting current region at lower currents than the standard electrode. Implications of this work are that the present methanol electrode is not mass transport limited and that catalyst surface is being well utilized. Representative results are shown in Figure D-4 and complete data are tabulated in Appendix D-7.

Figure D-4

Methanol Electrode Structure Study

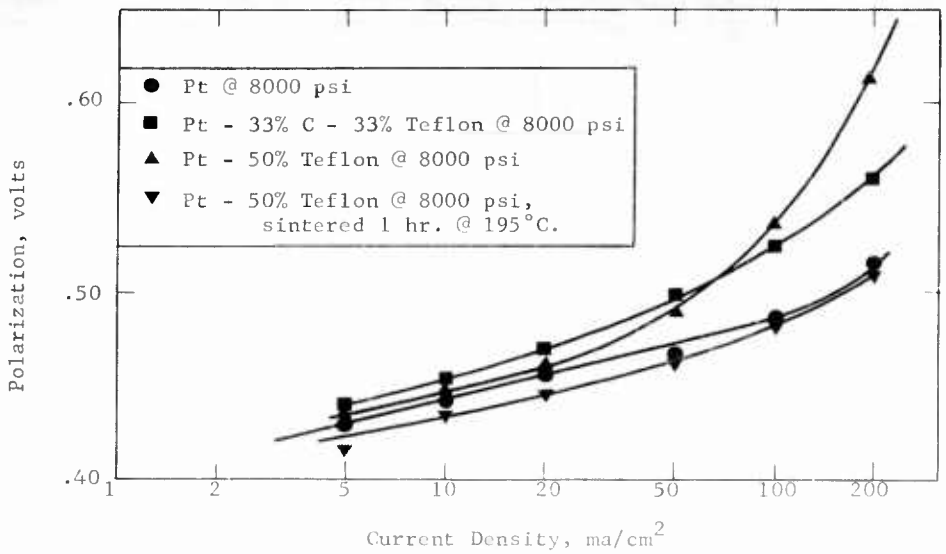

Part d - Noble Metal Catalysts Containing Ruthenium

A study of two component systems of certain noble metals with ruthenium was made to investigate the interactions of ruthenium with metals other than platinum. It comprised the preparation of equi-molar mixtures of ruthenium with gold, rhenium, iridium and rhodium using sodium borohydride as reducing agent. Tests of catalyst activity were made using 1 M methanol in 3.7 M sulfuric acid, at 60°C. The activities ranged from no activity, (Re-50 Ru) through slight activity, Au-50 Ru (0.4 volts polarized at 1 ma/cm^2), modest activity, Rh-50 Ru, (0.48 volts polarized at 50 ma/cm^2) to good activity, Ir-50 Ru (0.33 volts polarized at 50 ma/cm^2). The latter catalyst was stable to overpolarization but lost 40 millivolts when dried in air. These data are listed in Table D-15 and included in Appendix D-1.

Table D-15

Performance of Noble Metal Catalysts Containing Ruthenium

1 M methanol, 3.7 M H_2SO_4, 60°C

Catalyst	Polarization at Indicated ma/cm^2, volts			
	1	10	50	100
Re-50 Ru	---------- No activity ----------			
Au-50 Ru	0.40	--	--	--
Rh-50 Ru	0.28	0.36	0.48	--
Ir-50 Ru	0.25	0.30	0.33	0.36
Ir-50 Ru*	0.27	0.34	0.37	0.43

* Catalyst dried in air.

The activity of the iridium-ruthenium system is encouraging since it represents excellent methanol activity in a catalyst containing no platinum.

Phase 4 - Double Layer Capacitance
Studies on Pt-Re_2O_7-Methanol Systems

Additional studies were carried out during the period on the Pt-Re_2O_7-CH_3OH interaction in an effort to understand the improved performance of these systems. Double layer capacitance studies were used to define the adsorption of methanol on platinized platinum and to study the effect of Re_2O_7 pre-adsorption on subsequent methanol coverage at 25 and 80°C.

Part a - Effect of Methanol on
Double Layer Capacity

Adsorption of methanol on the platinized platinum electrode was studied by the double layer capacitance method described in a previous report(4). The effect of methanol on capacity was determined initially for 1 M methanol at 25°C in the voltage range from 0.2-0.9 volt vs N.H.E. Significant decreases in capacitance were noted in the range 0.3-0.7 volt vs N.H.E. (Appendix D-8). The effect of methanol concentration was then studied at a fixed voltage, 0.4 volt vs N.H.E., for methanol concentrations up to 0.05 M. It was found that capacitance decreased with increasing methanol concentration over this range and this variation was used to derive an apparent adsorption isotherm for the system. As described previously (4), data was treated by the parallel capacitor model, assuming:

$$C_{total} = \Gamma C^{o}_{Pt\text{-}X} + (1-\Gamma)\, C^{o}_{Pt}$$

where C_{total} = measured capacitance

$C^{o}_{Pt\text{-}X}$ = capacitance of covered platinum surface

C^{o}_{Pt} = capacitance of bare platinum

Γ = fractional surface coverage

Isotherms derived for systems at 25 and 80°C are shown in Figure D-5. Maximum coverage at 80°C is approached at methanol concentrations as low as 0.01 M. Corresponding 25°C coverage is about 80%.

Figure D-5

Coverage Versus Methanol
Concentration from Capacitance Measurements

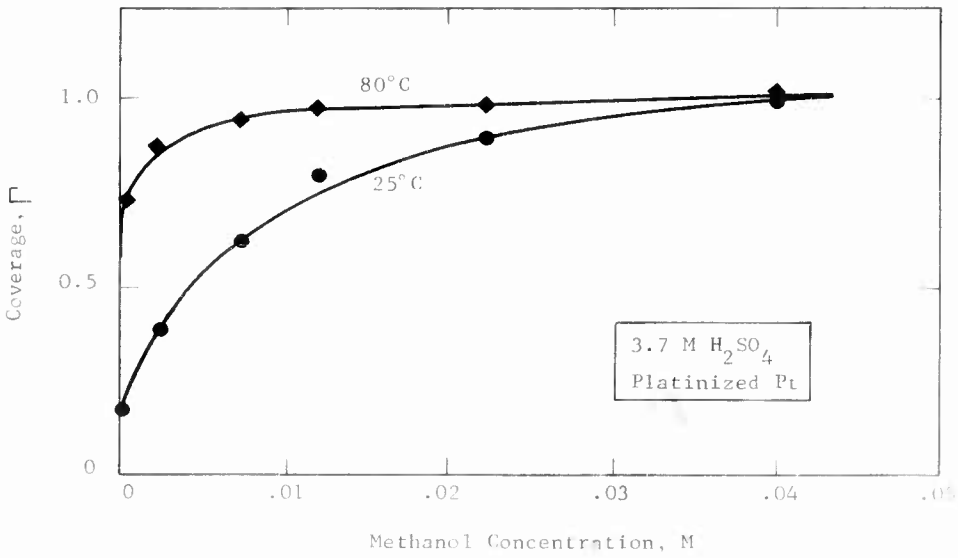

The coverage with methanol is found to be roughly logarithmic with concentration as shown by Appendix D-9.

Part b - Adsorption of Methanol
on Re_2O_7-Covered Platinum

The capacitance analysis of methanol adsorption on platinum serves as a guide in establishing the concentration range for maximizing methanol surface coverage. To gain more information on the Pt-Re_2O_7-methanol interaction, a study of methanol adsorption on a Re_2O_7-covered platinum surface was carried out. For this purpose, the platinized electrode was placed in a 3.7 M H_2SO_4 solution 0.001 M in Re_2O_7, and methanol additions up to 0.05 M made. Double layer capacitance was measured before and after Re_2O_7 addition and during the subsequent methanol additions. Surface coverage was derived from the total capacitance change produced by both the Re_2O_7 and methanol additions. This assumption has not been verified. However, the qualitative results obtained in this investigation should be valid.

Rhenium heptoxide initial coverage was found to be about 81 and 63% respectively for 80 and 25°C systems, based on this method of calculation. Surprisingly, methanol coverage with increasing concentration thereafter followed essentially identical curves for both temperatures, as shown in Figure D-6.

Figure D-6

Subsequent Methanol Adsorption
on Re_2O_7-Covered Platinum Surface

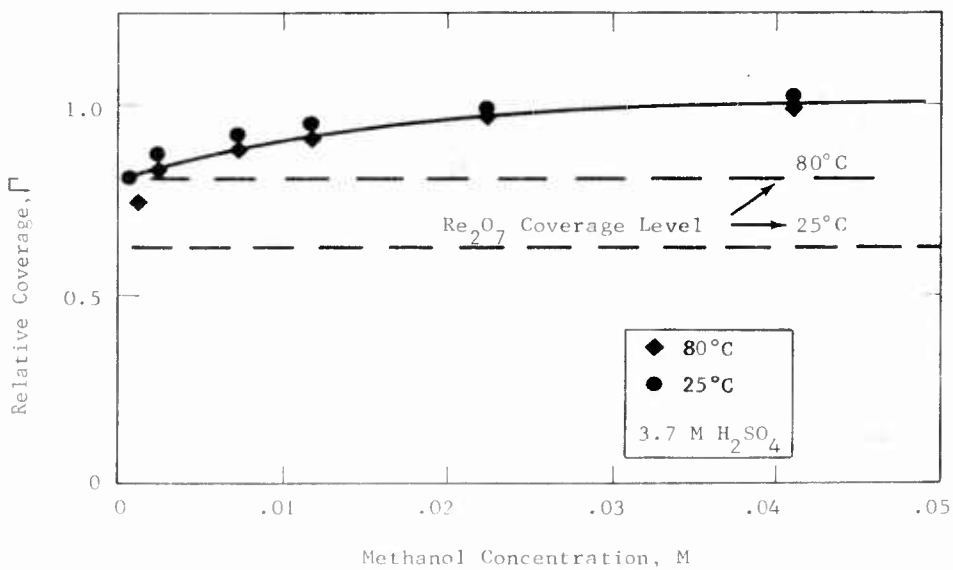

This lack of temperature dependence may simply mean that the sites left uncovered following Re_2O_7 adsorption are those sites most active for methanol adsorption. In any event, these coverages, even in the presence of methanol, are the levels previously shown (3, 4) to give optimum electrochemical performance.

4.5 Task E, Air Electrode

Laboratory studies have continued on the development of more active cathodes. Structural effects were investigated using thin carbon and platinum-Teflon electrodes. In addition, catalyst studies were carried out with platinum and platinum-gold alloys in sulfuric acid and with silver in potassium hydroxide and buffer solutions.

Phase 1 - Thin Carbon Electrodes

Thin catalyzed carbon structures were previously reported to make active cathodes, although scale-up problems existed due to electrode flooding under the increased hydrostatic pressure.(4) Experiments have been carried out aimed at overcoming the flooding problem as well as increasing catalytic activity. A number of different preparation variables were examined, in addition to the use of a porous Teflon barrier layer to control flooding.

Part a - Preparation Variables Study

A number of proprietary thin carbon electrodes which had been made previously for use in a hydrocarbon electrode development program were tested as oxygen electrodes. They represented studies of a variety of preparation variables including the porosity, type and amount of binder, and thickness of the electrode. Also investigated were the effects of catalyst composition, reduction method, support, treatment, and density. The experiments were run in the cell described in Appendix A-2 and details of electrode preparation and activity are shown in Appendix E-1.

Performances were compared in 3.7 M sulfuric acid at 100°C with oxygen, under sufficiently small hydrostatic pressure so that flooding was not a problem. It was found that the most active electrodes resulted from a re-impregnation technique with additional platinum catalyst. Thus, in one case polarizations as low as 0.24 and 0.34 volts from the theoretical oxygen potential were obtained at 10 and 100 ma/cm^2. It was also found that good performance could be obtained with very small catalyst loadings. Thus, an electrode containing only 1.3 mg/cm^2 of catalyst, but reduced by the radical anion method, was polarized only 0.38 volts at 100 ma/cm^2. Figure E-1 shows the detailed performance of this electrode.

Figure E-1

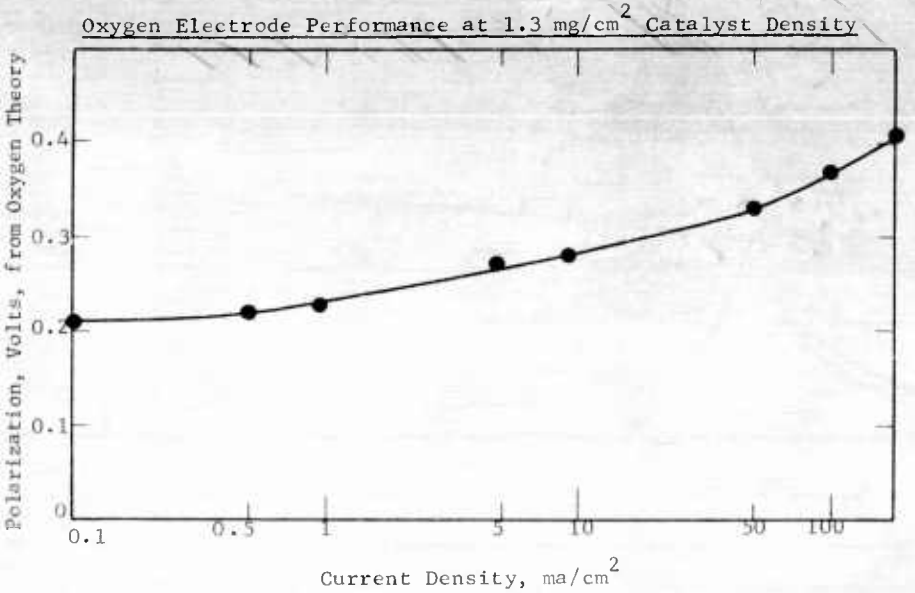

These cathodes also were stable for extended periods of operation. For example, an electrode was run at 35 ma/cm^2 for 552 hours with no change in activity. It appears then that the thin carbon electrode offers an active, stable structure able to efficiently utilize small quantities of catalyst, provided flooding is avoided by use of a sufficiently small electrolyte head or by means to be described in Part c.

Part b - Operating Variables Study

A comparison of oxygen electrode performance in 3.7 M sulfuric acid at 100°C and in 14.7 M phosphoric acid at 150°C was made using two types of thin carbon structures as well as platinum impregnated on platinum powder and platinum supported on titanium nitride. Although these differed widely in activity, as shown in Table E-1, the significant finding was the uniformly lower performance in phosphoric acid, especially at higher current densities. Therefore, screening runs will continue to be made in sulfuric acid.

Table E-1

Comparison of Cathode Activities in Sulfuric and Phosphoric Acids

Electrode	Acid	Polarization from Oxygen Theory at Indicated ma/cm^2		
		5	50	100
Thin Carbon, Re-impregnation with Platinum	Sulfuric	0.24	0.33	0.37
	Phosphoric	0.23	0.62	--
Thin Carbon, Radical Anion Reduction	Sulfuric	0.30	0.41	0.46
	Phosphoric	0.26	0.42	0.52
Platinum on Platinum	Sulfuric	0.28	0.37	0.41
	Phosphoric	0.29	0.51	0.64
Platinum on Titanium Nitride	Sulfuric	0.54	--	--
	Phosphoric	0.64	--	--

The effect of substituting air for oxygen was also investigated and found to result in a decrease in current density at a given polarization by a factor of 2.5 to 4, depending on the structure of the electrode. Appendix E-1 shows these results in more detail.

Part c - Teflon-Coated Thin Carbon Electrodes

The performance debit associated with thin carbon electrodes under larger hydrostatic pressures was found to be the result of increased seepage of electrolyte through the structure and consequently decreased air access to the catalyst (4). Therefore, experiments were carried out to determine if this seepage could be prevented by adding a porous wetproofing layer of Teflon on the gas side. The effect of hydrostatic head was determined by measuring and comparing the performances on air of standard carbon electrodes and carbon electrodes treated with the Teflon coatings. A description of the one inch electrodes used and the methods employed for studying the effects of increased hydrostatic pressures were detailed in the previous report (4).

These studies showed that the added layer of porous Teflon decreased electrolyte seepage and rendered the electrode insensitive to hydrostatic pressure. While the performance loss due to 5 inches of additional electrolyte head increased with current density to about 112 mv at 100 ma/cm^2 on the untreated electrodes, the debit in performance of those treated amounted to only 8 mv and was independent of current density. This is illustrated in Figure E-2 with the detailed data presented in Appendix E-2.

Figure E-2

Effect of Electrolyte Head on Performance
of Treated and Untreated Carbon Electrodes

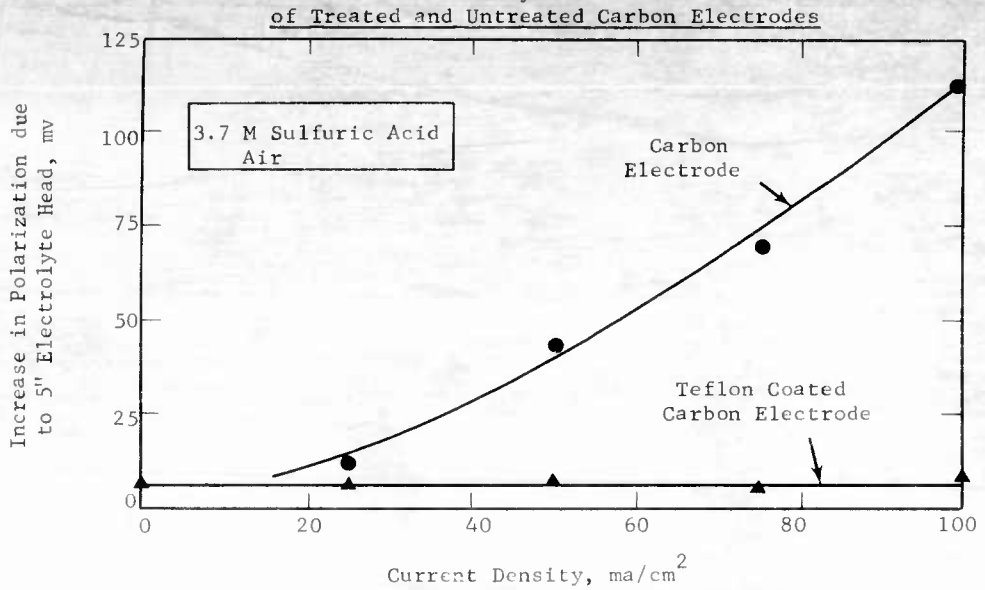

Thus, it should be possible to scale-up these carbon electrodes without incurring a significant loss of performance as a result of greater flooding.

Part d - Effect of Teflon Layer Porosity

An important variable in constructing these electrodes is the porosity of the Teflon coating. Therefore, a series of electrodes were tested in which the porosity of the Teflon layer was varied from 33 to 67%.

The tests showed that optimum performance was obtained with porosities in the range of 40 to 60%. Below 40%, the porosity became insufficient for the gaseous reactant to reach the catalyst by diffusion. This resulted in a rapid increase in polarization at current densities higher than 10 ma/cm^2. When the porosity of the Teflon layer was increased beyond 60%, the electrode tended to polarize more as the result of decreased effectiveness of the added Teflon layer in controlling electrolyte seepage. These data are presented in Appendix E-2.

Part e - Effect of Catalyst Loading on Performance

The addition of the porous Teflon layer had the added benefit of permitting upto a four-fold reduction in electrode thickness under the standard preparation techniques. Since the catalyst concentration on the carbon was maintained constant,

the catalyst loading was effectively reduced from the original 5 mg/cm^2 down to 1.2 mg/cm^2. The performance of these electrodes was then measured at 82°C with air in 3.7 M sulfuric acid to determine the effects of catalyst loading.

The tests showed that the reduction of catalyst loading to 1.2 mg/cm^2 by reducing the electrode thickness resulted in no loss of performance. These results are summarized in Table E-2 and detailed in Appendix E-2.

Table E-2

Effect of Catalyst Loading on Performance

Average Catalyst Density of the Catalyzed Layer, mg/cm^2	Polarization from Oxygen Theory at Indicated ma/cm^2				
	0	10	50	100	160
5	0.25	0.34	0.46	0.56	0.67
2.5	0.23	0.36	0.45	0.53	0.63
1.2	0.25	0.38	0.46	0.53	0.60

In order to further reduce electrode thickness it was necessary to use smaller sized particles of carbon. With these carefully screened particles, carbon electrodes could be successively reduced in thickness to about 2 mils and consequently to low catalyst loadings.

However, this reduction in catalyst loading below 1.2 mg/cm^2 resulted in corresponding decreases in performance. These data are presented in Appendix E-2. An analysis of these performance data showed that at a fixed polarization, the current density decreased approximately in proportion to the decrease in catalyst density. In other words, the results indicated an approximately constant catalyst utilization at catalyst densities below 1.2 mg/cm^2. This is shown in Table E-3.

Table E-3

Catalyst Utilization of Teflon-Coated Carbon Electrodes

Catalyst Loading, mg/cm^2	Catalyst Utilization at Indicated Polarization, ma/mg Catalyst	
	0.5	0.6
1.2	64	133
1.0	51	120
0.5	76	189
0.1	65	170

Because of the low catalyst loadings, a check was made of whether the carbon was contributing significantly as the active catalyst. A carbon electrode was therefore prepared with uncatalyzed carbon. At room temperature this electrode could maintain only one ma/cm^2. At 82°C, it was polarized 1.00 volt at 4 ma/cm^2. Thus, the activity of electrodes with 0.1 mg/cm^2 catalyst loading was due to the catalyst, not the carbon.

Phase 2 - Platinum-Teflon Electrodes

The Teflon coating technique developed for the thin carbon electrodes was also tested with the platinum-Teflon electrodes described previously (3,4). The work of this phase was designed to study the effect of catalyst loading on the performance of platinum-Teflon electrodes coated with porous Teflon layers and to test other structures to further improve the catalyst utilization at various levels of catalyst loading.

Part a - Effect of Catalyst Density on Performance

The catalyst density of Teflon-coated platinum-Teflon electrodes was varied over the range of 1.5 to 92 mg/cm^2 in order to determine how efficiently the catalyst was used in this structure. The tests were carried out in 3.7 M sulfuric acid with air as the oxidant and the data tabulated in Appendices E-3 and E-4.

The results showed that in the density range from 1.5 to 14 mg/cm^2, an increase in catalyst loading caused a proportional increase in current density at a constant potential, maintaining an approximately constant catalyst utilization as shown in Table E-4. Above 14 mg/cm^2, performance ceased to improve with increases in catalyst density.

Table E-4

Effect of Catalyst Density on the Performance of Platinum-Teflon Electrodes

Catalyst Density, mg/cm^2	Polarization from Oxygen Theory at 100 ma/cm^2	Catalyst Utilization at Indicated Polarization, ma/mg Catalyst	
		0.5	0.6
92	0.38	3	5
23	0.39	11	19
14	0.39	20	32
3	0.64	12	26
1.5	0.67	17	43

The test results also confirmed that the optimum porosity for the porous Teflon layer was in the 40 to 60% range. Some of the dual-layer platinum-Teflon electrodes were also tested with 5 inches of electrolyte head and found to be insensitive to the hydrostatic pressure. These results are shown in Appendix E-3.

Part b - Addition of Gold to Platinum-Teflon Electrodes

In an effort to improve the conductivity in platinum-Teflon electrodes of low catalyst density, gold powder was added to electrodes containing 1.5 mg/cm^2 of platinum. A significant improvement in performance was observed upon testing in 3.7 M sulfuric acid at 82°C with air. The data in Appendix E-4 show that the benefit increased with the amount of gold added, with 70 and 110 mv reductions in polarization at 100 ma/cm^2 for 7 and 28 mg/cm^2 of added gold respectively. In terms of catalyst utilization, the addition of 28 mg/cm^2 of gold caused a greater than 2-fold increase in current per unit amount of platinum, as shown in Table E-5.

Table E-5

Effect of Gold Addition on Platinum-Teflon Performance

Catalyst Density, mg/cm^2	Gold Density, mg/cm^2	Catalyst Utilization at Indicated Polarization, ma/mg Catalyst	
		0.5	0.6
1.5 to 14	0	16 (average)	34 (average)
1.5	7	30	67
1.5	28	39	95

Since gold is not a catalyst for the oxygen cathode, these improvements are probably due to the increased conductivity of the electrode structure caused by the addition of gold.

Part c - Tri-Layer Electrodes

It was shown earlier that increasing catalyst densities above about 14 mg/cm^2 did not result in further performance improvements. In an effort to more efficiently use higher catalyst loadings, several tri-layer electrodes were prepared. They consisted of a layer of porous Teflon on the gas side and two layers containing catalyzed carbon. Additional platinum black was added either to the middle layer or to the layer on the electrolyte side. Dual layer electrodes of equivalent composition and similar catalyst loading were also prepared. The data in Appendix E-5, as summarized in Table E-6, show no improvement in performance of the tri-layer electrodes over the dual-layer electrodes.

Table E-6

Comparison of Tri-Layer with Dual-Layer Electrodes

No. of Layers	Location of Platinum Layer	Catalyst Density, mg/cm^2	Polarization from Oxygen Theory at Indicated ma/cm^2		
			1	10	100
2	--	1.9	0.29	0.37	0.53
3	Middle	1.9	0.29	0.38	0.51
3	Electrolyte Side	1.9	0.30	0.40	0.60
2	--	1.1	0.31	0.40	0.58
3	Electrolyte Side	1.1	0.30	0.40	0.56

Part d - Multi-Layer Electrodes

Multi-layer platinum-Teflon electrodes were prepared by adding six to eight additional layers of platinum-Teflon to a single layer structure. Each additional layer consisted of alternate strips of platinum-Teflon and porous Teflon (or voids). The resultant electrode contained on the average 95 mg/cm^2 of platinum. It was found, in contrast to the dual and tri-layer structures, that the increased catalyst loading enhanced performance. Thus, as shown in Figure E-3, the best of these electrodes was polarized only 0.38 volts at 100 ma/cm^2 with air at 82°C. Its current density at 0.30 volts polarization was three times greater than that of a dual-layer electrode with an equivalent amount of catalyst. Complete performance details are given in Appendix E-6. This demonstrates that the multi-layer electrode could improve catalyst utilization at high densities, and should be a useful structure for less expensive catalysts.

Figure E-3

Performance of Multi-Layer Platinum-Teflon Electrodes

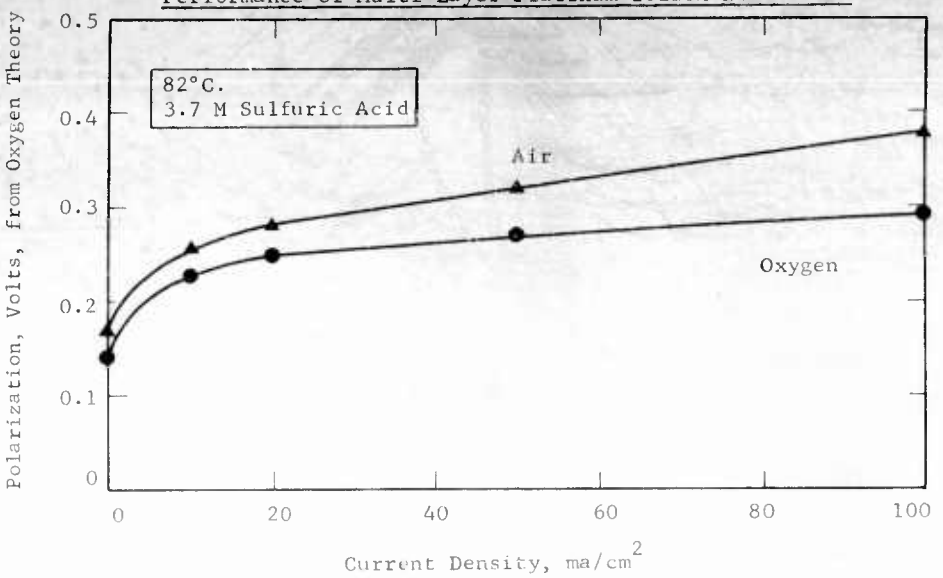

Phase 3 - Platinum and Gold Oxygen Catalysts

Platinum is the most active catalyst known for oxygen reduction. However, even though high current densities can be supported on this metal, a large initial polarization occurs at open-circuit and low current densities. Evidence has been published indicating that this characteristic of a platinum oxygen cathode may be related to surface oxide formation(13,14). Therefore, studies were made of the catalytic properties of oxidized and reduced platinum surfaces. In addition, attempts were made to alter the properties of the surface oxide by introduction of gold, which has a more anodic oxide formation potential than platinum. As part of this latter work, the activity of pure gold was also investigated.

Part a - Anodization and Cathodization of Platinum

A study of the effect of anodization and cathodization on the subsequent performance of a platinum black-catalyzed air electrode was made. The electrode consisted of a platinum black-Teflon mixture, pressed into a platinum screen. The steady state performance of the electrode was determined, using air, at 60°C in 3.7 M sulfuric acid in a conventional half cell described in Appendix A-2 . Then, the electrode was polarized either to oxygen evolution or hydrogen evolution to produce either an oxidized or reduced surface and the potential-time relationship observed as the electrode was returned to a given current density.

The return from the clean surface condition always produced lower polarizations and the return from the oxidized surface condition higher polarizations than the eventual steady state value. These changes, although temporary, were observable for periods of one-half hour or more and were larger for the less polarized steady state conditions at smaller current densities. In fact, at highly polarized positions, where the electrochemical reduction of the oxide was rapid, no difference was observable. Data obtained in this study are outlined in Table E-7.

Table E-7

Effect of Anodization and Cathodization on Air Electrode Performance

Current Density, ma/cm^2	Polarization, Volts, from Oxygen Theory(1)		Advantage in Cathodization, mv
	Pre-Anodized	Pre-Cathodized	
5	0.35	0.26	90
30	0.42	0.34	80(2)
50	0.43	0.36	70
100	0.47	0.43	40
200	0.58	0.58	0

(1) Two minutes after application of current.
(2) 40 mv advantage persisted after 1/2-hour operation.

Similar results were obtained with electrodes prepared from carbon catalyzed with platinum.

Although it was not definitely established that these results are due to the ratio of reduced to oxidized platinum existing on the surface after the pretreatment, the data are consistent with this hypothesis. For example, the electrochemical oxidation and reduction of platinum is highly irreversible, such that the condition established by the pretreatment could influence the activity of the catalyst for relatively long periods of time. The effect would also, as observed, decrease as the steady state potential of the electrode approached values where the reduction of the oxide becomes rapid.

Part b - Platinum-Gold Catalysts

A number of platinum-gold catalysts were made using several preparative techniques. Thus, powdered samples containing 30 atom % gold were obtained from solutions of the mixed metal chlorides by sodium borohydride reduction, by sodium borohydride reduction followed by a hydrogen reduction at 425°C, and by hydrogen reduction alone at 425°C. In addition, catalysts were also prepared by arc melting over the composition range of 5 to 40 atom % gold. These were examined for surface oxide properties in 3.7 M sulfuric acid, using the voltage scan technique described in Appendix E-7, over a voltage region of 0 to 1.5 volts from a hydrogen reference electrode in the same electrolyte.

The powdered samples were investigated at a temperature of 60°C, using a scan rate of 12 mv/sec. As shown in Table E-8, greatly different surface compositions were obtained by the three preparative methods, indicated by the gold/platinum reduction peak ratios. However, the potentials at which the platinum oxide reduction peaks occurred were not significantly shifted. The voltage scans themselves are shown in Appendix E-8, Figures E-2, 3, and 4.

Table E-8

Voltage Scans of Pt-30 Au Powdered Catalysts

Preparation	Gold/Platinum Reduction Peak Ratio	Potential of Platinum Reduction Peak, Volts from Standard Hydrogen
Sodium Borohydride	0.16	0.74
Sodium Borohydride + Hydrogen @ 425°C	0.60	0.79
Hydrogen @ 425°C	0.05	0.77

The smooth melted catalysts were scanned at 25°C at a rate of 24 mv/sec. Pure platinum and gold showed normal scans, but the alloys exhibited unexpected behavior. The 5 atomic % gold sample had greatly diminished platinum and hydrogen oxidation and reduction peaks, without at the same time showing gold peaks. At 10% and higher gold contents, all peaks had disappeared save for slight oxygen evolution and hydrogen reduction at the extreme ends of the scans. Appendix E-8, Figures E-5, 6, and 7 show these scans. The smooth catalysts were also tested directly as cathodes in 3.7 M sulfuric acid at 25 and 82°C by simply sparging oxygen over them. It was found that pure platinum was the most active sample, with performance decreasing with increasing gold content. These results are given in Appendix E-9. It is possible that the platinum oxide inhibition caused by gold accounts for the decreasing cathode activity with higher gold content.

Part c - Platinum-Gold Catalysts on Carbon

Platinum-gold catalysts of the same ratios as in the smooth samples were prepared on a carbon support by reduction of their mixed chlorides. These catalysts were evaluated for cathodic activity on oxygen in 3.7 M sulfuric acid at 100°C. They were also analyzed by X-ray diffraction to determine whether the two metals had formed alloys or were present as the separate metals.

X-ray studies indicated that there was some free gold present in compositions of Pt-10 Au, Pt-20 Au, and Pt-40 Au. Some of these were treated with an aqueous solution of iodine and potassium iodide, removing all signs of free gold. Chemical analysis of these treated catalysts indicated that most of the gold was still in the catalysts, presumably as an alloy.

Evaluation of these catalysts as cathodes operating on oxygen indicated the same performance for all untreated compositions except for the pure gold, which was not active. The catalysts that had been treated with iodine and potassium iodide solution were inactive, however, even though they had been reduced at 538°C under hydrogen in an attempt to remove the iodine. The activity of all these electrodes is shown in Appendix E-10.

The uniformity of activity of these electrodes probably reflects the characteristics of the electrode structure rather than any differences in catalyst activity. The open circuit potentials were not shifted toward the theoretical oxygen value as more gold was added, confirming the results found on the melted samples. However, the alloy catalysts supported on carbon did not show the low activity that the melted samples did. This indicates that some other factor is controlling the catalyst activity. This may be the state of catalyst subdivision or interaction between the metal catalyst and the carbon support.

Part d - Catalysis of Oxygen Reduction by Anodized Gold

It was discovered during the course of brief studies on gold electrodes that certain anodic films on gold were capable of sustaining the theoretical oxygen potential of 1.23 volts for significant periods of time. Thus, a copper-colored film produced by evolving oxygen from a gold wire in 3.7 M sulfuric acid for 1.5 hours achieved a potential of 1.23 volts versus the standard hydrogen electrode after one minute in an oxygenated solution. This potential remained essentially constant for three hours.

In order to determine whether this film was capable of supporting the oxygen reduction reaction, a study was carried out to measure the effect of anodization time on the coulombs required to reduce the electrode in the presence of oxygen and nitrogen respectively. Films produced by anodization of a gold wire at 2.2 volts from the normal hydrogen electrode for varying periods of time were reduced at constant currents of 2 to 20 ma/cm^2 and voltage-time transients recorded from an oscilloscope trace.

It was found that anodic film formation on this gold electrode in 3.7 M sulfuric acid was linear with anodization time in both cases. Film formation efficiency was surprisingly high, about 2%, over the ten minute range studied. There was no difference between reduction under nitrogen and reduction under oxygen, as shown in Figure E-4. However, due to the large number of coulombs on the electrode, large oxide film reduction currents were required and it would therefore have been impossible to detect small oxygen reduction currents in this way.

Figure E-4

Growth of Anodic Film on Smooth Gold

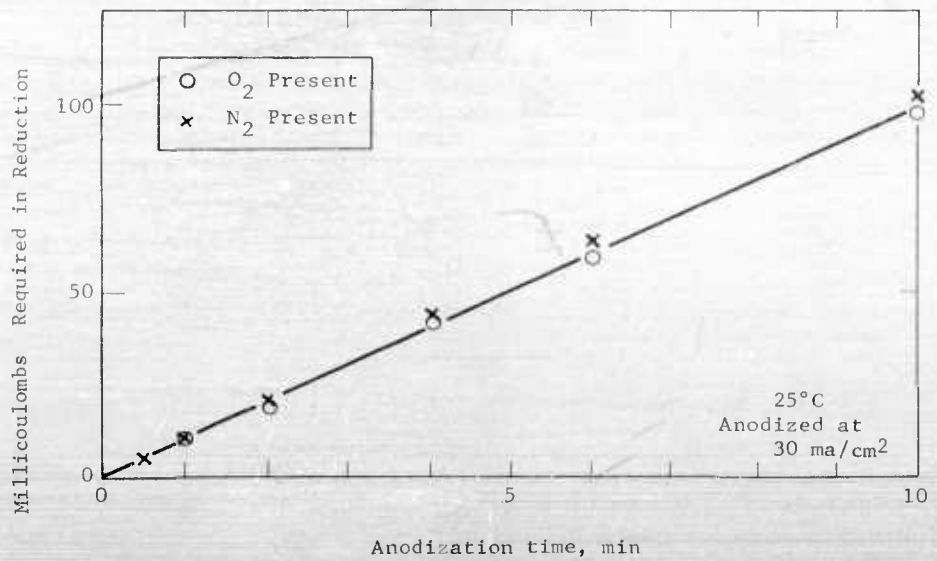

The reduction transition of these films was also studied briefly under low current conditions, 0.1 ma/cm^2, such that oxygen reduction currents, if present, would be correspondingly enhanced in the overall transition. Films were formed by only one minute anodization at 20 ma/cm^2, and low current reductions in the presence of oxygen and nitrogen were then compared.

It was found in this case also that transition times for oxygen and nitrogen sparged solutions were essentially identical within experimental accuracy, indicating negligible oxygen reduction. Thus it was concluded that the potential of 1.23 volts was due to an oxide that forms on the gold at high potentials and not to catalytic reduction of oxygen.

Phase 4 - Oxygen Catalysts for Buffer Electrolytes

With the finding that buffer electrolytes can support practical performance levels, the possibility arises of developing less expensive catalysts. In addition to the cost factor, catalysts insensitive to fuel are needed because of the requirement for bulk electrolyte flow through the cathode to minimize ionic concentration polarization. Preliminary studies have been carried out with silver catalysts, which are relatively inexpensive and are not expected to be active towards fuels such as methanol.

Part a - Oxygen Performance of Silver Catalysts

A variety of silver electrodes were tested with oxygen in potassium hydroxide and, in one case, a carbonate-bicarbonate buffer. The strong base was used to allow a clear determination of catalytic activity uncomplicated by ionic concentration polarization. The types of silver investigated were sodium borohydride reduced, and two types of commercial powders. One test was also run with palladium impregnated powder. Teflon was used as a binder with these catalysts. Finally, several experiments were performed using silver or silver-palladium impregnated carbon.

The most active preparations were those supported on carbon. Thus in 6.9 M potassium hydroxide at 82°C, the best performance was obtained with a silver-palladium sample, which was polarized 0.44 volts from the theoretical oxygen potential at 50 ma/cm^2. Pure silver catalysts on carbon were polarized from 0.47 to 0.50 volts at 50 ma/cm^2. In contrast, the best unsupported silver catalyst had a polarization of 0.62 volts at 50 ma/cm^2. In the carbonate-bicarbonate buffer, a sodium borohydride reduced powder which had a polarization in 3 M potassium hydroxide of 0.56 volts at 10 ma/cm^2, was polarized 0.82 volts at 60°C. However, although its performance was poor, the addition of 2 M methanol did not cause a further loss. Complete preparation and performance details are shown in Appendix E-11.

These results indicate that high current densities and insensitivity to methanol are possible with silver containing catalysts. However, polarizations are high, and the best catalysts are those supported on carbon. Since carbon structures are subject to high ionic concentration polarizations in buffer electrolytes, they are not satisfactory supports for these silver catalysts. Further work is therefore needed to find active forms of silver for use in buffer solutions.

4.6 Task F, Methanol Fuel Cell

Problems in maintaining performance in methanol-air fuel cells have been magnified in extending testing to larger multicell units. Therefore, analyses of performance characteristics of the individual cell components and their interrelationships during cell operation have been extended. As a result, improved cell assemblies and more stable methanol catalysts have been tested to increase the dependability and efficiency of cell operation.

Phase 1 - Engineering Research in the Methanol-Air Cell

An analysis of the internal resistance of the various components during cell operation revealed substantial ohmic loss at the cathode and membrane, see Appendix F-1. Additional loss with time resulted from CO_2 accumulation in the cell. Studies were carried out to eliminate the cause of this high resistance and minimize CO_2 accumulation. In addition, fuel and air distribution studies were made within the cell to determine their effect on performance.

Part a - Studies of the Membrane - Cathode Combination

In studies aimed at overcoming ohmic polarization at the air cathode, it was found that a major performance loss occurred because of poor contact between the membrane and cathode. This resulted in high internal resistance and decreased cathode activity. In addition, carbon dioxide accumulation in the spaces between the cathode and membrane during cell operation resulted in further performance loss with time. Several methods, such as using structural supports to improve contact and vents in the cathode to release trapped carbon dioxide, provided only partial solutions to the problem. The best technique was found to be pressing the membrane and cathode into a single, integral structure to produce a membrane clad cathode.

Tests of these clad cathodes were made in a 4" x 4" cell[4] in combination with a P-type anode. The cell was operated at 65°C with 1 M methanol and air in 3.7 M sulfuric acid. Cell performance improved by 0.1 volts to 0.44 volts at 40 ma/cm^2 and maximum power reached 31 mwatts/cm^2. Ohmic polarization was reduced from 0.04 volts to 0.025 volts at 40 ma/cm^2 and cathode activity reached expected values. This cell performance was maintained throughout 150 hours of intermittent operation. The cell performance is shown in Figure F-1 and detailed data are presented in Appendix F-2 and F-3.

Figure F-1

Effect of Pressing Membrane to Cathode on Performance

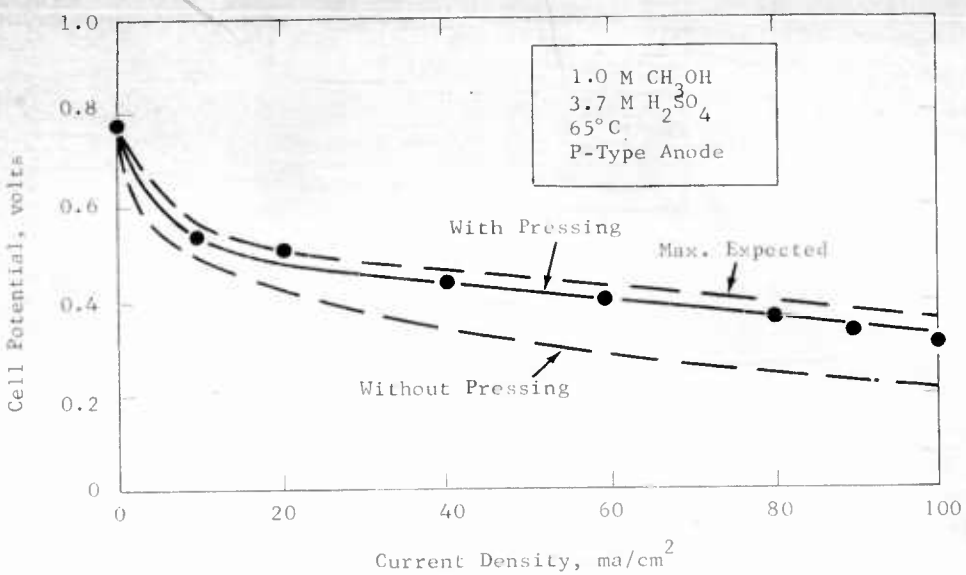

The performance with the clad cathode approaches the maximum performance for methanol and air expected with the P-type catalyst. The remaining loss is due to failure to achieve expected anode performance in this total cell.

Part b - Oxidation of Methanol at the Cathode

The extent of chemical oxidation at the cathode depends on the amount of methanol reaching the cathode. This in turn has been correlated with the concentration of methanol leaving the cell (4). Also, the electrochemical reduction of oxygen from air at the cathode helps in reducing the degree of methanol oxidation as pointed out in previous studies (4). Pressing the membrane to the cathode further reduces the chemical oxidation, apparently by improving the electrochemical efficiency of the cathode through good contact with the membrane. This was established in tests in a small cell at about 65°C with 1 M methanol in 3.7 M sulfuric acid at a current density of 40 ma/cm^2. The influence of pressing was found to reduce the chemical oxidation of methanol to insignificant levels when the methanol concentration at the exit of the fuel chamber was maintained below 0.65 M. This compares with 0.3 M in previous tests with no pressing. Results are shown in Figure F-2. The complete data are given in Appendix F-3.

Figure F-2

Effect of Pressing Membrane to Cathode
on Methanol Oxidation at Cathode

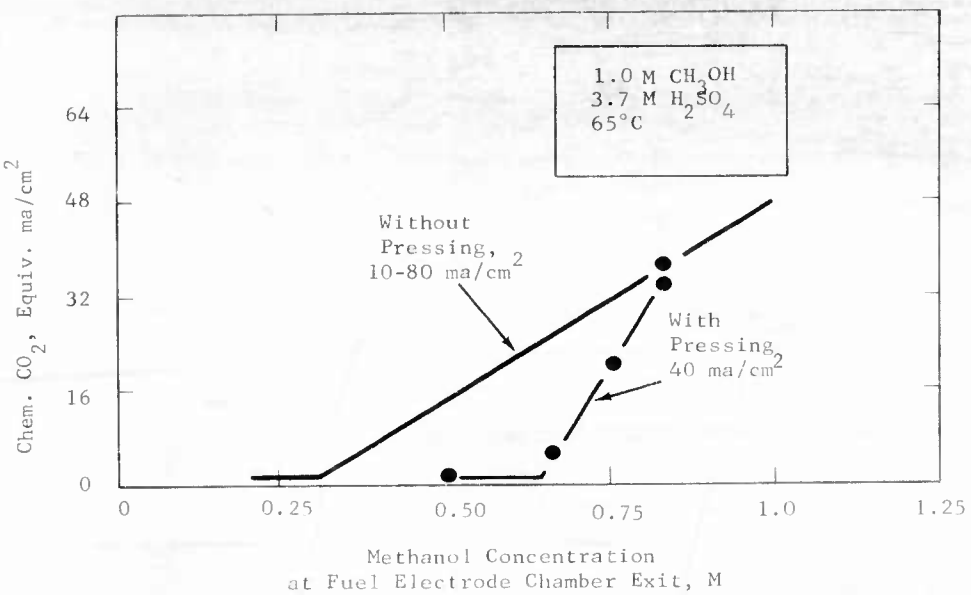

Thus the clad cathode reduces methanol loss resulting from oxidation at the cathode. This in turn minimizes the problem of CO_2 accumulation at the cathode.

Part c - Influence of Spacer Thickness on CO_2 Exhaust

Further attempts were made to assess the CO_2 exhaust problem at the anode. Previous work in the small cells was concerned with the effect of fuel chamber thickness on CO_2 release (3). These studies were extended to consider the effect of the thickness of the spacer which separates anode and membrane. The tests were conducted in a 9" x 5-3/4" cell with spacer thicknesses of 30 to 170 mils. These spacers showed only minor influence on performance, which is attributed to the variation of the conductance path through the electrolyte. No gas buildup was observed for the thinner spacers which are more desirable for compact cell assembly. These data are given in Appendix F-4.

Part d - Effect of Methanol and Air Distribution in 4" x 4" Cells

The effect of intracell fuel distribution on P-type anode performance was measured in a small cell. The circulating fuel-electrolyte solution was introduced alternately through one and two inlets at the bottom of the cell (4).

Performances of the anode and the cell were measured at 60°C with 1 M methanol and air in 3.7 M sulfuric acid. At currents as high as 100 ma/cm^2 and with fuel flow rates giving 50% methanol conversion per pass through the cell, the anode polarization showed negligible changes when switching from one to two fuel inlets. The results are shown in Table F-1.

Table F-1

Influence of Dual Feeding on
Intracell Methanol Distribution

1 M Methanol, 3.7 M Sulfuric Acid, 60°C

Current Density, ma/cm^2	Methanol Conversion Per Pass in the Cell, %	Reduction in Anode Polarization by Increasing Feed Points from One to Two, Millivolts
100	50	5
40	67	10
40	75	20

At extreme fuel conversions per pass, i.e. lower flow rates, the effect was only slightly more pronounced. Therefore, fuel distribution in the small cell in terms of cell performance is satisfactory. Problems in achieving and maintaining maximum P-type electrode performance appear to result from its sensitivity to oxidation.

Similar tests were conducted to assess the effect of air distribution on small cell performance. An air distributor described in Appendix Figure F-2 was designed to provide more even air flow over the surface of the cathode. Measurements were made of cell performance using a clad cathode at 60°C in 3.7 M sulfuric acid. The use of the distributor had no apparent effect on the cathode performance. The results are presented in Appendix F-5.

Phase 2 - Single Cell Operation with Improved Methanol Catalysts

Because of the sensitivity of the P-type catalyst to chemical and electrochemical oxidation, single cell work was extended to include more stable methanol catalysts. These included the potassium stabilized P-type catalyst, platinum-ruthenium catalyst, and ruthenium modified P-type catalyst.

Part a - Performance of Potassium Stabilized P-type Catalyst

Studies aimed at improving the stability of the P-type catalyst, described in Task D, have shown improvements for catalyst reduced in the presence of potassium ions. Therefore, three P-type electrodes were prepared by reduction with potassium borohydride. These electrodes were tested in a 4" diameter cell (4) in combination with a membrane clad cathode in 1 M methanol and air in 3.7 M sulfuric acid at 60°C.

Two of the electrodes gave performance comparable to the best obtained previously with the P-type catalyst, 0.35 volts at 80 ma/cm2. Furthermore, activity was maintained after polarization to 0.7 volt and 168 hours of storage in water or sulfuric acid with no methanol. However, the third electrode did not show the expected stability. It suffered performance loss after storage for 24 hours in 1 M methanol and 3.7 M sulfuric acid and was not stable to over-polarization. In addition, all three electrodes failed to achieve performance targets from half-cell measurements. Evidently, reduction with potassium borohydride is not sufficient to prevent chemical oxidation of this catalyst during assembly and storage. Performance of these electrodes is shown in Figure F-3 and the data are summarized in Appendix F-6.

Figure F-3

Performance of Potassium Stabilized P-Type Catalyst
In Methanol-Air Cells

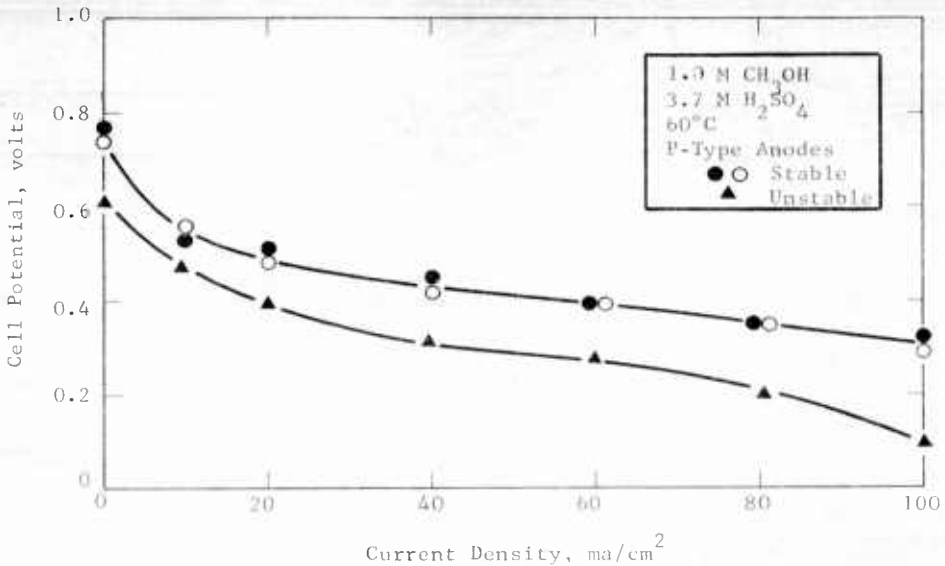

Thus, while good performance and improved stability were obtained in some cases, sensitivity to oxidation is still a problem in cell assembly and operation with the P-type catalyst.

Part b - Performance of Platinum-Ruthenium Catalyst

Because of good electrochemical stability demonstrated in catalyst studies described in Task-D, platinum-ruthenium electrodes were tested in single cells. However, difficulty was experienced in making physically rugged 4" electrodes with this catalyst which had poor adherance and coherance characteristics. The fabrication technique finally developed consisted of displacing the water in the catalyst with butanol and using 10 wt % Teflon as a binder. The butanol wets both the catalyst and binder making a more uniform dispersion. This catalyst mixture was used to make rugged electrode structures which were tested in 4" cells (4) in combination with clad cathodes. Typical performance measurements made at 60°C after repeated polarization to 0.8 volts on methanol and air are shown in Figure F-4 . Complete data are presented in Appendix F-7.

Figure F-4

Performance of Platinum-Ruthenium Catalyst
in Methanol-Air Cells

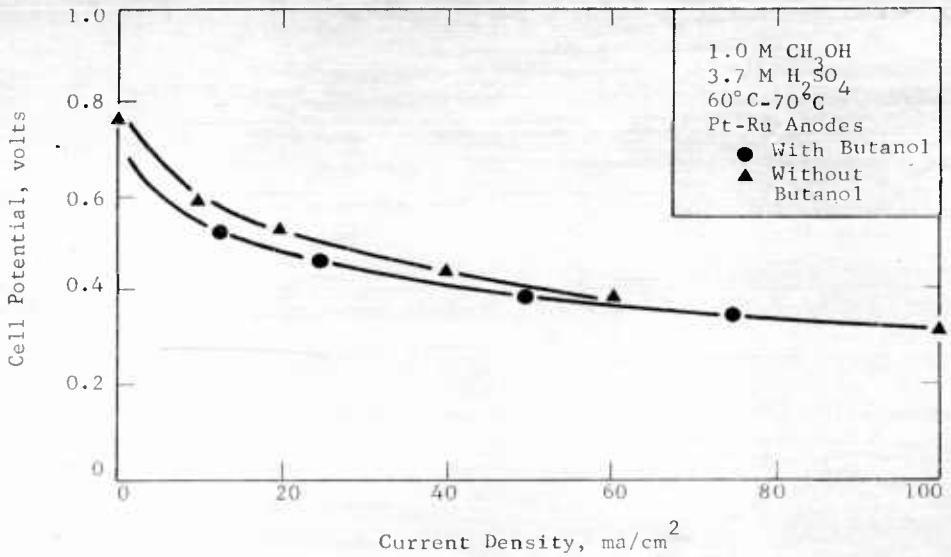

Initial performance with this catalyst preparation was much poorer, attributable to the presence of butanol. The residual butanol was removed by extensive washing and repeated anodic polarization to over 1.0 volt. Therefore, another electrode was prepared without butanol-Teflon addition. The platinum-ruthenium catalyst was washed extensively in 6 M potassium hydroxide in order to improve catalyst recovery. As a result, no purification of this electrode was required. However, during cell operation, catalyst erosion resulted in bare spots on the anode. Cell performance then dropped by 0.04 volts because of excessive methanol at the cathode. Results of this test are shown in Figure F-4 and data are presented in Appendix F-8.

Thus, while platinum-ruthenium electrodes have given good performance and electrochemical stability, electrode preparation remains a problem.

Part c - Performance of Ruthenium Modified P-Type Catalyst

Single cell tests were extended to include the P-type catalyst modified by the addition of ruthenium reported in Task D. This catalyst was made into an electrode by conventional techniques and tested in a total cell in combination with a clad cathode. Tests were made on 0.5 M methanol and air in 3.7 M sulfuric acid at 60°C and 82°C.

The anode gave good initial performance and improved after several polarizations to 0.8 volts in sulfuric acid. Following this treatment, the cell gave the best performance yet attained on methanol and air, 0.47 volts at 60°C and 0.52 volts at 82°C at 40 ma/cm^2. The performance is shown in Figure F-5 and more detailed data are given in Appendix F-9.

Figure F-5

Performance of Ruthenium Modified P-Type Catalyst in Methanol-Air Cells

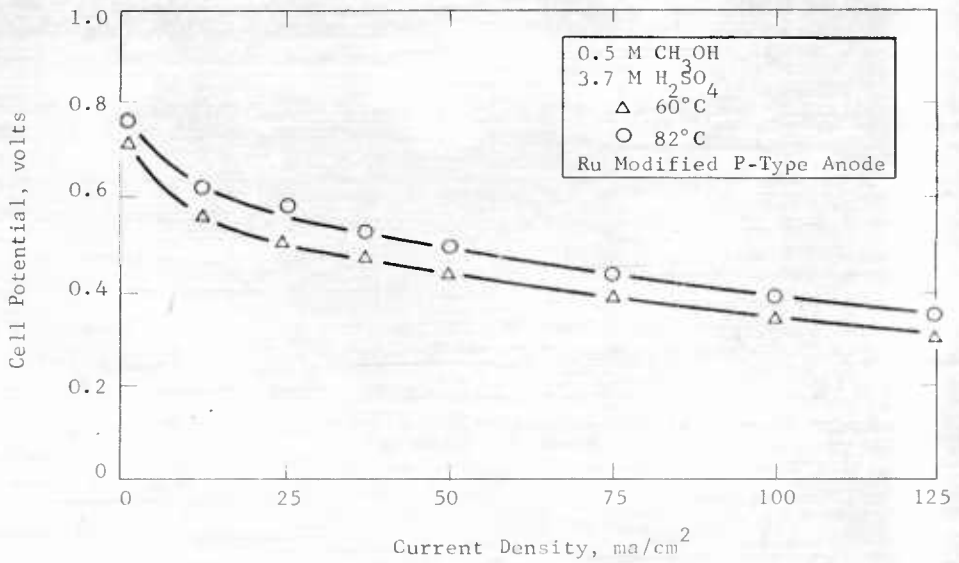

Stability of the modified P-type catalyst was much better than that of the unmodified P-type. During 168 hours of intermittent testing the electrode was subjected to storage in methanol-free electrolyte, polarization to oxygen evolution, and complete drying in air. It lost 25 mv from initial performance and 35 mv from best performance. A substantial portion of this loss was attributed to loss of catalyst from the electrode upon drying. A P-type catalyst is deactivated about 160 mv by any one of the above procedures.

Thus, of the new catalysts tested in total cells, the ruthenium modified P-type catalyst appears to have the best combination of characteristics of performance, stability, and electrode fabrication.

Part d - Scale-up of P-type and Ruthenium Modified P-type Catalysts

Performance evaluations with the P-type and ruthenium modified P-type anodes and pressed Permion 1010 membrane-Cyanamid AA1 cathodes were extended to larger 9" x 5-3/4" electrodes. These studies were made to assess scale-up problems with these catalysts.

Performance evaluations were made in a polypropylene single cell assembly (4) at 65°C with 1 M methanol in 3.7 M sulfuric acid.

The terminal performance of the cell was not equivalent to the 4" x 4" cell performance with the same components. At 40 ma/cm^2 the larger cells were 40 mv worse than the smaller cells. The poorer performance is attributable to a higher ohmic polarization in the larger cells amounting to about 0.060 volts at 40 ma/cm^2. The ohmic resistance free electrode performances were equivalent to 4" electrodes. The more stable ruthenium modified P-type catalyst gave a better terminal performance than the P-type and was almost equivalent to the P-type in the smaller cell. The performance curves are shown in Figure F-6. Detailed data are given in Appendices F-10 and F-11.

These studies with the larger 9" x 5-3/4" electrodes show that performances of the smaller 4" x 4" electrodes can be achieved providing the ohmic resistance in the larger cell is reduced.

Figure F-6

Performance of 9" x 5-3/4" Electrodes in Methanol-Air Cells

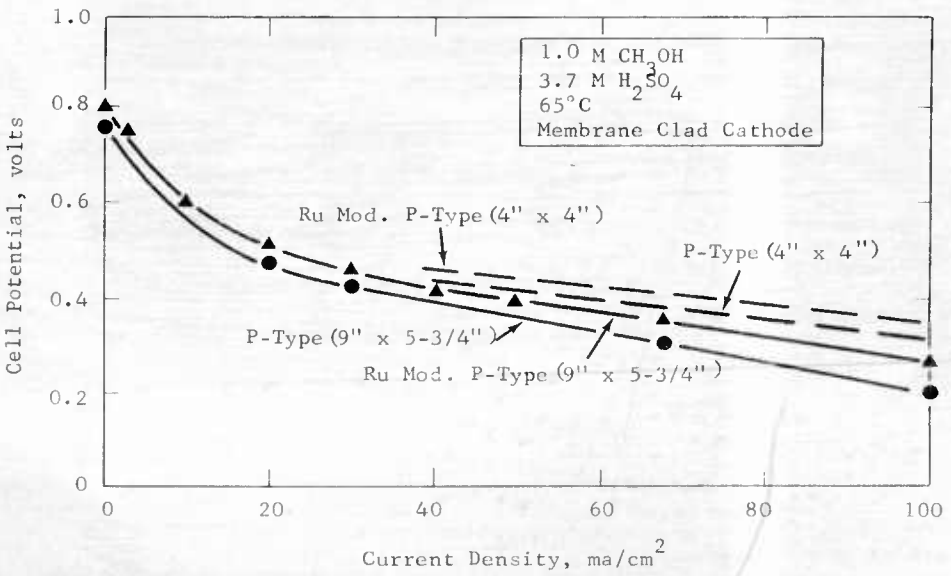

4.7 Task G, Prototype Development

The methanol-air prototype power system will consist of the fuel cell stack and the auxiliaries and controls needed to operate it. Engineering research directed toward the development of such a unit has been concerned with establishing a design as a basis for extending considerations of the problems of battery operation. In addition, studies in multicell stacks operating independently of the auxiliaries have been extended.

Phase 1 - Multicell Engineering Research

In order to better define the problems of methanol-air fuel cell battery operation, an experimental unit has been designed. This design which will be used in construction of a battery for research, has also served for analysis of problems of control, air distribution, and startup.

Part a - Methanol-Air Battery Design

An evaluation of all of the problems of methanol-air fuel cell construction and operation requires a self-contained fuel cell power system. This means a fuel cell battery unit operating to produce power in excess of its own requirements. The design of such a unit has been completed. It includes in addition to the methanol-air multicell assembly, the necessary auxiliaries and controls to permit self operation. The multicell assembly will consist of the 9" x 5-3/4" polypropylene cells already being used in single cell and multicell evaluations (4). The auxiliaries, which include electrical monitoring and control equipment, air blower, electrolyte pump, fuel pump, and heat and water balance equipment, have been assembled as pictured in Appendix G-1. The design of these components is largely based on engineering analyses reported earlier (3)(4). No attempt has been made to optimize this design as a prototype. Instead, this unit will be used for engineering research studies as the first step toward an eventual prototype.

The design originally aimed at sixty cells arranged in two - thirty cell stacks to produce 200 watts gross and 100 watts net. Recent improvements in performance in single cell tests with new catalysts, described in Task F, could more than double the gross output and reduce parasitic power requirements. The latter would be accomplished primarily by an improved electronic control system. The original system required a DC to DC converter plus a switching type voltage regulator to maintain a 28 volt DC output from the anticipated 12 volt input of the fuel cell stack. This system provided an overall electronic efficiency of 72% at maximum load. However, typical DC to DC converter performance resulted in 16% efficiency at 25% of the maximum load. Improved fuel cell stack voltage capability would eliminate the need for the DC to DC converter and regulation can be provided by a simple series regulator. This system has improved dynamic characteristics providing 89% efficiency at maximum design load and 67% efficiency at 25% maximum load. A comparison of the two electronic control systems is shown in Table G-1.

Table G-1

Voltage Regulator Efficiency

Fuel Cell Battery System			Regulator Efficiency
Input	Output		DC-DC Converter and
From Cells	1963 Performance		Voltage Regulator
13V	28V	40W	16%
12V	28V	69W	51%
10.7V	28V	111W	66%
10V	28V	152W	72%
	1964 Performance		Series Regulator
40V	28V	124W	67%
37V	28V	213W	73%
33V	28V	345W	85%
31V	28V	472W	89%

Thus, improved fuel cell performance increases overall efficiency and reduces problems in control.

Part b - Air Distribution Studies in 9" x 5-3/4" Cells

Assuring proper air distribution in the cells of a multicell stack is necessary for maintaining uniform fuel cell performance. This problem is complicated in batteries by the necessity of operating at relatively low pressure drops which can be supplied by conventional blowers. Therefore, studies of air distribution within and between the 9" x 5-3/4" cells have been made.

Studies of intracell air distribution were made by half-cell measurements on one and two electrodes operating in the same bicell module. This arrangement has been described previously (3)(4). The air ports, inlets and outlets, in the polypropylene frames were increased from 60 mil slots to 3/16" diameter holes for these tests because of air distribution problems noticed in multicell stack operation discussed in Phase 2, Part b. Tests were made at 60°C in 3.7 M sulfuric acid using the membrane clad cathodes described in Task G. The measurements were then repeated with the addition of 0.25 M methanol to the electrolyte. The results showed that air flow rates in excess of four times stoichiometric are required to insure expected cathode activity at each of the electrodes in the bicell module. In the presence of 0.25 M methanol, the air flow requirement is increased to five times stoichiometric. The results are shown in Figures G-1 and G-2 and data is recorded in Appendix G-2.

Figure G-1

Air Utilization in 9" x 5-3/4" Bicell Module
(without Methanol)

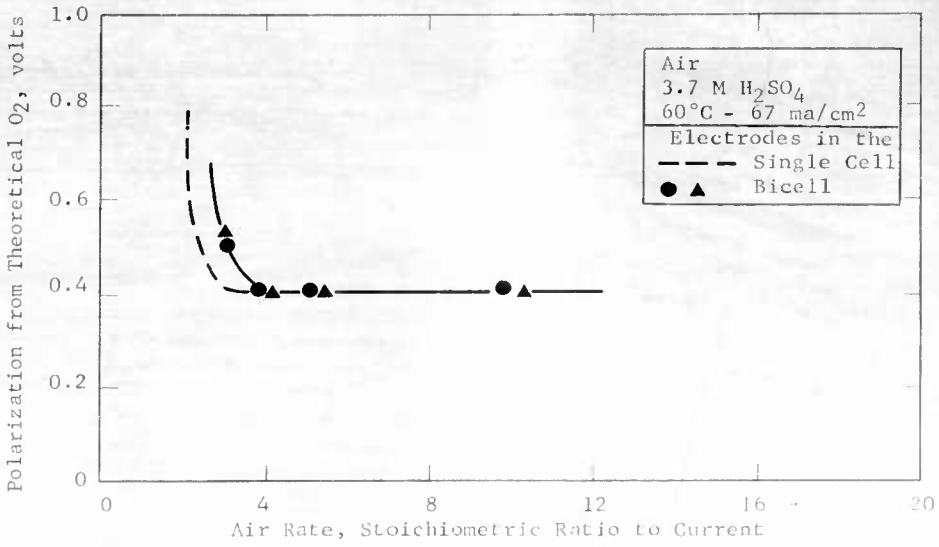

Figure G-2

Air Utilization in 9" x 5-3/4" Bicell Module
(with Methanol)

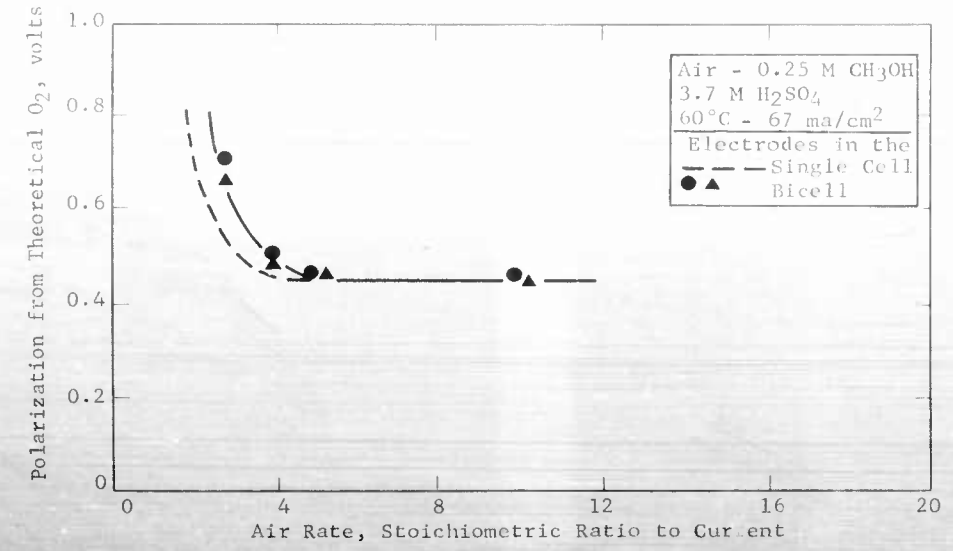

These half-cell studies were confirmed in total cell tests in the large bicell module. Performance fell off appreciably at air flow rates below five times stoichiometric. Attempts to improve air utilization by altering the flow pattern resulted in poorer performance. These results are shown in Figure G-3 and Appendix G-3.

Figure G-3

Air Utilization in 9" x 5-3/4" Cell

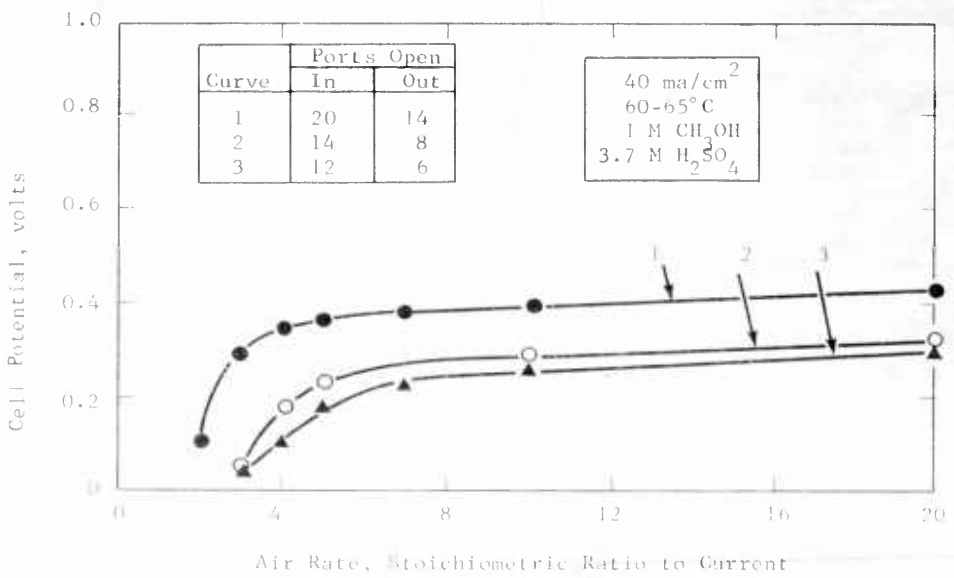

Finally, intercell air distribution studies were made in the six cell 9" x 5-3/4" stack. The tests were made at 65°C with 1 M methanol in 3.7 M sulfuric acid. The air utilization in each of the six cells operating in the multicell assembly was almost equivalent to that in the single module studies. The results are shown in Figure G-4 and Appendix G-12.

Figure G-4

Air Utilization in 9" x 5-3/4" Stack

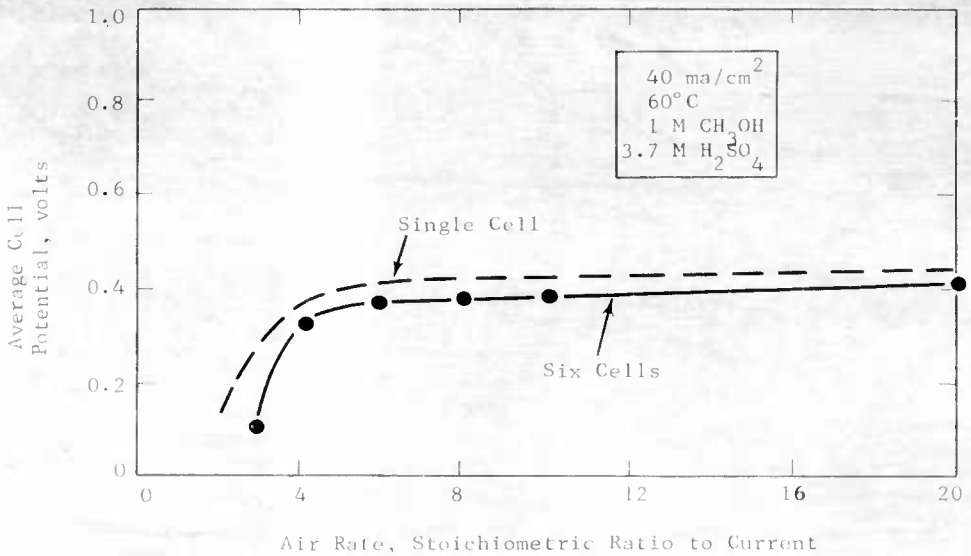

Thus air distribution in the large cells is satisfactory provided air flow rates in excess of five times the stoichiometric requirement are maintained.

Part c - Startup in Methanol-Air Cells

It is important to minimize the time required to reach operating temperatures in a methanol-air battery during startup. Previous engineering analysis of heating in this system (4) indicated that it would require about one hour to achieve the expected operating temperature range of 60°C to 80°C without the help of externally powered heaters. This analysis assumed that the irreversibility of the electrochemical reactions would provide the major heat source in the cells. However, chemical oxidation of methanol at the cathode provides an excellent source of heat inside of the cells. Therefore, tests were made to see if startup time could be reduced by favoring this reaction.

Tests were made in a six cell 9" x 5-3/4" stack operating on 1M methanol in 3.7 M sulfuric acid. Each cell contained a P-type anode and American Cyanamid AA1 cathode separated by Permion 1010 membrane. The heat released by the chemical oxidation of methanol at the cathode was an important factor in heating from room temperature. With the cells at open circuit, the unit reached 60°C in about 25 minutes. The rate of heating was increased further by applying a small load of 15 ma/cm^2 when the unit reached a temperature of 50°C. This permitted safe

operation of the P-type anodes without danger of over-polarization. By combining chemical heating and electrochemical operation at low currents, a temperature of 60°C was achieved within 12 minutes. These results are shown in figure G-5 and Appendix G-4.

Figure G-5

Effect of Methanol
Oxidation at the Cathode on Startup

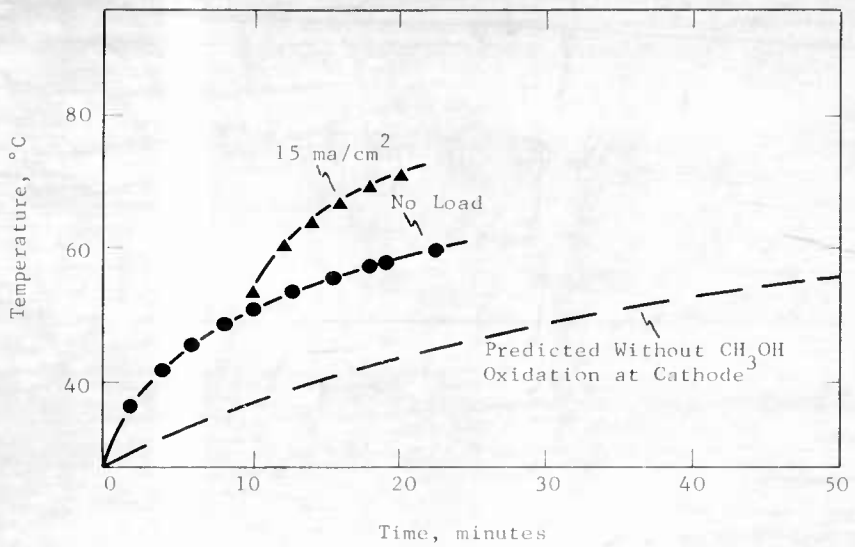

Thus, startup time is considerably reduced by favoring methanol oxidation at the cathode to produce initial heating to safe operating temperatures. Since each additional cell is an added heat source, it is expected that this result can be applied to larger multicell stacks.

Phase 2 - Multicell Operation

Multicell studies have continued on both the 4" x 4" cells and 9" x 5-3/4" cells. The smaller units provide a direct extension of the single cell technology to multicell operation while the larger units involve scale-up to a more practical size. In addition, multicell evaluations of the clad cathodes and ruthenium modified P-type anodes described in Task F were initiated to improve performance and stability.

Part a - Studies in 4" x 4" Stacks

Teflon cells, 4" x 4" described previously (4), were assembled in a stack of 10 cells. The overall dimensions of the ten cell stack were 5-3/4" x 5-3/4" x 3-3/4". The assembled fuel cell stack was provided with feed and exhaust connections, current collector bus bars, and hydrogen reference electrodes to

monitor anode polarizations. The laboratory equipment used for operating and monitoring the ten cell stack is shown in a flow schematic in Appendix G-5. Tests were made in the ten cell stack with methanol and air in sulfuric acid electrolyte to study the problemsof multicell operation. Each cell unit included a P-type anode, Permion 1010 membrane, and American Cyanamid AA1 cathode.

In the initial tests, the ten cell stack produced up to 10 watts at various terminal voltages when operating at 60°C to 70°C. At 24°C up to 5 watts power was produced. Terminal performances for both parallel-series and straight series connections are shown in Figures G-6 and G-7. The performance data are tabulated in Appendix G-7.

Figure G-6

Initial Performance Curve - Ten Cell Stack

Parallel-Series Connected(1)

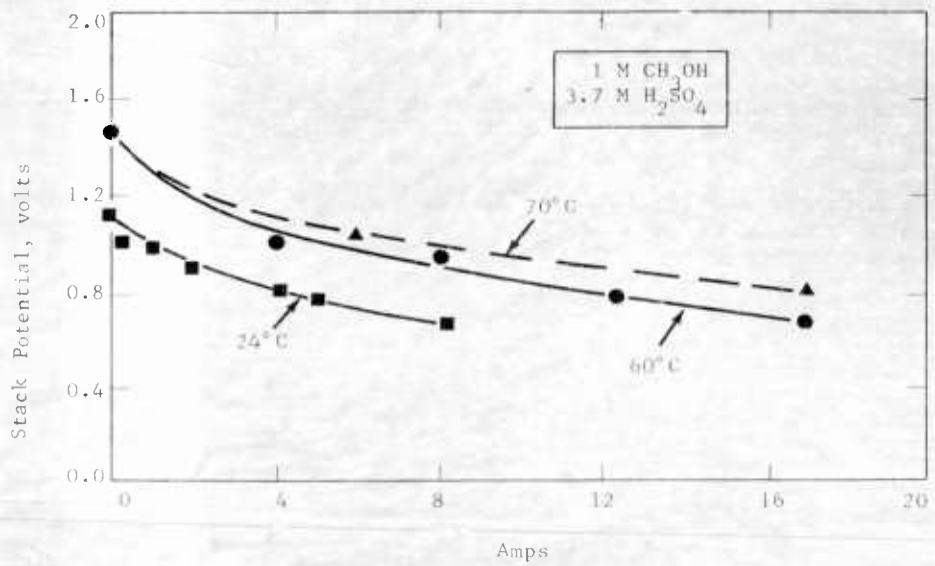

(1) The parallel-series circuit used in these tests is shown in Appendix G-6.

Figure G-7

Ten Cell Stack Performance with Time

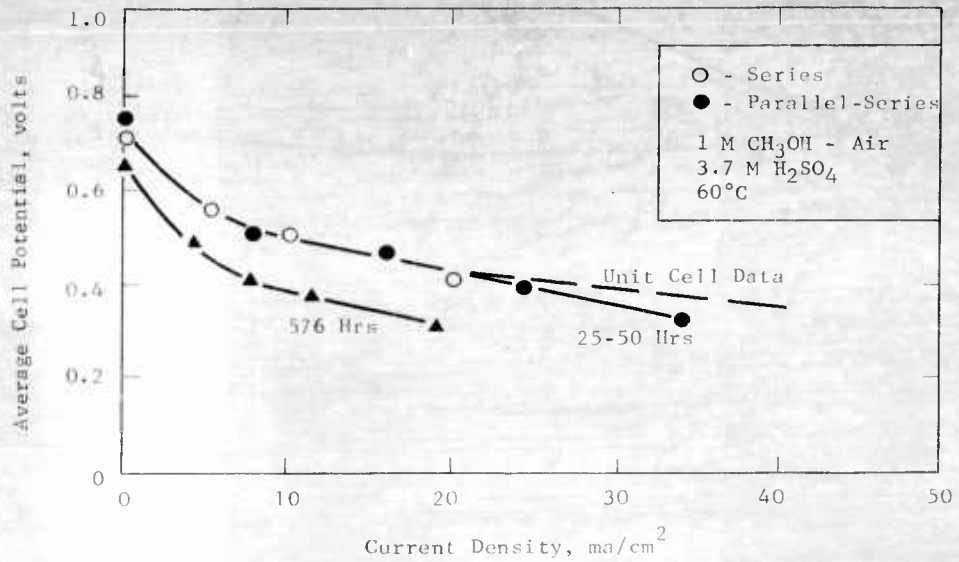

After initial tests, intermittent operation of the ten cell stack was continued for 576 hours with the cells parallel-series connected. The stack performance declined, largely attributable to loss in activity of the P-type catalyst as evidenced by increased polarization at the anodes. At 4 amperes the cell voltages declined by 100 millivolts, shown in Table G-2. Further data are given in Appendix G-8.

Table G-2

Testing of Ten Cell Stack

Hours in Service	50	576
Stack Amperes	4.1	3.9
Stack Voltage	1.01	0.80
Voltage of Parallel Bank:		
No. A	0.51	0.40
No. B	0.50	0.40
Anode Polarization, volts		
At Each Cell:		
No. 1	0.32	0.40
No. 2	0.24	0.45
No. 3	0.32	0.43
No. 4	0.32	0.46
No. 5	0.36	0.45
No. 6	0.34	0.41
No. 7	0.34	0.48
No. 8	0.45	0.37
No. 9	0.37	0.45
No. 10	0.33	0.37
Average	0.339	0.427
Deviation from Average	± 0.033	± 0.035

During operation of the ten cell stack, a storage test was made for 168 hours with 0.25 M methanol in 3.7 M sulfuric acid in both the anode and cathode compartments. A negligible activity loss of only 0.02 volts per cell occurred during this period.

Thus, while single cell performances were attained during initial testing of the 4" x 4" ten cell stack, performance declined with time.

Part b - Studies in 9" x 5-3/4" Stacks

The 9" x 5-3/4" polypropylene cells, previously described (4), were used for testing performance of larger P-type and ruthenium modified P-type electrodes in multicell assemblies. A six cell stack is pictured in Figure G-8.

Figure G-8

Six Cell 9" x 5-3/4" Polypropylene Stack

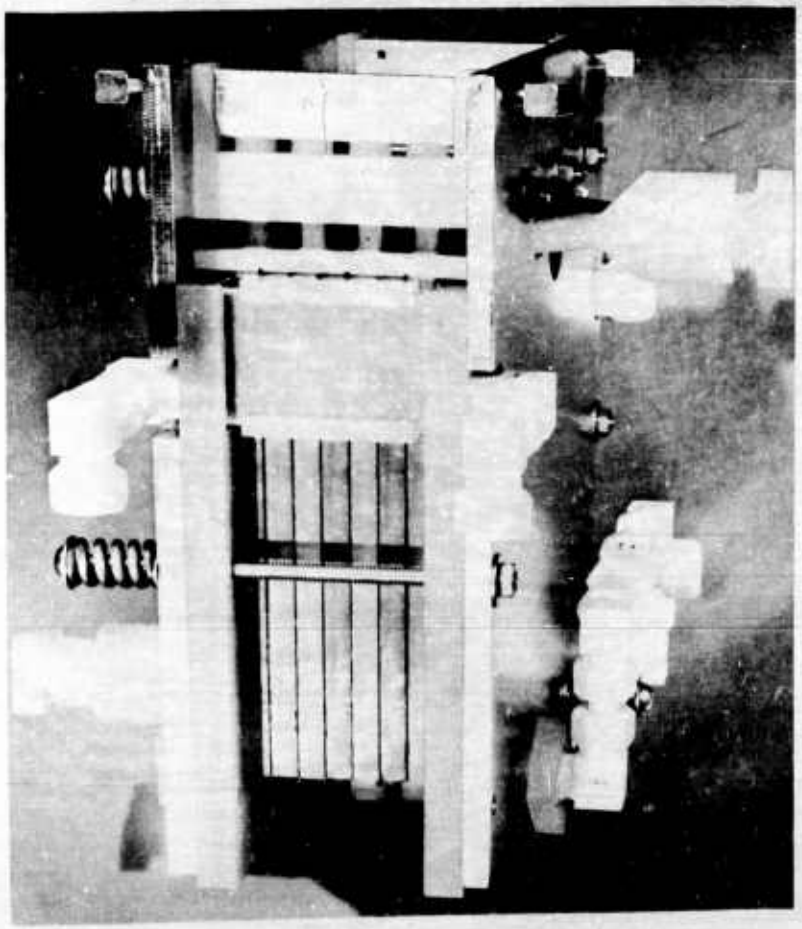

Tests were first made with P-type electrodes in cell assemblies similar to those used in the 4" x 4" multicell stacks. Results summarized in Appendix G-9 confirm the findings for this type cell assembly in small cells discussed in Part a. In addition, air distribution in the various cells was found to be sensitive to the inlet and outlet port sizes. Therefore, the air ports were enlarged from 60 mil slots to 3/16" diameter holes to give minimum resistance to flow and to improve intracell and intercell distribution. This was confirmed in air distribution studies described in Phase 1, Part b.

Studies were initiated with the ruthenium modified P-type catalyst and membrane clad cathodes at 60°C with 1 M methanol and air in 3.7 M sulfuric acid. In assemblies of two and six cells the performance was fairly uniform, averaging about 0.48 volts per cell at 20 ma/cm^2 with 0.02 volt variation. The six cell stack produced over 30 watts power. The ohmic loss was high, averaging about 0.03 volts/cell at 20 ma/cm^2. The average cell performance is compared with that of a single cell in Figure G-9. Detailed data are given in Appendices G-10, G-11, and G-12.

Figure G-9

9" x 5-3/4" Polypropylene Stack Performance

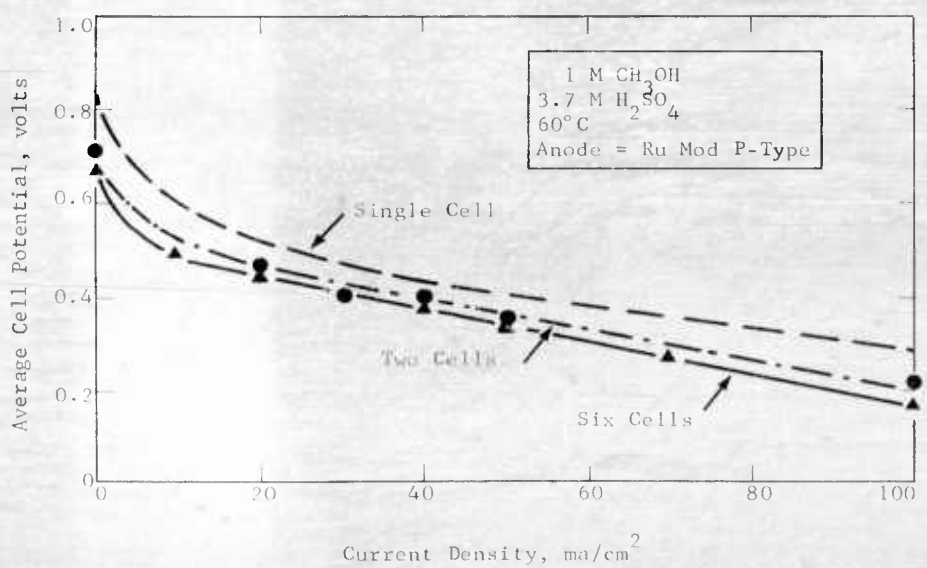

The multicell performances were lower than the single cell tests by about 60 to 80 mv in the 20 to 60 ma/cm^2 region, attributable to poorer performance at the methanol electrodes. This was indicated by higher than expected polarizations.

This loss in anode activity could have resulted from short circuiting through parallel electrolyte paths between the fuel chambers. Thus, further study of these problems is necessary.

SECTION 5

CONCLUSIONS

5.1 Task A, Hydrocarbon Electrode

Phases 1 and 2 - Study of Decane Reaction on Pt-Teflon Electrodes; Comparative Performance of Butane Fuel

Comparisons of the decane and butane reactions by both steady-state and voltage scan measurements indicate that the limiting rate of oxidation of both fuels is governed by a step that is chemical in nature, possibly fuel adsorption at the catalyst surface. The rates for this step are higher using butane, making it possible to observe a Tafel-like region in the performance curve. For this region, the reaction is presumably electron-discharge limited, wherein the butane surface concentration is governed by the adsorption equilibrium. In its general character, the gaseous butane reaction provides a more reliable and reproducible system for catalyst testing than does the liquid decane system. Catalytic limitations are believed to be sufficiently similar to justify the use of the lighter fuel for this purpose.

Phases 3 and 4 - Flooding Measurements; Electrode Structure

A variety of measurements, including voltage scans, electrode weight changes, and electrode response to methanol, showed that over 90% of the decane electrode becomes flooded with decane. Under these conditions the electrodes, when properly made, permit current densities at 100°C of about 10 ma/cm^2 at 0.5 volts polarization. Complete elimination of the decane flooding problem could theoretically improve this by an order of magnitude.

The extent of flooding can be reduced by inserting a porous barrier on the decane side of the electrode. The barrier, because of its preferential wetting and capilliarity, soaks up but does not easily discharge the fuel into the electrode. The use of the barrier also permits the use of better performing electrode structures which, by themselves, would be structurally weak. With these barriers, over twofold improvements in catalyst utilization can be obtained.

Phase 5 - Electrolyte Variations

The use of perfluoroacids as electrolytes demonstrate that electrolytes which have a greater tendency to wet electrode structures could aid in preventing decane flooding and improve cell performance. Such electrolytes are also stable to oxidation and hydrolysis, and have high conductances. Heptafluorobutyric acid was particularly useful in improving the performance of carbon as well as platinum based structures. Similar studies using electrolyte additives to improve the wettability of sulfuric acid indicated that improvements in performance could be obtained using this approach.

The use of phosphoric acid on an electrolyte for liquid decane was not beneficial. However, a mixed electrolyte consisting of sulfuric acid and phosphoric acid shows improved conductance at high acid concentrations and could prove useful in this region.

Phase 6 - Gas Phase Testing

Under very specific conditions gaseous hydrocarbons could be made to give excellent performance. Using a platinum-Teflon electrode made with Teflon emulsion, butane could be reacted at 150°C in concentrated phosphoric acid to give up to 400 ma/cm^2. Under these conditions decane vapor yields up to 100 ma/cm^2. These results could be used in designing a hydrocarbon fuel cell provided several serious engineering and materials problems could be overcome. The above electrodes were of no advantage with liquid decane, however. Their specificity again indicates the importance of structure and wetting properties and strengthens the hope that optimization of these factors could lead to large improvements in liquid fuel performance.

Phase 7 - Noble Metal Catalysts

In addition to the structural effects noted above the precipitation conditions were found to have a large effect on catalyst performance. A significantly higher surface area platinum, 60% greater than commercial platinum black, could be produced by co-precipitating platinum with aluminum hydroxide. This results in a two to threefold increase in performances on methanol as well as decane. Experiments using the P-type electrodes for decane oxidation showed that this catalyst has better initial activity than platinum. However, this catalyst irreversibly deactivates with use.

Phase 8 - Non-noble Steam Reforming Catalysts

Low cost steam reforming catalysts have enough activity for a practical system above 250°C. However, a twentyfold improvement in activity is needed for applications below 150°C. High hydrogen concentrations are attainable and the resultant hydrogen-rich gas is able to operate efficiently in a fuel cell without purification.

5.2 Task B, Hydrocarbon Fuel Cell

Phase 1 - Liquid Hydrocarbon-Air Fuel Cell

The total hydrocarbon fuel cell assembly has proven to be operable. The cell components, especially the liquid decane electrodes employed, performed with their same characteristics in total cell operation as they had in half cell tests. Power densities at about 100°C of 8.2 mwatts/cm^2 with cell voltages of 0.44 volts are attainable, with optimum performance favoring lower sulfuric acid concentrations.

5.3 Task C, New Systems

Phase 1 - Buffer Electrolytes

Buffer electrolytes can support practical performance levels at both electrodes and in total cells. Anode performances in methanol with present catalysts are as good or better than in acid and carbon dioxide is rejected. The best catalyst in both phosphate and carbonate solutions is the P-type. Cathode performances are somewhat poorer in buffer solutions, due to ionic concentration polarization within the porous electrodes, but can reach acceptable levels if suitable structures are used. In total cells the methanol incompatibility problem is more severe at the cathode in buffer than in acid due to the necessity for bulk flow through the electrode. However, successful operation at power outputs of more than 10 mwatts/cm^2 with air is possible if special precautions are taken to minimize methanol flow to the cathode. Further improvements in total cell performance can be gained by increasing the total concentration of the buffer and optimizing the ratio of the acidic and basic components.

Phase 2 - Hydrocarbon Redox Systems

Rhenium heptoxide is the only oxidizing agent found active for hydrocarbons at moderate conditions. When boiled as a slurry in decane, the hydrocarbon is converted partially to carbon dioxide and the heptoxide reduced to the trioxide and in some cases to the dioxide. The yield of carbon dioxide can be increased by the presence of certain catalysts, such as platinum or gold. The chemical reaction rate is equivalent to a current density of more than 50 ma/cm^2, so that this step would not be limiting in a complete redox cycle. The slow step, however, is the electrochemical reoxidation of the reduced species. This has not been achieved, due probably to the lack of electrical conductivity of the oxide.

Phase 3 - Dynamic Electrode Studies

No performance benefits are achieved with the flowing fuel system by preheating decane or by electrically heating the electrode. Open circuit pulsing is also of no benefit, since a slower rate of polarization is offset by the lowered time average current. Sintered platinum-Teflon electrodes and platinized gauzes are not active in the flowing fuel system.

Phase 4 - Slurry Catalyst Systems

The performance of slurry catalyst systems with a rotating electrode depends strongly on the cell geometry employed, as well as catalyst concentration. Optimum activity is achieved when sufficient turbulence is introduced. Under these conditions, performance with methanol and decane increases approximately linearly with the concentration of platinum black catalyst and the rotating speed becomes unimportant above a minimum value. Performance levels equal or superior to static systems can be reached at catalyst concentrations of 10 mg/ml or higher. At the same time, by assuming that the cell volume can be limited to that swept out by the electrode, catalyst utilizations can be calculated which are many times higher than for static systems. The practical significance of these results must await further engineering evaluation to determine the power requirements needed to operate a slurry catalyst system.

Other modifications to the slurry system do not improve performance. Supported platinum catalysts are not active, except with a carbon substrate. However, no additional catalyst utilization advantage is found in this case. Buffer electrolytes support low current density activities with methanol and decane equivalent to those in sulfuric acid, but at current densities above about 20 ma/cm2 instability and poorer performance occur. These effects appear related to catalyst wetting phenomena noted also in acid electrolyte.

Phase 5 - New Materials

Preliminary studies suggest that nuclear-grade zirconium, as well as boron carbide and boron nitride may resist anodic corrosion in sulfuric acid. Hence, they deserve further study to evaluate their usefulness in fuel cell components.

Phase 6 - Phthalocyanine-Based Catalysts

The phthalocyanine compounds of base metals are not active catalysts for the reduction of oxygen or the oxidation of hydrocarbons in sulfuric or phosphoric acids. Mixing platinum with these compounds does not result in any clear-cut synergistic effect, although certain of the phthalocyanines appear to beneficially

wetproof their carbon substrates. The phthalocyanines are stable under cathodic conditions in sulfuric acid and to a lesser extent in phosphoric acid. Under anodic conditions, however, considerable decomposition occurs.

5.4 Task D, Methanol Electrode

Phases 1 and 2 - Preparation and Performance of Platinum-Ruthenium Catalysts; Characteristics of Modified P-type Catalysts

The performance of platinum-ruthenium catalysts can be improved to levels comparable to those of the P-type catalyst by activating the catalyst in a basic solution. The stability of this catalyst, especially when overpolarized, is excellent and does not depend on the amount of methanol present.

The susceptibility of the P-type catalyst to losing performance as a result of overpolarization can be significantly reduced by stabilizing with potassium ions. However, the degree of stabilization depends upon the methanol concentration in the electrolyte. The P-type catalyst can be further improved in both performance and stability by the controlled addition of ruthenium. This catalyst is the most active methanol catalyst developed to date. The preparation of this catalyst is somewhat slow. However, a procedure that will produce a slightly less active catalyst, but is relatively fast is available. The procedure consists of fabricating the electrode in a less active, agglomerated form and then activating in base.

Phase 3 - Procedures Aimed at Enhancing Methanol Performance

Several new methods of preparing methanol catalysts were developed. One using radical anion reduction showed little advantage over other techniques presently in use. A second, involving the co-reduction and subsequent removal of silver, produced platinum electrodes with almost twice the surface area and three times the performance of commercially available platinum black. In addition, attempts to improve upon the structure of these electrodes through the addition of binders proved unsuccessful.

Studies of the preparation of co-metal catalysts of ruthenium and noble metals other than platinum showed that active methanol catalysts can be made without the use of platinum. An iridium-ruthenium catalyst proved to have exceptionally high activity.

Phase 4 - Double Layer Capacitance Studies on Pt-Re_2O_7-Methanol Systems

The adsorption of methanol and Re_2O_7 on a platinum surface has been shown to result in significant changes in the measured double layer capacitance. Under conditions of optimum performance, the rhenate ions occupy about 60 to 80% of the available platinum surface with methanol covering the remaining sites. This finding confirms the inferences of prior studies indicating that the fuel reacts with a pre-adsorbed rhenate layer that covers most of the surface.

5.5 Task E, Air Electrode

Phase 1 - Thin Carbon Electrodes

The most important variables in the preparation of thin carbon electrodes are the use of a platinum reimpregnation technique for maximum performance and a radical anion reduction for maximum catalyst utilization. These electrodes perform

better in 3.7 M sulfuric acid at 100°C than in 14.7 M phosphoric acid at 150°C. The former condition will, therefore, be retained for screening work. The flooding of the thin carbon structure, associated with high hydrostatic pressures, can be prevented by application of a 40 to 60% porous Teflon layer to the gas side. In this way scale-up of this electrode is permitted, as well as a reduction in the overall thickness. Catalyst densities down to 1.2 mg/cm^2 can be used with no loss in performance. Below this level, however, a constant catalyst utilization is reached, resulting in lower performance with decreasing catalyst loading. These results show that the thin carbon electrode with a porous Teflon layer offers an active and efficient air electrode structure.

Phase 2 - Platinum-Teflon Electrodes

Teflon-coated platinum-Teflon electrodes show proportional increases in performance with catalyst densities between about 1.5 and 14 mg/cm^2. Above 14 mg/cm^2 performance is constant, indicating a drop in catalyst utilization. At the 1.5 mg/cm^2 level, utilization is doubled by incorporating powdered gold to increase the electrical conductivity of the electrode. At very high catalyst densities, utilization is improved by use of a multi-layer structure consisting of alternate strips of platinum-Teflon and Teflon. Overall utilization is still inferior to the thin carbon structures, however.

Phase 3 - Platinum and Gold Oxygen Catalysts

The importance of surface oxide layers to the performance of platinum-containing oxygen catalysts was confirmed by experiments in which platinum was pretreated by either anodization or cathodization. In both cases, the subsequent return to steady state was slow and approached from a lower polarization in the case of the cathodized sample and from a higher polarization by the anodized sample. The addition of gold to platinum did not shift the potential at which the surface oxide formed. However, in the case of melted alloy samples, the presence of 10% or more gold inhibited completely the oxide formations of both metals. In addition, the catalytic activity decreased with increasing gold content. Powdered platinum-gold samples and those supported on carbon, however, gave normal oxide peak and catalytic behavior. Although the cause of these differences is not known, it does not appear that the oxygen catalytic activity of platinum is improved by gold addition. An open-circuit potential corresponding to that of oxygen, 1.23 volts, was observed on gold following vigorous anodization. However, this was traced to the formation of a gold oxide layer under these conditions rather than oxygen reduction.

Phase 4 - Oxygen Catalysts for Buffer Electrolytes

Silver catalysts for eventual use in buffer electrolytes are capable of high current densities and appear insensitive to methanol. However, they are highly polarized and the best activities are obtained only with carbon supports, which introduce high ionic concentration polarizations in buffer solutions.

5.6 Task F, Methanol Fuel Cell

Phase 1 - Single Cell Engineering Research

Use of a membrane clad cathode in total cell operation has resulted in improved performance. Maximum power increased from 26 mwatts/cm^2 to 31 mwatts/cm^2 at 60°C. The clad cathode insures uniform, intimate contact between the cathode and membrane which results in lower resistance and less tendency for CO_2 gas accumulation. Thus, ohmic polarization is reduced. It also permits more effective

reduction of O_2 over the entire cathode surface which reduces cathodic polarization. Finally, since O_2 reduction suppresses methanol oxidation at the cathode, the compatibility is improved. Tests of fuel and air distribution in the 4" x 4" single cells showed that reactant distribution is satisfactory.

Phase 2 - Single Cell Operation With Improved Methanol Catalysts

Evaluation of three new catalysts in total cell operation established that the ruthenium modified P-type catalyst is best for further single cell and multicell work. Performance in total cells with this catalyst improved, maximum power increasing to 45 mwatts/cm^2 at 82°C. Electrodes made with this catalyst were more chemically stable than P-type catalyst stabilized by potassium and more mechanically stable than platinum-ruthenium. Scale-up studies in 9" x 5-3/4" cells showed that electrode performance of both the ruthenium modified P-type anode and clad cathode was equivalent to results in 4" x 4" cells. However, higher resistance in the larger cell remains a problem.

5.7 Task G, Prototype Development

Phase 1 - Multicell Engineering Research

The design of a methanol battery for research was completed. Based on this design, considerations of problems of battery operation were extended. Considerable improvement in efficiency of electronic control is possible for the higher fuel cell performance demonstrated in single cell work with the ruthenium modified P-type catalyst. Results of air distribution studies in half cells, total cells, and multicell units have confirmed that the present 9" x 5-3/4" cell design requires at least five times stoichiometric air flow to insure uniform cell performance. In studies of start-up in multicell assemblies, methanol oxidation at the cathode has been shown to be an effective technique for accelerating the initial heating of the fuel cells.

Phase 2 - Multicell Operation

Studies in multicell stacks of 4" x 4" and 9" x 5-3/4" cells have been extended. In both sized units with P-type anodes, original performance targets (4) were achieved in initial testing but performances losses resulted in both electrodes after continued operation. Anode deactivation resulted from sensitivity of the P-type catalyst to chemical and electrochemical oxidation and cathode performance declined because of increased ohmic polarization. Studies with new components from single cell work have been initiated. Using ruthenium modified P-type anodes and clad cathodes, ohmic resistance free performance in a six cell 9" x 5-3/4" stack approached the new expected levels. However, high resistance in the large cell previously observed in single cell tests also appeared in the multicell evaluations. Thus, further changes in this cell design will be made.

SECTION 6

PROGRAM FOR NEXT INTERVAL

The studies carried out in hydrocarbon fuel cells during the first half of 1964 have been directed to uncovering the causes for performance limitations and exploring catalytic and electrode structural approaches for overcoming these limitations. The techniques used in this aspect of the program have been largely those applied successfully to bring the methanol cell to its present state of development. However, work on radically new approaches has been initiated and may prove even more effective. Both avenues will be followed during the remainder of the year with increasing emphasis on low cost catalyst systems and exploitation of the buffer electrolyte cell.

The methanol fuel cell has achieved promising performance levels in short term laboratory cells. Further work will be directed towards translating the new components into multicell systems. However, research on methanol cells will continue with the objective of improving catalyst performance and capabilities, as well as reduce costs.

The past and projected distribution of effort on each of these tasks are as follows. The emphasis will depend on the rates of progress in each area.

		Effort Expended in 1964, %	
		Actual	Projected
Task	Title	January-June	July-December
A	Hydrocarbon Electrode	31	37
B	Hydrocarbon Fuel Cell	2	1
C	New Systems	25	15
D	Methanol Electrode	13	10
E	Air Electrode	8	4
F	Methanol Fuel Cell	11	7
G	Prototype Development	10	26

Research and development is expected to concentrate during the latter half of the year as follows:

6.1 Task A, Hydrocarbon Electrode

Future research efforts will continue to deal with both electrode structure and electrode catalysis. The work will continue to be directed toward the use of liquid hydrocarbons in the jet fuel boiling range operating at the lowest possible operating temperatures with non-noble catalysts or catalysts containing less than 1 mg platinum per cm^2 or its equivalent. In the area of non-noble catalysts two approaches will be taken. One will be to incorporate Group VII or VIII metals into compounds stable enough to resist corrosion yet still active enough to be catalytic, such as mixed oxides, carbides, nitrides, borides, or silicides. Recently reported refractory mixed compounds of this type will be examined. The second approach will be to use alloys of non-noble metals in buffer electrolytes,

making use of regions of their phase diagrams in which unusual thermodynamic stabilization exists. This may provide added corrosion resistance. In the noble metals area the approach will be to prepare alloys to modify the catalyst structure or to augment its surface redox properties. In addition, means will be sought to use carbon and other supports to reduce the expensive metal requirements by a factor of at least ten. Following preliminary tests to verify that the butane system is sensitive to catalyst differences, as suggested by the mechanism studies, that system will be used to screen catalysts, with minimum electrode structure complications. Those catalysts which appear promising will be tested with liquid decane.

The work on the low temperature steam reforming catalysts will initially emphasize their incorporation into electrodes, which means solution of the conductivity and handling problems. Should the activity of these catalysts prove to be too low at 100°C attempts will be made to use non-corrosive electrolytes at temperatures up to 250°C. Consideration will also be given to the use of these catalysts in separate steam reforming chambers.

The structure work in the hydrocarbon area will involve control of the catalyst distribution and the wetting properties of the electrode. The variables to be studied include the binder type, form and particle size, the properties of the Teflon-catalyst gel, the sintering conditions, and the use of barriers or gas spaces. All of these variables will be altered when necessary to suit new catalysts or catalysts on carbon or other supports. In addition, the benefits of fluorocarbon acid electrolytes, or additives such as FC-95, will continue to be explored with the new structures. It is expected by these means to be to attain performances with liquid fuels at least equal to those now obtained with gases.

6.2 Task B, Hydrocarbon Fuel Cell

The total cell facility will continue to be used for evaluations of promising new electrode and electrolyte systems. The extent to which this unit is tested will depend upon the rate of progress in the development of new components. However, little effort in this area is expected during the next six months.

6.3 Task C, New Systems

Buffer solutions have been shown to be electrolytes capable of supporting high current densities at practical cell voltages. Therefore, work to further improve on these performance levels in these non-acid but CO_2 rejecting electrolytes will continue, largely emphasizing research on non-noble catalysts. In addition, buffer solutions of higher concentrations and of other compositions will be investigated. The slurry catalyst system will be examined from an engineering standpoint, with emphasis on establishing its feasibility. Studies of the effects of catalyst particle size and of gaseous reactants will also be made however, to provide data for the engineering evaluations.

Other areas to be investigated include new methods of hydrocarbon electrode operation, including various types of fuel delivery systems and the effects of intermittent fuel supply. These concepts will be combined with recent advances in electrode structures to see if further benefits are possible. Still another study will determine the feasibility of low temperature dehydrogenation of methanol to yield hydrogen and formaldehyde. These reactants, when fed to fuel electrodes, should offer enhanced reactivity compared to methanol.

6.4 Task D, Methanol Electrode

With the development of active methanol catalysts, the research effort will center on improving the performance of these catalysts, particularly with regard to extending their life under a variety of operating conditions, and to lowering their costs. Efforts will be made to establish high performance using less pure fuel stocks at low temperatures and high acid concentrations. Studies will be made on improving the electrodes by incorporating various plastic binders into the structures. Attempts will also be made to reduce the catalyst loading by supporting on carbon or dilution by conductive inerts. Also work aimed at finding less expensive active catalysts will continue.

6.5 Task E, Air Electrode

A variety of good structures are available for air electrode use in acid electrolyte. However, satisfactory structures are still needed for buffer electrolytes to minimize ionic concentration effects. Therefore studies will be carried out aimed at optimizing the flow-through properties of the cathode. Catalysis continues to be of prime importance, regardless of the electrolyte. Work will continue on developing more active and less expensive catalysts. One area will investigate the importance of geometric factors to air electrode catalysis. Another program will continue to study silver-containing catalysts, which have already demonstrated some activity and insensitivity to the presence of methanol. In addition, other non-noble catalysts will be tested in buffer electrolyte.

6.6 Task F, Methanol Fuel Cell

The large polypropylene cells have demonstrated their ruggedness and reliability. However, work is needed to improve their design to increase performance to the levels obtained in the smaller Teflon cells. This will require more detailed analysis of the problems of conduction of current in large cells. Specifically, sources of higher internal resistance must be found and corrected. These cells, together with smaller Teflon and polypropylene units, will be used to evaluate cell components during long term, sustained operation. In addition, studies will be made of lower temperature performance to establish operability during startup. Also, the mode of operation of the cell will be simplified, thereby minimizing requirements in the auxiliaries needed for battery operation. In particular, the need for electrolyte circulation will be evaluated and alternate methods for fuel injection and mixing and prevention of concentration polarization explored.

6.7 Task G, Prototype Development

Work is continuing on the development of operable multicell units. The entire effort will concentrate on the larger 9" x 5-3/4" polypropylene cell stacks. Additional units having greater numbers of cells will be employed. These units will be used to study the problems attendant to their operation in terms of their effects upon the performance of the individual cell components as well as the performance of the units as whole entities. Particular attention will be given to redesigning these units to eliminate cell inefficiencies caused by excessive ohmic losses in the current collection system, current leakage between cells, and maldistribution of both fuel and air in their manifolds.

Efforts will also be directed toward improving the techniques used in both the preparation of large quantities of catalyst and for the fabrication of the large electrodes. Identifying the causes of any voltage debits associated with the scale-up of these procedures and minimizing their effects will be of paramount concern. In addition attention will also be given to such problems as establishing methods for controlling fuel concentration, water balancing, temperature maintenance, and startup.

SECTION 7

IDENTIFICATION OF PERSONNEL AND DISTRIBUTION OF HOURS

7.1 Background of New Personnel

John S. Batzold (Ph.D., Physical Chemistry, McGill University) has been at Esso Research since 1952 engaged in research in the areas of gasoline combustion, lubrication, radio tracers, corrosion, surface chemistry, and electrochemistry, and has one publication concerning engine lubrication. His present assignment is directed toward improving the components of the methanol fuel cell.

Morton Beltzer (Ph.D., Physical Chemistry, Polytechnic Institute of Brooklyn) has been with Esso Research since 1959, most of that time in the Fuel Cell Section. His projects have included the development of new electrode structures. Dr. Beltzer has one publication on redox polymers and six patent applications in the area of fuel cells. He is presently working on buffer electrolytes.

George Ciprios (M.S., Chemical Engineering, Columbia University) has been at Esso Research since 1956 working on a variety of petroleum processes areas. His projects also included studies of the rheological behavior of lubricants and other petroleum components. He is co-author of a chapter on thermal and catalytic cracking, and refining in "Modern Petroleum Technology." He is currently engaged in the development of improved fuel electrode structures.

Hugh H. Horowitz (Ph.D., Organic Chemistry, Columbia University) has had eleven years of experience all with this company, in fuel cells and, prior to that, in organic, polymer, and surface chemistry, hydrodynamic lubrication and rheology. He has about 15 publications in lubrication, and polymer and organic chemistry, and has two patents and about seven pending.

Donald E. LeClair (B.S., Mechanical Engineering, University of Massachusetts) came to Esso Research in February, 1964 from Gilbert & Barker Manufacturing Company, the manufacturing affiliate of Standard Oil (N. J.). He has served in the Critical Skills Program of the U.S.A.F. and brings with him 7 years experience in such areas as design, manufacturing, and R & D. He has two patents in the field of valve design and manufacture and is presently working on design and development of fuel cell hardware and auxiliaries.

John M. Matsen (Ph.D., Chemical Engineering, Columbia University) has been at Esso Research since 1961. His doctoral dissertation was in the area of redox fuel cells. He has also worked in areas of catalysis, adsorption separations, equilibrium and transport properties and has twelve publications in those fields. Presently he is responsible for component and system development in the methanol cell.

Gershon Metzger (Ph.D., Columbia University) has been with Esso Research since 1960 after spending one year as a Post Doctoral Research Associate at Columbia. His specialty is organic chemistry -- synthetic as well as kinetic, mechanism and analytical work. He has 13 publications and presentations and 2 patents pending.

Charles E. Morrell (Ph.D., University of Minnesota) has 29 years of industrial experience, all at Esso Research. His work has been in various areas of organic and physical chemistry, and has resulted in about 30 publications and 75 patents.

William F. Taylor (M.S., Chemical Engineering, Ohio State University; M.S., Statistics, Rutgers University) has been with this company since 1957 working in petroleum process development and the preparation and kinetic and mechanism analysis of catalysts. He has 15 patent applications and three publications in the catalysis area.

Charles E. Thompson (Ph.D., University of Nebraska) has had 13 years experience in fuel cell research, organic synthesis and catalysis, all at Esso Research. He has 9 patents with 10 pending and two publications in the area of catalysis.

7.2 Distribution of Hours

The following are the technical personnel who have contributed to the work during the reporting period 1 Jan. 1964 - 30 June 1964 and the approximate number of hours of work performed by each:

John S. Batzold	906
Morton Beltzer	942
George Ciprios	655
I-Ming Feng	926
Carl E. Heath	926
Eugene L. Holt	958
Hugh H. Horowitz	956
Donald E. LeClair	934
Duane G. Levine	950
John M. Matsen	765
Gershon Metzger	925
Andreas W. Moerikofer	949
Charles E. Morrell	760
Eugene H. Okrent	938
Joseph A. Shropshire	936
Barry L. Tarmy	919
William F. Taylor	705
Charles E. Thompson	935
James A. Wilson	816
Charles H. Worsham	786
Total	17,587

SECTION 8

REFERENCES

(1) Heath, C. E., Tarmy, B. L., et al, Soluble Carbonaceous Fuel-Air Fuel Cell, Report No. 1, Contract DA 36-039 SC-89156, 1 Jan. 1962 - 30 June 1962.

(2) Tarmy, B. L., et al, Soluble Carbonaceous Fuel-Air Fuel Cell, Report No. 2, Contract DA 36-039 SC 89156, 1 Jan. 1962 - 31 Dec. 1962.

(3) Tarmy, B. L. et al, Soluble Carbonaceous Fuel-Air Fuel Cell, Report No. 3, Contract DA 36-039 AMC-00134(E), 1 Jan. 1963 - 30 June 1963.

(4) Tarmy, B. L. et al, Soluble Carbonaceous Fuel-Air Fuel Cell, Report No. 4, Contract DA 36-039 AMC-00134(E), 1 Jan. 1963 - 31 Dec. 1963.

(5) Osteryoung, R. A., et al, Anal. Chem., 34, 1833 (1962) also J. Electrochem. Soc., 110, 926 (1963).

(6) Demchenko, V. V., Zhur. Fiz.Khim., 37, 1849 (1963).

(7) Gerischer, H., Ber. Bunsenges physik. Chem., 67, 164 (1963).

(8) Gerischer H., Held, J., ibid, 921.

(9) U.S. Patent 2,177,412.

(10) Popat, P. V., Kuchar, A., Materials Compatibility Studies, Technical Summary Report 4, Contract DA-44-009-ENG-4909, 1 July 1963 - 31 December 1963.

(11) Smith, J. O., et al, Research To Improve Electrochemical Catalysts, First Quarterly Progress Report, Contract DA-44-009-AMC-202(T), 15 May 1963 - 15 August 1963.

(12) Dourif, H., Thomas, A. W., Phthalocyanine Compounds, Rheinhold Publishers, New York, New York, 1963.

(13) Hoare, J. P., J. Electrochem. Soc., 109, 858 (1962).

(14) Feldberg, S. W., et al, J. Electrochem. Soc., 110, 826 (1963).

(15) Buck, R. P., Griffith, L. I., J. Electrochem. Soc., 109, 1005 (1962).

(16) Bold, W., Breiter, M., Electrochemica Acta, 5, 145 (1961).

(17) Gilman, S., J. Phys. Chem., 66, 2657 (1962).

APPENDIX A-1

EVALUATION OF POLARIZATIONS

In order to place our reported polarizations on a realistic basis all reported values are corrected for the effects of liquid junction potentials. Use has been made of the calculated and measured parameters in Figure A-1 in determining the appropriate corrections.

Figure A-1

Calculated and Measured Potentials

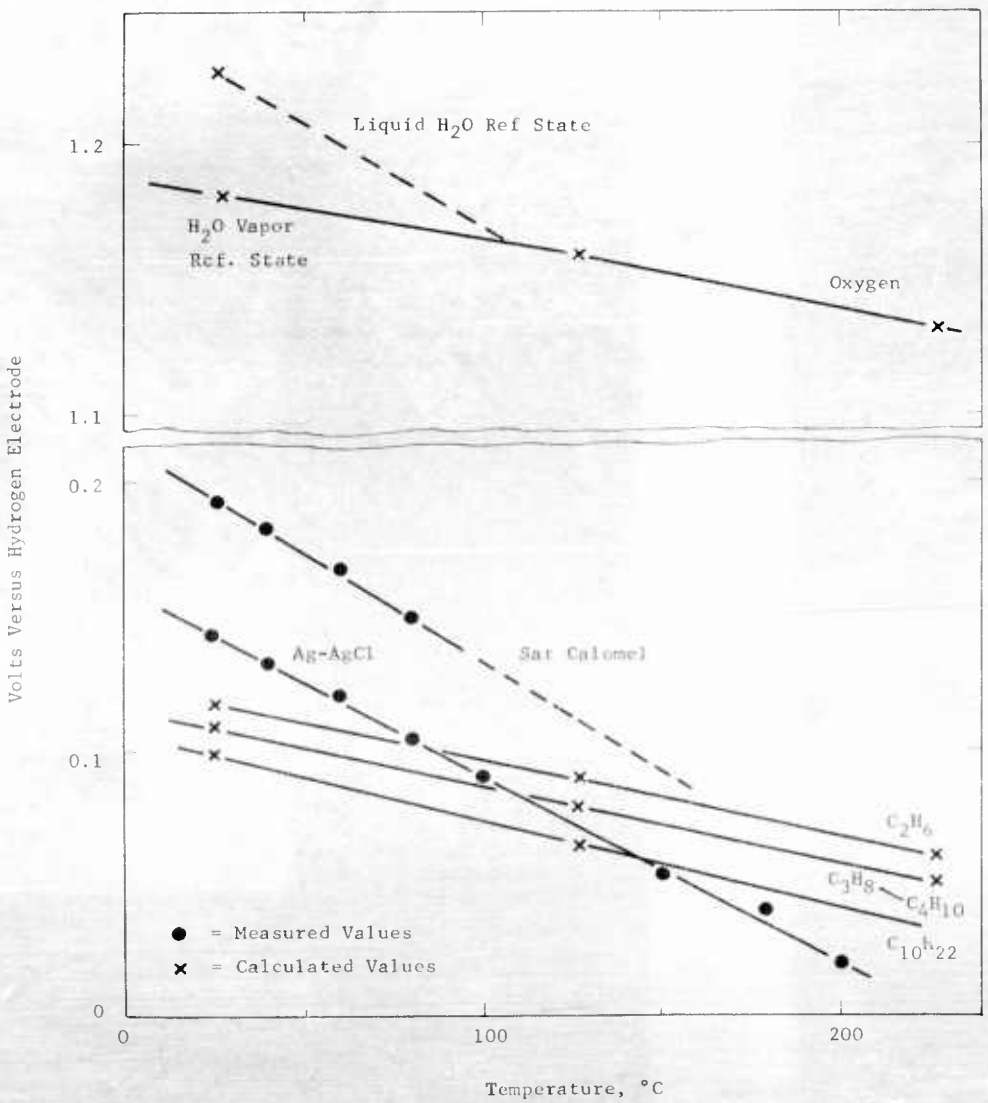

APPENDIX A-2

DIAGRAM OF FLANGE CELL

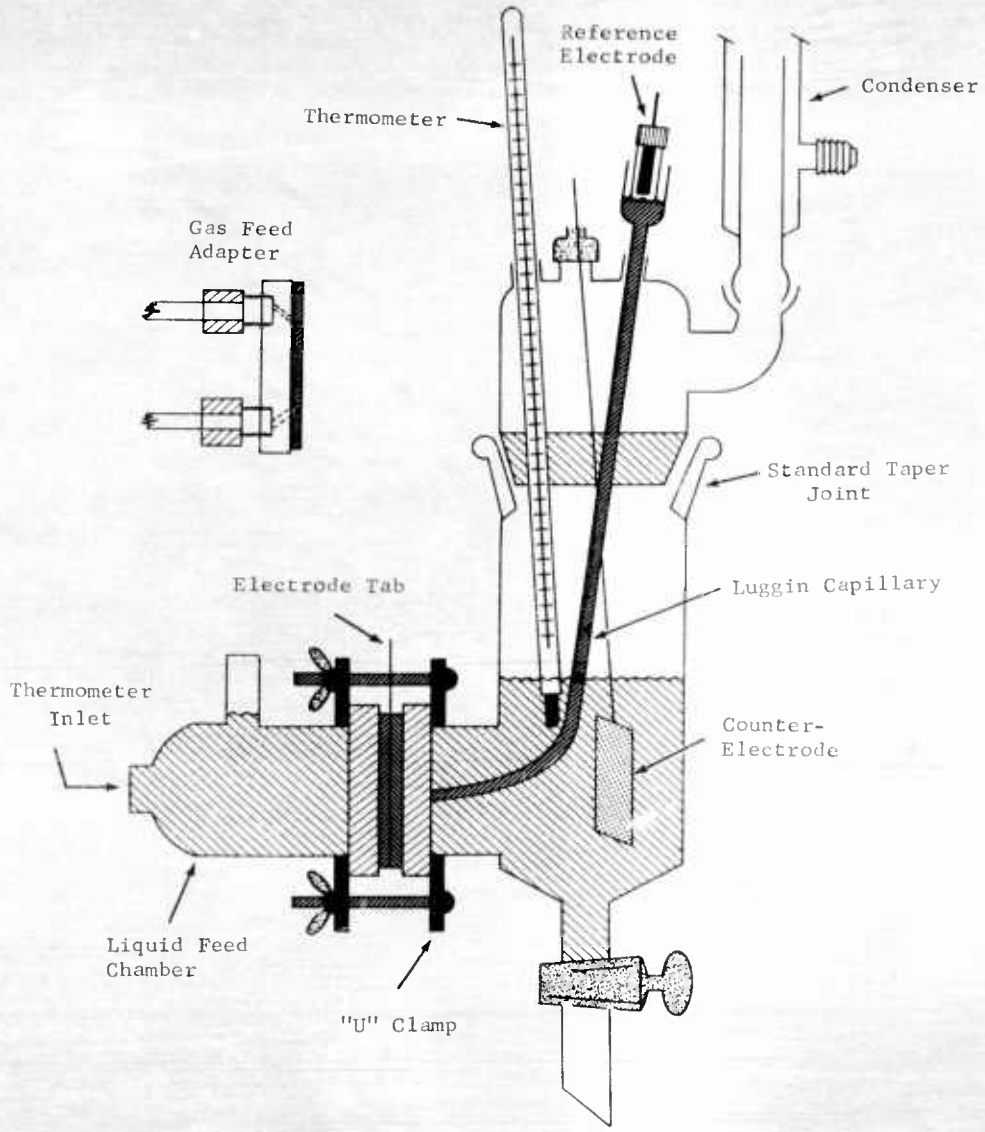

APPENDIX A-3

EXPLORATORY PERFORMANCE RUNS - DECANE

Temp, °C	Electrolyte	Polarization At Indicated ma/cm², volts 0	0.5	1	2	5	10	Limiting Current, ma/cm²	Remarks
100	3.7 M H_2SO_4	0.18	0.20	0.22	0.23	0.29	0.37	20	Liquid Decane
105	6 M H_2SO_4	0.12	0.16	0.18	0.20	0.25	0.34	18	"
100	3.7 M H_2SO_4	0.18	0.24	0.28	0.33	0.46	--	9	"
100	"	0.08	0.19	0.24	0.28	0.36	--	10	"
100	"	0.05	0.22	0.27	0.31	0.40	--	8	"
100	"	0.03	0.16	0.20	0.24	0.31	--	8	Steam distilled feed.
100	"	0.03	0.16	0.20	0.27	0.34	--	7	Steam distilled feed.
100	"	0.30	0.38	0.43	0.47	--	--	3	Pt on carbon-steam distilled feed.
140	14.7 M H_3PO_4	0.07	0.09	0.11	0.15	0.24	0.40	15	Argon carrier gas through decane feed reservoir at 120°C. Pt-on carbon + Teflon electrode.
100	0.5 M H_2SO_4	0.06	0.08	0.13	0.27	0.35	--	8	Steam distilled feed.
140	14.7 M H_3PO_4	0.13	0.21	0.24	0.26	0.38	--	7.5	Pt-on-carbon-heptane + Argon feed at 75°C.
150	14.7 M H_3PO_4	0.10	0.16	0.18	0.23	0.39	--	6	Pt-Teflon-heptane + Argon - 88°C.
100	3.7 M H_2SO_4	0.15	0.28	--	--	--	--	1	Pt-Teflon-Argon + heptane at 90°C.

1. Pt-Teflon (2:1) electrode, 1 cm^2 area, 30-35 mg Pt/cm^2, except as noted.

APPENDIX A-4

Typical Voltage Scan on Decane Fuel

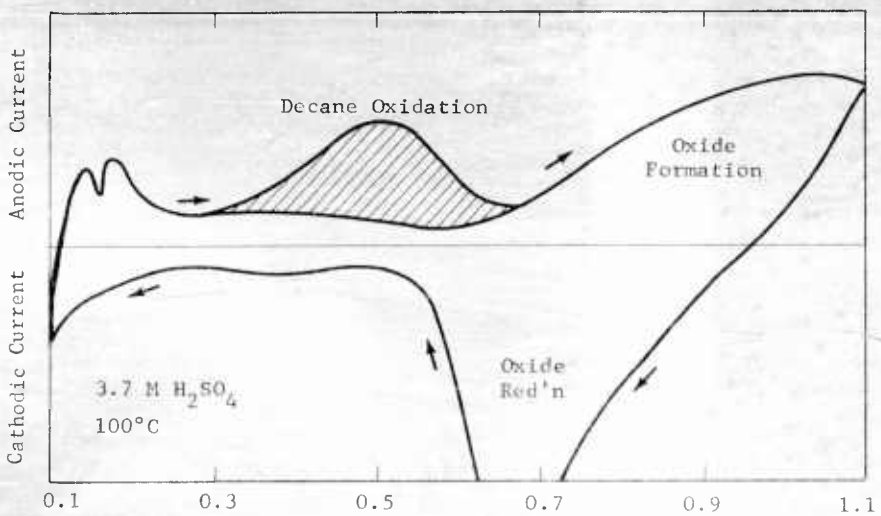

Volts Versus Hydrogen in Same Electrolyte

APPENDIX A-5

VOLTAGE SCAN MEASUREMENTS ON DECANE

Pt Teflon (2:1) Electrode, 1 cm^2 Apparent Area, 0.0-1.0 volts versus S.C.E. Scan

Electrolyte	Temp. °C	Scan Rate sec/volt	Decane Peak (Millicoulombs/cm^2)	Remarks
3.7 M H_2SO_4	100	30	212.5	Continuous sweep.
"	"	"	311	15 sec wait @ 0.0 versus S.C.E.
"	"	"	376	30 sec wait @ 0.0 versus S.C.E.
"	"	"	469	1 min wait @ 0.0 versus S.C.E.
"	"	"	589	2 min wait @ 0.0 versus S.C.E.
"	"	"	772	5 min wait @ 0.0 versus S.C.E.
"	"	"	794	7 min wait @ 0.0 versus S.C.E.
"	"	"	925	10 min wait @ 0.0 versus S.C.E.
"	"	"	1028	30 min wait @ 0.0 versus S.C.E.
3.7 M H_2SO_4	60	10	5.2	
"	"	20	18.5	
"	"	30	30.4	
"	"	40	39.3	
3.7 M H_2SO_4	80	10	12.0	
"	"	20	32.6	Temperature effect study--liquid
"	"	30	55.9	decane feed.
"	"	40	84.5	
3.7 M H_2SO_4	100	10	15.4	
"	"	20	111.0	
"	"	30	234.5	
"	"	40	319.5	
3.7 M H_2SO_4	100	30	160	$C_{10}H_{22}$ 5.13 M.
"	"	"	85.8	2.56 M $C_{10}H_{22}$ in cetane.
"	"	"	10.8	0.856 M $C_{10}H_{22}$ in cetane.
"	"	"	~ 0	0.513 M $C_{10}H_{22}$ in cetane.
"	"	30	130.0	5.13 M $C_{10}H_{22}$.
"	"	"	74.9	2.56 M $C_{10}H_{22}$ in cetane.
"	"	"	12.4	0.856 M $C_{10}H_{22}$ in cetane.
"	"	"	~ 0	0.513 M $C_{10}H_{22}$ in cetane.
0.5 M H_2SO_4	80	40	130.2	
1 M H_2SO_4	"	"	95.5	
3 M H_2SO_4	"	"	73.0	
5 M H_2SO_4	"	"	33.4	
7 M H_2SO_4	"	"	56.8	
9 M H_2SO_4	"	"	105.6	
0.5 M H_2SO_4	"	20	99.2	Acid concentration study.
1 M H_2SO_4	"	"	80.3	
3 M H_2SO_4	"	"	32.4	
5 M H_2SO_4	"	"	26.8	
7 M H_2SO_4	"	"	33.5	
9 M H_2SO_4	"	"	80.5	
3.7 M H_2SO_4	100	20	79.0	Silica gel treated decane.
"	"	30	94.7	
"	"	60	186.3	
"	"	120	362.0	
14.7 M H_3PO_4	80	40	13.7	H_3PO_4 electrolyte comparison.
"	100	"	37.1	ΔE^* apparent 14.4 kcal/mole.
"	120	"	152.0	
"	140	"	current oscillation-erratic	

(1) Liquid decane feed except as noted.

APPENDIX A-6

PERFORMANCE RUNS ON BUTANE

Temp, °C	Electrolyte	Polarization At Indicated ma/cm², volts 0	1	5	10	20	Limiting Current, ma/cm²	Remarks
95	3.7 M H_2SO_4	-0.06	0.07	0.15	0.19	0.27	25	Temperature study, same electrode, internally consistent set
75	"	0.08	0.160	0.24	0.31	--	15	
55	"	0.80	0.25	0.41	--	--	7.5	
95	"	-0.05	0.03	0.12	0.16	0.24	25	Acid concentration change.
95	0.5 M H_2SO_4	-0.03	0.05	0.12	0.17	0.27	25	
95	3.7 M H_2SO_4	0.0	0.04	0.12	0.18	--	20	
95	3.7 M H_2SO_4	0.07	0.08	0.20	--	--	6.5	14 mol % butane in Argon.
150	14.7 M H_3PO_4	-0.03	0.06	0.13	0.17	0.47	20	
95	3.7 M H_2SO_4	-0.15	0.03	0.15	--	--	7	Electrode activity poor.
75	3.7 M H_2SO_4	0.03	0.12	--	--	--	5	Temperature study
55	3.7 M H_2SO_4	-0.03	0.24	--	--	--	3.5	
100	3.7 M H_2SO_4	-0.10	-0.06	0.01	0.06	--	20	
80	3.7 M H_2SO_4	-0.09	0.01	0.10	0.15	--	15	
100	3.7 M H_2SO_4	-0.02	0.02	0.11	0.18	--	15	Butane.
100	"	-0.02	0.04	0.12	--	--	10	1:1 butane/Argon.
100	"	-0.01	0.06	0.29	--	--	6	1:3 butane/Argon.
100	"	-0.05	--	--	--	--	0.8	1:3/98.7 butane/Argon.
110	3.3 M H_2SO_4	-0.06	0.03	0.09	0.15	--	15	
115	3.3 M H_2SO_4	0.05	0.15	0.25	0.40	--	10	
95	3.7 M H_2SO_4	0.10	0.15	0.23	0.30	--	15	Dry butane feed.
95	3.7 M H_2SO_4	0.10	0.15	0.23	0.30	--	15	Pre-equilibrated feed.
95	3.7 M H_2SO_4	-0.01	0.12	0.19	0.25	0.38	25	Pre-equilibrated feed
95	3.7 M H_2SO_4	0.10	0.13	0.20	0.25	0.50	20	Dry butane feed.
150	14.7 M H_3PO_4	-0.01	0.04	0.10	0.17	0.37	20	Pre-equilibrated feed
150	"	-0.02	0.05	0.14	0.20	0.29	25	Dry feed.
95	3.7 M H_2SO_4	0.03	0.06	0.17	--	--	6	P-type electrode, Ru modified.

Butane feed, pre-equilibrated with electrolyte, except as noted.
Pt-Teflon (2:1) by wt. 1 cm² area, 30-35 mg Pt/cm², hand pressed unless otherwise noted.

APPENDIX A-7

VOLTAGE SCAN MEASUREMENTS ON BUTANE

Pt-Teflon (2:1) Electrode, 1 cm^2 Area (Apparent), Butane Feed Pre-equilibrated

Electrolyte	Temp, °C	Scan Rate, sec/volt	Butane Peak, millicoulombs	Remarks
3.7 M H_2SO_4	95	20	759	Feed pre-equilibrated with
"	"	40	1263	electrolyte at 95°C, corrected
"	"	60	1791	with Argon blanks. See Fig. A-2.
"	"	100	2372	
3.7 M H_2SO_4	55	60	276	Temperature study-estimated
"	"	100	358	zero correction from Argon
3.7 M H_2SO_4	75	60	598	blanks above. See Fig. A-3.
"	"	100	847	
3.7 M H_2SO_4	95	60	1475	
"	"	100	1850	
0.5 M H_2SO_4	95	100	2185	Acid concentration study.
1 M H_2SO_4	"	"	2190	See Fig. A-4
3 M H_2SO_4	"	"	2320	
3.7 M H_2SO_4	"	"	2372	
5 M H_2SO_4	"	"	2830	
3.7 M H_2SO_4	95	20	335	Butane, pre-equilibrated.
"	"	40	633	Comparison set for runs below.
"	"	60	909	
"	"	100	1223	
3.7 M H_2SO_4	95	20	221	1:1 vol Argon-butane
"	"	40	400	
"	"	60	616	
"	"	100	997	
3.7 M H_2SO_4	95	100	884	Butane
"	"	100	315	3:1 vol Argon/butane

Figure A-2

Effect of Scan Rate on Butane Peak Coulombs

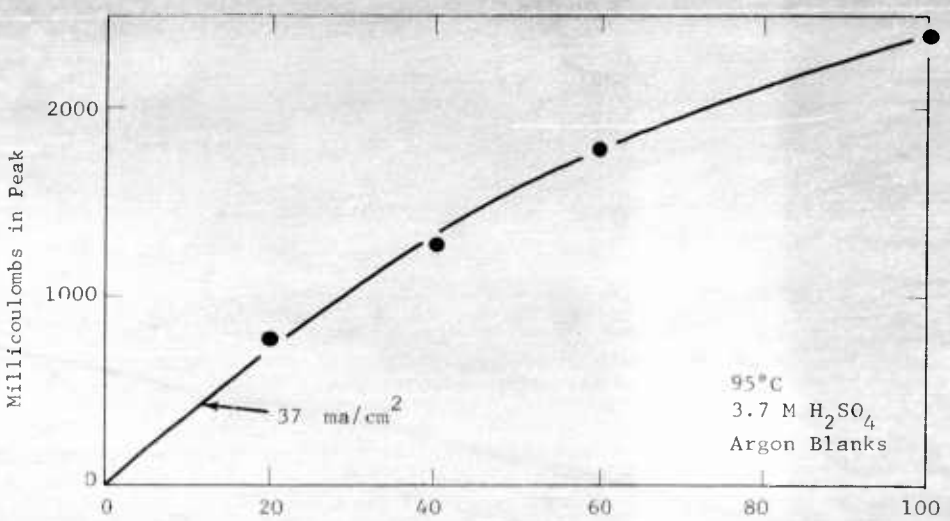

Reciprocal Scan Rate, sec/volt

Figure A-3

Effect of Temperature on Coulombs in Butane Peak

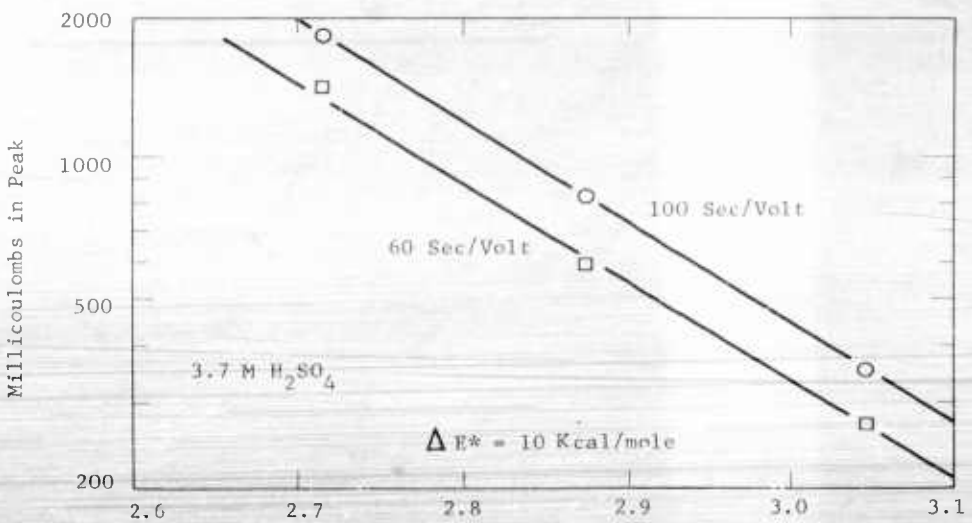

$1/T \times 10^3$ ($°K^{-1}$)

Figure $\overline{A}$-4

Effect of Acid
Concentration on Coulombs in Butane Peak

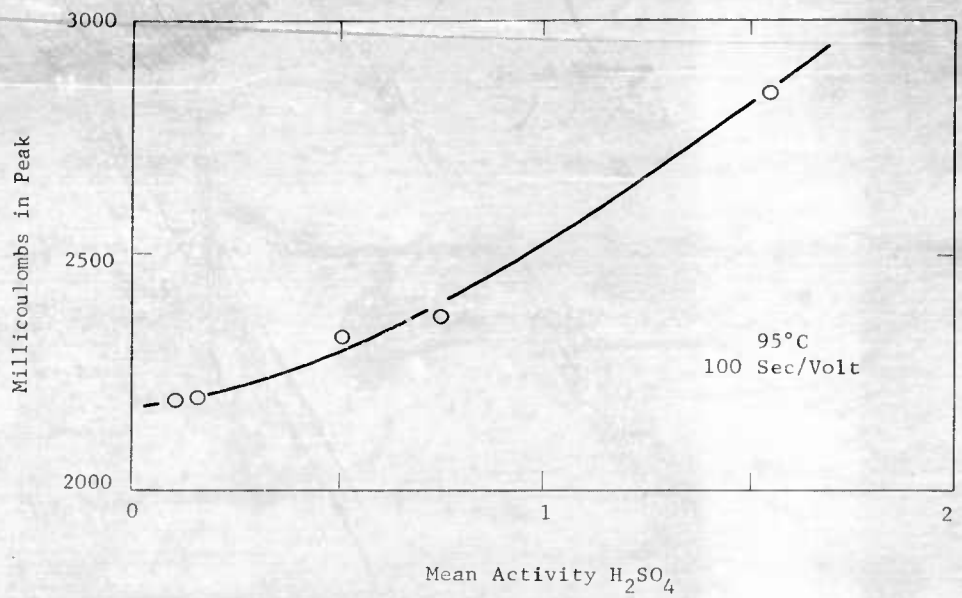

APPENDIX A-8

EFFECTS OF BUTANE CONCENTRATION ON PERFORMANCE

Steady State Performance

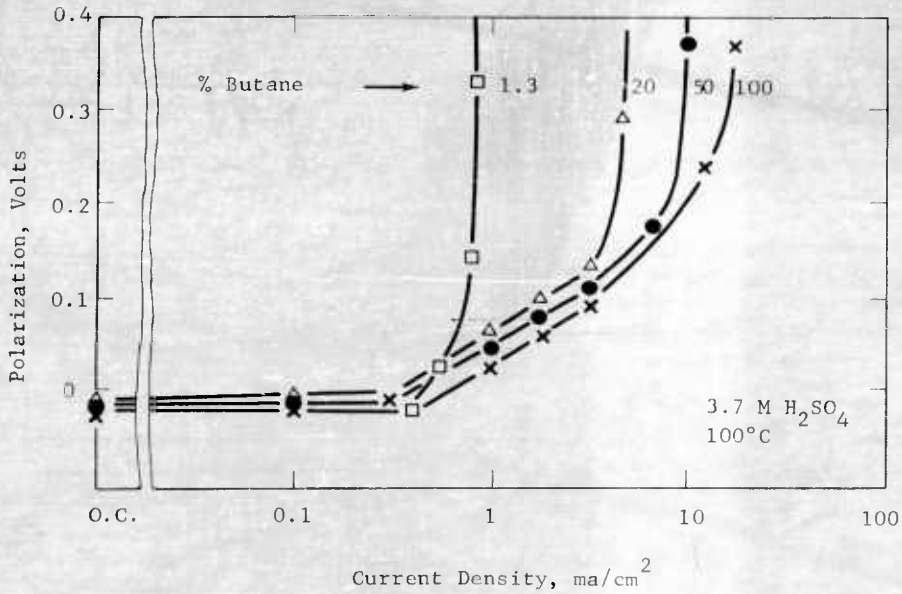

Coulombs in Voltage Scan

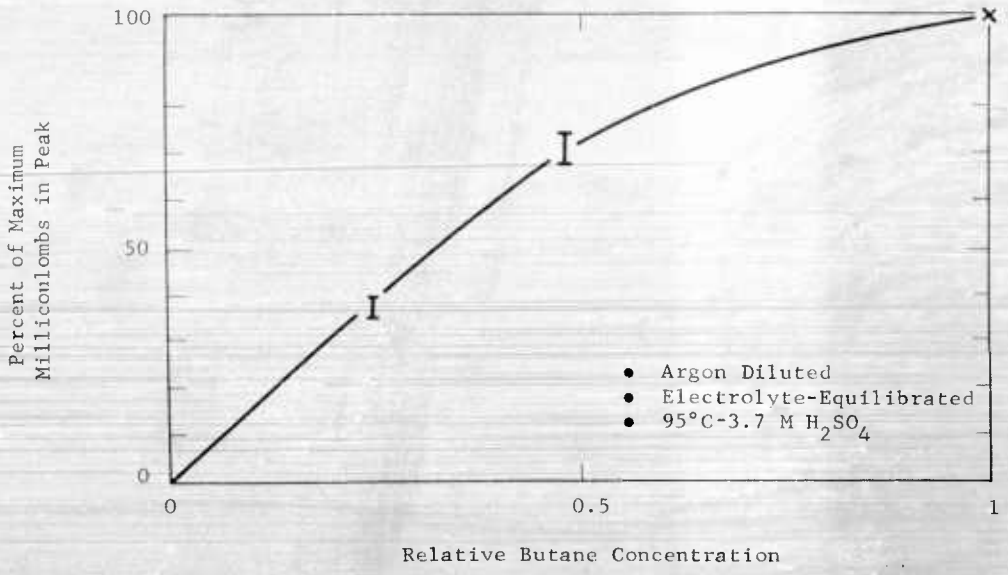

APPENDIX A-2

NCAKE ELECTRODE DATA SUMMARY - INTERFACE MAINTAINING ELECTRODES

Electrode	Catalyst Loading mg cm^{-2}	Fabrication Pressure, psi	Fabrication Thickness, mils	Designation Number	Temp °C	Electrolyte Composition M(e)	Polarization At Indicated ma cm^{-2}, Volts 0	2.1	7.2	7.1	23	12.2	13	17.2	Remarks
PDT 211	50	1500(a)	--	2318-3	25	3.7	0.14	--	0.36	--	0.55	X(d)	0.95	--	30 minutes per point.
PDT 211	25	1500(a)	--	2318-12	25	3.7	--	--	0.32	0.46	0.66	X(d)	--	--	Repeat.
PDT 211	100	1500(a)	--	2318-12	25	3.7	0.15	--	0.38	0.54	0.92	--	--	--	2 hours per point.
PDT 211	100	1500(a)	--	2318-12	25	3.7	0.18	--	0.46	0.93	0.73	--	--	--	
Catalyst Loading Study															
PDT 211	25	1500	--	2318-21A	25	3.7	0.13	0.38	0.46	0.60	0.60	--	--	--	
PDT 211	50	1500	--	2318-31B	25	3.7	0.12	0.34	0.44	0.52	0.67	--	--	--	
PDT 211	100	1500	--	2318-21B	25	3.7	0.14	0.22	0.34	0.38	0.42	0.48	0.58	0.64	
PDT 211	100	1500	--	2318-31A	25	3.7	0.10	0.30	0.41	0.44	0.56	0.64	--	--	1% TD-135 in electrolyte.
PDT 211	200	1500	--	2318-21A	25	3.7	0.13	0.24	0.28	0.34	0.38	0.56	0.70	--	
PDT 211	400	1500	--	2318-2E	25	3.7	0.38	0.21	0.35	0.47	0.60	0.72	--	--	Steam distillation.
Ballmill Study															
PDT 211	100	1500	33	2318-41-1	25	3.7	--	0.27	0.36	0.40	0.49	0.62	0.98	--	0 minutes ballmill(b).
PDT 211	100	1500	44	2318-41-2	25	3.7	--	0.22	0.39	0.55	0.57	0.83	--	--	3 minutes ballmill(b).
PDT 211	100	1500	--	2318-2E	25	3.7	0.10	0.20	0.38	0.38	0.52	0.38	--	--	8 minutes ballmill(b).
PDT 211	100	1500	--	2318-2	25	3.7	0.13	0.25	0.42	0.50	0.98	--	--	--	16 minutes ballmill(b).
PDT 211	100	1500	--	GC-7	25	3.7	0.09	0.31	0.40	0.44	0.50	0.64	X(d)	--	8 minutes ballmill(b).
PDT 211(c)	50	1500	--	2313-116	25	3.7	0.08	0.16	0.30	--	--	--	--	--	
PDT 211	50	1500	--	2313-33	25	3.7	0.11	0.20	0.39	0.56	0.92	--	--	--	IR study run.
Composition Study															
PDT 211	100	1500	33	90-1	25	3.7	0.16	0.34	0.40	0.46	0.84	--	--	--	
PT 13	100	1500	32	92-3	25	3.7	0.06	0.31	0.40	0.46	0.63	0.74	--	--	
PDT 8315	100	1500	103	92-1	25	3.7	0.09	0.31	0.73	0.94	--	--	--	--	
PDT 312	100	1500	124	92-3	25	3.7	0.13	0.49	0.60	X(d)	--	--	--	--	
PT 64	100	1500	34	92-8	25	3.7	0.09	0.30	0.35	0.40	0.46	0.66	--	--	
PD 11	50	1500	29	92-9	25	3.7	0.10	0.42	0.71	X(d)	--	--	--	--	
PDT 341	50	1500	38	92-11	25	3.7	0.10	X(d)	--	--	--	--	--	--	
PB 14	50	1500	32	92-12	25	3.7	0.01	X(d)	--	--	--	--	--	--	
PDT 211	100	1500	34	92-13	25	3.7	0.06	0.30	0.32	0.38	0.46	0.57	0.66	X(d)	
PT 8315	100	1500	29	92-14	25	3.7	0.16	0.27	0.41	0.56	0.90	--	--	--	
CY AA1	10	1500	8	92-15	25	3.7	---------- (0.45 v @ 0.035 ma cm^{-2}) ----------								Cyanamid AA1 anode.
PDT 211	25	1500	12	92-21	25	3.7	0.11	0.42	X(d)	--	--	--	--	--	
							0.17	0.40	X(d)	--	--	--	--	--	1% TD-135 added to electrolyte.
PT 8315	300	1500	29	92-22	25	3.7	0.09	0.23	0.36	X(d)	--	--	--	--	
							0.06	--	0.26	0.62	X(d)	--	--	--	1% TD-135 added to electrolyte. Maintained at 1.0 ma cm^{-2} for 12 hours.
Methanol Feed Wetting Study							0	10	20	50	100	200	500	1000	
PDT 211(f)	100	1500	44	92-24	60	3.7	0.12	0.17	0.19	0.24	0.35	0.37	0.96	0.39	Fuel and electrolyte chambers contained 2 vol % MeOH in 3.7 M H_2SO_4.
					90	3.7	0.12	0.21	0.21	0.27	0.34	0.44	0.54	--	Electrolyte chamber contained above solution; fuel chamber contained decane.
					25	3.7	0	2.5	5.0	10.0	20.0				Fuel chamber filled with decane, electrolyte filled with 3.7 M H_2SO_4.
							0	20	50	75	100	200	500	1000	
						3.7	0.11	0.12	0.21	0.27	0.4	0.73	--	--	Fuel chamber filled with decane, electrolyte chamber contained 2 vol % MeOH.
						3.7	0.10	0.10	0.21	0.24	0.4	X(d)	--	--	Fuel chamber filled with decane.
Emulsion Feed Study							0	0.5	2	5.0	10.0				
PDT 211	100	1500	33	92-18	25	3.7	0.12	0.41	1.07	--	--				Fuel chamber contained a mechanically-agitated solution of 1.2 gms 100 cc Dowfax 9 N 4 in decane.
PDT 211	100	1500	44	92-19	25	3.7	0.08	X(d)	--	--	--				Fuel chamber contained a mechanically-agitated dispersion of 10 vol % decane, 90 vol % electrolyte and 1.2 gms/100 cc of Dowfax 9N4 surfactant in decane.

(a) Not pressed in form. All subsequent electrodes pressed in Teflon restraining rings.
(b) Pre-imbibed with 30% H_2SO_4 for relative wettability measurements.
(c) Platinized (12 wt % Pt) Teflon used. Final catalyst loading was 50 mg Pt/cm^2.
(d) X means positive failure.
(e) Sulfuric acid electrolyte.
(f) Single electrode used in methanol study.

APPENDIX A-10

PECATE ELECTRODE DATA SUMMARY - BARRIER TYPE ELECTRODES

Electrode	Catalyst Loading mg/cm²	Fabrication Pressure	Fabrication Thickness, mils	Designation Number	Temp °C	Sulfuric Acid Concentration, M	Polarization At Indicated ma/cm², Volts 0	2.5	5.0	7.5	10	12.5	15	17.5	20	Remarks
9 Micron Porous Teflon Barriers 1.16" Thick																
PDT 211	50	1500	27	2363-11	105	1	0.08	0.26	0.33	0.54	0.66	--	--	--	--	
PDT 211	50	200	34	2363-12	105	3.7	0.13	0.32	0.37	0.41	0.43	0.53	0.57	0.62	0.59	
PDT 211	50	200	34	2363-12	105	1	0.12	0.34	0.40	0.50	0.50	0.55	0.57	0.57	0.63	
PDC 211	50	200	34	2363-12	105	6	Dead at 2.5 ma/cm²									
PDA 21.7.3	50	200	34	2363-13	105	3.7	0.08	0.36	0.41	0.53	0.61	--	--	--	--	
PT 11	50	200	--	2363-14A	105	3.7	0.08	0.30	0.36	0.41	0.56	--	--	--	--	
PT 11	50	200	--	2363-14B	105	3.7	0.08	0.36	0.42	0.46	0.50	--	--	--	--	Silica treated decane
PS 11	50	1500	37	2363-22	105	3.7	0.02	0.17	0.23	0.51	--	--	--	--	--	Poisoned
PDT 211	50	200	37	2363-26	105	3.7	0.06	0.30	0.36	0.43	0.58	--	--	--	--	
PDT 211	100	200	--	2363-29	105	3.7	0.07	0.24	0.23	0.36	0.39	0.46	0.52	0.57	--	
PDT 211	50	350	--	2363-28	105	3.7	0.06	0.26	0.38	0.54	0.66	--	--	--	--	
PDT 211	50	200	Sintered	2363-38	105	3.7	0.08	0.28	0.36	0.60	--	--	--	--	--	After O_2 evolution
PDT 211	50	200	34	2363-46	105	3.7	0.05	0.26	0.36	0.54	0.72	--	--	--	--	Barrier pressed to elec trode
PDT 211	50	200	34	2363-46	105	3.7 (0.1% surfactant)	0.12	0.30	0.40	0.45	0.48	0.52	0.54	0.58	0.62	
PDT 211	50	200	34	2363-47	105	3.7	0.04	0.26	0.38	0.61	--	--	--	--	--	1/8" thick barrier
PDT 211	50	200	34	2363-47	105	same with 0.1% surfactant	0.08	0.36	0.41	0.45	0.52	0.56	0.62	--	--	
PDT 211	50	200	34	2363-48	105	3.7	0.06	0.27	0.39	0.43	--	--	--	--	--	3/8" barriers
PDT 211	50	200	34	2363-46	105	same with 0.1% surfactant	0.11	0.33	0.40	0.44	0.49	0.54	0.65	--	--	
PDT 211	50	200	34	2363-49	105	3.7 (0.1% surfactant)	0.08	0.26	0.37	0.40	0.46	0.50	0.56	0.66	--	
Emulsion Fabrication Systems																
PT 91	50	200	12	2615-3	105	3.7 (0.1% surfactant)	0.14	0.37	0.44	0.49	0.51	0.90	--	--	--	
PDT 523	50	200	27	2615-4	105	"	0.14	0.37	0.47	0.53	0.58	0.36	0.90	--	--	
PT 46	50	200	30	2615-5	105	"	0.12	0.30	0.44	0.48	0.53	0.55	0.64	--	--	
PS 73	50	200	22	2615-6	105	"	0.06	0.44	0.54	0.58	0.66	0.82	--	--	--	
PDT 211	50	200	35	2615-7	105	"	0.08	0.40	0.50	0.56	0.68	--	--	--	--	
PDT 212	50	200	37	2615-8	105	"	0.10	0.34	0.41	0.44	0.48	0.52	0.56	--	--	
PDT 451	50	200	43	2615-9	105	"	0.07	0.32	0.38	0.47	0.53	0.62	--	--	--	
PDT 731	50	200	43	2615-10	105	"	0.08	0.36	0.44	0.50	0.53	0.60	0.65	0.71	--	
PT 8615	50	200	13	2363-40	105	"	0.05	0.28	0.36	0.44	0.53	--	--	--	--	
PDT 334	50	200	63	2615-11	105	3.7 (0.1% surfactant)	0.11	0.37	0.46	0.53	0.59	0.64	0.72	--	--	
PDT 243	50	200	[illegible]	2315-12	105	"	0.13	0.53	0.50	--	--	--	--	--	--	
PDT 361	50	200	[illegible]	2315-13	105	"	0.08	0.33	0.49	0.58	0.[illegible]	--	--	--	--	
PDT 434	50	200	[illegible]	2315-14	105	"	0.09	0.35	0.41	0.43	0.[illegible]	0.[illegible]	0.[illegible]	0.66	0.[illegible]	
PDT 413	50	200	[illegible]	2315-15	105	"	0.12	0.39	0.45	0.53	0.60	0.[illegible]	--	--	--	
PDT 442	50	200	[illegible]	2315-16	105	"	0.07	0.30	0.42	0.43	0.50	0.[illegible]	0.[illegible]	0.64	--	
PT 37	50	200	[illegible]	2315-17	105	"	0.12	0.39	0.50	0.57	0.65	--	--	--	--	
PDT 443	50	200	[illegible]	2315-23	105	"	0.08	0.34	0.42	0.47	0.37	--	--	--	--	
PDT 443	50	100	[illegible]	2315-26	105	"	0.08	0.33	0.41	0.51	0.[illegible]	--	--	--	--	
PDT 443	50	1000	22	2315-31	105	"	0.11	0.33	0.42	0.53	--	--	--	--	--	
PDT 443	50	10000	--	2315-32	105	"	0.11	0.43	0.52	--	--	--	--	--	--	
PST 211	50	200	40	2315-22	105	"	0.[illegible]	0.29	0.41	0.[illegible]	0.[illegible]	--	--	--	--	
PST 451	50	200	[illegible]	2315-35	105	"	0.[illegible]	0.28	0.[illegible]	--	--	--	--	--	--	
PST 731	50	200	24	2315-26	105	"	0.[illegible]	0.[illegible]	0.[illegible]	0.[illegible]	0.[illegible]	--	--	--	--	Saran binder
PST 434	50	200	[illegible]	2315-37	105	"	0.[illegible]	0.[illegible]	0.41	0.[illegible]	--	--	--	--	--	
PDT 211	50	200	[illegible]	2315-14	102	"	0.12	0.[illegible]	0.[illegible]	0.[illegible]	0.[illegible]	--	--	--	--	
PDT 211	50	200	[illegible]	2315-19	102	"	--	--	--	--	0.43	0.[illegible]	--	--	--	
PDC 211	50	200	[illegible]	2315-30	102	"	0.[illegible]	0.[illegible]	0.[illegible]	--	--	--	--	--	--	
PDT 211	50	200	[illegible]	2315-21	105	"	0.[illegible]	0.34	Dead							
Other Barriers																
PT 11	50	200	--	2363-4	105	3.7	0.14	0.30	0.44	0.54	0.61	0.70	--	--	--	Porous Carbon Teflon barrier
PT 11	50	200	--	2363-4	105	14.7*	0.14	0.43	0.69	--	--	--	--	--	--	
PT 11	50	200	--	2363-4	105	14.7*	0.14	--	0.43	0.49	0.52	0.62	--	--	--	
PDT 211	50	200	34	2363-19-1	105	3.7	0.07	0.29	0.35	0.46	0.51	0.90	--	--	--	350 psi pressed Teflon barrier
PDT 212	50	200	37	2363-19-2	105	3.7	0.04	0.22	0.31	0.51	--	--	--	--	--	1000 psi pressed Teflon

Additional Teflon Barrier Electrodes Tested Using Ownamid A/1 Electrode as Anode

							Polarization At Indicated ma/cm², Volts 0	0.1	0.2	1.0	2.5	5.0	7.5	
CY AA1	9	--	6	GC-19	105	3.7	0.30	0.38	0.43	0.49	0.69	--	--	Fermion 1010 membrane on electrolyte side
CY AA1	9	--	6	GC-25	105	3.7	0.24	0.38	0.45	0.49	0.55	0.62	--	
CY AA1	9	--	12	GC-26	105	3.7	0.26	0.36	0.40	0.42	0.45	0.49	0.66	

*65% H_3PO_4

APPENDIX A-11

FLUORINATED ACID ELECTROLYTE STUDIES ON DECANE

Notebook and Page	Description of Electrode	Electrolyte	Current Density @ 100°C ma/cm²	Current Density @ 100°C ma/mg of catalyst	Polarization, volts
2263-38	PDT-211, 50 mg Pt/cm² Teflon Barrier	30% aq. Heptafluoro-butyric Acid	5	0.1	.37
	"	"	8	0.16	.47
	"	"	14	0.28	.66
2263-41	Carbon 1211 - Electrode		2	0.7	.37
	"	"	4	1.3	.47
2263-42	1:1 Pt-Rh, Pt PDT 211 50 mg. metal/cm², Teflon Barrier	"	5	--	.34
2263-43	Pt-Ru PDT 211 50 mg Pt-Ru/cm² Teflon Barrier	"	5	--	.46
2263-49	Pt(A.F.)(1) PDT-211 50 mg Pt/cm² Teflon Barrier	30% Sulfuric Acid + 2% Pentadecafluorooctanoic Acid	7	--	.34
2263-50	PDT 211 50 mg Pt/cm² Teflon Barrier	30% Hexafluoroglutaric Acid	5, [10](2)		.3
2263-50	Pt(A.F.)(1) PDT 211 50 mg Pt/cm² Teflon Barrier	"	3.5	--	.3

(1) Prepared by aluminate-formaldehyde, coprecipitation-reduction technique.
(2) This number was observed once and was never reproduced.

APPENDIX A-12

Conductance of Mixed H_2SO_4 and H_3PO_4

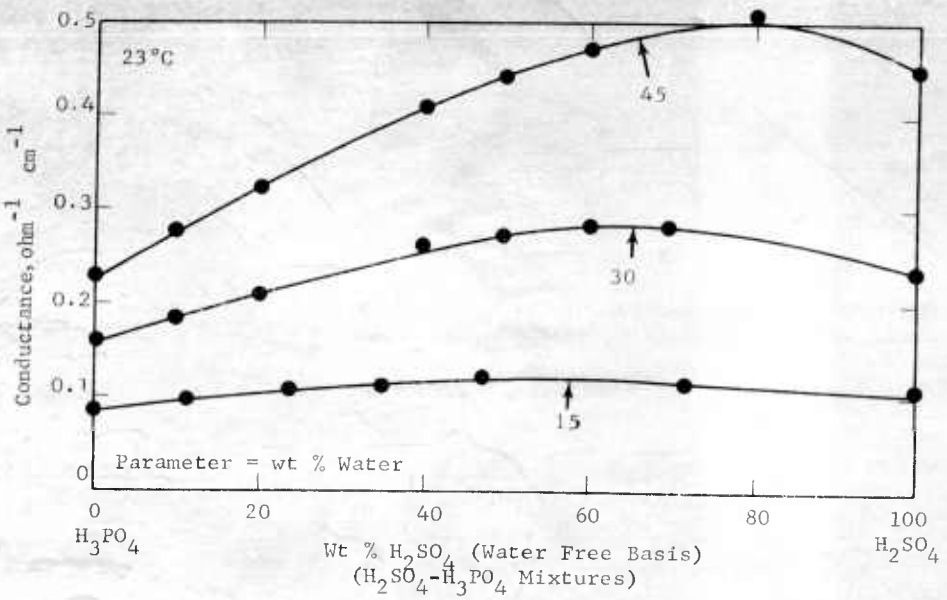

APPENDIX A-13

PERFORMANCE RUNS-PLATINUM-TEFLON SINTERED ELECTRODES(1)

Gaseous Fuels

Temp, °C.	Electrolyte	Feed(2)	Polarization At Indicated ma/cm², volts 0	1	10	25	50	100	Limiting Current, ma/cm²	Remarks
150	14.7 M H_3PO_4	Butane	0.08	0.09	0.16	0.21	0.25	0.27	400	Held at 100 ma/cm² steady one hour.
100	3.7 M H_2SO_4	"	-0.02	0.0	0.10	0.20	--	--	30	
150	14.7 M H_3PO_4	"	-0.03	-0.03	0.07	0.13	0.16	0.23	150	
150	"	"	-0.06	--	0.07	0.13	0.17	0.23	150	Dry feed.
150	"	"	-0.03	-0.05	0.04	0.09	0.12	0.16	400	Pre-equilibrated feed.
150	"	"	-0.08	-0.05	0.02	0.07	0.12	0.17	400	Dry feed.
150	"	Decane	0.07	0.09	0.19	0.29	0.32	0.42(3)	100	Steam distilled feed.
150	"	"	0.12	0.16	0.31	0.46	--	--	40	Steam distilled feed.
150	"	"	0.08	0.11	0.21	0.32	0.52	--	90	Vapor feed decane.
150	"	"	--	0.16	0.25	0.32	0.42	0.55	150	Vapor feed -- 9 micron Teflon barrier at electrode.

(1.) 85% commercial Pt-15% Teflon emulsion. Sintered one minute at 343°C., 1100 psig, - 30 mg Pt/cm².
(2.) All feeds electrolyte-equilibrated except as noted.
(3.) Oscillations about this point.

APPENDIX A-14

NOBLE METAL CATALYSTS EXAMINED ON HYDROCARBONS

Notebook and Page	Metal	Reduction Technique	Electrode Structure and Fabrication	100°C, 3.7 M Sulfuric Acid		
				Ethane	Decane	
				Current Density (ma/cm^2) at 0.4 volts Polarization	Current Density (ma/cm^2)	Polarization (volts)
2263-23	Pt	Commercial	100 mg Pt/cm^2 PDT 211	6	5,10(2)	0.7
2263-25	Pt	H_2 at 650°C	~ 80 mg Pt/cm^2 PDT 211	0.7	0.8	0.7
2263-32	Pt	$NaBH_4$	100 mg Pt/cm^2 PDT 211	2	1	0.7
2263-34	Pt	Commercial	50 mg Pt/cm^2 PDT 211 Teflon Barrier	-	3.5,3.5(2)	0.34
2263-48	Pt	Formaldehyde-Aluminate	50 mg Pt/cm^2 PDT 211 Teflon Barrier	-	7	0.34
2263-26	Ir	H_2 at 650°C	60 mg Ir/cm^2 PDT 211	1	0.5	0.7
2263-33	Ir	$NaBH_4$	100 mg Ir/cm^2 PDT 211	-	< 1	0.7
2263-45	Zr	High Temp.	Doesn't reduce under these conditions			
2263-44	Rh	$NaBH_4$	50 mg Rh/cm^2 PDT 211 Teflon Barrier	< 1	< 0.5	0.7
2263-36	Pt-Ru(40%)	H_2 at 650°C	50 mg Pt-Ru/cm^2 PDT 211 Teflon Barrier	< 3.5	< 2.5, < 2(2)	0.7
2263-42	Pt-Ru(40%)	H_2 at 650°C	50 mg Pt-Rh/cm^2 PDT 211 Teflon Barrier	-	< 1.5	0.34
2619-7	Pt-Rh(13%)	Formaldehyde - Aluminate	50 mg Pt-Rh/cm^2 PDT 211 Teflon Barrier	-	~ 2	0.34

(1) Teflon was substituted for Dynel in structures evaluated on ethane.
(2) Replicate runs.

APPENDIX A-15

BENCH SCALE STEAM REFORMER

The bench scale steam reformer was operated as follows. The catalyst was charged to the reactor, and the reactor then mounted in a vertical position, with the catalyst supported on a porous disk. A thermocouple probe was inserted into the catalyst bed and the void space above the catalyst bed filled with quartz wool. The reactor was then closed and the catalyst given the appropriate preactivation treatment. Then the reactor temperature was adjusted to the desired operating level and the decane and water introduced. The effluent from the reactor passed through a condenser and then into a gas-liquid separator. The gas from the separator was then passed through a wet test meter. Gas samples were then taken in stainless steel bombs for analysis by mass spectrometer. The flow of decane and water was measured by feeding the pumps from graduated dropping cyclinders. The temperature of the catalyst bed was controlled by a "Guardsman" temperature regulator which operated the reactor heater.

Figure A-5

Bench Scale Laboratory Reactor

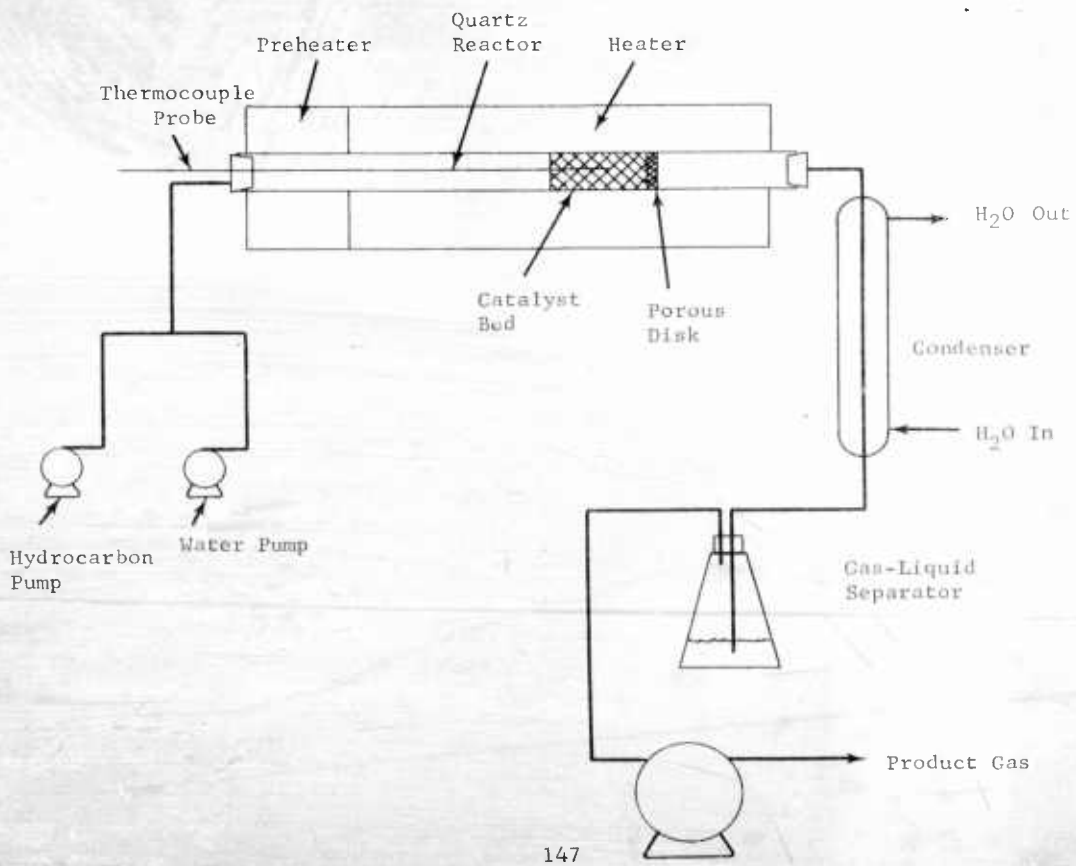

APPENDIX A-16

DECANE STEAM REFORMING STUDIES

Run	1	1	2	2	3	3	3
Part	A	B	A	B	A	B	C
Catalyst	T-1						
Catalyst Charge, grams	40	40	20	20	20	20	20
Bed Temperature, °C	1[illegible]	260	370	370	260	260	315
Feed Rate							
Decane, cc/hr	27	28	27	25	27	26	26
Water, cc/hr	85	80	82	80	50	84	84
W/hr/W, hours^{-1}	0.[illegible]0	0.51	0.99	0.92	0.99	0.95	0.95
Product Gas							
Liters/hr	0.35	4.20	48.66	41.86	1.23	2.75	20.38
Composition, mol %							
Hydrogen	--	--	62.78	60.17	--	--	74.13
Methane	--	--	13.95	18.58	--	--	1.45
Total C_2	--	--	.02	.08	--	--	.06
Total C_3	--	--	.01	.02	--	--	.03
Total C_4	--	--	.01	.04	--	--	.05
Total C_5	--	--	.03	.06	--	--	.03
Total C_6	--	--	.02	.03	--	--	.04
Carbon dioxide	--	--	22.78	20.17	--	--	23.67
Carbon monoxide	--	--	0.40	0.85	--	--	0.54
			100.00	100.00			100.00
% Decane converted	3.25(3)	2.95(3)	54.3(2)	53.9(2)	0.89(3)	2.1(3)	16.7(2)
Rate of Conversion of Decane g/hr/g catalyst(4)	1.25 x 10^{-3}	1.51 x 10^{-2}	.536	.485	.87 x 10^{-2}	2.0 x 10^{-2}	.158

(1) Analysis by mass spectrometer.
(2) Based on quantity and composition of gas product.
(3) Based on quantity of gas produced and stoichiometry $C_{10}H_{22} + 20\ H_2O \longrightarrow 10\ CO_2 + 31\ H_2$.
(4) Rate = fraction decane converted times W/hr/W.

APPENDIX A-16 (CONT'D)

DECANE STEAM REFORMING STUDIES

Run	4	4	5	5	6	6	6	7	7	7
Part	A	B	A	B	A	B	C	A	B	C
Catalyst	T-1-A		T-1-B		T-1-C			T-1-D		
Catalyst Charge, grams	40		40		20			20		
Bed Temperature, °C	260	315	260	315	315	260	315	315	205	370
Feed Rate										
Decane, cc/hr	30	27	24	26	54	26	35	31	30	30
Water, cc/hr	83	82	79	85	80	78	68	73	30	80
W/hr/W, hours^{-1}	0.99	0.49	0.91	0.48	1.98	0.95	1.2	1.14	1.10	1.10
Product Gas										
Liters/hr	1.29	0.96	2.81	13.13	16.30	1.71	13.00	29.13	0.66	61.58
Composition, mol %(1)										
Hydrogen	--	--	76.02	74.89	--	75.58	73.82	--	--	54.32
Methane	--	--	0.89	1.43	--	.44	1.02	--	--	20.56
Total C_2	--	--	.12	.12	--	.03	.04	--	--	.06
Total C_3	--	--	.04	.01	--	--	--	--	--	.04
Total C_4	--	--	.14	.14	--	.05	.06	--	--	.04
Total C_5	--	--	.34	.42	--	.23	.16	--	--	.06
Total C_6	--	--	.04	.06	--	.04	.03	--	--	.03
Carbon dioxide	--	--	21.64	22.44	--	23.65	23.26	--	--	21.43
Carbon monoxide	--	--	0.77	0.49	--	--	0.41	--	--	3.44
			100.00	100.00		100.00	100.00			100.00
% Decane Converted	8.84(3)	7.1	2.02(2)	11.1(2)	--	1.35(2)	7.79(2)	--	0.43(3)	75.4(2)
Rate of Conversion of Decane g hr/g Catalyst(4)	6.82×10^{-3}	1.96×10^{-2}	1.83×10^{-2}	9.32×10^{-2}	--	1.28×10^{-2}	0.99×10^{-1}	--	4.73×10^{-3}	.829

(1) Analysis by mass spectrometer.
(2) Based on quantity and composition of gas produced.
(3) Based on quantity of gas produced and stoichiometry $C_{10}H_{22} + 20\ H_2O \longrightarrow 10\ CO_2 + 31\ H_2$.
(4) Rate = fraction decane converted times W hr W.

APPENDIX A-16 (CONT'D)

DECANE STEAM REFORMING STUDIES

Run	8			9				10		
Part	A	B	C	A	B	C	D	A	B	C
Catalyst	T-1-E			T-1-F				T-1-G		
Catalyst Charge, grams	40			20				20		
Bed Temperature, °C	315	260	370	315	260	370	315	315	260	370
Feed Rate										
Decane, cc/hr	33	32	32	33	32	32	30	31	32	32
Water, cc/hr	69	82	82	80	82	80	76	80	80	84
W/hr/W, hour^{-1}	3.60	3.99	3.99	1.21	1.17	1.17	1.10	1.14	1.17	1.17
Product Gas										
Liters/hr	21.31	2.18	23.89	18.71	2.78	31.30	16.14	19.52	3.42	33.14
Composition, mol %(1)										
Hydrogen	--	74.31	--	71.95	--	--	--	--	--	--
Methane	--	1.30	--	4.40	--	--	--	--	--	--
Total C_2	--	.04	--	.13	--	--	--	--	--	--
Total C_3	--	.03	--	.08	--	--	--	--	--	--
Total C_4	--	.03	--	.08	--	--	--	--	--	--
Total C_5	--	.03	--	.07	--	--	--	--	--	--
Total C_6	--	.02	--	.07	--	--	--	--	--	--
Carbon Dioxide	--	22.93	--	23.22	--	--	--	--	--	--
Carbon Monoxide	--	1.15	--	0.90	--	--	--	--	--	--
		100.00		100.00						
% Decane Converted	--	1.36(2)	--	13.7(2)	1.70(3)	--	--	--	2.09(3)	--
Rate of Conversion of Decane g/hr/g Catalyst(4)	--	$.302 \times 10^{-2}$	--	0.166	1.99×10^{-2}	--	--	--	2.44×10^{-2}	--

(1) Analysis by mass spectrometer.
(2) Based on quantity and composition of gas product.
(3) Based on quantity of gas produced and stoichiometry $C_{10}H_{22} + 20\ H_2O \longrightarrow 10\ CO_2 + 31\ H_2$.
(4) Rate = fraction decane converted times W/hr/W.

APPENDIX A-16 (CONT'D)

DECANE STEAM REFORMING STUDIES

Run	11	11	11	11	12	12	13	13	14	14	14	14
Part	A	B	C	D	A	B	A	B	A	B	C	D
Catalyst	T-1-H				T-1-I		T-1-J		T-1-K			
Catalyst Charge, grams	20				50		50		20			
Bed Temperature, °C	315	290	315	290	315	290	260	205	315	290	205	150
Feed Rate												
Decane, cc/hr	34	32	33	32	33	30	32	32	31	30	30	30
Water, cc/hr	85	82	84	83	79	78	84	81	84	90	80	84
W/hr/W, hour^{-1}	1.24	1.17	1.21	1.43	0.53	0.53	0.47	0.47	1.14	1.10	1.10	1.10
Product Gas												
Liter/hr	16.73	3.96	46.1	3.79	7.76	0.62	0.87	0.21	19.77	3.44	0.44	0.12
Composition, mol %(1)												
Hydrogen	74.06	--	--	--	--	--	--	--	70.30	73.08	--	--
Methane	2.35	--	--	--	--	--	--	--	4.49	2.23	--	--
Total C_2	.07	--	--	--	--	--	--	--	.16	.12	--	--
Total C_3	.04	--	--	--	--	--	--	--	.09	.06	--	--
Total C_4	.04	--	--	--	--	--	--	--	.09	.08	--	--
Total C_5	.03	--	--	--	--	--	--	--	.08	.06	--	--
Total C_6	.05	--	--	--	--	--	--	--	.07	.06	--	--
Carbon Dioxide	22.92	--	--	--	--	--	--	--	22.83	22.67	--	--
Carbon Monoxide	0.22	--	--	--	--	--	--	--	1.39	1.62	--	--
	100.00								100.00	100.00		
% Decane Converted	10.5(2)	2.1(3)	--	1.99(3)	--	0.34(3)	--	0.13(3)	15.6	2.6	0.28(3)	0.078(3)
Rate of Conversion of Decane g hr/g Catalyst(4)	1.31×10^{-1}	2.31×10^{-2}	--	2.72×10^{-2}	--	1.30×10^{-3}	--	0.61×10^{-3}	0.178	0.0286	3.08×10^{-3}	8.60×10^{-4}

(1) Analysis by mass spectrometer.
(2) Based on quantity and composition of gas product.
(3) Based on quantity of gas produced and stoichiometry $C_{10}H_{22} + 20\ H_2O \longrightarrow 10\ CO_2 + 31\ H_2$.
(4) Rate = fraction decane converted times W/hr/W.

APPENDIX A-16 (CONT'D)

DECANE STEAM REFORMING ACTIVITIES

Run	11	13	13	13	16	16	16	16
Part	A	B	C	D	A	B	C	D
Catalyst	T-1-L				T-1-G			
Catalyst Charge, grms	20				20			
Bed Temperature, °C	315	260	205	150	315	260	205	150
Feed Rate								
Decane, ml/hr	33	32	32	32	33	32	32	32
Water, ml/hr	62	62	62	62	62	62	62	62
W/C, g/g	1.7	1.7	1.7	1.7	1.7	1.7	1.7	1.7
F								
Liters/hr	1.0	0.96	0.93	0.93	1.03	0.99	0.89	0.95
Composition, mol % (1)								
Hydrogen	71.48	--	--	--	--	--	--	--
Methane	2.47	--	--	--	--	--	--	--
Total C_2	.11	--	--	--	--	--	--	--
Total C_3	.05	--	--	--	--	--	--	--
Total C_4	.03	--	--	--	--	--	--	--
Total C_5	.03	--	--	--	--	--	--	--
Total C_6	.04	--	--	--	--	--	--	--
Carbon Dioxide	22.77	--	--	--	--	--	--	--
Carbon Monoxide	.52	--	--	--	--	--	--	--
	100.00							
% Decane Converted	--	--	0.092(3)	0.099(3)	--	5.29(3)	0.17(3)	0.11(3)
Rate of Conversion of Decane g/hr/g Catalyst(4)	--	--	1.70×10^{-3}	0.863×10^{-3}	--	0.18×10^{-2}	1.99×10^{-3}	1.09×10^{-3}

(1) Analysis by mass spectrometer.
(2) Based on quantity and composition of gas product.
(3) Based on quantity of gas produced and stoichiometry $C_{10}H_{22} + 20\ H_2O \longrightarrow 10\ CO_2 + 31\ H_2$.
(4) Rate = fraction decane converted times W or W.

APPENDIX A-17

LIQUID PHASE REFORMING SYSTEM

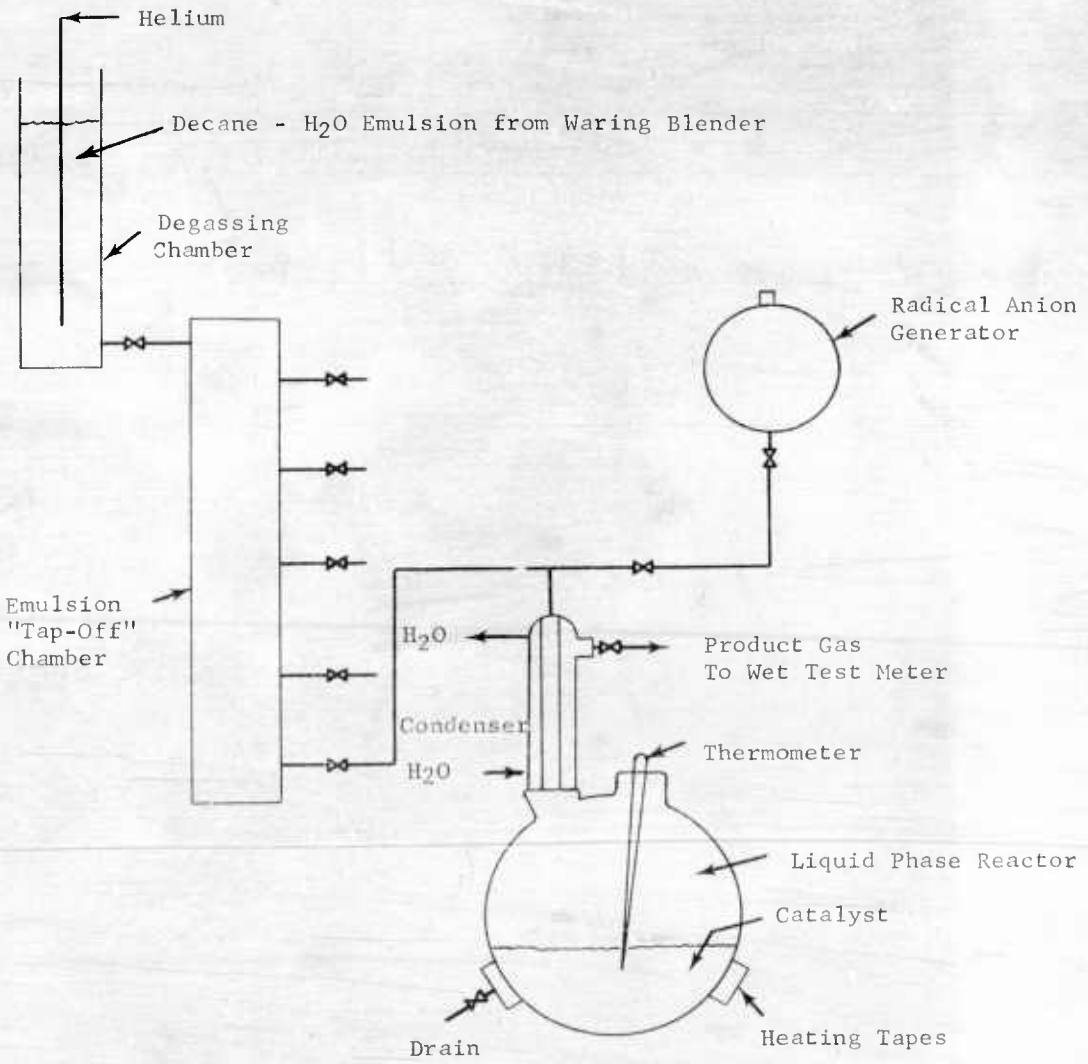

APPENDIX B-1

THE HYDROCARBON FUEL CELL DESIGN

The total cell used in evaluating hydrocarbon cell components is shown schematically in Figure B-1. The basic cell is constructed of Teflon and consists of three chambers: a central electrolyte chamber sandwiched between the fuel and oxidant chambers.

Figure B-1

Hydrocarbon Total Cell

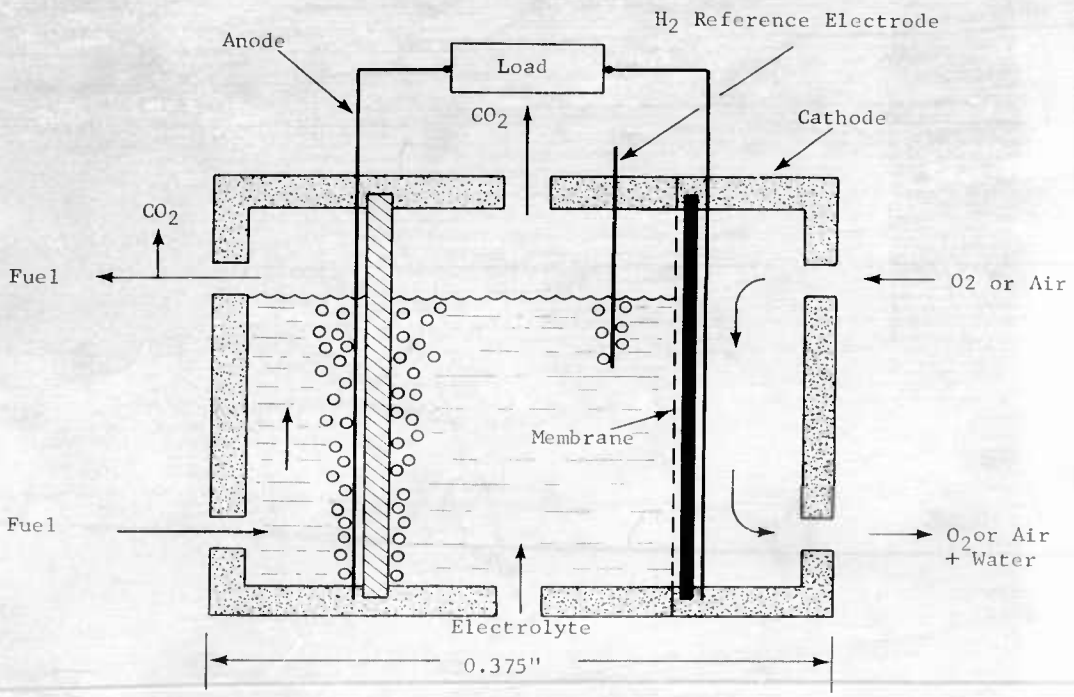

The interface between the fuel and electrolyte chambers is maintained by the electrode itself, while the electrolyte-oxidant (Air or O_2) interface can be maintained by either a membrane or by a suitable electrode structure. The electrodes are 1-3/8" in diameter, with an area of 11.3 cm^2. Both liquid fuel and electrolyte are fed from the bottom, and carbon dioxide can be vented from both the fuel and electrolyte chambers. When used with condensable fuel vapors, the fuel flow is reversed.

APPENDIX B-2

LIQUID DECANE-OXYGEN CELL PERFORMANCE

Electrode Description	Fabrication Pressure, psi	Catalyst Loading, mg/cm^2	Sulfuric Acid Conc, M	Fuel Temp, °C	Cell Potential At Indicated Current Density ma/cm^2, volts 0	2.5	5.0	7.5	10	12.5	15	20	25	Remarks
PDT-1	1500	50	3.7	126	0.81	0.63	0.51	0.43	0.37	0.30	0.27	0.16	--	Heating by lamps and blower.
PDT-1	1500	50	3.7	126	0.81	0.68	0.59	0.54	0.49	0.47	0.44	0.40	0.37	Electrolyte added to fuel; 20 and 25 ma/cm^2 points not stable.
PDT-2	1500	50	3.7	126	0.81	0.58	0.50	0.41	0.33	0.18	--	--	--	Initial performance.
PDT-2	1500	50	3.7	126	0.81	0.48	0.30	--	--	--	--	--	--	After anode deterioration.
PDT-2	1500	50	8.1	126	0.71	0.40	0.20	--	--	--	--	--	--	Electrolyte darkened--Permion
			10.3	126	0.58	0.16	--	--	--	--	--	--	--	membrane attacked.
PDT-3	1500	100	3.7	103	0.79	0.62	0.56	0.51	0.45	0.36	--	--	--	Heating mantle in use.
PDT-4	1500	100	3.7	103	0.81	0.66	0.62	0.58	0.54	--	--	--	--	
PDT-5	1500	100	3.7	103	0.84	0.54	0.21	0.12	--	--	--	--	--	Severe leakage; electrode cracked.

APPENDIX C-1

METHANOL PERFORMANCE IN BUFFER ELECTROLYTES

Electrolyte 1 M each KH_2PO_4, K_2HPO_4

Polarization, Volts, from Methanol Theory

Current Density, ma/cm2	Platinum						Platinum-Ruthenium						P-Type					
	25°C		60°C		80°C		25°C		60°C		80°C		25°C		60°C		80°C	
	Unstirred	Stirred	Unstirred	Stirred	Unstirred	Stirred	Unstirred	Stirred	Unstirred	Stirred	Unstirred	Stirred	Unstirred	Stirred	Unstirred	Stirred	Unstirred	Stirred
5	0.47	0.47	0.37	0.37	0.31	0.31	0.33	0.33	0.22	0.22	0.17	0.17	0.37	0.35	0.14	0.14	0.10	0.10
10	0.51	0.50	0.40	0.39	0.32	0.32	0.38	0.38	0.27	0.26	0.22	0.22	0.41	0.39	0.19	0.19	0.16	0.16
25	0.58	0.55	0.46	0.43	0.37	0.35	0.50	0.47	0.37	0.33	0.29	0.29	0.49	0.45	0.26	0.25	0.20	0.20
50	--	--	0.51	0.47	0.40	0.39	--	--	0.41	0.38	--	0.32	0.54	0.51	0.32	0.30	0.27	0.25
75	--	--	0.53	0.49	0.43	0.41	--	--	--	0.41	--	0.35	--	--	0.35	0.33	0.30	0.27
100	--	--	0.56	0.51	0.46	0.42	--	--	--	0.44	--	0.37	--	--	0.37	0.35	0.32	0.29
150	--	--	0.59	0.54	0.49	0.45	--	--	--	0.46	--	0.40	--	--	0.41	0.37	0.34	0.32
							Electrolyte 1 M each $KHCO_3$, K_2CO_3											
5	0.42	0.42	0.27	0.27	0.23	0.23	0.30	0.30	--	--	0.15	0.15	0.37	0.35	0.14	0.14	0.11	0.11
10	0.46	0.45	0.30	0.30	0.26	0.26	0.34	0.34	0.23	0.22	0.18	0.18	0.41	0.39	0.18	0.18	0.14	0.14
25	0.53	0.50	0.33	0.33	0.29	0.29	0.42	0.39	0.27	0.26	0.23	0.23	0.49	0.45	0.22	0.22	0.18	0.18
50	0.58	0.54	0.40	0.38	0.34	0.32	0.52	0.47	0.33	0.31	0.28	0.27	0.54	0.51	0.26	0.25	0.22	0.21
75	0.63	0.58	0.44	0.40	0.35	0.33	0.59	0.53	0.36	0.33	0.31	0.30	--	--	0.30	0.28	0.26	0.23
100	0.64	0.59	0.46	0.42	0.38	0.35	0.66	0.58	0.39	0.36	0.34	0.31	--	--	0.33	0.29	0.27	0.24
150	0.69	0.64	0.49	0.46	0.41	0.38	--	--	0.45	0.39	0.38	0.34	--	--	0.35	0.31	0.32	0.27
200	0.72	0.68	0.51	0.47	--	--	--	--	--	--	--	--	--	--	--	--	0.34	0.30

APPENDIX C-2

CATHODE PERFORMANCE AT 60°C

Electrolyte 1 M each KH_2PO_4, K_2HPO_4

Current Density, ma/cm²	Polarization, Volts, from Oxygen Theory						
	Nalfilm Clad Cyanamid		Gelman Clad Cyanamid		Felt Clad Cyanamid		Double Cyanamid
	Oxygen	Air	Oxygen	Air	Oxygen	Air	Air
5	0.32	0.39	0.31	0.31	0.25	0.34	--
10	0.41	0.55	0.35	0.39	0.28	0.38	--
25	0.60	0.99	0.41	0.49	0.34	0.45	0.38
50	0.79	--	0.47	0.68	0.42	0.61	0.46
75	--	--	0.55	0.78	0.50	0.71	--
100	--	--	0.61	--	0.56	--	0.65

Electrolyte 1 M each $KHCO_3$, K_2CO_3

Current Density, ma/cm²	Polarization, Volts, from Oxygen Theory		
	Gelman Clad Cyanamid		Felt Clad Cyanamid
	Oxygen	Air	Oxygen
5	0.34	0.45	0.27
10	0.38	0.49	0.30
25	0.44	0.54	0.36
50	0.48	0.59	0.42
75	0.53	0.62	0.47
100	0.55	0.66	0.53

APPENDIX C-3

INITIAL BUFFER TOTAL CELL PERFORMANCE

Electrolyte 1 M each KH_2PO_4, K_2HPO_4
Anode P-5
Cathode Gelman-backed American Cyanamid Type AA-1
Oxidant Oxygen

Test No	CH_3OH Conc, moles/liter	Temp, °C	Current Density, ma/cm^2	Terminal Cell Voltage	Terminal Power, $mwatts/cm^2$
2272-3	0.5	22	0	0.35	0
			0.5	0.33	0.2
			5.0	0.15	0.8
			12.0	0.00	0
		60	0	0.33	0
			0.5	0.26	0.1
			5.0	0.15	0.8
			15.0	0.00	0
2272-3	0.05	22	0	0.51	0
			1.0	0.40	0.4
			2.0	0.31	0.6
			5.0	0.26	1.3
			7.5	0.19	1.4
			10.0	0.12	1.2
			15.0	0.01	0.2
2272-5*	0.75	60	15.0	0.33	5.0
			21.0	0.26	5.5
2272-6**	0.75	60	15.0	0.42	6.3
			21.0	0.33	6.9
			27.0	0.26	7.0

* Additional Gelman membrane between electrodes.
** Additional Permion membrane between electrodes.

APPENDIX C-4

EFFECT OF FUEL CONCENTRATION ON BUFFER TOTAL CELL PERFORMANCE

Anode	P-5
Membrane	Gelman
Cathode	American Cyanamid
Fuel Anolyte	CH_3OH + 1 M K_2HPO_4 + 1 M KH_2PO_4
Plain Anolyte	1 M KH_2PO_4 + 1 M K_2HPO_4

Test No	2272-4														
Cell Temp, °C	22					60									
Fuel Conc, moles/liter	0.05										0.125				
Fuel Anolyte Flow Rate, ml/min	12					11.5					12				
Fuel Anolyte Inlet Temp, °C	Rm														
Plain Anolyte Flow Rate, ml/min	0					2.5					2.8				
Plain Anolyte Inlet Temp, °C	Rm														
Anolyte Flow Rate Through Membrane, ml/min	2.5					7.0					4.0				
Oxidant	O_2														
Current Density, ma/cm^2	0	1	5	7.5	10	1	5	7.5	10	12	5	7.5	10	12	15
Cell Voltage, volts	0.61	0.51	0.33	0.21	0.05	0.53	0.37	0.30	0.24	0.20	0.35	0.30	0.25	0.20	0.13
Anode Polarization, volts	0.15	0.26	0.42	0.50	0.59	0.08	0.22	0.28	0.34	0.37	0.17	0.23	0.28	0.33	0.38
IR, volts	--	--	0.01	0.01	0.02	--	0.01	0.02	0.02	0.03	0.01	0.02	0.02	0.03	0.03
Cathode Polarization (calculated), volts	0.44	0.43	0.44	0.48	0.54	0.59	0.60	0.60	0.60	0.62	0.67	0.65	0.65	0.64	0.66
Cell Voltage, ExIR, volts	0.61	0.51	0.34	0.22	0.07	0.53	0.38	0.32	0.26	0.23	0.36	0.32	0.27	0.23	0.16
Terminal Power Output, mwatt/cm^2	--	0.5	1.65	1.6	0.5	0.5	1.85	2.25	2.4	2.4	1.75	2.25	2.5	2.4	1.95
Power, ExIR, mwatt/cm^2	--	0.5	1.7	1.7	0.7	0.5	1.9	2.4	2.6	2.76	1.8	2.4	2.7	2.76	2.4

APPENDIX C-5

EFFECT OF ANOLYTE FLOW RATE ON BUFFER TOTAL CELL PERFORMANCE

No 2272-4
Anode P-5
Cathode American Cyanamid
Anolyte Methanol + 1M KH_2PO_4 + 1M K_2HPO_4; Methanol free phosphate solution between membrane and anode
Membrane Gelman 5A
Fuel Anolyte Flow rate 12 ml/min
Anolyte through membrane flow rate 3-6 ml/min
Current density 5 ma/cm^2
Oxidant O_2

Fuel Conc, moles/liter	---------- 0.05 ----------				
Temp, °C	----------22----------				
Anolyte Circulation Rate, ml/min	0	1.5	2.5	5.5	8
Cell Voltage, volts	0.33	0.32	0.30	0.23	0.12
Anode Polarization, volts	0.42	0.43	0.45	0.50	0.59
Cathode Polarization, volts	0.44	0.44	0.44	0.46	0.48
IR Loss, volts	0.01	0.01	0.01	0.01	0.01
Power Output, mwatts/cm^2	1.65	1.60	1.50	1.15	0.60

Methanol Conc. moles/liter	---------- 0.05 ----------				
Temp, °C	---------- 60 ----------				
Anolyte Circulation Rate, ml/min	0	1.5	2.5	5.5	11
Cell Voltage, volts	0.35	0.36	0.38	0.33	0.29
Anode Polarization, volts	-	0.22	0.20	0.24	0.28
Cathode Polarization, volts	-	0.61	0.61	0.62	0.62
IR Loss, volts	-	0.01	0.01	0.01	0.01
Power Output, mwatt/cm^2	1.75	1.8	1.9	1.65	1.45

Methanol Conc, moles/liter	---------- 0.125 ----------				
Temp, °C	---------- 60 ----------				
Anolyte Circulation Rate, ml/min	0	1.5	3.0	5.0	11
Cell Voltage, volts	0.33	0.34	0.33	0.30	0.29
Anode Polarization, volts	0.19	0.19	0.19	0.22	0.24
Cathode Polarization, volts	0.68	0.67	0.68	0.68	0.67
IR Loss, volts	0.01	0.01	0.01	0.01	0.01
Power Output, mwatt/cm^2	1.65	1.70	1.65	1.50	1.45

APPENDIX C-6

PERFORMANCE OF DUAL ANOLYTE CHAMBER BUFFER TOTAL CELL

Anode	P-5
Membrane	Gelman
Cathode	American Cyanamid
Fuel Anolyte	CH_3OH + 1 M K_2HPO_4 + 1 M KH_2PO_4
Plain Anolyte	1 M KH_2PO_4 + 1 M K_2HPO_4
Additional Membrane	Gelman

Test No	2272-6									2272-5					
Cell Temp, °C	60									60					
Fuel Conc, moles/liter	1.5									0.5					
Fuel Anolyte Flow Rate, ml/min	12									11.5					
Fuel Anolyte Inlet Temp, °C	78									Rm					
Plain Anolyte Flow Rate, ml/min	13.5									11.0					
Plain Anolyte Inlet Temp, °C	78									Rm					
Anolyte Through Membrane Flow Rate, ml/min	8.5									7.0					
Oxidant	O_2									O_2					
Current Density, ma/cm^2	0	27	30	27	21	15	10	5	1	0	1	5	10	15	21
Cell Voltage, volts	0.90	0.29	0.28	0.33	0.39	0.46	0.55	0.64	0.79	0.84	0.62	0.45	0.33	0.26	0.16
Anode Polarization, volts	0.08	0.30	0.29	0.28	0.26	0.25	0.18	0.16	0.09	0.10	0.32	0.40	0.41	0.45	0.49
IR, volts	--	0.06	0.07	0.06	0.05	0.04	0.02	0.01	--	--	--	0.01	0.02	0.04	0.05
Cathode Polarization (calculated), volts	0.22	0.55	0.55	0.53	0.50	0.45	0.45	0.39	0.32	0.26	0.26	0.34	0.45	0.45	0.50
Cell Voltage, ExIR, volts	0.90	0.35	0.35	0.39	0.44	0.50	0.57	0.65	0.79	0.84	0.62	0.46	0.35	0.30	0.21
Terminal Power Output, mwatt/cm^2	--	7.8	8.4	8.9	8.2	6.9	5.5	3.2	0.8	--	0.6	2.2	3.3	3.9	3.4
Power, ExIR, mwatt/cm^2	--	9.5	10.5	10.5	9.2	7.5	5.7	3.2	0.8	--	0.6	2.3	3.5	4.5	4.4

APPENDIX C-7

EFFECT OF TEMPERATURE ON BUFFER TRIAL CELL PERFORMANCE

No. 2272-7
Anode P-5
Membrane Gelman
Cathode American Cyanamid
Fuel Anolyte Methanol + 1M KH_2PO_4 + 1M K_2HPO_4
Anolyte 1M KH_2PO_4 + 1M K_2HPO_4
Additional Membrane Gelman

Test Period	A					B														C				
Cell Temp, °C	43	43	49	54	60	60														45	50	55	60	65	70	74
Fuel Conc, moles/liter	1.5					1.5														1.5						
Fuel Anolyte flow rate, ml/min	11					11														12						
Anolyte flow rate, ml/min	16					16														16						
Anolyte Inlet Temp, °C	65	68	72	73	75	75														72						
Anolyte Flow Rate Through Membrane, ml/min	11					11														9						
Oxidant	O_2					O_2														O_2						
Current Density, ma/cm²	0	27	27	27	27	1	5	10	15	21	30	35	38	40	45	50	27	27	27	27	27	27	27			
Cell Voltage, volts	0.86	0.33	0.35	0.37	0.39	0.82	0.69	0.60	0.52	0.46	0.37	0.32	0.30	0.28	0.24	0.20	0.35	0.36	0.37	0.39	0.41	0.43	0.45			
Anode Polarization, volts	0.11	0.36	0.34	0.33	0.32	0.15	0.21	0.25	0.29	0.31	0.33	0.34	0.35	0.36	0.37	0.37	0.36	0.35	0.35	0.33	0.32	0.31	0.28			
IR, volts	0.00	0.05	0.05	0.05	0.05	-	0.01	0.02	0.03	0.04	0.06	0.07	0.08	0.08	0.09	0.10	0.05	0.05	0.05	0.05	0.05	0.05	0.05			
Cathode Polarization (calc), volts	0.23	0.46	0.46	0.45	0.44	0.23	0.29	0.33	0.36	0.39	0.44	0.47	0.47	0.48	0.50	0.53	0.44	0.44	0.43	0.43	0.42	0.41	0.42			
Cell Voltage Ex IR, volts	0.86	0.38	0.40	0.42	0.44	0.82	0.70	0.62	0.55	0.50	0.43	0.39	0.38	0.36	0.33	0.30	0.40	0.41	0.42	0.44	0.46	0.48	0.50			
Terminal Power Output, mwatts/cm²	-	8.9	9.4	10.0	10.5	0.8	3.5	6.0	7.8	9.6	11.1	11.2	11.4	11.2	10.8	10.0	9.4	9.7	10.0	10.5	11.0	11.6	12.1			
Power Ex IR, mwatts/cm²	-	10.2	10.8	11.3	11.9	0.8	3.5	6.2	8.2	10.5	12.9	13.6	14.4	14.4	14.8	15.0	10.8	11.0	11.3	11.9	12.4	12.9	13.5			

Test Period	C							D																E				
Cell Temp, °C	45	50	55	60	65	70	74	76																76				
Fuel Conc, moles/liter	1.5							2.0																2.0				
Fuel Anolyte Flow Rate, ml/min	12							11.5																11				
Anolyte Flow Rate, ml/min	16							16																15				
Anolyte Inlet Temp, °C	72							81																80				
Anolyte Flow Rate Through Membrane, ml/min	9							8																75				
Oxidant	O_2							O_2																Air				
Current Density, ma/cm²	32.4	33.6	34.7	38.0	41.1	42.0	43.8	0	1	5	10	21	27	30	38	40	42	45	51	0	1	5	10	15	21	27	30	
Cell Voltage, volts	0.3	0.3	0.3	0.3	0.3	0.3	0.3	0.92	0.86	0.74	0.66	0.53	0.46	0.44	0.37	0.35	0.34	0.31	0.25	0.86	0.80	0.65	0.56	0.47	0.40	0.34	0.30	
Anode Polarization, volts	0.37	0.37	0.36	0.35	0.34	0.33	0.31	0.07	0.11	0.17	0.19	0.24	0.26	0.26	0.28	0.28	0.28	0.29	0.30	0.07	0.11	0.17	0.21	0.23	0.25	0.27	0.27	
IR, volts	-	-	-	-	-	-	-	-	-	0.01	0.02	0.04	0.05	0.06	0.08	0.08	0.08	0.09	0.10	-	-	0.01	0.02	0.03	0.04	0.05	0.06	
Cathode Polarization, volts (calc)	-	-	-	-	-	-	-	0.21	0.23	0.28	0.33	0.39	0.43	0.44	0.47	0.49	0.50	0.51	0.55	0.27	0.29	0.37	0.41	0.47	0.51	0.54	0.57	
Cell voltage Ex IR, volts	-	-	-	-	-	-	-	0.92	0.86	0.75	0.68	0.57	0.51	0.50	0.45	0.43	0.42	0.40	0.35	0.86	0.80	0.66	0.58	0.50	0.44	0.39	0.36	
Terminal Power Output, mwatts/cm²	9.7	10.0	10.4	11.4	12.3	12.6	13.2	-	0.86	3.7	6.6	11.1	12.4	13.2	14.0	14.0	14.2	13.9	12.7	-	0.8	3.2	5.6	7.1	8.4	9.2	9.6	
Power Ex IR, mwatts/cm²	-	-	-	-	-	-	-	-	0.86	3.8	6.8	12.0	13.7	15.0	17.1	17.2	17.6	18.0	17.8	-	0.8	3.3	5.8	7.5	8.8	10.5	10.8	

APPENDIX C-8

PERFORMANCE OF BUFFER TOTAL CELL WITH DUAL AMERICAN CYANAMID ELECTRODE

No 2272-10
Anode P-5
Membrane None
Cathode Double American Cyanamid
Fuel Anolyte Methanol + 1 M KH_2PO_4 + 1 M K_2HPO_4
Anolyte: 1 M KH_2PO_4 + 1 M K_2HPO_4
Additional Membrane Gelman

Cell Temp, °C	---------- 72 ----------								
Fuel Conc, moles/liter	---------- 2.0 ----------								
Fuel Anolyte Flow Rate, ml/min	---------- 45 ----------								
Anolyte Flow Rate, ml/min	---------- 19 ----------								
Anolyte Inlet Temp., °C.	---------- 72 ----------								
Anolyte Flow Rate Through Membrane, ml/min	---------- 11 ----------								
Oxidant	---------- Air ----------								
Current Density, ma/cm^2	0	10	15	20	25	30	35	40	45
Cell Voltage, volts	0.93	0.60	0.54	0.48	0.44	0.40	0.36	0.30	0.25
Anode Polarization, volts	--	0.21	--	0.26	--	0.29	--	0.31	--
IR, volts	--	0.02	0.03	0.04	0.05	0.06	0.07	0.08	0.09
Cathode Polarization (calc), volts	--	0.37	--	0.42	--	0.45	--	0.51	--
Cell Voltage ExIR, volts	0.93	0.62	0.57	0.52	0.49	0.46	0.43	0.38	0.34
Terminal Power Output, mwatts/cm^2	--	6.0	8.1	9.6	11.0	12.0	12.6	12.0	11.2
Power ExIR, mwatts/cm^2	--	6.2	8.5	10.4	12.2	13.8	15.0	15.2	15.3

APPENDIX C-9

CELL CONSTRUCTION FOR CATALYST SLURRY MEASUREMENTS

The cells used for all but the first few measurements with the catalyst slurry system were round bottom tubes (12 cm high, diameter from 3 to 5 cm), with perpendicular ribs attached to the cell walls to increase turbulent flow. A bright Pt foil of varying size (2 to 8 cm^2 area on both sides) served as anode. It was perforated with a number of holes of 3 mm diameter. It was welded to a Pt wire which was glued into a glass capillary and served a dual function as current collector and stirrer, rotating at speeds up to 4000 rpm. A Pt wire was placed in a fritted gas dispenser to serve as cathode and a Ag-AgCl electrode with a Luggin capillary was the reference electrode. Temperature was controlled by a thermoelement and the cell atmosphere was continuously flushed with a small amount of nitrogen. The cell is shown in Figure C-1.

Figure C-1

Cell For Catalyst Slurry Experiments

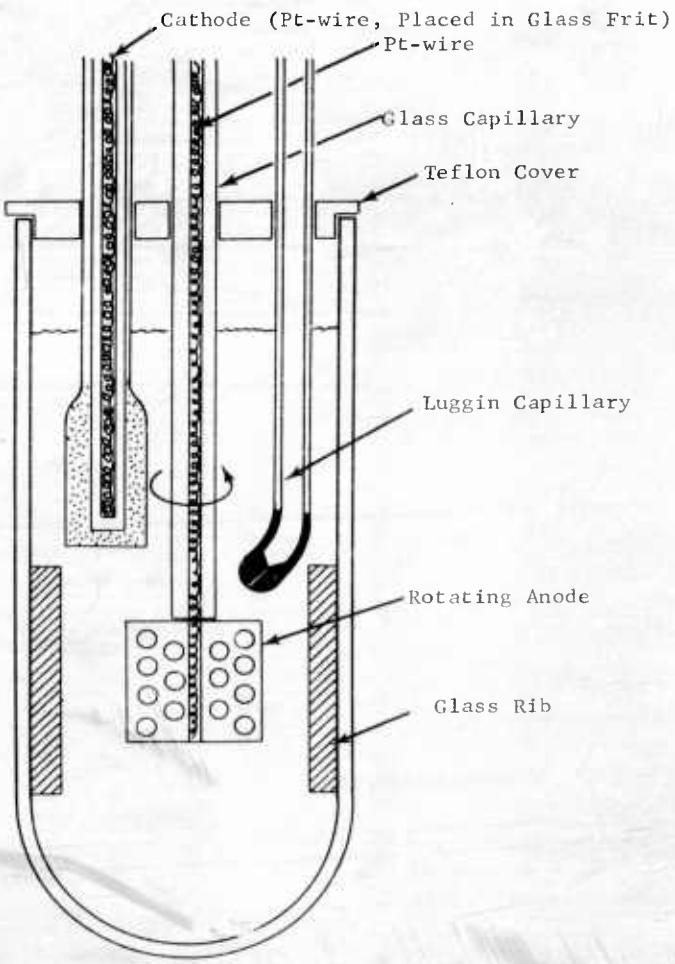

APPENDIX C-10

PERFORMANCE OF CATALYST SLURRY SYSTEM

Temperature 60°C
Electrolyte 3.7 M H_2SO_4
Fuel 1 M CH_3OH (unless otherwise noted)

Reference	Polarization At Indicated ma/cm^2, volts 0	1	10	50	100	Rotation Speed, rpm	Catalyst	Catalyst Conc, mg/ml	Cell Type	Anolyte Volume, ml	Anode Area, cm^2	Remarks
1971-44	0.09	0.63	--	--	--	550	Pt ($NaBH_4$ red)	5	H-shaped	100	8	
1971-46-1	0.52	0.59	--	--	--	2300	"	10	" "	"	"	
1971-46-2	0.26	0.56	0.74	--	--	550	"	10	" "	"	"	
1971-48-1	0.54	0.59	0.74	--	--	2300	"	20	" "	"	"	
1971-48-2	0.07	0.46	0.70	--	--	"	"	20	" "	"	4, perforated	
--	--	0.37	0.44	0.57	--	"	Commercial Pt-black	20	Round, 4.5 cm dia	50	"	
1971-50	--	0.37	0.54	--	--	2400	"	10	" "	"	"	
--	0.30	0.34	0.41	0.58	--	"	"	50	" "	"	"	
2274-04	0.19	0.29	0.38	0.51	0.61	"	"	100	" "	"	"	
2274-05	--	0.40	0.48	0.64	--	1400	"	50	", perpendicular ribs	"	"	
2274-09	--	0.17	0.29	0.42	0.53	2500	"	50	" 3 cm dia, ribbed	"	"	
2274-13	--	0.36	0.46	0.57	0.61	"	"	1	" 4 cm dia, ribbed	"	"	
2274-16-1	--	0.19	0.36	0.48	0.54	"	"	10	" "	"	"	
2274-17	--	0.23	0.37	0.48	0.52	"	"	20	" "	"	"	
2274-16-2	--	--	0.20	0.32	0.38	"	"	100	" "	"	"	
2274-18	--	0.31	0.45	0.52	0.57	"	"	1	" 5 cm dia, ribbed	100	"	
2274-19	--	0.21	0.35	0.47	0.52	"	"	10	" "	"	"	
2274-20	--	--	0.22	0.34	0.39	"	"	100	" "	"	"	
2274-22-1	--	0.32	0.42	0.51	0.56	"	"	1	" 3 cm dia, ribbed	50	"	
2274-21	--	0.27	0.39	0.48	0.53	"	"	10	" "	"	"	
2274-24-1	--	0.15	0.32	0.43	0.50	"	"	50	" "	"	"	
2274-22-2	--	--	0.23	0.40	0.47	"	"	100	" "	"	"	
2274-24-2	--	--	--	0.36	0.42	"	"	200	" "	"	"	
2274-26	--	0.17	0.39	0.54	0.61	"	P-7 (KBH_4 red)	10	" "	"	"	
2274-41-1	0.20	0.33	--	--	--	3500	Commercial Pt	1	" 5 cm dia, ribbed	80	"	100°C, 50 vol % decane.
2274-41-2	--	--	0.39	--	--	"	"	10	" "	"	"	" "
2274-42-1	--	0.15	0.21	0.41	0.57	"	"	50	" "	"	"	" "
2274-42-2	--	0.12	0.15	0.27	0.41	"	"	100	" "	"	"	" "
2274-42-3	--	--	--	0.15	0.22	"	"	270	" "	"	"	" "
2635-8	--	--	0.22	0.38	0.64	1500	"	100	" "	60	"	60°C, electrolyte 1 M K_2HPO_4, 1 M KE_2PO_4.
2635-9	--	--	0.21	--	--	"	"	50	" "	"	"	95°C, "
2274-44	0.10	--	--	--	--	3500	Pt coated Teflon	33	" 4 cm dia, ribbed	"	"	100, 33 vol % decane.
2274-45	--	--	--	0.58	--	"	Commercial Pt	50	" 5 cm dia, ribbed	"	"	105, "
2274-46-1	--	--	--	0.30*	--	"	Pt, exclusively H_2SO_4-wetted	50	" "	"	"	100, "
2274-46-2	--	--	0.37*	0.46*	--	"	Pt, exclusively Decane-Wetted	50	" "	"	"	" "
2274-49	0.14	0.17	0.44*	--	--	"	P7 with Ru	12	" "	"	"	" "
2635-10	0.60	--	--	--	--	"	Pt Coated Sand (by Exchange)	160	" "	"	"	" "
2635-14	0.46	--	--	--	--	2500	Pt Coated Sand (H_2 reduced)	100	" "	"	"	" "

* Unstable

Electrode designation	Phthalocyanine	Catalyst Density, wt % on Carbon	Electrolyte	Temp, °C	Electrode Pretreatment	Polarization at Indicated ma cm^{-2}, Volts 0	1	2	10	20	50	100	Electrolyte Coloration
1776-9	Fe	9	3.7 M H_3PO_4	130	None	0.41	.4	0.54	0.68	0.725	0.72	0.84	Colorless
					Anodized under H_2	0.39	.54	.74	.8	1.0	--	--	Yellow
1776-2	Fe				None	0.39	.46	0.55	0.61	0.66	0.76	0.87	Colorless
					Cathodized to constant readings	0.44	0.525	0.64	0.70	0.77	0.89	1.03	Colorless
					Anodized under H_2	0.40	0.54	0.76	0.94	--	--	--	Deep Yellow
1776-29, 32					None	0.41	0.47	0.54	0.57	0.62	0.70 (extrap)	--	Colorless
"					Cathodized to constant readings (maximum current density = 55 ma cm^{-2}).	0.41	0.50	0.58	0.62	0.67	--	--	Colorless
					Cathodized to constant readings (maximum current density = 100 ma cm^{-2}).	0.41	0.50	0.61	0.67	0.74	0.90	--	Colorless
1776-32	Fe				None	.44	0.53	0.61	0.69	0.71	0.83	--	Colorless
					Cathodized to constant readings	0.44	0.565	0.68	0.74	0.81	0.93	--	Colorless
1776-41, 46	Fe		12.1 M H_3PO_4	130	None	0.43	0.50	0.60	0.67	0.84	--	--	Slight color
					Cathodized to constant readings	0.44	0.53	0.65	0.75	0.90	--	--	Slight color
1776-48	Fe				None	0.39	0.44	0.53	0.595	0.72	--	--	Slight color
					Cathodized to constant readings	0.41	0.49	0.60	0.74	1.00	--	--	Slight color
1776-16	Co		3.7 M H_3PO_4	130	None	0.42	0.54	0.68	0.745	0.82	0.92	1.04	Colorless
					Cathodized to constant readings	0.43	0.58	0.71	0.765	0.82	0.92	1.02	Colorless
					Anodized under O_2	1.30	0.90	1.50	1.84	--	--	--	Yellow
1776-18	Co				None	0.43	0.515	0.71	0.88	0.99	1.125	--	Colorless
					Repeatedly cathodized	0.43	0.455	0.62	0.815	0.91	1.07	--	Colorless
					Anodized	0.36	0.515	0.71	0.825	0.94	1.13	--	Yellow-brown
1776-49	Mn		12.1 M H_3PO_4	130	None	0.43	0.53	0.655	0.72	0.795	1.06	--	Slightly pink
1775-3													
1775-8	Zn				None	0.45	0.7	0.83	0.38	0.98	--	--	Slightly yellow
					Cathodized to constant readings	0.45	0.66	0.84	0.73	0.845	0.975	--	Slightly yellow
1776-50	Cu				None	0.41	0.42	0.53	0.58	0.64	0.97	--	Very slight color
1775-3					Repeatedly cathodized	0.41	0.64	0.74	0.85	0.88	1.01	--	Very slight color
1776-9	V		3.7 M H_3PO_4	130	None	0.48	0.61	0.73	0.88	1.08	--	--	Colorless
					Anodized 30 minutes at 1.0 volts	0.37	0.52	0.64	0.71	0.795	0.945	--	Colorless
1776-33	V				None	0.48	0.63	0.765	0.89	0.98	--	--	Colorless
					Anodized one hr	0.40	0.56	0.74	0.81	0.86	--	--	Yellow color
					Anodized 2.1 hrs	0.37	0.54	0.78	0.89	0.995	--	--	Yellow color
1776-37	V				None	0.47	0.64	0.83	0.90	1.01	--	--	Colorless
					Anodized five hrs	0.30	.37	0.54	0.92	1.04	--	--	Deep yellow
1776-13	None	--			None	0.42	0.495	0.62	0.68	0.79	0.875	0.98	--
		--			Cathodized to constant readings	0.40	0.50	0.625	0.69	0.79	0.875	0.98	--
1776-25, 27		--			None	0.40	0.495	0.62	0.68	0.745	0.85	0.97	--
		--			Cathodized to constant readings	0.39	0.495	0.63	0.695	0.765	0.875	1.00	--
		--			After use as anode-ethylene and H_2	0.40	0.52	0.725	0.89	1.12	--	--	--
1775-41, 46		--	12.1 M NaH_2PO_4	130	None	0.37	0.485	0.60	0.68	0.785	1.06	--	--
					Three cathodic cycles	0.34	0.505	1.065	-------	(Flooded Badly)	-------		--

APPENDIX C-12

METAL PHTHALOCYANINES AS FUEL ELECTRODES

Group 12a

Electrode Designation	Phthalocyanine	Catalyst Density, wt % on Carbon	Electrolyte	Temp, °C	Fuel	Polarization at Indicated ma/cm², volts 0	0.18	0.54	1.1	1.8	Remarks
1776-26	Ni	5	3.1 M H_2SO_4	100	Ethane	0.45	>0.55	>0.76	--	0.87	Before anodization.
"	"	"	"	"	"	0.42	>0.45	--	--	>0.78	After anodization.
1776-24	Co	"	"	"	"	0.45	>0.55	>0.73	--	0.83(a)	Before anodization.
"	"	"	"	"	"	0.44	>0.49	>0.71	0.90	--	--
1776-28, 45	None	--	"	"	"	0.57	0.60	0.81(b)	0.85	0.88	--
1775-5, 12, 19											
"	"	--	"	"	Ethylene	0.49	0.55	0.82	--	--	--
"	"	--	"	"	Hydrogen	0.05	--	--	--	>0.63	--
"	"	--	12.1 M H_3PO_4	130	Ethylene	0.61	--	0.89	--	--	--
1776-41, 48	Fe	5	"	"	"	0.48	--	0.56-0.73(c)	0.81	--	Before cathodization.
"	"	"	"	"	"	0.42	--	0.72	--	--	After cathodization.
1776-47	Fe	20	"	"	"	0.38	0.80	--	--	--	No change on cathodization.
1775-3	Mn	5	"	"	"	0.40	>0.68	--	--	--	No change on cathodization.
1775-4	Cu	10	"	"	"	0.225	>0.9	--	--	--	Before cathodization.
"	"	"	"	"	"	0.20	Ca0.7	--	--	--	After brief cathodization.

Group 12b

						0	0.05	0.1	0.5	1.0	
1775-28, 45	None	--	12.1 M H_3PO_4	130	Ethylene	0.53	0.64	0.78	--	--	--
1775-5, 12, 19											
"	"	--	"	"	Ethane	0.57	0.68	0.78	--	--	--
"	"	--	"	"	Hydrogen	0.64	0.72	0.82	--	--	--
"	"	--	"	"	N_2	0.60	0.68	0.78	--	--	--
1775-10	Zn	10	"	"	Ethylene	0.48-0.54	0.54-0.65	0.64-0.75	--	--	Run as a metal derivative regarded as least likely to show activity.
1775-4	Cu	10	"	"	"	0.235	0.33	0.42	0.69	0.82	Electrode extensively cathodized before run.

(a) Replacement of ethane with N_2 raises polarization to 0.89 volts.
(b) Replacement of ethane with N_2 raises polarization to 0.85 volts.
(c) At current density of 0.9 ma/cm².

APPENDIX C-11

MIXTURES OF PLATINUM AND METAL PHTHALOCYANINES IN CATHODES

Electrode Designation	Phthalocyanine	Catalyst Density, wt % in Carbon	Electrolyte	Temp, °C	Pt Content, mg/cm²	Polarization from Oxygen Theory at Indicated ma/cm² 0	1	5	10	20	50	100	Cycle No.
					Series I: Physical Mixtures								
1773-15, 16	None (Electrode A) (a)	--	12.1 M H_3PO_4	130	1.8	0.38	0.32	0.38	0.42	0.46	0.52	0.61	1
"	"	--	"	"	"	0.24	0.275	0.345	0.38	0.435	0.64	>1.0	4
"	"	--	"	"	"	0.25	0.295	0.38	0.48	0.72	--	--	7
"	"	--	"	"	"	0.22	0.295	0.40	0.43	0.95	--	--	10
1773-26	None (Electrode B) (b)	--	"	"	"	0.195	0.275	0.335	0.375	0.43	0.53	0.61	Best
"	"	--	"	"	"	0.26	0.31	0.49	0.435	0.49	0.62	0.80	1
"	"	--	"	"	"	0.24	0.27	0.335	0.295	0.345	0.56	0.74	4
"	"	--	"	"	"	0.23	0.26	0.35	0.39	0.43	0.56	0.73	
"	"	--	"	"	"	0.23	0.26	0.35	0.39	0.43	0.56	0.60	Best individual values in all cycles
"	"	--	"	"	"	0.35	0.43	1.0(c)	--	--	--	--	(e)
1773-38	Cu	7.1	"	"	"	0.33	0.32	0.41	0.45	0.48	--	--	1
"	(Electrode C)	"	"	"	"	0.205	0.26	0.29	0.39	0.43	0.49	0.585	4
"	"	"	"	"	"	0.24	0.3	0.37	0.43	0.45	0.51	0.59	8
"	"	"	"	"	"	0.20	0.295	0.34	0.38	0.42	0.48	0.56	12(c)
"	"	"	"	"	"	0.16	0.26	0.335	0.37	0.415	0.48	0.525	Best(d)
"	"	"	"	"	"	0.23	0.285	0.385	0.405	0.45	0.70(c)	--	(e)
1775-39	Cu	"	"	"	"	0.31	0.29	0.39	0.435	0.48	0.56	0.76	1(e)
"	(Electrode D)	"	"	"	"	0.17	0.24	0.335	0.39	0.47	0.60	>1.0	4
"	"	"	"	"	"	0.19	0.26	0.365	0.48	0.71	>1.0	--	6
1775-39	Cu	"	"	"	"	0.27	0.27	0.30	0.345	0.42	0.53	0.76	Best
"	(Electrode E)	"	"	"	"	0.28	0.30	0.395	0.56	0.655	0.81	--	1
"	"	"	"	"	"	0.19	0.25	0.365	0.43	0.48	0.605	0.78	4
"	"	"	"	"	"	0.22	0.3	0.4	0.44	0.49	0.605	0.77	7
1775-48	V	5.1	"	"	"	0.24	0.26	0.355	0.415	0.465	0.58	0.72	10(best)
2814-3, 7	(Electrode F)	"	"	"	"	0.145	0.28	0.34	0.435	0.48	0.61	0.815	
"	"	"	"	"	"	0.25	0.305	0.44	0.55	0.745	--	--	4
"	"	"	"	"	"	0.31	0.37	0.474	0.59	0.85	--	--	7(=steady)
					Series II: Pt-on-Pc Impregnation								
3838-4	Cu	10	9.1 M H_3PO_4	130	1.0	0.18	0.365	0.46	0.53	0.68	0.75	1.06	1 (=2)
	(Electrode G)												

(a) Diluent carbon treated with conc H_2SO_4.
(b) Diluent carbon not treated with conc H_2SO_4.
(c) Steady state values after electroreduction.
(d) Regardless of cycle, but later than Cycle 5.
(e) After testing anodically. See Appendix C-14.
(f) At 2 ma/cm².
(g) Later cathodic cycles show electrode flooding.

APPENDIX C-14

MIXTURES OF PLATINUM AND METAL PHTHALOCYANINES IN ANODES

Electrode Designation	Phthalocyanine	Cat Density, wt % on Carbon	Pt Content, mg/cm²	Electrolyte	Temp. °C	Fuel	Polarization from Fuel Theory at Indicated ma/cm², Volts 0	1	5	10	20	50	100	Cycle No.	Prior Test History
Series I: Physical Mixtures															
1775-11, 15	None (Electrode A)	--	1.3	12.1 M H_2SO_4	130	Ethylene	0.21	0.36	0.48	0.53	0.58	1.01	--	1	4 cathodic cycles
"	"	--	"	"	"	"	0.22	0.42	0.53	0.59	0.67	1.04	--	3	
1775-26	None (Electrode B)	--	"	"	"	"	0.26	0.435	0.57	0.63	0.75	--	--	1	6 cathodic cycles
"	"	--	"	"	"	"	0.26	0.433	0.57	0.63	0.75	--	--	2	
"	"	--	"	"	100	Hydrogen	0.00	0.08	0.33	--	--	--	--		Equilibrated on O_2
"	"	--	"	"	130	"	0.04	0.05	0.06	0.21	>0.8	--	--		Flooded badly on H_2
"	"	--	"	14. M H_3PO_4	100	Ethylene	0.22	0.365	0.7	>1.0	--	--	--		Equilibrated on O_2
"	"	--	"	"	"	Ethane	0.22	0.32	--	--	--	--	--		
1775-18	Cu (Electrode C)	7.5	"	12.1 M H_3PO_4	130	Ethylene	0.235	0.405	0.51	0.55	0.605	0.715	0.84	1	13 cathodic cycles
"	"	"	"	"	"	"	0.22	0.40	0.51	0.55	0.605	0.72	0.85	2	
1775-39	Cu (Electrode D,	"	"	"	"	"	0.38	0.495	0.61	0.675	0.76	--	--	1	Electrode fresh
"	"	"	"	"	"	"	0.26	0.44	0.56	0.615	0.675	0.755	0.82	3	
1775-18	Cu (Electrode C)	"	"	"	"	Hydrogen	0.02	0.02	0.02	0.03	0.03	0.04	0.09	1	
"	"	"	"	"	100	"	0.00	0.002	0.002	0.004	0.005	0.028	0.22	1	None
"	"	"	"	14.7 M H_3PO_4	100	Ethylene	0.21	0.325	0.445	0.50	0.57	0.68	1.02	1	None
"	"	"	"	"	"	Ethane	0.27	0.48	0.82	1.00	--	--	--	1	
1775-28	Fe (Electrode F)	"	"	12.1 M H_3PO_4	130	Hydrogen	0.004	0.004	0.004	0.019	0.034	0.087	0.184		Equilibrated on O_2
"	"	"	"	"	"	Ethylene	0.24	0.385	0.515	0.58	0.66	0.91	--	1	Equilibrated on O_2
"	"	"	"	"	"	"	0.24	0.38	0.51	0.58	0.67	0.91	--	2	
1775-43	V (Electrode G)	3.75	"	"	"	"	0.245	0.42	0.79	>1.0	--	--	--	1	
Series II: Pt-on-Pc Impregnation															
2814-3,	None (Electrode I)	--	1.	3.7 M H_2SO_4	100	Ethylene	0.20	0.38	0.49	0.56	0.635	>1.0	--	--	--
"	"	--	"	"	"	Ethane	0.12	0.30	>1.0	--	--	--	--	--	--
"	"	--	"	"	50	Hydrogen	--	--	--	-0.00-	--	--	0.10	Ca 1.0	--
2814-4	Cu (Electrode H)	10	"	"	100	Ethylene	0.19	0.45	0.67	0.90	--	--	--	--	--
"	"	"	"	"	"	Ethane	0.16	0.29	Ca 1.0	--	--	--	--	--	--
"	"	"	"	"	50	Hydrogen	--	--	--	-0.00-	--	--	0.13	0.39	--

APPENDIX D-1

METHANOL CATALYST PERFORMANCE

Electrode Identification	Catalyst Identification	Catalyst Loading, mg/cm^2	Nominal Composition at %	Polarization vs Theoretical Methanol at Indicated ma/cm^2 1	10	50	100	Tafel Slope	Test Temp, °C	Reduction	Catalyst Treatment	Electrode Preparation
2051-43-1	2051-31-2	20	Pt-10Ir	0.40	0.78	0.87	--	--	60	CO at 370°C H_2 at 650°C	6 M KOH	10% Teflon, dry
2051-47-1	Comm'l. Pt	20	Pt	0.39	0.43	0.48	--	--	60	--	--	10% Teflon, dry
2051-50-1	2051-45-1	20	Pt-20Ru	0.25	0.32	0.38	0.41	0.06	60	$NaBH_4$	6 M KOH	10% Teflon, dry
2269-5-1	517-18	--	P-7	0.13	0.30	0.38	0.42	--	60	$NaBH_4$	None	Wet press
2269-6-1	2269-6-1	20	Pt-20Ru	0.35	0.42	0.50	0.55	0.08	60	$NaBH_4$	None	10% Teflon, dry
2269-9-1	2051-45-2	20	Pt-33Ru	0.24	0.29	0.34	0.37	0.06	60	$NaBH_4$	6 M KOH	10% Teflon, dry
				--	0.27	0.32	0.35	0.07	80			
				--	0.30	0.35	0.38	0.07	60			
				--	0.34	0.40	0.44	0.09	40			
2269-16-1	2051-45-2	25	½ P-7 & ½Pt-33Ru	0.19	0.28	0.35	0.39	0.09	60	$NaBH_4$	None	Wet press
				--	0.22	0.29	0.33	0.105	80	$NaBH_4$	6 M KOH	
				--	0.28	0.34	0.37	0.08	60			
				--	0.31	0.37	0.41	0.09	45			
Same electrode after overpolarization to .90 volts 15 minutes				0.25	0.33	0.39	0.43					
2269-21-1	2269-15-1	20	Pt-33Ru	0.25	0.31	0.36	0.41	0.06	60	$NaBH_4$	6 M KOH	10% Teflon, dry
2269-24-1	2269-15-2	20	Pt-33Ru	--	0.29	0.34	0.38	0.06	60	$NaBH_4$	6 M KOH	10% Teflon, dry
2269-25-1	2269-17-2	20	Pt-20Ru	0.30	0.37	0.42	0.45	0.07	60	$NaBH_4$(1)	6 M KOH	10% Teflon, dry
2269-26-1	2269-17-3	20	Pt-20Ru	0.33	0.40	0.48	--	0.07	60	CO at 370°C(1)	6 M KOH	10% Teflon, dry
2269-27-1	2269-17-4	20	Pt-20Ru	--	0.31	0.39	0.46	--	60	CO at 370°C	KOH soak	10% Teflon, dry
2269-28-1			P-7	--	0.28	0.36	0.41		60	KBH_4	None	Wet press
2269-29-1	2269-29-1		P-7	--	0.41	0.50	0.53	0.09	60	$NaBH_4$	KOH soak	Wet press
2269-30-1	2269-17-1	20	Pt-20Ru	--	0.33	0.42	0.47		60	CO at 370°C(2)	KOH soak	10% Teflon, dry
2269-33-1	2269-15-2	17	Pt-33Ru	--	0.30	0.35	0.37	0.06	60	$NaBH_4$	KOH soak	Wet press(3)
2269-34-1	2269-18-2-1	20	Pt-30Rh	--	0.40	0.46	0.51	0.09	60	$NaBH_4$	KOH soak	10% Teflon, dry
2269-36-1	2269-18-4	20	Pt-70Rh	0.40	0.44	0.50	0.56		60	$NaBH_4$	KOH soak	10% Teflon, dry
2269-38-1	2269-36-1		Pt-33Ru	0.31	0.38	0.44	0.49	0.07	60	$NaBH_4$	None	Wet press
2269-39-1	2269-29-1	20	P-7	0.32	0.41	0.49	0.54		60	$NaBH_4$	KOH soak	10% Teflon, dry
2269-41-1	2269-37-2-1	20	Pt-30Ru	0.27	0.33	0.38	0.42	0.06	60	$NaBH_4$	KOH soak	10% Teflon, dry
2269-44-1	2269-37-3	20	Pt-50Ru	0.22	0.28	0.34	0.39	0.05	60	$NaBH_4$	KOH soak	10% Teflon, dry
2269-45-1	2269-37-4	20	Pt-70Ru	0.21	0.28	0.32	0.38	0.06	60	$NaBH_4$	KOH soak	10% Teflon, dry
2269-46-1	2269-43-1	6(4)	Pt-40Ru	0.24	0.30	0.36	0.40	0.07	60	$NaBH_4$	KOH soak	Wet press
2269-47-1	2269-43-2	6(4)	Pt-40Ru	0.25	0.31	0.36	0.39	0.07	60	$NaBH_4$	KOH soak	Wet press
2269-48-1	2269-42-1	9(4)	P-7	0.25	0.34	0.45	0.50	(5)	60	KBH_4	KOH soak	Wet press
2051-22-1	2013-50-A		Pt	0.38	0.47	0.56	0.65	0.11	60	CO at 370°C	6 M KOH	Wet press
2051-23-1	2013-50-B	16(4)	Pt-33Ru	0.27	0.32	0.39	0.44	--	60	CO at 370°C	6 M KOH	Wet press
2051-25-1	2013-48-B	43(4)	Pt-30Ru	0.25	0.31	0.37	0.40	0.06	60	$NaBH_4$	6 M KOH	Wet press
2051-26-1	2013-48-C	17(4)	Pt-33Ru	0.26	0.33	0.42	0.50		60	$NaBH_4$	6 M KOH	Wet press
2051-27-1	2051-24-1	12(4)	Pt-33Ru	0.32	0.42	0.53	0.62	0.11	60	CO at 370°C	6 M KOH	Wet press
2051-28-1	2051-24-3	29(4)	Pt-10Ir	0.31	0.39	0.45	0.50	0.09	60	CO at 370°C	6 M KOH	Wet press
2051-29-1	2051-24-1	20	Pt-33Ru	0.23	0.30	0.38	0.44	0.08	60	CO at 370°C	6 M KOH	10% Teflon, dry
2051-30-1	2051-24-1	10	Pt-33Ru	0.25	0.32	0.44	--	0.08	60	CO at 370°C	6 M KOH	10% Teflon, dry
2051-32-1	2051-24-3	22	Pt-10Ir	0.33	0.40	0.46	0.50	0.07	60	CO at 370°C	6 M KOH	10% Teflon, dry
2051-34-1	2051-33-5	20	Pt-33Ru	0.35	0.44	0.52	--	0.08	60	(6)		
2051-35-1			Pt-20Ru	0.27	0.36	0.42	--	0.10	60	Radical anion	None	Wet press
2051-36-1	2051-29-1	20	Pt-33Ru	0.28	0.33	0.42	--	0.06	60	CO at 370°C	6 M KOH	10% Teflon, dry
2051-38-1	2051-29-2	20	Pt-5Au	0.37	0.44	0.50	--	0.08	60	CO at 370°C	6 M KOH	10% Teflon, dry
2051-39-1	2051-34-1	20	Pt-20Ru	0.27	0.32	0.40	--	0.06	60	CO at 370°C H_2 at 650°C	6 M KOH	10% Teflon, dry
2051-40-1	2051-34-2	20	Pt-20Ru	0.27	0.32	0.39	--	0.06	60	CO at 370°C H_2 at 650°C	6 M KOH	10% Teflon, dry

(1) Pretreated at 600°C in air, 2 hours.
(2) Pretreat-air 595°C.
(3) Catalyst previously dried, moistened with H_2O before press.
(4) At end of run.
(5) 0.07 at low current density, 0.11 at high current density.
(6) Physical mixture, commercial Pt Black + Ru, reduced by CO at 370°C.

APPENDIX D-1 (CONT'D)

METHANOL CATALYST PERFORMANCE

Electrode Identification	Catalyst Identification	Catalyst Loading, mg/cm^2	Nominal Composition, at %	Polarization vs Theoretical Methanol at indicated ma/cm^2 1	10	50	100	Tafel Slope	Reduction	Treatment	Electrode Preparation
2623-23-1	2623-22-1CA		Pt-40Ru	0.24	0.31	0.37	0.40	0.07	$NaBH_4$(2)	None	Wet press
Same				--	0.27	0.33	0.36	0.07		1 min, KOH	
Same				--	0.28	0.32	0.35	0.07		16 hr, KOH	
2623-24-1	2623-22-1CB	15(1)		0.23	0.30	0.36	0.38	0.07		20 min, KOH	Wet press
2623-25-1	2623-22-1CC			0.22	0.28	0.33	0.36	0.06		16 hr, KOH	Wet press
2623-26-1	2623-22-3CA		RuP-5	0.25	0.34	0.40	--	0.09	$NaBH_4$(2)	None	Wet press
Same				0.23	0.30	0.35	0.38	0.07		2 min, KOH	
Same				0.21	0.28	0.35	0.38	0.07		1 hr, KOH	
Same				--	0.28	0.35	0.38	--		16 hr, KOH	
2623-27-1	2623-22-3CB			0.20	0.27	0.33	0.35	0.08		10 min, KOH	Wet press
2623-28-1	2623-22-3CC			0.20	0.28	0.34	0.37	0.08		2 hr, KOH	Wet press
2623-29-1	2623-22-3CD			0.20	0.28	0.34	0.36	0.08		16 hr, KOH	Wet press
2623-30-1	2623-22-2C		Pt-40Ru	0.25	0.34	0.40	0.43	0.09	$NaBH_4$(2)	None	Wet press
Same				--	.31	.35	.38			1 min, KOH	
Same				0.23	0.28	0.33	0.36	0.06		10 min, KOH	
2623-37-2	2623-22-2C1	23(1)		0.22	0.28	0.34	0.45	0.07		64 hr, KOH	Wet press
2623-31-1	2623-32-1B		Ru-50Ir	0.30	0.42	0.74	--	--	$NaBH_4$(2)	None	Wet press
Same				--	0.30	0.34	0.37	0.06		1 min, KOH	
Same				--	0.31	0.34	0.37	0.06		10 min, KOH	
Same				0.21	0.30	0.33	0.36	0.06		16 hr, KOH	
2623-36-2	2623-32-3C	17.5		--	0.31	0.36	0.41	0.06		10 min, KOH	Wet press
Same				--	--	0.34	0.36	--		5 min, KOH	
2623-32-1	2623-32-2C	17(1)		--	0.24	0.33	0.35	0.06		64 hr, KOH	Wet press
2623-33-1	2623-34-1C	16(1)	RuP-5	0.24	0.32	0.39	0.42	0.08	$NaBH_4$(2)	None	Wet press
Same				--	0.28	0.33	0.36	0.07		3 min, KOH	
Same				0.21	0.28	0.34	0.38	0.07		16 hr, KOH	
2623-36-1	2623-34-2C	17(1)		0.22	0.29	0.35	0.38	0.07		10 min, KOH	Wet press
2623-37-1	2623-34-3C	26(1)		0.21	0.27	0.33	0.35	0.07		64 hr, KOH	Wet press
2623-38-2	2465-40-3	20	Ru-50Ir	0.27	0.34	0.37	0.43	0.07	$NaBH_4$	6 M KOH(3)	Dry + 10% Teflon
2623-45-1			Pt-40Ru	0.27	0.35	0.41	0.45	--	H_2O(4)	6 M KOH	Wet press
2623-42-1		20		0.28	0.34	0.38	0.41	0.06			Dry + 10% Teflon
2623-43-1	2623-41-2		RuP-5	0.24	0.31	0.37	0.40	0.07	$KABH_4$(5)	None	Wet press
Same				--	0.28	0.34	0.37	0.08		2 min, KOH(3)	
Same				--	0.28	0.34	0.37	0.06		5 min, KOH(3)	
Same				--	0.28	0.34	0.37	0.08		16 hr, KOH(3)	
2623-45-1	2623-41-2A		RuP-5	0.20	0.28	0.34	0.37	0.08		18 hr, KOH(3)	Wet press
2623-43-1	2623-41-1		RuP-5	0.20	0.29	0.34	0.37	0.08	$NaBH_4$(6)	None	Wet press
Same				--	0.27	0.32	0.35	0.08		2 min, KOH	
Same				--	0.27	0.32	0.35	0.08		5 min, KOH	
Same				--	0.29	0.33	0.33	0.08		16 hr, KOH	
2623-45-2	2623-39-1	16(1)	Pt-40Ru	0.16	0.25	0.29	0.32	0.08	H_2 185°C	16 hr, KOH	Wet press
2623-47-1		20		0.18	0.25	0.29	0.32	0.07			Dry + 10% Teflon
2623-47-2		20		--	0.24	0.29	0.32	0.07			Dry + 10% Teflon
Same				--	0.22	0.26	0.28(7)	--			
2623-48-2	2623-39-2	20	Pt-40Ru	0.19	0.25	0.30	0.32	0.07	H_2 185°C	16 hr, KOH	Dry + 10% Teflon
2623-50-1	2623-49-1	20(1)	RuP-5	--	0.26	0.32	0.34	0.08	$NaBH_4$(6)	None	Wet press
Same				--	0.29	0.31	0.33	0.08		5 min, KOH	
2623-50-2	2623-49-2	20(1)	RuP-5	--	0.24	0.29	0.32	0.08		10 min, KOH	Wet press
2623-51-1	2623-49-1	20(1)	RuP-5	0.12	0.19	0.25	0.28	0.08	H_2 185°C	16 hrs, KOH(3)	Wet press
After two Overpolarizations(8)				0.16	0.23	0.26	0.28	0.06			
2623-52-1	2623-49-3	20(1)	RuP-5	0.15	0.21	0.28	0.30	0.08			
After two Overpolarizations(8)				--	0.24	0.28	0.31	0.07			
2623-53-1	2623-Unknown	20	Pt-25 Ag(8)	--	0.42	0.50	0.54	0.14	H_2 260°C	6M KOH	Dry + 10% Teflon
2623-54-1	Comm. Pt Black	20	Pt	0.32	0.38	0.48	0.53	0.08			Dry + 10% Teflon
2623-55-1	2623-49-4	20	Pt-25 Ag_2O(9)	--	0.34	0.38	0.40	0.06			Dry + 10% Teflon
Same				0.42	0.47	0.46	0.49	0.05		4 M $NaNO_3$	
2623-56-1	2623-Unknown	20	Pt	--	0.41	0.48	0.50	0.08	H_2O_2(4)	6M KOH	Dry + 10% Teflon
2623-57-1	2623-49-5	20	Pt-25 Ag_2O	--	0.46	0.46	0.50	0.06		4 M HNO_3(10)	Dry + 10% Teflon
2623-58-1	2623-49-6	20(1)	RuP-5	--	0.25	0.30	0.31	0.09	H_2 185°C	16 hr, KOH	Wet press
After two Overpolarizations(8)				0.18	0.26	0.31	0.33	0.07			
2623-59-1	2623-49-7	5(1)	Pt-40Ru	0.09	0.16	0.41	0.44	0.07	$NaBH_4$	HNO_3	Wet press
Same				--	0.11	0.16	0.38	0.07		3 min, KOH	
2623-60-1		10(1)		--	0.15	0.42	0.46	--			Dry + 10% Teflon
Same				--	0.11	0.36	0.39	0.07		3 min, KOH	
2623-15-1		10(1)		0.07	0.15	0.40	0.43	0.08			Dry + 10% Teflon
Same				--	0.09	0.34	0.38	0.07		3 min, KOH	
2623-16-1	2623-12-1		RuP-5	--	--	0.34	0.37	--	H_2 260°C	Anodization(10)	Wet press
2623-18-1	2623-12-2	9.5(1)	RuP-5	--	0.30	0.37	--	0.09	H_2 260°C	4 M HNO_3 (10)	Wet press
2623-17-1	2623-15-1	14(1)	Pt-40Ru	--	0.33	0.55	--	--	$NaBH_4$	HNO_3	Dry + 10% Teflon
Same				0.24	0.28	0.33	0.36	--		3 min, KOH	
Same				0.22	0.28	0.31	0.34	0.06		5 min, KOH	
2623-19-1	2623-15-2	11(1)	Pt-40Ru	0.33	0.36	--	--	--	H_2 260°C	HNO_3	Wet press
Same				--	0.36	0.45	--	--		3 min, KOH	

(1) Measured at end of test.
(2) 75°C reduction step.
(3) Containing 2M methanol.
(4) Precipitation of alumina simultaneous with catalyst pptn.
(5) Methanol present during reduction.
(6) Formaldehyde present during reduction.
(7) 0.30 volts at 200 ma/cm^2, 0.36 volts at 500 ma/cm^2, 82°C.
(8) Silver removed by anodization.
(9) Overpolarized to 0.80 volts, 0.05 M methanol, twice.
(10) To remove Ag (25 at %) co-reduced with catalyst.

METHANOL CATALYST PERFORMANCE

Electrode Identification	Catalyst Identification	Catalyst Loading mg/cm²	Nominal Composition, at.%	Polarization vs Theoretical Methanol at Indicated ma/cm² 1	10	50	100	Tafel Slope	Reduction	Treatment	Electrode Preparation
2464- 3-1	2269-37-1	20	Pt-10Ru	0.29	0.36	0.42	0.45	.06	$NaBH_4$	6 M KOH	10% Teflon, dry
2464- 5-1	2269-32-2	13(1)	P-7	0.33	0.40	0.46	0.50	.08	CO 427°C H_2 650°C	6 M KOH	Wet press
2464- 7-1	2464- 6-1	20	Pt-33Ru	0.23	0.29	0.35	0.38	.06	KBH_4	6 M KOH	10% Teflon, dry
2464- 8-1	2464- 8-1	10(1)	P-7	0.19	0.27	0.37	0.42	.10	KBH_4	6 M KOH(2)	Wet press
Same-Overpolarized(3)				0.27	0.34	0.41	0.47				
2464-10-1	2464- 6-3	9(1)	Pt-33Ru	0.24	0.33	0.47	0.54	.07	Kal. anion(4)	6 M KOH	10% Teflon, dry
2464-11-1	2464- 6-2	16	Pt-33Ru	0.22	0.29	0.40	0.44	.07	H_2 at 650°C	6 M KOH	10% Teflon, dry
2464-12-1	2464-12	20	Pt-50Ru(5)	0.35	0.42	0.48	0.50	.07	(5)		
Same-After Pot. Scanning(6)				0.26	0.34	0.40	0.44	.08			
2464-16-1	2464-14-1-1	11(1)	Ru-P-3	0.17	0.27	0.35	0.41	.10	KBH_4	6 M KOH	Wet press
2464-17-1	2464-14-3	17(1)	Ru-P-3	0.25	0.32	0.38	0.41	.07	KBH_4	6 M KOH	Wet press
2464-20-1	2464-14-2-1	6(1)	Ru-P-2	0.24	0.32	0.39	0.43	.07	KBH_4	6 M KOH	Wet press
2464-21-1	2464-13-2	11(1)	P-7	0.27	0.37	0.52	0.58	.11	CO 427°C	6 M KOH(2)	Wet press
2464-22-1	2464-13-2	20(1)	P-7	0.26	0.37	0.49	0.52	.11	CO 427°C	6 M KOH(2)	Wet press
2464-24-1	2464-18-1	14(1)	Ru-P-3	0.15	0.26	0.37	0.41	.10	KBH_4	6 M KOH(2)	Wet press
Same-Overpolarized(3)				-	0.28	0.35	0.41				
2464-25-1	2464-18-2	17(1)	Ru-P-1	0.19	0.28	0.34	0.38	.08	KBH_4	6 M KOH(2)	Wet press
Same After Overpolarization(3)				0.23	0.30	0.37	0.41	.08			
2464-28-1	2464-23-1	36(1)	P-7	0.32	0.45	-	-	.13	CO 427°C H_2 650°C	6 M KOH	Wet press
2464-30-1	2464-23-2	30(1)	P-7	0.29	0.42	0.54	-	.12	CO 427°C H_2 650°C	6 M KOH	Wet press
2464-31-1		35(1)	P-7(8)	0.17	0.26	0.34	0.38	.07	KBH_4	None	Wet press
Same After Overpolarization(3)				0.22	-	0.39	0.43				
2464-31-2		29(1)	P-7(8)	0.18	0.26	0.35	0.39(10)	.12	KBH_4	None	Wet press
Same After Overpolarization(3)				-	0.33	0.40	-				
2464-34-1		37(1)	P-7(8)	0.16	0.24	0.31	0.36(10)	.10	KBH_4	None	Wet press
Same After Overpolarization(3)				-	0.31	0.37	0.40				
2464-34-2		35(1)	P-7(8)	0.16	0.24	0.31	0.36(11)	(7)	KBH_4	None	Wet press
Same After Overpolarization(3)				-	0.31	0.37	0.40				
2464-38-1	2464-18-2		Ru-P-2	0.13	0.22	0.28	0.31	.09	KBH_4	6 M KOH(2)	Wet press
Same After Overpolarization(3)				0.17	0.23	0.28	0.31	.07			
2464-39-1	2464-18-2	20	Ru-P-2	0.13	0.21	0.26	0.31	.09	KBH_4	6 M KOH(2)	Wet press
Same After Overpolarization(3)				0.17	0.24	0.30	0.42	.07			
2464-40-1		20	P-7(8)	0.15	0.24	0.31	0.36(12)	.09	KBH_4	None	Wet press
Same After Overpolarization(3)				-	0.31	0.37	0.41	.08			
2464-41-1	2464-17-2	19(1)	Pt-40Ru	0.22	0.28	0.32	0.36		$NaBH_4$	6 M KOH	Wet press
Same After Overpolarization(3)				-	0.27	0.34	0.38	.08			
2464-43-1	2464-18-1	22(1)	Ru-P-3	0.17	0.26	0.34	0.38	.09	KBH_4	6 M KOH(2)	Wet press
Same After Overpolarization(3)				-	0.30	0.36	0.40				
2464-44-1	2464-18-3	13(1)	Ru-P-3	0.18	0.27	0.34	0.38	.09	KBH_4	6 M KOH(2)	Wet press
Same After Overpolarization(3)				-	0.29	0.36	0.39	.09			
2464-49-1	2464-18-2	20	Ru-P-2	0.19	0.24	0.31	0.36	.08	KBH_4	6 M KOH(2)	10% Teflon, dry
Same After Overpolarization(3)				-	0.28	0.34	-				
2464- 6-1	2464-18-2		Ru-P-2	0.13	0.20	0.26	0.30	.09	KBH_4	6 M KOH(2)	Wet press
Same After Overpolarization(3)				-	0.29	0.36	-				
2465- 5-1			P-7	0.12	0.21	0.30	0.38(13)	.12	KBH_4	None	Wet press
Same After Overpolarization(3)				0.16	0.28	0.44	0.52				
				0.27	0.41	0.55	-				
2465- 7-1	2464-17-2	10	Ru-P-2	0.18	0.26	0.34	0.37	.11	KBH_4	6 M KOH	Wet press
Same After Overpolarization(3)				-	0.28	0.34	0.38				
2464-50-1	2464-47-2		Ru-P-2	0.16	0.24	0.31	0.34	.10	KBH_4	6 M KOH	Wet press
Same After Overpolarization(3)				-	0.29	0.35	0.38				
2465- 9-1	2464-47-2		Ru-P-2	0.22	0.30	0.37	0.40	.09	KBH_4	6 M KOH	Wet press
2465-10-1	2469- 8-1		Pt-40Ru	0.21	0.34	0.42	0.48	.07	$NaBH_4$	3 M H_2SO_4	Wet press
Same After Overpolarization(3)				-	0.32	0.38	-				
2465-11-1	2469- 8-2		Pt-40Ru	0.16	0.25	0.30	0.33	.08	$NaBH_4$	6 M KOH	Wet press
Same After Overpolarization(3)				-	0.24	0.31	0.34				

(1) Measured at end of test.
(2) Containing 2 M methanol.
(3) Twice to .80 volts, 15 min each, 0.05 M methanol.
(4) Li, biphenyl in tetrahydrofuran.
(5) Phys. mix. comm. Pt black + Ru, reduced with CO at 427°C.
(6) Potential driven between 0 and 1.5 volts, 10 times, [illegible].
(7) No pronounced Tafel region.
(8) Same catalyst preparation.
(9) 0.01 M K_2SO_4 in electrolyte.
(10) 0.05 M K_2SO_4 in electrolyte.
(11) 0.10 M K_2SO_4 in electrolyte.
(12) 0.5 M K_2SO_4 in electrolyte.
(13) Electrolyte 1 M potassium carbonate, 1 M potassium bicarbonate.

APPENDIX D-1 (CONT'D)

METHANOL CATALYST PERFORMANCE

Electrode Identification	Catalyst Identification	Catalyst Loading, mg/cm²	Nominal Composition, At %	Polarization vs Theoretical Methanol at Indicated mA/cm² 1	10	50	100	Tafel Slope	Reduction	Treatment	Electrode Preparation
2465-12-1	2465- 8-3	14(1)	Pt-40Ru	0.21	0.27	0.34	0.37	.07	$NaBH_4$	6 M KOH	Wet press
After Overpolarization(2)				0.22	0.28	0.34	0.36				
2465-13-1	2465- 8-1	20(1)	Pt-40Ru	0.21	0.27	0.32	0.35	.06	$NaBH_4$	(4)	Wet press
After Overpolarization(3)				0.19	0.25	0.30	0.32				
2465-15-1	2465-14-1	9(1)	Ru-P-4	0.24	0.32	0.38	0.41	.08	$NaBH_4$	6 M KOH	Wet press
After Overpolarization(3)				0.26	0.33	0.40	-				
2465-19-1	2465-18-1	7(1)	Ru-P-4	0.25	0.29	0.34	0.38	.08	$NaBH_4$	6 M KOH(2)	Wet press
After Overpolarization(3)				-	0.29	0.36	0.39				
2465-20-2	2465-18-2	16(1)	Ru-P-4	0.21	0.26	0.35	0.40	.07	KBH_4	6 M KOH(2)	Wet press
After Overpolarization(3)				-	0.29	0.34	0.37				
2465- 3-1	---		P-7	0.35	0.41	-	-		---	(5)	
2465-23-1	2465-22-1	9(1)	Pt-40Ru	0.20	0.26	0.30	0.33	.06	$NaBH_4$(5)	6 M KOH	Wet press
2465-24-1	2465-15-1	14(1)	Ru-P-5	0.16	0.24	0.30	0.33	.09	$NaBH_4$	6 M KOH(2)(7)	Wet press
After Overpolarization(3)				0.19	0.25	0.31	0.34				
2465-25-1	2465-18-2	15(1)	Ru-P-6	0.16	0.25	0.30	0.33	.08	$NaBH_4$	6 M KOH(2)	Wet press
After Overpolarization(3)				-	0.27	0.33	0.37				
2465-28-1	2465-26-1	27(1)	Pt-40Ru	0.21	0.27	0.33	0.36		$NaBH_4$	6 M KOH	Wet press(8)
After Overpolarization(2)				0.21	0.27	0.30	0.33	.05			Wet press(9)
				0.20	0.24	0.30	0.32				
2465-30-1	2465-14-1	21(1)	Ru-P-4	0.23	0.30	0.35	0.38	.07	$NaBH_4$	6 M KOH(2)(7)	Wet press
After Overpolarization(3)				0.20	0.28	0.33	0.36				
2465-32-1	2465-31-1	19(1)	Pt-40Ru	0.24	0.30	0.34	0.36	.06	$NaBH_4$(10)	6 M KOH	Wet press
After Overpolarization(3)				0.24	0.28	0.32	0.34				
2465-33-1	2465-31-2	8(1)	Pt-40Ru	0.26	0.33	0.39	0.43	.07	$NaBH_4$(10)	6 M KOH	Wet press
After Overpolarization(3)				0.24	0.30	0.38	0.45				
2465-34-1	---	35(1)	Pt-20Ru	0.21	0.32	0.46	0.56		Rad. anion(11)	6 M KOH	Wet press
2465-35-1	---		Ru-P-5	0.15	0.22	0.28	0.30	.08	KBH_4	6 M KOH(2)	Wet press
After Overpolarization(3)				-	0.24	0.29	0.31				
2465-41-1	2465-40-1		Ru-50Au	0.40	-	-	-		$NaBH_4$	6 M KOH(2)	Wet press
2465-41-2	2465-40-2		Ru-50Rh	0.28	0.36	0.48	-	.08	$NaBH_4$	6 M KOH(2)	Wet press
2465-42-1	2465-40-3		Ru-50Ir	0.25	0.30	0.33	0.36	.06	$NaBH_4$	6 M KOH(2)	Wet press
2465-42-2	2465-40-4		Ru-50Re		No Activity				$NaBH_4$	6 M KOH(2)	Wet press
2465-45-1	2465-43-2		Pt-40Ru	0.34	0.41	0.46	0.49	.07	$NaBH_4$	H_2O_2	Wet press
2465-46-1	2465-43-1		Pt-40Ru	0.35	0.42	0.48	0.50	.07	$NaBH_4$	None	Wet press
2465-48-1	2465-[illegible]		Pt-40Ru	0.29	0.36	0.42	0.46	.08	$NaBH_4$	KOH	Wet press
2465-49-1	2465-49-1		Ru-50Ir	-	0.31	0.35	0.37	.06	$NaBH_4$	6 M KOH(2)	Wet press
2465-46-1	2465-47-1		Pt-40Ru	-	0.30	0.34	0.38	.06	HCHO	None	Wet press
2465-[illegible]-1	2465-47-2		Pt-40Ru	0.27	0.32	0.37	0.40	.04	HCHO	None	Wet press
				0.29	0.35	0.42	0.50	.06			
				0.23	0.29	0.34	0.37	.06			
2623-[illegible]-1	2465-40-2		Ru-50Rh	0.30	0.35	0.40	-		$NaBH_4$	6 M KOH(7)	Wet press
2623-[illegible]-1	2465-47-3		Pt-40Ru	-	0.31	0.37	0.39		HCHO	6 M KOH	Wet press
				-	0.33	0.38	0.39				
				0.23	0.28	0.32	0.34				
2623-[illegible]-1	2623- 9-1	16.5(1)	Pt-40Ru	0.24	0.29	0.34	0.37	.06	$NaBH_4$	6 M KOH(12)	Wet press
2623-17-1	2623- 9-3	20(1)	Pt-40Ru	0.22	0.28	0.32	0.34				10% Teflon, dry
2623-13-1	2623- 9-2	12(1)	Pt-40Ru	0.24	0.30	0.34	0.36	.06	$NaBH_4$	12 M KOH(12)	Wet press
2623-18-1	"	10(1)	Pt-40Ru	0.22	0.28	0.32	0.34				10% Teflon, dry
2623-14-2	2623- 8-1	17(1)	Pt-40Ru	0.23	0.29	0.34	0.36		$NaBH_4$	6 M KOH(12)	Wet press
2623-21-1	"	20	Pt-40Ru	0.22	0.28	0.32	0.34				10% Teflon, dry
2623-16-1	2623- 9-1	11(2)	Pt-40Ru	0.24	0.30	0.34	0.36		$NaBH_4$	H_2O, Sat. K_2SO_4(12)	Wet press
2623-19-1	2623- 9-2	--	Pt-40Ru	0.28	0.36	0.40	0.42		$NaBH_4$	12 M KOH(12)	Wet press
2623-20-1	"	20	Pt-40Ru	0.24	0.29	0.34	0.36				10% Teflon, dry

(1) Measured at end of test
(2) Containing 2 M methanol.
(3) Twice to 0.6 volts, 30 min., 0.05 M methanol
(4) Catr. 2465-8-1, soaked overnight in 6 M KOH
(5) Attempt to reactivate electrode by $NaBH_4$ treat
(6) Formaldehyde present during reduction.
(7) Borane treat. of this catalyst.
(8) From KOH soln
(9) After normal acid wash.
(10) Solution of catalyst which contained 2 wt % polyox
(11) Tetraphenylbiphenol in THF.
(12) [illegible]

APPENDIX D-2

VOLTAGE SCAN-PT-33 Ru, PHYSICAL MIXTURE

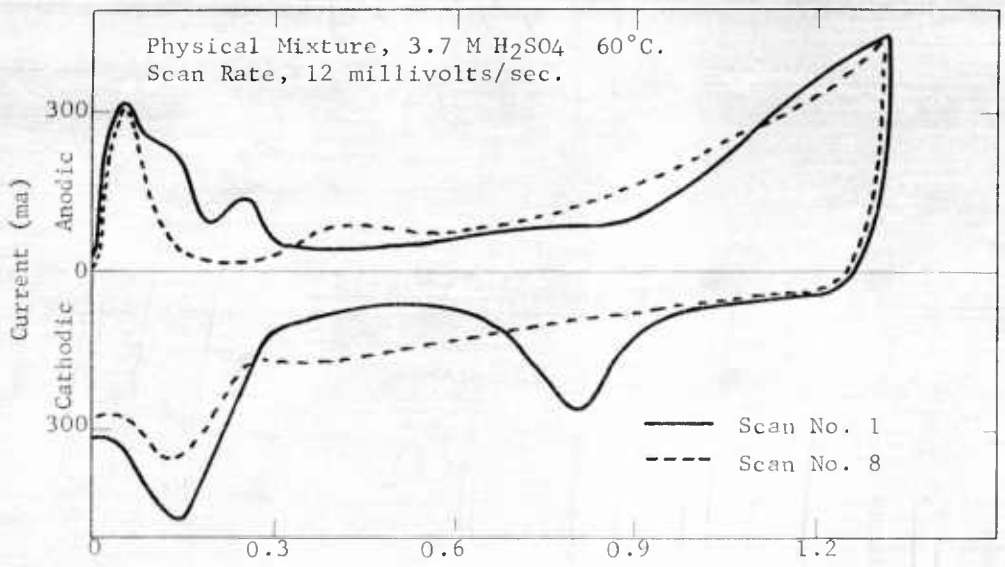

APPENDIX D-3

METHANOL CATALYST LIFE STUDIES

Electrode No.	Catalyst	Polarization from Methanol Theory at Indicated Hours, 50 ma/cm^2, 1 M Methanol						Comments
		1	500	1000	2000	4000	6000	
(2)	P-Type[1] 82°C	.28	.31	.32	.34	.35	.38	P Catalyst on Pt Screen
(3)	P-Type[2] 82°C	.28	.28	.30	.30	.33	.32	P Catalyst on Ta Screen
(4)	Pt-33 Ru 82°C	.33	.34	.34[3]				On Pt Screen + 10% Teflon
(5)	RuP-2 82°C	.25	.30[5]	.31	.33[4][5]			Catalyst on Pt Screen
(6)	RuP-5 60°C	.35	.34[5][6]					Catalyst on Pt Screen
(7)	RuP-5 60°C	.32	.33					Catalyst on Pt Screen

(1) 5000 hour life reported in ref (4); had polarized to 0.45 at 7000 hours.
(2) 2000 hour life reported in ref (4).
(3) Voluntarily shut down at 1340 hours at a polarization of 0.35.
(4) 1500 hours on test; 50 millivolt loss between 0 and 500 hours attributed to catalyst loss.
(5) Tests in progress.
(6) 410 hour value.

APPENDIX D-4

COMPOSITION OF RADICAL ANION REDUCED CATALYSTS

Reference No.	Catalyst Composition Based On Composition of Reaction Solution	Wet Chemical Analysis
235	Pt-20 Ru	Pt-8.9 Ru
260	Pt-20 Ru	Pt-19.0 Ru
268	Pt-33 Ru	Pt-9.5 Ru
238	Pt-25 Zn	Pt-24.9 Zn
239	Pt-50 Zn	Pt-50.0 Zn
240	Pt-25 Nb	Pt-0.4 Nb
241	Pt-50 Nb	Pt-2.6 Nb
242	Pt-25 V	Pt-5.2 V
243	Pt-50 V	Pt-11.7 V
244	Pt-25 W	Pt-0.1 W
245	Pt-50 W	Pt (traces of W)
247	Pt-50 Ta	Pt-13 Ta
248	Pt-25 Zr	Pt-1.8 Zr
265	Pt-25 Zr	Pt-3.5 Zr
249	Pt-50 Zr	Pt-0.6 Zr
252	Pt-25 Mo	Pt-1 Mo
253	Pt-50 Mo	Pt-0.9 Mo
254	Pt-25 Ti	Pt-2.0 Ti
255	Pt-50 Ti	Pt-6.1 Ti
256	Pt-25 Cr	Pt-4.2 Cr
257	Pt-50 Cr	Pt-9.9 Cr
259	Pt-50 Mn	Pt-37.5 Mn

APPENDIX D-5

PREPARATION AND TESTING OF RADICAL ANION REDUCED CATALYSTS

Run No.	Catalyst Composition*	Polarization at Indicated ma/cm², volts 0	1	10	50	100	Tafel Slope b	Catalyst Loading, mg/cm²	Remarks**
13	Pt	0.34	0.44	0.49	0.52	0.55	0.05	20	Standard, reduced with $NaBH_4$.
226	Pt	0.18	0.27	0.43	0.47	0.50	0.11	26	
229	Pt	0.22	0.30	0.39	0.45	0.48	0.08	26	
227	P7	0.17	0.24	0.39	0.46	0.49	0.08	14	
228A	P7	0.18	0.28	0.39	0.47	0.51	0.11	25	
235	Pt-20 Ru	0.20	0.24	0.31	0.36	0.38	0.07	22	First batch.
250	Pt-20 Ru	0.20	0.25	0.32	0.37	0.40	0.08	22	Stored in H_2O for three days.
260	Pt-20 Ru	0.23	0.31	0.40	0.46	0.49	0.09	10	Second batch stored in H_2SO_4 for three days.
261	Pt-20 Ru	0.26	0.32	0.39	0.44	0.46	0.07	8	Second batch.
262	Pt-20 Ru	0.24	0.28	0.33	0.37	0.38	0.05	20	Third batch washed with benzene and CH_3OH.
271	Pt-20 Ru	0.21	0.26	0.34	0.40	0.43	0.09	--	Third batch washed with CH_3OH.
263	Pt-20 Ru	0.20	0.27	0.34	0.39	0.42	0.08	18	" " " "
233	Pt-33 Ru	0.20	0.25	0.31	0.36	0.38	0.07	16	First batch.
234	Pt-33 Ru	0.20	0.24	0.29	0.34	0.36	0.07	20	
236	Pt-33 Ru	0.20	0.24	0.30	0.34	0.37	0.06	20	
268	Pt-33 Ru	0.20	0.26	0.30	0.38	0.40	0.07		Second batch.
251	Pt-33 Ru	0.17	0.23	0.30	0.34	0.37	0.07	20	First batch stored in H_2O for three days.
238	Pt-25 Zn	0.35	0.40	0.43	0.47	0.49	0.05	8	
239	Pt-50 Zn	0.35	0.45	0.49	0.54	0.58	0.05	9	
240	Pt-25 Nb	0.32	0.36	0.41	0.45	0.47	0.05	14	
241	Pt-50 Nb	0.23	0.33	0.40	0.44	0.43	0.06	26	
242	Pt-25 V	0.28	0.34	0.41	0.45	0.47	0.07	9	
243	Pt-50 V	0.26	0.34	0.41	0.45	0.47	0.065	10	
244	Pt-25 W	0.25	0.37	0.40	0.45	0.47	0.07	17	
245	Pt-50 W	0.18	0.34	0.40	0.45	0.47	0.07	14	
246	Pt-25 Ta	0.21	0.33	0.48	0.53	0.55	0.07	30	
247	Pt-50 Ta	0.34	0.42	0.55	0.62	0.67	0.09	5	
248	Pt-25 Zr	0.31	0.36	0.40	0.44	0.47	0.04/0.09***	18	
265	Pt-25 Zr	0.24	0.38	0.44	0.47	0.49	0.035	11	Traces of unreduced ZrO_2 observed.
249	Pt-50 Zr	0.31	0.40	0.42	0.44	0.47	0.02/0.09***	23	
252	Pt-25 Mo	0.14	0.33	0.38	0.43	0.46	0.055	23	
253	Pt-50 Mo	0.31	0.37	0.44	0.52	0.56	0.07	13	
254	Pt-25 Ti	0.35	0.39	0.44	0.50	0.53	0.06	10	Storage water became milky. Second run 20 mv less polarized.
255	Pt-50 Ti	0.32	0.36	0.42	0.47	0.50	0.05	9	
256	Pt-25 Cr	0.13	0.21	0.43	0.48	0.51	.05	8	Second run 150 mv less below 5 ma/cm².
257	Pt-50 Cr	0.18	0.31	0.47	0.50	0.52	.05	8	
258	Pt-25 Mn	0.32	0.40	0.45	0.48	0.50	.05	10	
259	Pt-50 Mn	0.32	0.42	0.53	0.62	0.66	0.12	5	
264	Pt-20 Ru-20 Ta	0.16	0.28	0.34	0.39	0.41	0.07	--	

* Based on composition in mol % of reaction solution.

** Catalyst preparation from corresponding salt solutions or slurries in THF or diglyme by reduction at room temperature with radical anion prepared in situ or separately by addition of Li or Na to polycyclic aromatics (biphenyl). The precipitates were washed with degassed, benzene, methanol and H_2O and stored under N_2.

*** A/B denotes change in Tafel slope at 30 ma/cm² to the second value (B).

APPENDIX D-6

EXTENDED PERFORMANCE TESTS ON RADICAL ANION REDUCED CATALYSTS

Run No.	Catalyst[1] Composition	Initial Polarization at 50 ma/cm^2, volts	Polarization Increase, mv	Length of Test, hrs
262	Pt-20 Ru[2]	0.38	10	336
260	Pt-20 Ru[3]	0.47	100	20
261	Pt-20 Ru[3]	0.44	220	20
251	Pt-33 Ru	0.37 (at 100 ma/cm^2)	100	100
238	Pt-25 Zn	0.47	50	20
239	Pt-50 Zn	0.54	30	20
263	Pt-25 Zr	0.47	60	16
254	Pt-25 Ti	0.50	35	16
255	Pt-50 Ti	0.47	110	16
257	Pt-50 Cr	0.50	180	28
259	Pt-50 Mn	0.62	600	10
264	Pt-20 Ru-20 Ta	0.39	90	72

(1) Based on reaction solution composition.
(2) Third preparation.
(3) Second preparation.

APPENDIX B-7

EFFECT OF STRUCTURE VARIABLES ON METHANOL ELECTRODE PERFORMANCE

Electrode No.	Preparation(1)	Temp °C	Methanol Conc, M	Polarization at Indicated ma/cm^2, volts					
				5	10	20	50	100	200
2292-3A	100% Pt pressed @ 8000 psi	82	1	0.39	0.41	0.43	0.44	0.46	0.49
2292-3A	100% Pt pressed @ 8000 psi	60	1	0.43	0.45	0.46	0.47	0.49	0.52
2292-3B	50% Pt - 50% activated carbon pressed @ 8000 psi	--	-	Did not press into coherent electrodes					
2292-3C	50% Pt - 50% Teflon pressed at 8000 psi	82	1	0.39	0.41	0.43	0.46	0.50	0.57
2292-3C	50% Pt - 50% Teflon pressed at 8000 psi	60	1	0.42	0.44	0.46	0.48	--	0.63
2292-4A	33% Pt + 33% C + 33% Teflon pressed at 8000 psi	60	1	0.43	0.44	0.45	0.47	0.48	0.51
2292-4B	50% Pt - 50% Teflon pressed at 50 psi	60	1	0.42	0.44	0.45	0.47	0.49	0.51
2292-4C	33% Pt - 33% Teflon - 33% additional porosifier	60	1	0.44	0.46	0.47	0.50	0.53	0.56
2292-4D	50% Pt - 25% C - 25% Teflon pressed at 500 psi	60	1	0.43	0.45	0.46	0.47	0.49	0.52
2292-5A	50% Pt - 50% Teflon ballmilled, pressed at 1000 psi								
2292-5B	75% Pt + 25% Teflon ballmilled, pressed at 1000 psi			Did not press into coherent electrodes					
2292-5C	75% Pt + 25% Teflon pressed at 1000 psi								

All runs in 3.7 M sulfuric acid with one inch diameter electrodes in half cell.

(1) Commercial Pt black, Engelhard Lot 8250, used in all electrodes. All loadings were 20 mg/cm^2.

APPENDIX D-8

DOUBLE LAYER CAPACITANCE IN THE PRESENCE OF METHANOL

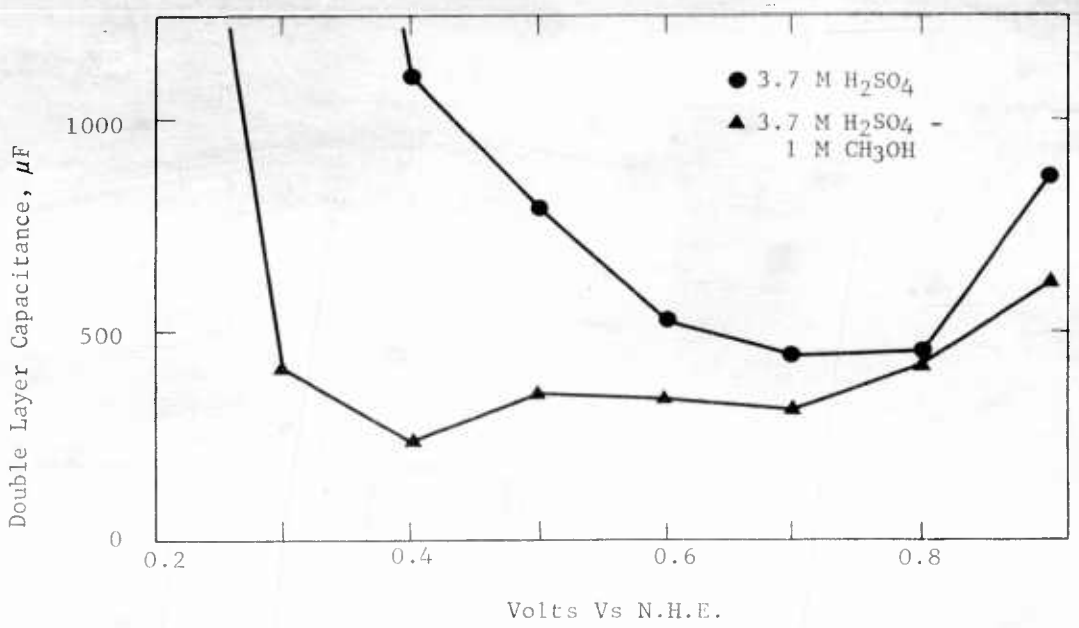

APPENDIX D-9

COVERAGE ON PLATINIZED PLATINUM
AS A FUNCTION OF METHANOL CONCENTRATION

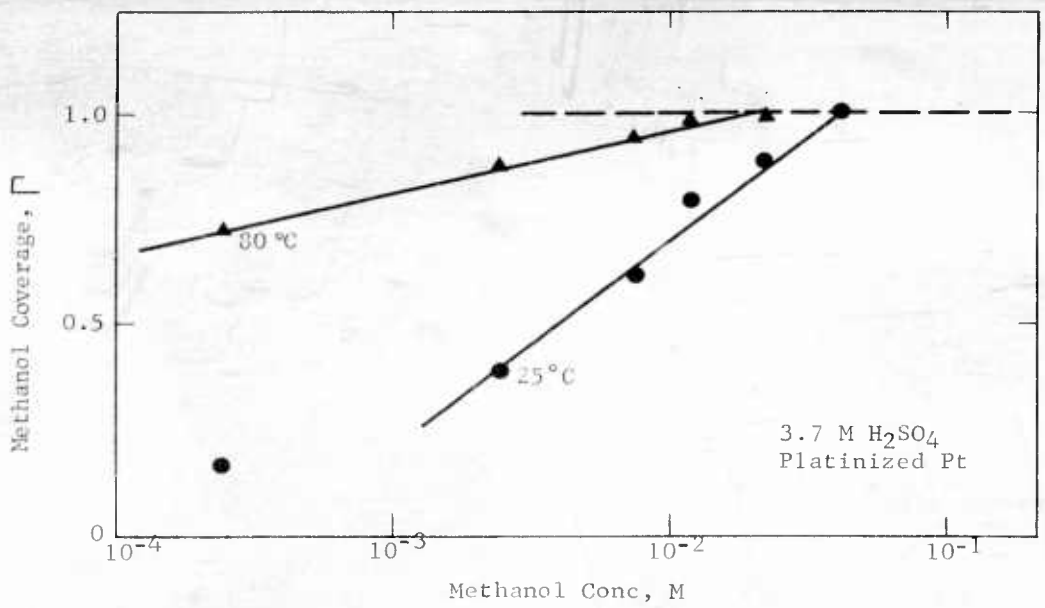

APPENDIX E-1

SCREENING STUDIES ON POROUS OXYGEN ELECTRODES

Electrode No.	Catalyst	Oxidant	Variable	Electrolyte	Temp °C	Polarization from Oxygen Theory at Indicated ma/cm² 0	5	10	20	50	100	200
109B III	CT-1	Air	Standard preparation(1)	30% H_2SO_4	82	0.29	0.31	0.33	0.36	0.43	0.64	--
155-19	CT-1 + Pt	O_2	Std prep, reimpregnated with Pt	30% H_2SO_4	100	0.19	0.24	0.27	0.29	0.34	0.44	0.53
		Air			100	0.20	0.28	0.30	0.34	0.47	0.71	--
155-20	CT-1 + Pt	O_2	Std prep, reimpregnated with Pt	30% H_2SO_4	100	0.19	0.24	0.26	0.28	0.33	0.37	0.45
		Air			100	0.19	0.27	0.29	0.32	0.39	0.53	--
159-2	Pt	O_2	Pt powder impregnated with Pt	30% H_2SO_4	100	0.17	0.26	0.30	0.32	0.37	0.41	0.47
161B-2	CT-1	O_2	Radical anion reduction,	30% H_2SO_4	100	0.23	0.30	0.33	0.35	0.41	0.46	0.55
150A-2	Pt	O_2	Supported on TiN	30% H_2SO_4	100	0.38	0.59	0.66	0.79	--	--	--
139-4	CT-1	O_2	41B X Teflon binder	30% H_2SO_4	100	0.27	0.43	0.46	0.50	0.61	--	--
145-4	CT-1	O_2	Coconut charcoal catalyst support	30% H_2SO_4	100	0.47	0.51	0.57	0.68	--	--	--
119-4	Pt	O_2	Engelhard Pt black, Teflon 7	30% H_2SO_4	100	0.25	0.44	0.47	0.51	0.57	0.62	0.69
155-20	CT-1 + Pt	O_2	Std prep, reimpregnated with Pt	85% H_3PO_4	150	0.22	0.25	0.27	0.30	0.38	0.52	--
159-2	Pt	O_2	Std prep, reimpregnated with Pt	85% H_3PO_4	150	0.17	0.29	0.34	0.40	0.51	0.64	--
161B2	CT-1	O_2	Std prep, reimpregnated with Pt	85% H_3PO_4	150	0.29	0.30	0.33	0.36	0.42	0.51	--
155-21	CT-1 + Pt	O_2	Std prep except half electrode thickness reimpregnation with Pt	30% H_2SO_4	100	0.17	0.22	0.26	0.27	0.33	0.39	0.48
155-23	CT-1 + Pt	O_2	Std prep, reimpregnated with Pt	30% H_2SO_4	100	0.17	0.22	0.24	0.27	0.30	0.34	0.43
155-22	CT-1	O_2	Std prep, except half electrode thickness	30% H_2SO_4	100	0.20	0.28	0.30	0.33	0.38	0.43	0.50
155-24	CT-1	O_2	Standard preparation	30% H_2SO_4	100	0.21	0.28	0.30	0.33	0.38	0.44	0.55
155-17	CT-1 + Pt	O_2	Std prep, reimpregnated with Pt	30% H_2SO_4	100	0.19	0.24	0.27	0.30	0.34	0.41	--
160A-7	CT-1	O_2	Std prep except higher catalyst loading	30% H_2SO_4	100	0.22	0.30	0.33	0.37	0.43	0.50	0.59
160A-5	CT-1 + Pt	O_2	Std prep except higher catalyst loading, reimpregnate with Pt	30% H_2SO_4	100	0.17	0.24	0.26	0.29	0.33	0.37	0.44
150B-1	Pt	O_2	Supported on TiN	30% H_2SO_4	100	0.39	0.54	0.61	0.70	--	--	--
		O_2		85% H_3PO_4	150	0.41	0.53	--	--	--	--	--
160A-6	CT-1 + Pt	O_2	Std prep except higher catalyst loading, reimpregnate with Pt	30% H_2SO_4	100	0.17	0.23	0.25	0.27	0.31	0.35	--
162A-1	CT-2	O_2	Radical anion reduction	30% H_2SO_4	100	0.21	0.28	0.30	0.32	0.36	0.40	0.46
				85% H_3PO_4	150	0.25	0.29	0.33	0.37	0.45	0.54	--
162A-2	CT-2	O_2	Radical anion reduction	30% H_2SO_4	100	0.21	0.29	0.30	0.33	0.38	0.44	0.53
160A-8	CT-1	O_2	Std prep except higher catalyst loading, reimpregnate	30% H_2SO_4	100	0.19	0.30	0.33	0.39	0.41	0.45	0.52
162A-3	CT-2	O_2	Radical anion reduction reimpregnation with Pt	30% H_2SO_4	100	0.15	0.25	0.28	0.31	0.38	0.46	0.58
162A-4	CT-2	O_2	Radical anion reduction reimpregnation with Pt	30% H_2SO_4	100	0.17	0.23	0.27	0.32	0.40	0.50	0.59
162A-5	CT-2	O_2	Radical anion reduction	30% H_2SO_4	100	0.21	0.27	0.28	0.30	0.33	0.37	0.42
		Air			100	0.23	0.30	0.32	0.36	0.42	0.51	0.70
160A-5	CT-1	Air	Std prep except higher catalyst loading	30% H_2SO_4	100	0.17	0.24	0.27	0.30	0.39	0.56	--
150B-2		O_2	TiN support	30% H_2SO_4	100	0.37	0.56	0.65	--	--	--	--
162A-6	CT-2	O_2	Radical anion reduction	30% H_2SO_4	100	0.19	0.25	0.28	0.30	0.34	0.38	0.43
165A-1	Au	O_2	Standard preparation	30% H_2SO_4	100	0.43	0.55	0.73	--	--	--	--
		O_2				0.45	0.64	0.74	--	--	--	--
165A-2	Au	Air	Standard preparation	30% H_2SO_4	100	0.45	0.62	--	--	--	--	--
166A-1	CT-2 Pt-Au	O_2	Standard preparation	30% H_2SO_4	100	0.23	0.31	0.34	0.38	0.44	0.57	--
167A-1	P-type	O_2	Standard preparation	30% H_2SO_4	100	0.25	0.30	0.32	0.35	0.40	0.46	0.55
168A-1	Pt_3Zn	O_2	Standard preparation	30% H_2SO_4	100	0.23	0.29	0.31	0.34	0.37	0.41	0.47
168A-3	Pt_3Zn	O_2	Standard preparation	30% H_2SO_4	100	0.23	0.28	0.30	0.32	0.36	0.40	0.46
160A-8R	CT-1 + Pt	O_2	Std prep except higher catalyst loading, reimpregnated with B_2H_6 reduced Pt	30% H_2SO_4	100	0.17	0.39	0.44	0.50	0.62	0.74	--
175A-1	Pt-Au-Pd-Ag	O_2	Standard preparation	30% H_2SO_4	100	0.41	0.57	0.61	0.66	0.74	--	--
175A-2	Pt-Au-Pd-Ag	O_2	Standard preparation	30% H_2SO_4	100	0.34	0.43	0.47	0.51	0.59	0.71	--
185A-1	Pt-20 Au	O_2	$NaBH_4$ reduction	30% H_2SO_4	100	0.23	0.30	0.32	0.36	0.41	0.49	0.58
185A-2	Pt-20 Au	O_2	$NaBH_4$ reduction	30% H_2SO_4	100	0.23	0.30	0.32	0.34	0.39	0.45	0.53
185B-1	Pt-20 Au	O_2	Standard preparation	30% H_2SO_4	100	0.29	0.38	0.41	0.45	0.53	0.63	--
185B-2	Pt-20 Au	O_2	Standard preparation	30% H_2SO_4	100	0.29	0.37	0.40	0.44	0.49	0.57	0.67

(1) Catalyzed carbon compounded with a binder and having a porosity of about 40%.

APPENDIX E-2

PERFORMANCE OF CARBON ELECTRODES

Oxidant: Air
Electrolyte: 3.7 M H_2SO_4

Test No.	Average Thickness, mils: Catalyzed Layer	Teflon Layer	Teflon Layer Average Porosity, %	Temp, °C	Electrolyte Head, Inches	Catalyst Density, mg/cm²	Polarization from Oxygen Theory at Indicated ma/cm²: 0	0.8	4	8	16	40	80	120	160
2060-16 I	20	20	43	24	0	2.5	0.29	0.30	0.39	0.44	0.50	0.59	0.68	0.77	0.91
				22	5	2.5	0.28	0.31	0.43	0.48	0.52	0.61	0.72	0.86	--
2060-16 II	20	20	43	82	0	2.5	0.31	0.32	0.37	0.41	0.44	0.51	0.59	0.67	0.88
				82	5	2.5	0.30	0.31	0.37	0.41	0.43	0.50	0.59	0.73	--
2060-15 III	20	20	43	23	0	2.5	0.28	0.29	0.35	0.41	0.46	0.55	0.66	0.76	0.90
				82	0	2.5	0.25	0.27	0.31	0.36	0.40	0.48	0.57	0.68	0.85
2060-15 I	40	0	-	21	0	5.0	0.41	0.43	0.47	0.47	0.54	0.64	0.74	0.82	0.89
				53	0	5.0	0.25	0.26	0.29	0.33	0.37	0.44	0.52	0.60	0.67
2060-15 II	40	20	50	24	6	2.5	0.33	0.34	0.40	0.50	0.56	0.66	0.72	0.78	0.85
				21	0	2.5	0.23	0.25	0.31	0.43	0.49	0.57	0.66	0.75	0.80
				82	0	2.5	0.23	0.25	0.32	0.35	0.38	0.43	0.50	0.56	0.63
2060-23 I	30	10	43	23	0	2.5	0.30	0.33	0.44	0.48	0.53	0.62	0.72	0.80	0.86
				82	0	2.5	0.29	0.29	0.33	0.37	0.40	0.47	0.54	0.59	0.65
2060-23 II	30	20	50	24	6	2.5	0.28	0.32	0.41	0.45	0.50	0.58	0.66	0.71	0.77
				82	0	2.5	0.20	0.23	0.33	0.38	0.41	0.47	0.54	0.60	0.67
2060-23 III	30	10	43	23	0	2.5	0.31	0.30	0.42	0.41	0.46	0.53	0.64	0.80	0.87
				73	5	2.5	0.25	0.24	0.30	0.36	0.39	0.48	0.56	0.80	0.89
2060-23 IV	30	10	43	48	0	2.5	0.27	0.31	0.37	0.39	0.43	0.50	0.59	0.69	0.86
				82	5	2.5	0.29	0.33	0.38	0.41	0.45	0.54	0.58	0.61	0.66
2060-27 I	10	10	43	23	0	1.2	0.25	0.43	0.58	0.58	0.66	0.86	0.72	0.78	0.84
2060-27 II	10	10	50	22	5	1.2	0.43	0.44	0.52	0.56	0.59	0.68	0.76	0.80	0.86
2060-27 III	10	10	50	82	0	1.2	0.30	0.32	0.38	0.41	0.46	0.54	0.58	0.64	0.71
				82	5	1.2	0.28	0.33	0.41	0.43	0.47	0.52	0.59	0.66	0.71
2060-31	30	10	43	23	0	2.5	0.24	0.26	0.44	0.46	0.50	0.58	0.64	0.69	0.72
				71	5	2.5	0.25	0.31	0.42	0.43	0.48	0.55	0.61	0.67	0.74
				80	0	2.5	0.25	0.28	0.34	0.40	0.44	0.50	0.56	0.58	0.63
				81	5	2.5	0.27	0.29	0.34	0.37	0.40	0.45	0.51	0.55	0.60
				82	5	1.2	0.24	0.29	0.35	0.38	0.39	0.46	0.50	0.56	0.59
2060-32	30	10	43	22	0	2.5	0.22	0.26	0.43	0.46	0.50	0.57	0.68	0.73	0.78
				22	5	2.5	0.28	0.28	0.34	0.38	0.42	0.48	0.59	0.73	0.88
				80	0	2.5	0.29	0.30	0.38	0.41	0.45	0.52	0.59	0.65	0.70
				80	5	2.5	0.27	0.28	0.34	0.38	0.41	0.48	0.54	0.59	0.64
				81	5	2.5	0.27	0.30	0.34	0.38	0.43	0.49	0.56	0.60	0.66

APPENDIX E-2 (CONT'D)

PERFORMANCE OF CARBON ELECTRODES

Oxidant Air
Electrolyte 3.7 M H_2SO_4

Test No	Average Thickness, mils: Catalyzed Layer	Average Thickness, mils: Teflon Layer	Teflon Layer Average Porosity, %	Temp, °C	Electrolyte Head, Inches	Catalyst Density, mg/cm²	Polarization from Oxygen Theory at Indicated ma/cm²: 0	0.8	4	8	16	40	80	120	160
2060-43 VIII	20	20	60	22	0	2.5	0.32	0.42	0.52	0.58	0.66	0.82	--	--	--
				22	5	2.5	0.34	0.46	0.57	0.64	0.71	0.84	--	--	--
				82	0	2.5	0.26	0.30	0.34	0.38	0.43	0.50	0.57	0.62	0.67
				82	5	2.5	0.29	0.31	0.35	0.38	0.43	0.50	0.57	0.63	0.69
2061-13	10	10	60	20	0	1.2	0.33	0.42	0.48	0.50	0.54	0.64	0.72	0.78	0.84
				20	5	1.2	0.32	0.45	0.50	0.53	0.58	0.64	0.73	0.79	0.87
				80	0	1.2	0.28	0.33	0.39	0.42	0.45	0.50	0.55	0.60	0.63
				81	5	1.2	0.30	0.33	0.41	0.43	0.46	0.51	0.57	0.61	0.65
2061-13	10	10	50	20	0	1.2	0.33	0.44	0.51	0.55	0.61	0.73	0.84	0.93	--
				20	5	1.2	0.33	0.46	0.53	0.58	0.64	0.74	0.87	0.99	--
				80	0	1.2	0.29	0.35	0.41	0.44	0.47	0.53	0.60	0.65	0.70
				81	5	1.2	0.31	0.39	0.43	0.45	0.49	0.55	0.62	0.67	0.72
2060-112-13-613	10	10	60	22	0	1.2	0.34	0.46	0.52	0.56	0.60	0.68	0.72	0.78	
				22	5	1.2	0.34	0.47	0.54	0.57	0.61	0.68	0.74	0.80	
				82	0	1.2	0.25	0.28	0.34	0.36	0.40	0.46	0.54	0.60	0.67
				82	5	1.2	0.27	0.29	0.34	0.37	0.41	0.46	0.54	0.60	0.67
2061-13	10	10	50	22	0	1.2	0.30	0.36	0.41	0.45	0.49	0.56	0.63	0.69	0.77
				22	5	1.2	0.33	0.41	0.47	0.48	0.52	0.58	0.66	0.72	0.80
				82	0	1.2	0.23	0.29	0.33	0.37	0.41	0.47	0.54	0.61	0.68
				82	5	1.2	0.23	0.29	0.33	0.38	0.41	0.48	0.56	0.61	0.68
2061-13	10	10	60	20	0	1.2	0.33	0.42	0.48	0.50	0.54	0.64	0.72	0.78	0.84
				20	5	1.2	0.32	0.45	0.50	0.53	0.58	0.64	0.73	0.79	0.87
				81	0	1.2	0.28	0.33	0.39	0.42	0.45	0.50	0.55	0.60	0.63
				82	5	1.2	0.30	0.35	0.41	0.43	0.46	0.51	0.57	0.61	0.65

Test No	Average Thickness, mils: Catalyzed Layer	Average Thickness, mils: Teflon Layer	Teflon Layer Average Porosity, %	Temp, °C	Electrolyte Head, Inches	Catalyst Density, mg/cm²	Polarization from Oxygen Theory at Indicated ma/cm: 0	1	10	20	50	100	150
2061-34	8	8	60	22	0	0.9	0.49	0.93	--	--	--	--	--
				82	0	0.9	0.51	0.85	--	--	--	--	--
2061-27	8	8	60	22	0	0.9	0.37	0.58	0.64	0.68	0.75	0.84	--
2061-30	8	8	60	22	0	0.9	0.42	0.52	0.57	0.58	0.66	0.74	0.81
				82	0	0.9	0.34	0.42	0.47	0.48	0.53	0.61	0.67
2061-34	8	8	60	22	0	0.9	0.33	0.44	0.52	0.52	0.59	0.68	0.76
				82	0	0.9	0.25	0.30	0.39	0.43	0.50	0.57	0.63

APPENDIX E-3

PERFORMANCE OF PLATINUM-TEFLON ELECTRODES

Oxidant: Air
Electrolyte: 3.7 M H_2SO_4

Test No.	Average Thickness, mils: Platinum Layer	Average Thickness, mils: Teflon Layer	Teflon Layer Average Porosity, %	Catalyst Density, mg/cm^2	Temp, °C	Electrolyte Head, Inches	Polarization from Oxygen Theory at Indicated ma/cm^2: 0	0.8	4	8	16	40	80	120	160
2060-16 III	20	20	33	46	23	0	0.18	0.19	0.22	0.26	0.30	0.36	0.43	0.52	0.59
					21	5	0.14	0.15	0.25	0.30	0.34	0.39	0.44	0.54	0.70
2060-16 IV	20	20	33	46	82	0	0.17	0.17	0.19	0.22	0.25	0.28	0.32	0.43	0.53
					82	5	0.15	0.16	0.19	0.22	0.25	0.29	0.33	0.43	0.63
2060-26 III	20	10	33	46	21	0	0.26	0.29	0.31	0.35	0.40	0.49	0.61	0.73	0.87
					21	5	0.28	0.33	0.38	0.42	0.46	0.52	0.61	0.69	0.86
2060-27 III	20	10	33	46	82	0	0.20	0.22	0.28	0.30	0.33	0.36	0.49	0.61	0.79
2060-26 V	20	10	33	46	21	5	0.22	0.23	0.27	0.30	0.33	0.40	0.50	0.63	0.79
2061-5	20	10	33	46	22	0	0.26	0.27	0.31	0.36	0.40	0.48	0.57	0.64	0.68
					21	5	0.21	0.35	0.40	0.44	0.46	0.52	0.59	0.64	0.70
2061-6	20	10	33	46	83	0	0.20	0.21	0.26	0.28	0.31	0.38	0.45	0.51	0.57
					82	5	0.19	0.21	0.26	0.29	0.32	0.38	0.46	0.51	0.56
2061-5	10	10	50	23	22	0	0.22	0.26	0.31	0.34	0.37	0.42	0.47	0.51	0.54
					22	5	0.20	0.27	0.34	0.36	0.38	0.43	0.47	0.51	0.54
2061-6	10	10	50	23	82	0	0.19	0.22	0.26	0.28	0.30	0.33	0.37	0.40	0.44
					82	5	0.19	0.22	0.26	0.28	0.30	0.33	0.37	0.40	0.44
2060-41 I	7	7	60	16	23	0	0.28	0.29	0.34	0.36	0.38	0.42	0.46	0.49	0.52
					82	0	0.23	0.24	0.26	0.28	0.31	0.34	0.38	0.40	0.42
2061-16	7	7	50	16	20	0	0.23	0.35	0.39	0.41	0.42	0.45	0.48	0.49	0.50
					21	5	0.19	0.30	0.34	0.36	0.38	0.42	0.45	0.47	0.49
					82	0	0.20	0.24	0.27	0.29	0.31	0.34	0.37	0.40	0.42
					82	5	0.19	0.22	0.26	0.28	0.30	0.33	0.36	0.40	0.42
2060-20 I	10	10	67	23	25	0	0.24	0.26	0.29	0.31	0.34	0.39	0.43	0.46	0.49
					82	0	0.28	0.29	0.30	0.31	0.33	0.35	0.39	0.42	0.45
2060-20 II	20	10	67	46	23	0	0.26	0.28	0.29	0.32	0.36	0.42	0.49	0.54	0.60
					82	0	0.23	0.24	0.27	0.29	0.31	0.35	0.40	0.45	0.50
2060-10 III	40	--	--	92	82	0	0.19	0.20	--	0.26	--	0.33	0.36	0.40	0.43

APPENDIX E-4

ADDITION OF GOLD TO PLATINUM TEFLON ELECTRODES

Oxidant Air
Electrolyte 3.7 M H_2SO_4
Temperature 82°C

Test No	Average Thickness, mils: Platinum Layer	Average Thickness, mils: Teflon Layer	Teflon Layer Average Porosity, %	Catalyst Loading, mg/cm^2	Gold Loading, mg/cm^2	Polarization from Oxygen Theory at Indicated ma/cm^2: 0	1	10	20	50	100	160
2061-27	3	8	50	3	0	0.26	0.30	0.40	0.45	0.54	0.64	0.74
2061-27	2	8	50	1.5	0	0.22	0.32	0.44	0.49	0.57	0.67	0.76
2061-39	4	12	60	1.5	28	0.22	0.30	0.38	0.42	0.49	0.56	0.62
2061-40	3	12	60	1.5	7	0.21	0.30	0.38	0.42	0.51	0.60	0.70

APPENDIX E-5

TRI-LAYER PLATINUM-TEFLON ELECTRODES

Oxidant Air
Electrolyte 3.7 M H_2SO_4

Test No	Number of Layers	Location of Platinum Catalyst	Average Thickness, mils		Catalyst Density, mg/cm^2	Temp, °C	Polarization from Oxygen Theory at Indicated ma/cm^2						
			Total	Teflon Layer			0	1	10	20	50	100	160
2061-32	3	Layer on electrolyte side	11	8	1.9	82	0.24	0.30	0.40	0.45	0.52	0.60	0.65
2061-32	3	Layer on electrolyte side	11	8	1.1	82	0.24	0.30	0.40	0.45	0.51	0.56	0.62
2061-34	3	Middle layer	11	8	1.9	82	0.23	0.30	0.39	0.44	0.51	0.56	0.63
2061-35	3	Middle layer	19	16	1.9	82	0.22	0.29	0.38	0.43	0.50	0.56	0.62
2061-30	2	--	11	8	1.9	82	0.22	0.29	0.37	0.41	0.48	0.53	0.57
						24	0.24	0.38	0.48	0.52	0.56	0.62	0.66
2061-30	2	--	11	8	1.1	82	0.25	0.31	0.40	0.44	0.51	0.58	0.63
						24	0.26	0.41	0.52	0.57	0.65	0.72	0.79

APPENDIX E-6

MULTI-LAYER PLATINUM-TEFLON ELECTRODES

Electrolyte 3.7 M H_2SO_4

Test No	Electrode	Temp, °C	Oxidant	Polarization from Oxygen Theory at Indicated ma/cm²						
				0	1	10	20	50	100	160
2061-48	Multilayer(1)	82	Air	0.17	0.25	0.35	0.41	0.54	0.71	--
		82	O_2	0.14	0.21	0.29	0.32	0.39	0.47	0.53
		102	O_2	0.14	0.21	0.29	0.33	0.41	0.49	0.56
2061-50	Multilayer(2)	22	Air	0.18	0.22	0.30	0.33	0.40	0.46	0.52
		60	Air	0.17	0.21	0.28	0.30	0.34	0.39	0.46
		82	Air	0.17	0.20	0.26	0.28	0.32	0.38	0.45
		20	O_2	0.15	0.19	0.27	0.29	0.33	0.36	0.39
		62	O_2	0.14	0.18	0.25	0.26	0.29	0.31	0.33
		83	O_2	0.14	0.17	0.23	--	0.27	0.29	0.31
2271-4	Multilayer(3)	23	Air	0.20	0.25	0.34	0.38	0.44	0.49	0.54
		60	Air	0.19	0.23	0.31	0.33	0.36	0.41	0.46
		82	Air	0.19	0.21	0.28	0.30	0.34	0.39	0.44
		60	O_2	0.15	0.20	0.27	0.29	0.32	0.35	0.37
		82	O_2	0.16	0.19	0.25	0.27	0.30	0.32	0.34
		100	O_2	0.16	0.19	0.25	0.26	0.29	0.31	0.33

(1) Eight additional layers, each consisting of alternating strips of Pt-Teflon and 60% porous Teflon.
(2) Six additional layers, each consisting of alternating strips of Pt-Teflon and voids.
(3) Six additional layers, each consisting of alternating strips of Pt-Teflon and 80% porous Teflon.

APPENDIX E-7

VOLTAGE SCAN TECHNIQUE

The voltage scan technique has been used by many workers in the field of electrochemistry(15,16,17). Basically, the technique requires a potentiostat controlled by an external triangular wave signal, and a means for recording potential and current. For fast scans, an electronic signal generator and oscilloscope are used. For slow scans, such as those used in this report, a motor driven potentiometer and an x-y plotter are quite satisfactory.

The voltage signal to the x-y plotter in this work was furnished by the output of a Keithley electrometer, calibrated by a variable potentiometer. The current signal to the x-y plotter was furnished by the voltage drop across precision resistors of appropriate values. Scan rate was controlled by a gear box driving a potentiometer. A schematic of the equipment used is shown in Appendix Figure E-1.

Figure E-1

Diagram of Equipment Used in Voltage Scans

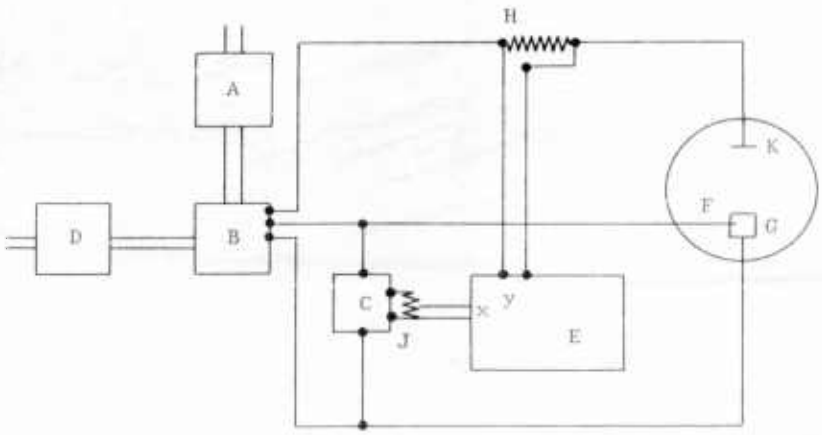

A. Potentiostat Power Supply
B. Potentiostat, Duffers Model 600
C. Electrometer, Keithley Model 610A
D. Triangular Wave Generator
E. x-y Plotter, Moseley Model 2D
F. Saturated Calomel Reference Electrode, Luggin Capillary
G. Test Electrode
H. Precision Resistor
J. Voltage Divider for Calibration
K. Counter Electrode

APPENDIX E-8

VOLTAGE SCANS OF PLATINUM-GOLD SAMPLES

Figure E-2

Pt-30Au, Sodium Borohydride Reduced

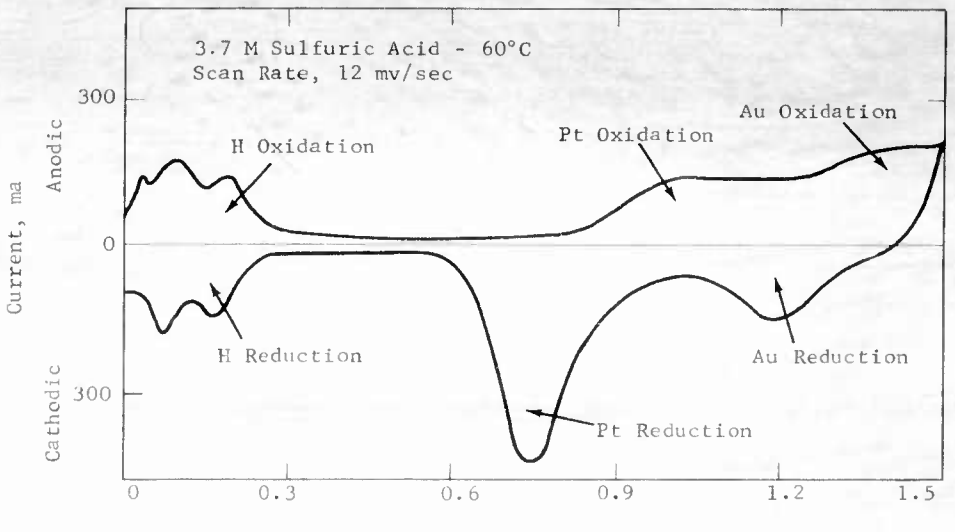

Figure E-3

Pt-30Au, Sodium Borohydride Reduced and Hydrogen Treated at 425°C

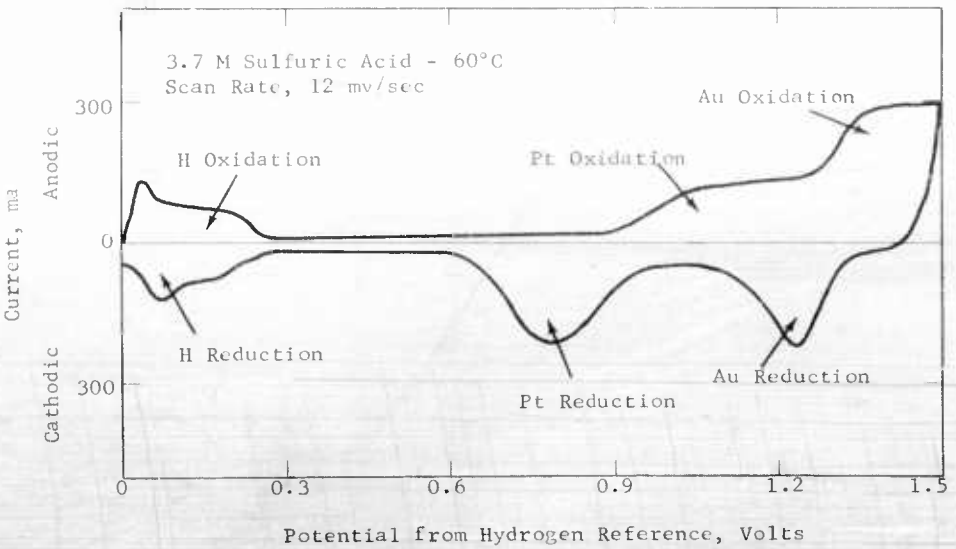

Figure $\bar{E}$ 4

Pt-30Au, Hydrogen
Reduced at 425°C

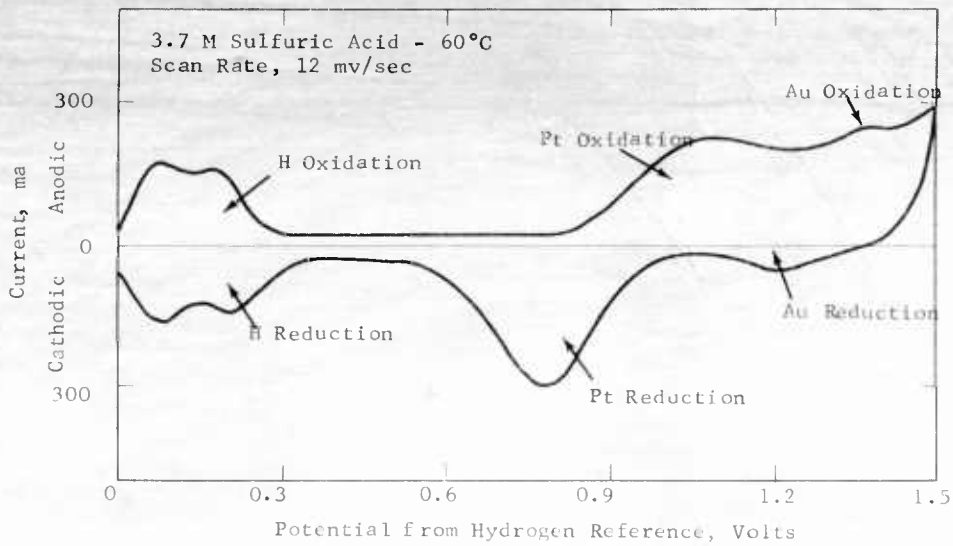

Figure $\bar{E}$-5

Smooth Pt Sample

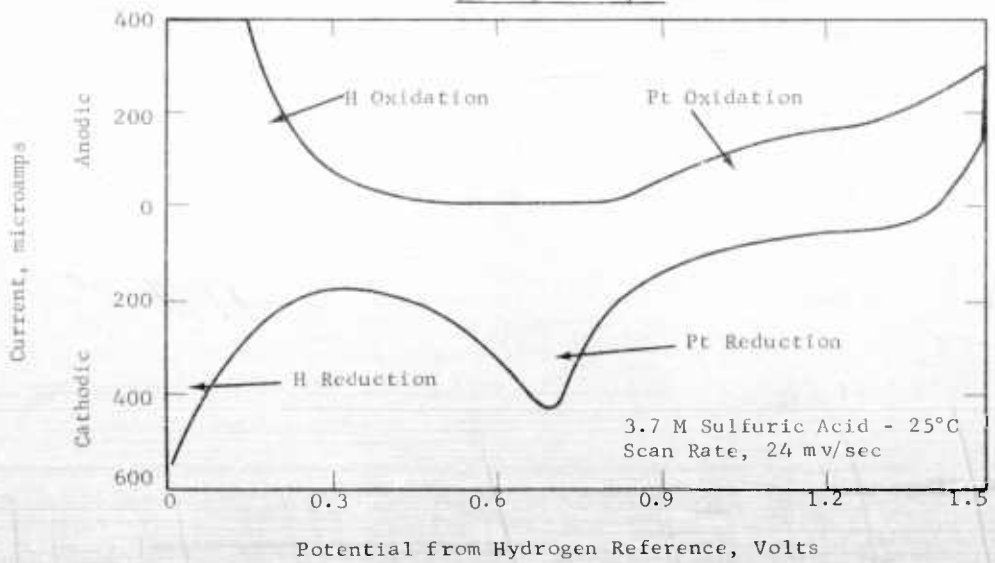

APPENDIX E-8 (CONTINUED)

Figure E-6

Smooth Pt-5Au Sample

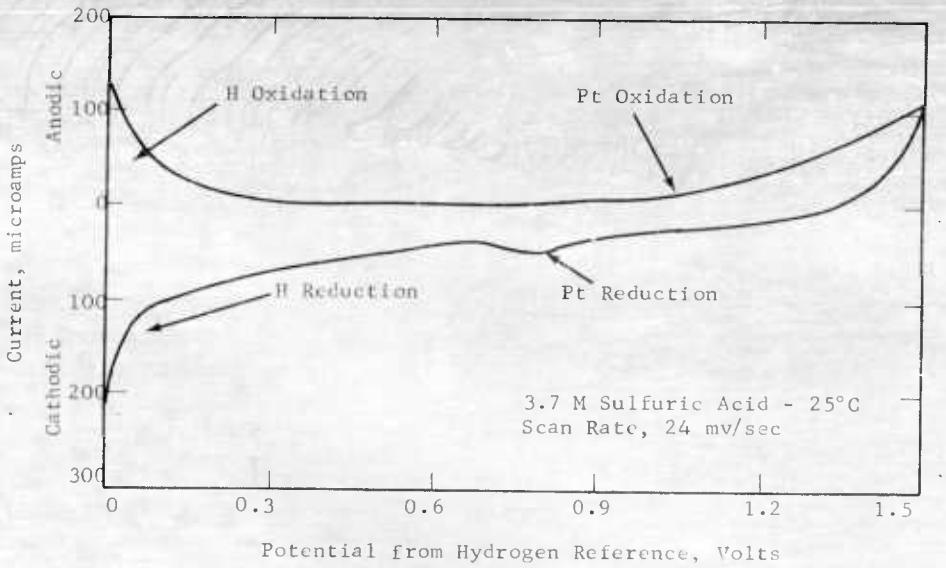

Figure E-7

Smooth Pt-10Au Sample

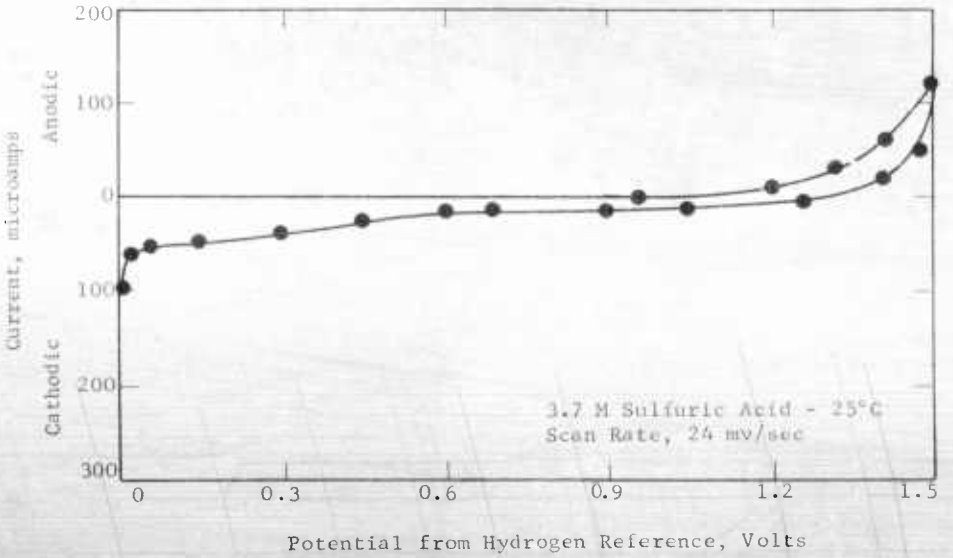

APPENDIX E-9

PLATINUM-GOLD ALLOY BUTTONS EVALUATED AS OXYGEN ELECTRODES

Electrode No	Catalyst	Variable(1)	Temp, °C	Polarization from Oxygen Theory at Indicated ma/cm²				
				O.C.	10^{-6}	10^{-5}	10^{-4}	10^{-3}
187F	Pt	--	25	0.32	0.37	0.47	0.59	0.79
187A	5 Au-Pt	5 minutes treat in aqua regia at 80°C	25	--	0.38	0.42	0.51	0.65
187B	10 Au-Pt	5 minutes treat in aqua regia at 80°C	25	0.31	0.40	0.52	0.67	--
187C	20 Au-Pt	5 minutes treat in aqua regia at 80°C	25	0.29	0.34	0.39	0.49	0.65
187D	40 Au-Pt	5 minutes treat in aqua regia	25	0.31	0.33	0.37	0.48	0.66
187G	Au	--	25	0.52	0.55	0.61	--	--
187A	5 Au-Pt	--	82	0.30	0.32	0.44	0.78	--
			25	--	0.42	0.69	--	--
187B	10 Au-Pt	--	82	0.37	0.40	0.55	--	--
			25	--	0.47	0.72	--	--
187C	20 Au-Pt	--	82	--	0.34	0.38	0.63	--
			25	--	0.59	0.84	--	--
187D	40 Au-Pt	--	25	0.56	0.64	0.84	--	--
			82	0.53	0.59	0.69	--	--

(1) Buttons of metals weighing 25 g evaluated by bubbling O_2 over the immersed button.

APPENDIX E-10

PLATINUM-GOLD CATALYSTS ON CARBON AS OXYGEN ELECTRODES

Electrode No	Catalyst	Variable	Polarization from Oxygen Theory at Indicated ma/cm^2(1) 0	5	10	20	50	100	200
166A-1	Pt 5 Au	Standard preparation	0.23	0.31	0.34	0.38	0.44	0.57	--
166B-2	Pt 5 Au	Std prep, I_2-KI extraction	0.43	0.74(2)	--	--	--	--	--
169B-2	Pt 10 Au	Std prep, I_2-KI extraction	0.43	0.72(2)	--	--	--	--	--
170A-1	Pt 20 Au	Standard preparation	0.45	0.69(2)	--	--	--	--	--
170B-2	Pt 20 Au	Std prep, I_2-KI extraction	0.43	0.67(2)	--	--	--	--	--
171A-1	Pt 40 Au	Standard preparation	0.43	0.72(2)	--	--	--	--	--
171B-1	Pt 40 Au	Std prep, I_2-KI extraction	0.47	0.67	0.74(2)	--	--	--	--
172B-1	Pt	Std prep, I_2-KI extraction	0.45	0.62	0.71(2)	--	--	--	--
176A-1	Pt 5 Au	Standard preparation	0.23	0.26	0.28	0.31	0.34	0.38	0.44
176A-2	Pt 5 Au	Standard preparation	0.21	0.28	0.32	0.35	0.41	0.47	0.58
176B-1	Pt 5 Au	I_2-KI extraction	0.44	0.66	--	--	--	--	--
177A-2	Pt Au	Standard preparation	0.22	0.28	0.31	0.34	0.39	0.45	0.54
178A-1	Pt 20 Au	Standard preparation	0.23	0.30	0.32	0.35	0.40	0.48	0.58
179A-1	Pt 40 Au	Standard preparation	0.24	0.30	0.32	0.35	0.40	0.45	0.52
180A-1	Pt	Standard preparation	0.23	0.30	0.32	0.35	0.40	0.46	0.50
177C-1	Pt 10 Au	I_2-KI extraction	0.42	0.62	--	--	--	--	--
178C-1	Pt 20 Au	I_2-KI extraction	0.49	0.74	--	--	--	--	--
179C-1	Pt 40 Au	I_2-KI extraction	0.45	0.79	--	--	--	--	--
180C-1	Pt	Standard preparation	0.42	0.70	--	--	--	--	--
176A-1	Pt 5 Au	Standard preparation	0.22	0.29	0.31	0.34	0.39	0.44	0.51
177A-1	Pt 10 Au	Standard preparation	0.21	0.28	0.31	0.34	0.40	0.46	0.57
178A-2	Pt 20 Au	Standard preparation	0.23	0.30	0.32	0.35	0.40	0.47	0.56
179A-2	Pt 40 Au	Standard preparation	0.22	0.30	0.32	0.35	0.40	0.45	0.52
180A-1	Pt	Standard preparation	0.23	0.31	0.33	0.37	0.44	0.52	0.65

(1) All electrodes evaluated on oxygen at atmospheric pressure in 3.7M sulfuric acid at 100° C.
(2) Catalyst poisoned by contamination during treating.

APPENDIX E-11

OXYGEN ELECTRODES EVALUATED IN 6.9 M POTASSIUM HYDROXIDE

Oxygen at 1 atm, 82°C

Electrode No	Catalyst	Variable	Polarization from Oxygen Theory at Indicated ma/cm²					
			0	5	10	50	100	200
181A-1	Ag	DuPont type 6216 Ag-Teflon binder	0.34	0.87	--	--	--	--
181A-2	Ag	Composition of 181A-1, air treat at 260°C	0.32	0.56	0.66	0.91	--	--
181B-1	Ag	Composition of 181A-1, impregnated with Ag	0.22	0.66	--	--	--	--
181C-1	Ag-Pd	Composition of 181A-1, impregnated with Pd	0.26	--	--	--	--	--
181D-2	Ag	Composition of 181A-1 except double proportion of binder, air treat at 288°C	0.36	0.48	0.53	0.73	0.88	--
182A-1	Ag on C	20% Ag on FC-30 type carbon, Teflon binder	0.34	0.40	0.42	0.48	0.53	0.67
182B-2	Ag on C	Same as 182A-1 except greater porosity	0.35	0.41	0.42	0.47	0.52	0.62
183A-2	Ag-Pd on C	10% Ag-Pd on FC-30 type carbon, Teflon binder	0.32	0.36	0.38	0.44	0.49	0.54
186A-1	Ag	Handy Harmon type 130 Ag, air treat at 343°C, Teflon binder	0.24	0.38	0.43	0.62	0.83	--
			0.24	0.44	0.51	0.73	--	--
186B-1	Ag	Handy Harmon type 130 Ag, impregnated with Ag, Teflon binder	0.25	0.41	0.47	0.69	0.89	--
186B-2	Ag	Same as 186B-1, air treat at 316°C	0.22	0.40	0.46	0.68	0.84	--
184A-1	Ag on C	Same as 182A-1 except lower porosity	0.36	0.42	0.44	0.50	0.54	0.63
184A-2	Ag on C	Same as 184A-1	0.36	0.41	0.43	0.48	0.52	0.58
--	Ag*	Sodium Borohydride Reduced	0.20	0.40	0.56	--	--	--
--	Ag**	"	0.20	0.55	0.82	--	--	--

* Tested in 3 M potassium hydroxide at 60°C.
** Tested in 1 M each carbonate-bicarbonate buffer at 60°C.

APPENDIX F-1

RESISTANCE MEASUREMENTS IN THE METHANOL-AIR FUEL CELL

Studies of IR losses were made in a 4" x 4" cell (4) operating on 1 M methanol and air in 3.7 M sulfuric acid at 60°C. These studies were made while using rapid square wave current switching to determine fuel cell voltage changes during large rapid changes in current. The results showed some poorly defined IR conditions at the cathode.

Tests were made switching between 0 and 30 ma/cm^2 at a rate of 15 CPS using a square wave signal generator and a mercury switching relay. Oscilloscope patterns of the electrode potentials indicated the current switching effects as shown in Figure F-1. An analysis of the effective capacitive slopes indicates a cell capacitance of about 8 farads. This should result in an operating system havin a very stiff characteristic during sharp changes in load. Anode voltage change characteristics during switching present a very clear-cut picture of 4 mv of IR and a well defined capacitive slope. The voltage/time characteristic of the cathode showed a possible total IR of about 50 mv. However, a large part of this apparent IR was manifested in a very sharp voltage change occurring in 2 or 3 milliseconds after current switching. Previous experience with square wave currents through partially platinized platinum wire electrodes suggested that these long voltage tails are related to resistive components in the system. The primary portion of the cathode trace indicated high capacitance values and suggested that IR reduction in the cathode structure might be possible.

Figure F-1

Cell Testing with Square Wave Current Signal

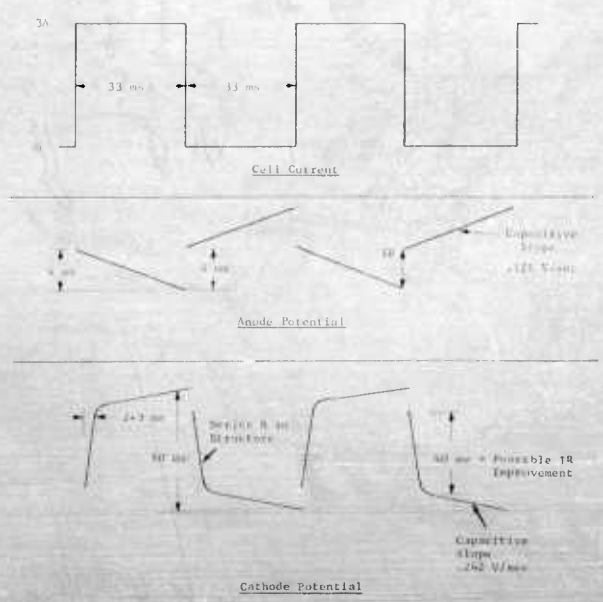

APPENDIX F-2

UNIT 4" x 4" CELL TESTS WITH METHANOL-AIR SYSTEM

Air Cathode Backed With 50 Mesh Tantalum Screen

Run Number	1511-13											
Cell Temp, °C	62	62	62	64	62	62	62	62	62	62	62	62
Electrolyte, M H_2SO_4	3.7							3.7				
CH_3OH In Electrolyte, M	1.0							1.0				
Run Period, hours	46-47							1-4				
Current Density, ma/cm^2	0	10	20	40	60	80	100	10	20	40	80	100
Observed Terminal Voltage:	0.72	0.59	0.53	0.44	0.37	0.30	0.24	0.51	0.45	0.35	0.23	0.17
Polarization At CH_3OH Anode, volts	0.16	0.25	0.20	0.31	0.33	0.35	0.35	0.33	0.36	0.39	0.41	0.43
IR Loss, volts	--	--	--	0.03	--	--	--	--	--	0.04	--	--
Polarization At Cathode, volts (calc)	0.32	0.35	0.37	0.42	0.45	0.49	0.53	0.35	0.37	0.38	0.48	0.50
Efficiency Of Cell, %	57.1	46.8	42.1	34.9	29.4	23.8	19.0	40.5	3.56	27.8	18.2	13.5
Total Terminal Power, mwatts/cm^2	0.0	5.9	10.6	17.6	22.2	24.0	24.0	5.1	9.0	14.0	18.4	17.0
Oxidant	Air (Saturated with H_2O At 89°C)							Dry Air				
Stoichiometric Ratio To Current	--	40.7	20.3	9.6	7.0	5.8	5.8	42.0	21.0	10.5	6.2	5.0
Rate, cc/min (STP)	680	680	680	640	700	770	970	700	700	700	830	830
Electrolyte, ml/hr through cell	71.6	71.6	71.6	71.6	71.6	71.6	71.6	24.8	24.8	49.8	49.8	125
CH_3OH Conversion Per Pass, %	0.0	8.7	17.4	34.8	52.3	69.6	87.0	25.2	50.4	--	--	50.0
Cathode	CW-30 (Cyanamid)											
Anode	FW-12 (P -Type)											

APPENDIX F-2 (Cont'd)

UNIT 4" x 4" CELL TESTS WITH METHANOL-AIR SYSTEM

Air Cathode Backed With 50 Mesh Tantalum Screen

Run Number	1511-13 (Cont'd)						
Cell Temp, °C	84	84	84	84	84	83	83
Electrolyte, M H_2SO_4	3.7						
CH_3OH In Electrolyte, M	1.0						
Run Period, hours	69-70						
Current Density, ma/cm^2	0	10	20	40	60	80	100
Observed Terminal Voltage:	0.74	0.61	0.54	0.45	0.38	0.31	0.26
Polarization At CH_3OH Anode, volts	0.12	0.23	0.27	0.30	0.32	0.33	0.34
IR Loss, volts	--	--	--	0.03	--	--	--
Polarization At Cathode, volts (calc)	0.34	0.35	0.37	0.42	0.45	0.49	0.52
Efficiency Of Cell, %	58.7	48.4	42.8	35.7	30.2	24.6	20.6
Total Terminal Power, mwatts/cm^2	0	6.1	10.8	18.0	22.8	24.8	26.0
Oxidant	Air (Saturated With H_2O At 89°C)						
Stoichiometric Ratio To Current	--	40.7	20.3	11.4	7.6	6.3	10.9
Rate, cc/min (STP)	680	680	680	760	760	840	1820
Electrolyte, ml/hr through stack	71.6	71.6	71.6	71.6	107.5	107.5	314
CH_3OH Conversion Per Pass, %	0.0	8.7	17.4	34.8	34.8	46.5	19.9

APPENDIX F-3

UNIT 4" x 4" CELL TESTS WITH METHANOL-AIR SYSTEM

Air Cathode Backed with Pressed Permion Membrane

Run Number	1511-16											
Cell Temp, °C	62	69	69	69	69	69	69	70	64	64	63	63
Electrolyte, M H_2SO_4	3.7											
CH_3OH In Electrolyte, M	1.0	1.0										
Run Period, hours	2-3								23	23	25	26
Current Density, ma/cm^2	0	10	20	40	60	80	90	100	40	80	40	40
Observed Terminal Voltage:	0.78	0.53	0.50	0.44	0.39	0.35	0.33	0.31	0.44	0.34	0.43	0.40
Polarization At CH_3OH Anode, volts	0.09	0.29	0.31	0.36	0.39	0.40	0.41	0.41	0.34	0.35	0.36	0.41
IR Loss, volts	0.00	--	--	0.024	--	--	--	(0.06)	--	--	--	--
Polarization At Cathode, volts (calc)	0.33	0.38	0.38	0.38	0.38	0.40	0.41	0.42	0.40	0.46	0.39	0.37
Efficiency Of Cell Stack, %	61.8	42.1	39.7	34.9	31.0	27.8	26.2	24.6	34.9	27.0	34.1	32.5
Total Terminal Power, $mwatts/cm^2$	0.0	5.3	10.0	17.6	23.4	28.0	29.7	31.0	17.6	27.2	17.2	16.0
Oxidant	Air (Saturated with H_2O at 45 to 53°C)											
Stoichiometric Ratio To Current	--	76	38	19	12.6	9.5	8.4	7.6	12.7	8.3	12.7	12.7
Rate, cc/min (STP)	450	1260	1260	1260	1260	1260	1260	1260	840	1100	840	840
Electrolyte, ml/hr through cell	50.0	28.5	28.5	50.0	74.8	138	138	138	138	138	100	50.0
CH_3OH Conversion Per Pass, %	0.0	21.9	43.8	50.0	50.0	36.2	40.8	45.3	18.1	--	25.0	50.0
CO_2 Produced Chemically, gm moles/hr	--	--	--	--	--	--	--	--	0.022	--	0.013	0.000
Cathode	CYW-31											
Anode	FW-10 (P-type)											

APPENDIX F-3 (Cont'd)

UNIT 4" x 4" CELL TESTS WITH METHANOL-AIR SYSTEM

Air Cathode Backed With Pressed Permion Membrane

Run Number	1511-16 (cont'd)							
Cell Temp, °C	68	69	69	69	69	68	68	68
Electrolyte, M H_2SO_4	3.7							
CH_3OH In Electrolyte, M	1.0							
Run Period, hours	3-3.5							
Current Density, ma/cm^2	0	10	20	40	60	80	90	100
Observed Terminal Voltage:	0.70	0.65	0.59	0.51	0.47	0.43	0.42	0.40
Polarization At CH_3OH Anode, volts	0.21	0.27	0.30	0.34	0.37	0.39	0.39	0.40
IR Loss, volts	--	--	--	0.024	--	--	--	--
Polarization At Cathode, volts (calc)	0.29	0.28	0.30	0.33	0.32	0.34	0.34	0.34
Efficiency Of Cell Stack, %	55.5	51.5	46.8	40.5	37.3	34.2	33.3	31.7
Total Terminal Power, mwatts/cm^2	0	6.5	11.8	20.4	28.2	34.4	37.8	40.0
Oxidant	Oxygen (wet at 37°C)							
Stoichiometric Ratio To Current	--	316	158	79	53	39	35	32
Rate, cc/min (STP)	1100							
Electrolyte, ml/hr through stack	71.7							
CH_3OH Conversion Per Pass, %	0.0	8.7	17.4	34.8	52.2	69.6	78.2	87.0

APPENDIX F-4

POLYPROPYLENE SINGLE CELL 9" x 5-3/4" TESTS WITH METHANOL-AIR SYSTEM

Experiments with Variations in Spacer Between Electrodes

Experiment Code	(1)			(2)		(3)	(3)and(4)	(4)and(5)	(6)
Run Number	1511-34			1511-35		1511-40	1511-41	1511-42	1511-43
Cell Temp, °C	65	68	71	59	59	63	66	62	61
Electrolyte,M (H_2SO_4)	3.7			3.7		3.7			
CH_3OH in Electrolyte, M	1			1		1			0.5
Current Density, ma/cm^2	0.0	40	100	40	100	40	40	40	40
Observed Terminal Voltage, volts	0.81	0.45	0.27	0.46	0.27	0.32	0.29	0.40	0.40
Voltage Efficiency, %	64.2	35.7	21.4	36.5	21.4	25.4	23.0	31.7	31.7
Terminal Power, mwatts/cm^2	0.0	18.0	27.0	18.4	27.0	12.8	11.6	16.0	16.0
Anode Polarization, volts	--	--	--	--	--	0.39	0.37	0.40	0.40
IR Loss, volts	--	--	--	--	--	0.07	0.07	0.08	0.07
C thode Polarization, volts	--	--	--	--	--	0.42	0.47	0.32	0.33
IR Loss Polarization, volts	--	--	0.15	--	0.11	0.17	0.17	0.20	0.17
Oxidant	Air (Sat. with water at 44-46°C)					Air (Sat. with water at 27°C)			
Stoichiometric Ratio to Current	--	10.2	10.2	18.0	7.2	20.0	20.0	20.0	11.0
Rate, cc/min (STP)	1800	4100	10200	7200	7200	8000	8000	8000	4400
Electrolyte, ml/hour	10.2	616	616	616	616	205	--	--	--
CH_3OH Elec Chem Conv/Pass, %	0.0	12.1	30.3	12.1	30.3	36.6	--	--	--
Cathode Number	CYW-36			CYW-36		CYW-40	CYW-40	CYW-41	CYW-41
Anode Number	FW-27 (Ru Mod P-Type)			FW-27		FW-27	FW-27	FW-27	FW-28(Ru Mod P-Type)

Experiment:
(1) Spaces between electrodes = 30 mil soft Viton rubber. Current collector = 1 - 0.006 mil thickness gold.
(2) Spaces between electrodes = 90 mil soft Viton rubber. Current collector = 2 - 0.006 mil thickness gold.
(3) Spaces between electrodes = polypropylene springs (30 mil space). Current collector = 2 - 0.006 mil thinkness gold.
(4) Also cut "V" slats at top of anode to permit better CO_2 release.
(5) Spaces between electrodes = 120 mil Teflon. Current collector = 2 - 0.006 mil thickness gold.
(6) Doubled thickness of gold collectors on approaches to terminals.

APPENDIX F-5

DATA ON AIR DISTRIBUTOR IN 4" x 4" TEFLON CELL

Temp = 62°C
1 M CH_3OH in 3.7 M H_2SO_4
Current = 40 ma/cm^2
Current Density = 40 ma/cm^2
Run 1511-16

Air Stoichiometric Ratio to Current	Cell Voltage Without Distributor	Cell Voltage With Distributor
10	0.42	0.42
8	0.42	0.42
5	0.42	0.42
4	--	0.36
3	0.23	0.20
2.5	0.08	0.04

Figure F-2

Teflon Cathode Support Section Showing Air Distributor

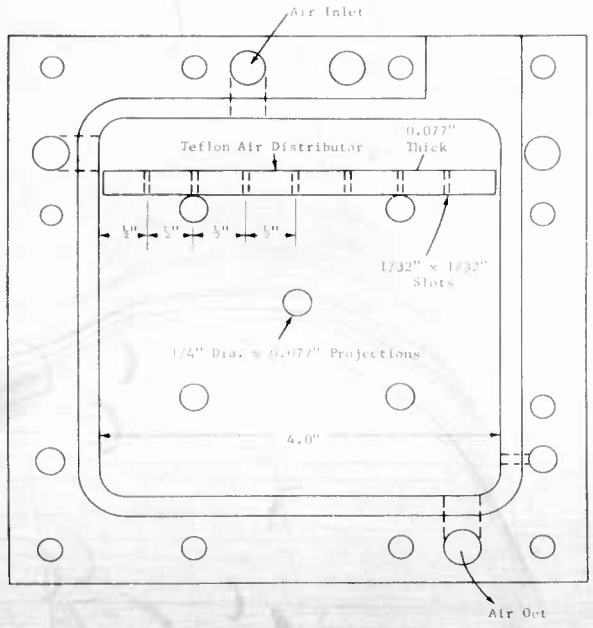

APPENDIX F-6

PERFORMANCE OF POTASSIUM STABILIZED P-TYPE ELECTRODES IN TOTAL CELLS

60°C
1 M CH_3OH in 3.7 M H_2SO_4
American Cyanamid AA-1 Cathode
Clad with Permion 1010 Membrane

Current Density, ma/cm^2	Cell Potential, Volts			Anode Polarization from Theory, Volts			
				Half-Cells	Total Cell		
	#1	#2	#3		#1	#2	#3
0	.76	.75	.60	--	--	--	--
10	.53	.54	.47	.23	.29	.30	.43
20	.50	.49	.40	.27	.31	.31	.40
40	.44	.43	.31	.32	.37	.36	.48
60	.39	.39	.27	.34	.40	.40	.52
80	.35	.35	.20	.35	.41	.41	.56
100	.30	.29	.10	.36	.42	.42	.61

Cells #1 and #2: Performance after polarization to 0.7 volts.
Cell #1 stored in 3.7 M H_2SO_4 for 168 hours.
Cell #2 stored in H_2O for 168 hours.
Cell #3 : Performance after polarization to 0.7 volts.
Cell #3 stored in 1M CH_3OH 3.7 M H_2SO_4 for 24 hours.

APPENDIX F-7

CATALYST TESTING IN 4" DIAMETER TOTAL CELL

Run	Anode No.	Anode Preparation And Comments	Methanol Conc, M	Oxidant	Temp °C	Performance Criteria	Cell Performance At Indicated ma/cm^2 12.5	25	50	75	100	125
	2292-6	Pt-30% Ru dry powder. Made into water paste and spread. Pressed at 1000 psi. Catalyst did not adhere to electrode when immersed.										
	2292-7	Undried Pt 33% Ru spread and pressed at 1000 psi. Handled better than 2292-6 but still did not adhere to screen.										
31764A*	2292-8	Pt-33% Ru never dried; pressed from butanol paste.	1	Air	60	Anode polar.	0.33	0.34	0.40	--	--	--
						Cell volts	0.42	0.37	0.26	--	--	--
						Power, mw/cm^2	5.2	9.3	13	--	--	--
31764B*	2292-8	Pt-33% Ru never dried; pressed from butanol paste.	.25	Air	59	Anode polar	0.36	0.40	0.47	--	--	--
						Cell volts	0.41	0.34	0.22	--	--	--
						Power, mw/cm^2	5.1	8.5	11	--	--	--
32464	P-type	Stored two weeks in water.	1	Air	61	Anode polar	0.39	0.42	0.46	--	--	0.50
						Cell volts	0.43	0.36	0.24	--	--	0.13
						Power, mw/cm^2	5.4	9.0	12.0	--	--	16.3
33064	2292-9	Pt-40% Ru with 10% Teflon pressed from butanol paste.	.1	Air	60	Anode polar	0.36	0.39	0.43	0.49	--	--
						Cell volts	0.50	0.43	0.32	0.17	--	--
						Power, mw/cm^2	6.3	10.8	16.0	12.8	--	--
33164A	2292-9	Pt-40% Ru with 10% Teflon pressed from butanol paste.	1	Air	59	Anode polar	0.39	0.41	0.46	0.45	0.46	--
						Cell volts	0.47	0.39	0.30	0.23	0.17	--
						Power, mw/cm^2	5.9	9.8	15.0	17.3	17.0	--
33164B	2292-10	Pt-40% Ru pressed from butanol paste. Polarized to 1.3 volts versus [illegible].	1	Air	59	Anode polar	0.32	0.35	0.37	0.40	0.41	0.42
						Cell volts	0.50	0.46	0.40	0.33	0.29	0.23
						Power, mw/cm^2	6.3	11.5	20.0	24.8	29.0	28.8
33164C	2292-10	Activated again by polarizing twice to 1.2 volts.	[illegible]	Air	[illegible]	Anode polar	0.31	0.34	0.37	0.39	--	0.41
						Cell volts	0.52	0.47	0.40	0.35	--	0.25
						Power, mw/cm^2	6.5	11.8	20.0	26.3	--	32.3

Anode catalyst loadings: approximately 20 mg/cm^2 in all cases.
Electrolyte: 3.7 M sulfuric acid.
Cathode: American Cyanamid AA1 with pressed Permion 1010 membrane.
Oxidant flow rates: high enough for performance to be insensitive to rate.

* Run in 4" x 4" Teflon cell.

APPENDIX F-8

CATALYST TESTING IN 4" x 4" TOTAL CELL (1)

Run Number	1511-32											
Cell Temp, °C	68	67	67	67	67	67	67	68	68	82	82	82
Electrolyte M, H_2SO_4	3.7											
CH_3OH in Electrolyte, M	1.0											
Current Density, ma/cm^2	0.0	10	20	40	60	80	100	150	200	20	40	100
Observed Terminal Voltage, volts	0.77	0.59	0.53	0.45	0.39	0.34	0.32	0.25	0.17	0.54	0.46	0.33
Voltage Efficiency, %	61.0	46.7	42.0	35.6	47.5	36.9	25.3	19.8	13.5	42.8	31.7	26.1
Terminal Power, mwatts/cm^2	0.0	5.9	10.6	18.0	23.4	27.2	32.0	37.5	34.0	10.8	18.4	33.0
Anode Polarization, volts	0.08	0.25	0.29	0.33	0.35	0.36	0.37	0.37	0.38	0.30	0.35	0.39
IR Loss, Volts	0.00	--	--	--	--	--	0.06	--	--	--	--	--
Cathode Polarization, volts	0.35	0.36	0.37	0.40	0.42	0.45	0.45	0.49	0.53	0.35	0.37	0.42
Oxidant	Air (Sat. with water at 50-55°C)									--Air (Sat. at 61°C)-		
Stoichiometric Ratio to Current	--	32.4	16.2	8.1	10.0	10.0	37.2	24.8	18.6	17.4	8.1	7.5
Rate, cc/min (STP)	6200	540	540	540	1000	1330	6200	6200	6200	580	540	1250
Electrolyte, ml/hour	205	42	42	42	62	82	102	154	205	102	41	102
CH_3OH Elec Chem Conv/Pass, %	0.0	14.9	29.8	59.5	60.2	60.8	61.2	60.8	60.8	12.2	61.0	61.2
Cathode Number	CYW-35 (Permion membrane pressed into American Cyanamid (AA1) electrode)											
Anode Number	FW-26 (Pt-Ru Catalyst) (2)											

(1) Initial Performance.
(2) Soaked in 6 M KOH for 72 hours.

APPENDIX F-5

CATALYST TESTING IN 4" DIAMETER TOTAL CELL

Run	Anode No.	Anode Preparation And Comments	Methanol Conc. M	Oxidant	Temp °C	Performance Criteria	Cell Performance At Indicated ma/cm² 12.5	25	50	75	100	125
4164	2292-12	P-type modified by controlled addition of Ru. Spread as water paste pressed at 1000 psi.	1	Air	60	Anode polar	0.34	0.38	0.42	--	--	
						Cell volts	0.46	0.40	0.31	--	--	--
						Power, mw/cm²	5.8	10.0	15.5	--	--	--
4264	2292-12	Activated by polarizing twice to .9 volts versus H_2	1	Air	60	Anode polar	0.31	0.33	0.37	0.40	0.42	0.43
						Cell volts	0.52	0.46	0.39	0.33	0.27	0.22
						Power, mw/cm²	6.5	11.5	19.5	24.8	27.0	27.5
4364	2292-13	Replicate of 2292-12 but wet with 1 M methanol when exposed to air.	1	Air	60	Anode polar	0.29	0.33	0.38	0.41	0.45	0.47
						Cell volts	0.50	0.44	0.34	0.26	0.19	0.12
						Power, mw/cm²	6.3	11.0	17.0	19.5	19.0	15.0
4964	2292-15	Pt-40% Ru pressed with Saran binder.	1	Air	60	Anode polar	0.31	0.34	0.38	0.40	0.41	0.42
						Cell volts	0.46	0.41	0.34	0.29	0.21	0.15
						Power, mw/cm²	5.7	10.3	17.0	21.8	21.0	18.6
41064A	2292-16	Ruthenium modified P-type after polarization to .8 volts.	1	Air	60	Anode polar	0.25	0.27	0.30	0.32	0.34	0.35
						Cell volts	0.54	0.50	0.44	0.39	0.35	0.30
						Power, mw/cm²	6.8	12.5	22.0	29.3	35.0	37.5
41064	2292-16	After two additional polarizations for activation.	.5	Air	60	Anode polar	0.26	0.28	0.31	0.33	0.35	0.36
						Cell volts	0.56	0.51	0.45	0.39	0.35	0.30
						Power, mw/cm²	7.0	12.8	22.5	29.3	35.0	37.5
41464B	2292-16	After weekend storage.	.5	Air	82	Anode polar	0.23	0.26	0.28	0.30	0.32	0.33
						Cell volts	0.62	0.59	0.50	0.44	0.39	0.35
						Power, mw/cm²	7.8	14.8	25.0	33.0	39.0	43.8
41464C	2292-16	After weekend storage.	.5	Oxygen	82	Anode polar	0.23	0.26	0.29	0.31	0.33	0.34
						Cell volts	0.68	0.63	0.56	0.50	0.45	0.41
						Power, mw/cm²	8.5	15.8	28.0	37.5	45.0	51.4
41664A	2292-16	After overpolarization to oxygen evolution, complete drying in air and appreciable attrition.	1	Air	60	Anode polar	0.29	0.32	0.35	0.38	0.40	0.41
						Cell volts	0.52	0.46	0.38	0.32	0.26	0.21
						Power, mw/cm²	6.5	11.5	19.0	24.0	26.0	26.3
41664B	2292-18	Ruthenium modified P-type.	1	Air	60	Anode polar	0.25	0.28	0.32	0.34	0.36	0.38
						Cell volts	0.54	0.49	0.42	0.36	0.31	0.26
						Power, mw/cm²	6.8	12.3	21.0	27.0	31.0	32.5

Anode catalyst loadings: approximately 20 mg/cm² in all cases.
Cathode: American Cyanamid AA1 with pressed Permion 1010 membrane.
Electrolyte: 3.7 M sulfuric acid.
Oxidant flow rates: high enough for performance to be insensitive to rate.

APPENDIX F-10

SINGLE CELL TEST OF 9" x 5-3/4" POLYPROPYLENE METHANOL-AIR FUEL CELL

Cathode : Permion membrane pressed into Cyanamid AA-1 Electrode

Run Number	1511-28						1511-29				
Cell Temp, °C	56	59	60	60	60	62	59	66	66	65	65
Electrolyte, M H_2SO_4	3.7										
CH_3OH In Electrolyte, M	1.0										
Current Density, ma/cm^2	0	10	20	30	41.6	66.6	0	20	30	66.6	100
Terminal Current, amps	0	3	6	9	12.5	20.0	0	6.0	9.0	20.0	30.0
Terminal Voltage	0.70	0.48	0.40	0.36	0.30	0.20	0.76	0.49	0.44	0.30	0.20
Voltage Efficiency, %	55.6	38.1	31.7	28.6	23.8	15.9	60.3	38.9	34.9	23.8	15.9
Terminal Power, mwatts/cm^2	0	4.8	8.0	10.8	12.5	13.3	0	9.8	13.2	20.0	20.0
Terminal Power, watts	0	1.4	2.4	3.2	3.8	4.0	0	2.9	4.0	6.0	6.0
Anode Polarization, volts	0.13	0.28	0.33	0.36	0.37	0.41	0.13	0.32	0.35	0.40	0.43
IR Loss, volts	--	--	0.036	--	--	--	--	0.036	--	--	--
Cathode Polarization, volts	0.36	0.42	0.43	0.43	0.46	0.49	0.31	0.35	0.36	0.40	0.40
Oxidant	Air (Saturated with H_2O at 40°C)						Air (Saturated with H_2O at 58°C)				
Stoichiometric Ratio To Current	--	59	30	20	14	9	--	31	20	10	6
Rate, cc/min (STP)	5900						1800	6200	6200	6200	7600
Electrolyte, ml/hour	1800						1800				
CH_3OH Elec Chem Conv/Pass, %	0.0	1.0	2.2	3.1	4.3	7.0	0.0	2.2	3.1	7.0	10.4
Cathode	CYW-33(1)						CYW-34				
Anode	FW-25(2)						FW-25				

(1) Used in single cell test prior to run 1511-28, exposed to air and methanol in cell over weekend possibly causing deactivation.
(2) Freshly prepared electrode (liquid blotted from surface before pressing to give smooth surface) p-Type Catalyst.

APPENDIX F-11

POLYPROPYLENE SINGLE CELL PERFORMANCE WITH 9" x 5-3/4" ELECTRODES USING METHANOL AND AIR

Run Number	1511-34								
Cell Temp, °C	65								
Electrolyte, M H_2SO_4	3.7								
CH_3OH in Electrolyte, M	1.0								
Current Density, ma/cm^2	0.0	3.3	10	20	30	40	50	66.7	100
Current, amps	0.0	1.0	3.0	6.0	9.0	12.0	15.0	20.0	30.0
Observed Terminal Voltage	0.81	0.76	0.60	0.52	0.47	0.43	0.41	0.37	0.27
Voltage Efficiency, %	64.2	60.3	47.5	41.2	38.1	34.1	32.5	29.4	21.4
Terminal Power, mwatts/cm^2	0.0	2.5	6.0	10.4	14.1	17.2	20.5	24.7	27.0
Oxidant	Air (Sat. with water at 44-51°C)								
Stoichiometric Ratio to Current	--	54.0	18.0	9.0	10.0	10.1	10.2	10.3	10.2
Rate, cc/min (STP)	1800	1800	1800	1800	3000	4050	5100	6900	10200
Electrolyte, ml/hour	10.3	10.3	32.4	61.5	112	112	154	205	247
CH_3OH Elec Chem Conv/Pass, %									
Cathode Number	CYW-36								
Anode Number	FW-27 (Ru Mod. P-Type)								

APPENDIX G-1

AUXILIARY AND CONTROL SYSTEM
FOR METHANOL-AIR POWER UNIT

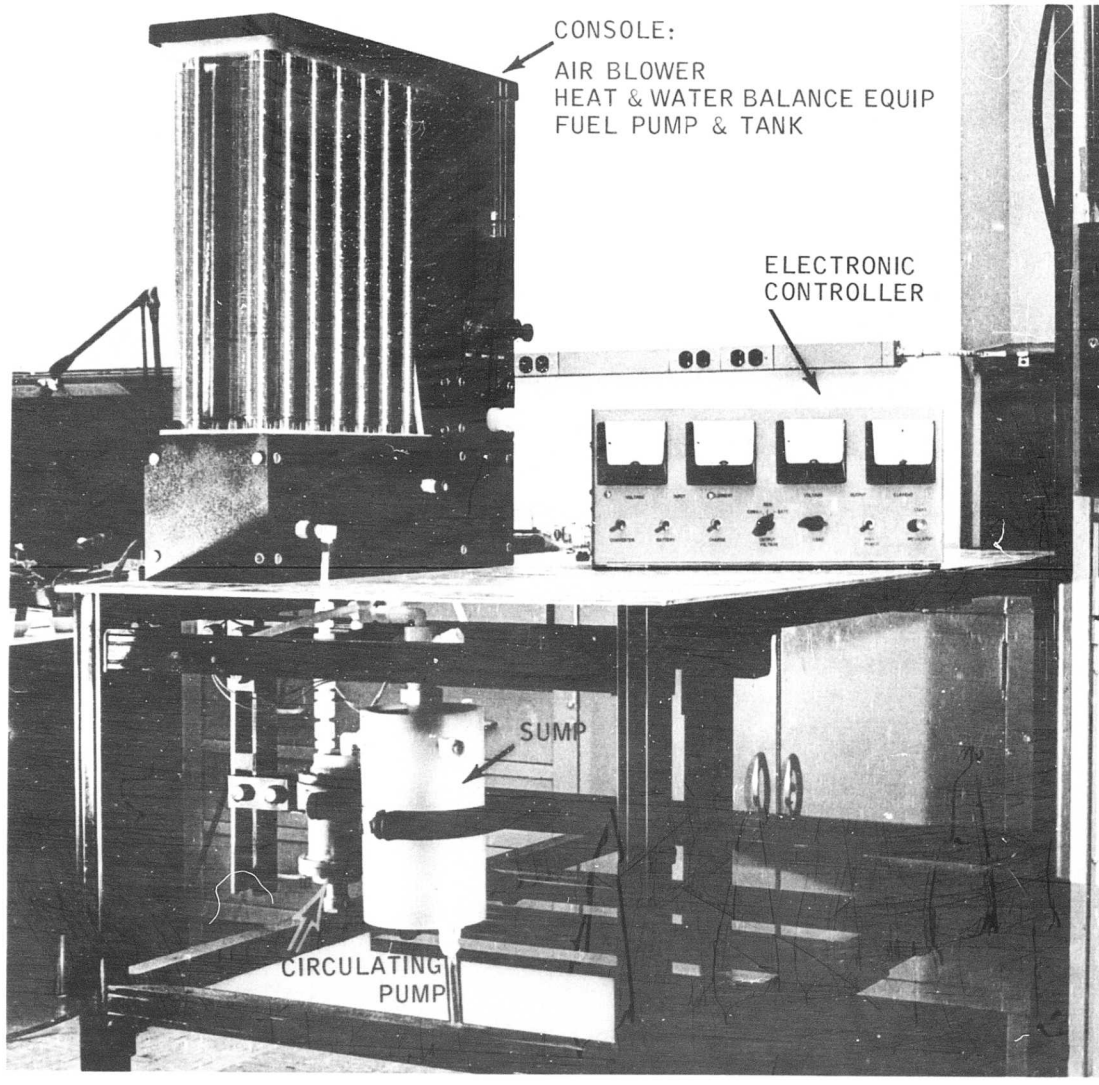

APPENDIX G-2

HALF-CELL STUDIES OF AIR UTILIZATION IN 9" x 5-3/4" BI-CELL MODULE

Air
3.7 M H_2SO_4
American Cyanamid AA-1 Cathode Clad
with Permion 1010 Membrane
Ohmic Free Performance

Current Density, ma/cm^2	Air Rate, Stoichiometric Ratio to Current	Polarization, Volts from Theoretical O_2		Pressure Drop, mm H_2O
		Cell #1	Cell #2	
100	3	0.57	0.59	~ 2
100	4	0.47	0.47	
100	5	0.46	0.47	~ 2
100	10	0.46	0.46	~ 6
67	3	0.48	0.51	
67	4	0.41	0.42	~1
67	5	0.41	0.42	~2
67	10	0.41	0.40	~4
33	4	0.37	0.37	~1
33	5	0.37	0.37	~1
33	10	0.37	0.36	

APPENDIX G-2 (CONT'D)

HALF-CELL STUDIES OF AIR UTILIZATION IN 9" x 5-3/4"BI-CELL MODULE

Air
0.25 M CH_3OH in 3.7 M H_2SO_4
American Cyanamid AA-1 Cathode Clad
with Permion 1010 Membrane
Ohmic Free Performance

Current Density, ma/cm^2	Air Rate, Stoichiometric Ratio to Current	Polarization, Volts from Theoretical O_2 Cell #1	Cell #2	Pressure Drop, mm H_2O
100	3	0.67	0.72	
100	4	0.49	0.52	
100	5	0.47	0.47	
100	10	0.46	0.45	
67	3	0.65	0.70	
67	4	0.48	0.45	
67	5	0.44	0.43	
67	10	0.42	0.40	
33	4	0.76	0.76	
33	5	0.39	0.39	~ 1
33	10	0.36	0.34	~ 1

APPENDIX G-3

INFLUENCE OF AIR PORT LOCATION ON UTILIZATION
OF AIR IN 9" x 5-3/4" POLYPROPYLENE METHANOL-AIR FUEL CELL

Conditions: Temp = 60-65°C
Electrolyte = 3.7 M H_2SO_4
Methanol in Electrolyte = 1M

Run Number	Air Port Design	Air Stoichiometric Ratio to Current	Cell Voltages at Current Density of 20 ma/cm^2	40 ma/cm^2	60 ma/cm^2
1511-41	(1)	3	0.07	0.03	0.00
	Single Cell	4	0.12	0.10	0.10
		5	0.15	0.18	0.14
		7	0.21	0.23	0.16
		10	0.33	0.26	0.18
		12	--	--	0.20
		20	0.35	0.29	0.22
1511-40	(2)	3	0.10	0.04	0.02
	Single Cell	4	0.18	0.18	0.09
		5	0.27	0.24	0.19
		10	0.40	0.29	0.22
		20	0.41	0.32	0.25
1511-42	(3)	2	0.09	--	--
	Single Cell	3	0.20	0.08	0.21
		4	0.27	0.27	0.26
		5	0.37	0.35	0.27
		7	0.45	0.37	0.29
		10	0.46	0.38	0.30
		20	0.48	0.40	0.30
1511-43	(4)	2	0.20	0.12	--
	Single Cell	3	0.38	0.28	0.04
		4	0.45	0.35	0.24
		5	0.46	0.37	0.30
		7	0.47	0.38	0.31
		10	0.48	0.40	0.34
		20	0.50	0.43	--
1511-45	(4)	3	--	0.10	--
	6 Cell Stack	4	0.28	0.33	--
	(Average Voltages	6	0.44	0.37	--
	Shown Only)	8	0.46	0.38	--
		10	0.47	0.38	--
		20	0.48	0.41	--

3/16" Diameter Air Port Arrangement Across Frames (Solid circles refer to closed air ports)

(1) Inlets oo ●oo●●●oo oo●●●oo● oo
Outlets oo●●●●● ●o●●●oo

(2) Inlets oo ooo●●●oo oo●●●ooo oo
Outlets oo●●●oo oo●●●oo

(3) Inlets oo oo●o●o●o o●o●o●oo oo
Outlets oo●●●oo oo●●●oo

(4) Inlets oo oooooooo oooooooo oo
Outlets ooooooo ooooooo

APPENDIX G-4

STARTUP MEASUREMENTS IN METHANOL-AIR CELLS

6 Cell 9" x 5-3/4" Stack
P-type Anodes
American Cyanamid Cathodes
Permion 1010 Membrane
1.0 M CH_3OH
3.7 M H_2SO_4

Time, min	Temp, °C	Air Rate, cc/min	Current Density, ma/cm^2
0	23.89	0	0
2.5	32.22	1600	0
5.0	37.78	1600	0
12.0	43.33	3300	0
14.0	48.89	3300	0
16.5	54.44	3300	0
18.5	57.22	3300	0
22	60.00	3300	0
25	65.56	3300	15
28	71.11	5000	"
35	79.44	5000	"
40	82.22	5000	"
0	22.89	0	0
2	32.22	2500	0
4	37.78	"	0
6	43.33	"	0
8	46.11	"	0
10	50.00	"	15
12	58.85	"	"
14	63.90	"	"
16	66.65	"	"
18	68.33	"	"
20	71.11	"	"

APPENDIX G-4 (CONT'D)

STARTUP MEASUREMENTS IN METHANOL-AIR CELLS

Time, min	Temp, °C	Air Rate, cc/min	Current Density, ma/cm^2
0	23.89	0	0
2	32.22	2500	0
4	36.7	"	0
6	40.55	"	0
8	46.11	"	0
10	48.89	5000	0
12	48.89	"	0
14	51.67	3300	0
16	52.80	2500	0
18	56.15	"	0
0	23.89	0	0
2	32.22	1600	0
4	35.00	"	0
6	37.78	"	0
8	40.55	"	0
10	41.7	"	0
12	45.0	"	0
14	46.7	"	0
16	48.35	"	0
18	48.89	3300	0
20	48.89	"	0
22	50.00	"	0
24	51.67	"	15
26	60.00	"	"
34	76.67	"	"
40	81.10	"	"

APPENDIX G-5

FLOW SCHEMATIC - TEN CELL STACK

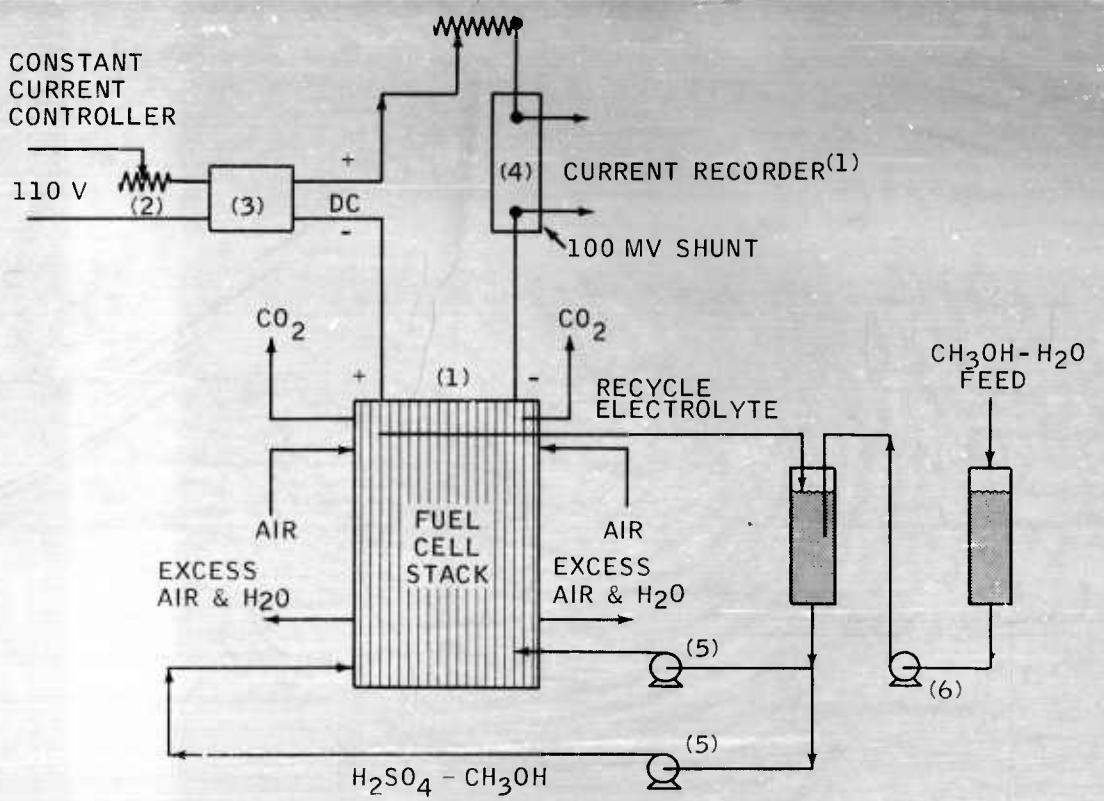

(1) Stack voltage and current, and individual cell voltages and anode polarizations measured on a multipoint recording millivolt meter, Model 6702, Daystrom, Inc., Poughkeepsie, New York.

(2) Variac Type W10MT 3, General Radio Co., Concord, Massachusetts.

(3) ATR rectifier, Model 620C-Elit, ATR Mfg. Co., St. Paul, Minnesota.

(4) 100 mv Shunt, Esterline-Angus Co., Indianapolis, Indiana, made for use with Model AW DC AMM ETER.

(5) Pump, Model 2-6000, 14 RPM, Buchler Instruments, Inc., Fort Lee, N.J.

(6) Pump, Model 2-6000, 5.7 RPM, Buchler Instruments, Inc., Fort Lee, N.J.

APPENDIX G-6

WIRING DIAGRAM FOR TEN CELL STACK

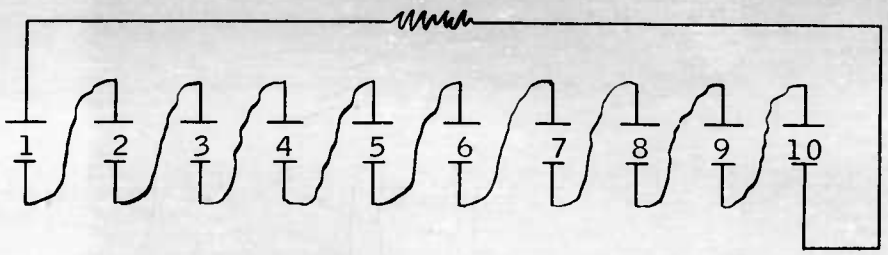

SERIES CONNECTION

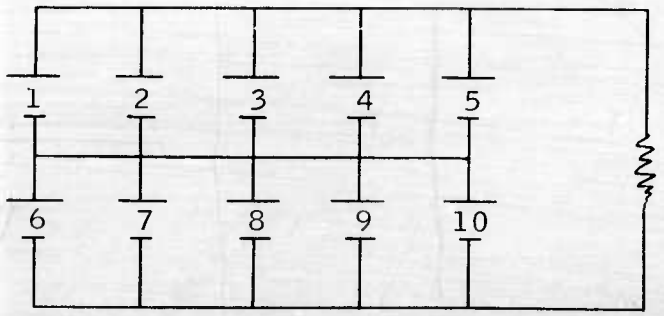

SERIES-PARALLEL CONNECTION

APPENDIX G-7

TEN CELL STACK METHANOL-AIR FUEL CELL - 4" x 4" ELECTRODES

Delivered To Fort Monmouth
USAER and DL

Run Number	1511-10											
Cell Temp, °C	58	58	58	57	60	58	61	59	60	73	71	54
Elctrolyte, M H_2SO_4	3.7				3.7							
CH_3OH In Electrolyte, M	1.0				1.0							
Test Duration, hours	25				50-52				75	77	100	47
Electrical Connections	Series				2 banks of 5 cells in Parallel, each bank in series with each other							
Stack Current Amperes	0.0	0.55	1.0	2.0	0.0	4.1	8.0	12.2	17.0	6.0	17.0	4.1
Stack Voltage	7.0	5.6	5.0	4.1	1.47	1.02	0.96	0.78	0.63	1.00	0.80	1.0
Stack Power, watts	0.0	3.1	5.0	8.2	0.0	4.2	7.7	9.5	10.7	6.0	13.6	4.1
Efficiency Of Stack, %	56.0	44.8	40.0	32.8	58.8	40.8	38.4	31.2	25.2	40.0	32.0	40.0
Voltage Of Cells:												
No. 1	0.67	0.55	0.48	0.39	0.75	0.51	0.49	0.42	0.34	0.51	0.43	0.49
No. 2	0.70	0.55	0.46	0.38	"	"	"	"	"	"	"	"
No. 3	0.70	0.58	0.52	0.40	"	"	"	"	"	"	"	"
No. 4	0.69	0.58	0.53	0.40	"	"	"	"	"	"	"	"
No. 5	0.67	0.57	0.51	0.41	"	"	"	"	"	"	"	"
No. 6	0.70	0.57	0.50	0.39	0.73	0.50	0.47	0.39	0.31	0.50	0.39	0.50
No. 7	0.68	0.55	0.50	0.42	"	"	"	"	"	"	"	"
No. 8	0.70	0.57	0.51	0.41	"	"	"	"	"	"	"	"
No. 9	0.69	0.56	0.46	0.38	"	"	"	"	"	"	"	"
No. 10	0.75	0.63	0.57	0.46	"	"	"	"	"	"	"	"
Anode Polarizations, Volts At Cell:												
No. 1	0.25	0.35	0.39	0.46	0.10	0.32	0.32	0.36	0.38	0.31	0.30	0.36
No. 2	0.37	0.38	0.41	0.48	0.12	0.24	0.32	0.36	0.45	0.29	0.40	0.38
No. 3	0.23	0.30	0.33	0.37	0.14	0.32	0.30	0.31	0.35	0.30	0.27	0.34
No. 4	0.25	0.32	0.34	0.41	0.14	0.32	0.31	0.37	0.35	0.31	0.28	0.34
No. 5	0.26	0.33	0.36	0.42	0.19	0.36	0.37	0.41	0.38	0.35	0.31	0.35
No. 6	0.23	0.30	0.32	0.36	0.17	0.34	0.30	0.34	0.37	0.28	0.28	0.34
No. 7	0.25	0.34	0.36	0.37	0.15	0.34	0.33	0.35	0.39	0.33	0.33	0.35
No. 8	0.23	0.32	0.36	0.44	0.19	0.45	0.37	0.46	0.42	0.34	0.42	0.38
No. 9	0.25	0.35	0.41	0.48	0.17	0.37	0.34	0.40	0.46	0.30	0.35	0.37
No. 10	0.12	0.24	0.27	0.34	0.14	0.33	0.28	0.32	0.38	0.25	0.27	0.36
Air, cc/min (@ 32°F)	2000	2000	2000	3780	2000	2000	2000	2000	5450	2600	5450	2000
Air, Stoichiometric Ratio To Current	--	21.8	12.0	11.3	--	14.6	7.5	4.9	9.6	13.0	12.0	14.6
Electrolyte, ml/hr	98	74	148	296	49	589	535	589	589	589	589	589
CH_3OH Elec Chem Conv/Pass, %	0.0	46.4	42.2	42.2	0.0	9.2	20.2	28.0	39.0	13.7	39.0	9.2
CO_2 Produced, gm moles/hr	0.070	0.070	0.079	--	0.170	0.130	0.220	0.275	--	--	--	0.040

APPENDIX G-8

TEN CELL STACK METHANOL-AIR FUEL CELL - 4" x 4" ELECTRODES

Run Number	1511-10													
Cell Temp, °C	20	20	20	23	23	23	24	77	60	62	61	69	62	62
Electrolyte, M H_2SO_4	3.7													
CH_3OH In Electrolyte, M	1.0													
Test Duration, hours	195-196							245	408	576				
Electrical Connections	2 banks of five cells in parallel, each bank in series with each other													
Stack Current, amperes	0.0	0.5	1.1	2.1	4.2	5.2	8.2	20.5	4.0	2.1	3.9	5.8	9.5	0.0
Stack Voltage	1.18	1.01	0.98	0.92	0.80	0.75	0.63	0.49	0.84	1.05	0.80	0.81	0.62	1.30
Stack Power, watts	0.0	0.50	1.1	1.9	3.4	3.9	5.2	10.0	3.4	2.2	3.1	4.7	5.9	0.0
Efficiency Of Stack, %	47.2	40.4	39.2	36.8	32.0	30.0	25.2	19.6	33.6	42.0	32.0	32.4	24.8	52.3
Voltage Of Cells:														
No. 1	0.55	0.51	0.48	0.45	0.39	0.37	0.32	0.26	0.43	0.51	0.40	0.39	0.32	0.66
No. 2	"	"	"	"	"	"	"	"	"	"	"	"	"	"
No. 3	"	"	"	"	"	"	"	"	"	"	"	"	"	"
No. 4	"	"	"	"	"	"	"	"	"	"	"	"	"	"
No. 5	"	"	"	"	"	"	"	"	"	"	"	"	"	"
No. 6	0.61	0.54	0.50	0.56	0.40	0.37	0.32	0.23	0.40	0.50	0.40	0.37	0.31	0.66
No. 7	"	"	"	"	"	"	"	"	"	"	"	"	"	"
No. 8	"	"	"	"	"	"	"	"	"	"	"	"	"	"
No. 9	"	"	"	"	"	"	"	"	"	"	"	"	"	"
No. 10	"	"	"	"	"	"	"	"	"	"	"	"	"	"
Anode Polarization, Volts At Cell:														
No. 1	0.24	0.26	0.28	0.30	0.33	0.34	0.30	0.39	0.38	0.34	0.40	0.29	0.39	0.21
No. 2	0.10*	0.04	0.07	0.09	0.13	0.15	0.07	0.35	0.41	0.38	0.45	0.37	0.43	0.22
No. 3	0.26	0.28	0.29	0.31	0.32	0.32	0.32	0.41	0.41	0.37	0.43	0.37	0.40	0.22
No. 4	0.27	0.28	0.29	0.31	0.32	0.33	0.33	0.44	0.41	0.37	0.46	0.37	0.42	0.22
No. 5	0.07	0.28	0.30	0.32	0.33	0.34	0.40	0.44	0.41	0.37	0.45	0.41	0.44	0.23
No. 6	0.20	0.25	0.28	0.30	0.31	0.32	0.32	0.40	0.40	0.35	0.41	0.39	0.41	0.32
No. 7	0.20	0.23	0.27	0.30	0.33	0.34	0.37	0.46	0.41	0.39	0.48	0.41	0.44	0.34
No. 8	0.20*	0.25	0.27	0.30	0.32	0.33	0.36	0.41	0.41	0.32	0.37	0.36	0.36	0.20
No. 9	0.08	0.25	0.27	0.32	0.37	0.40	0.45	0.41	0.43	0.37	0.45	0.36	0.38	0.24
No. 10	--	0.26	0.28	0.31	0.33	0.33	0.34	0.40	0.41	0.33	0.37	0.34	0.37	0.20
Air, cc/min (@ 32°F)	2580							5350	2480	2960	2960	5160	5160	2200
Air, Stoichiometric Ratio To Current	-	62.0	28.0	14.7	7.4	6.0	3.7	3.1	7.5	16.9	9.1	10.7	6.5	--
Electrolyte, ml/hr	580							589	589	98	196	589	589	598
CH_3OH Elec Chem Conv/Pass, %	0.0	2.7	5.8	11.2	11.3	27.6	43.5	11.2	21.2	11.2	20.7	30.8	50.5	0.0
Cathodes	(Cyanamid CYW 19-28)													
Anodes	FW 1-9 and 14 (P-Type)													

* New anodes in No. 2 and No. 8 cells.

APPENDIX G-9

SIX CELL STACK 9" x 5-3/4" POLYPROPYLENE METHANOL-AIR FUEL CELL

(Cathodes And Anodes Used Previously In A Number Of Tests(4))
Series Connected

Run Number	1511-18		1511-21				
Cell Temp, °C	51	52	65	69	69	69	67
Electrolyte, M H_2SO_4	3.7						
CH_3OH In Electrolyte, M	1.0						
Current Density, ma/cm^2	11	32	0	10	20	30	50
Terminal Current, amps	3.2	9.5	0	3.0	6.0	9.0	15.0
Terminal Voltages:							
Cell No. 1	0.42	0.26	0.62	0.48	0.41	0.35	0.24
Cell No. 2	--(5)	--(5)	0.61	0.49	0.44	0.36	0.20
Cell No. 3	0.45	0.31	0.58	0.44	0.44	0.36	0.19
Cell No. 4	0.00	0.00(2)	0.74(3)	0.45	0.37	0.33	0.04
Cell No. 5	0.00	0.00(2)	0.78(3)	0.43	0.36	0.32	0.04
Cell No. 6	0.46	0.34	0.76	0.52	0.45	0.40	0.30
Total Stack Voltage	1.33	0.91	4.09	2.81	2.47	2.12	1.01
Total Voltage Efficiency, %	17.6	12.0	54.2	37.2	32.7	28.1	13.4
Terminal Power, mwatts/cm^2	2.4	4.8	0.0	4.7	8.2	14.0	8.4
Terminal Power, watts	4.2	8.6	0.0	8.4	14.8	19.1	15.1
Anode Polarizations, volts							
Cell No. 1	0.39	0.53	0.22	0.34	0.37	0.41	0.50
Cell No. 2	--	--	0.21	0.27	0.33	0.36	0.47
Cell No. 3	0.39	0.47	0.07	0.14	0.31	0.33	0.36
Cell No. 4	--	--	0.13	0.26	0.28	0.31	0.37
Cell No. 5	--	--	0.13	0.33	0.37	0.40	0.47
Cell No. 6	0.37	0.45	0.08	0.28	0.30	0.33	0.43
IR Loss, volts	0.135/100 amps/ft^2(1)						
Oxidant	Air (Saturated with water at 40°C)						
Stoichiometric Ratio To Current	42.3	14.2	--	50.2	25.1	16.7	10.0
Rate, cc/min (STP)	13,500		7000	15,000			
Electrolyte, ml/hour	900	900	1800				
CH_3OH, elec chem conv/pass, %	13.3	39.6	0.0	6.2	12.5	18.7	31.2

(1) With weak springs behind current collectors.
(2) Air Frame to cells 4 and 5 were 40 mils wide compared to 63 mils in the other cells.
(3) The air slots feeding to cells 4 and 5 were opened to about 60 mils by means of a hand drill.
(4) Cathodes were Cyanamid electrodes backed with Permion membranes. Anodes were P-type.
(5) Air cathode reversed, thus no contact with collector.

APPENDIX G-10

TWO CELL STACK PERFORMANCE WITH 9" x 5-3/4" ELECTRODES USING METHANOL AND AIR

Run Number	1511-37										
Cell Temp, °C	69	67	67	68	70	70	80	81	81	82	81
Electrolyte, M H_2SO_4	3.7										
CH_3OH in electrolyte, M	1.0										
Current Density, ma/cm^2	0.0	20	30	40	50	100	0.0	10	20	50	100
Stack Current, Amps	0.0	6.0	9.0	12.0	15.0	30.0	0.0	3.0	6.0	15.0	30.0
Terminal Voltages:											
Cell No. 1	0.72	0.46	0.42	0.38	0.35	0.21	0.71	0.51	0.41	0.36	0.10
Cell No. 2	0.68	0.47	0.40	0.38	0.35	0.21	0.72	0.57	0.49	0.36	0.16
Total Stack Voltage	1.40	0.94	0.84	0.76	0.71	0.43	1.45	1.10	0.90	0.72	0.28
Total Voltage Efficiency, %	55.5	37.3	33.3	30.1	28.2	17.1	57.5	43.7	35.7	28.6	11.1
Terminal Power, mwatts/cm^2	0.0	9.4	12.3	15.2	17.5	21.0	0.0	5.4	9.1	18.0	13.0
Terminal Power, watts	0.0	5.6	7.5	9.1	10.6	12.3	0.0	3.3	5.4	10.8	8.4
Anode Polarization, Volts:											
Cell No. 1	0.19	0.35	0.36	0.37	0.38	0.42	0.07	0.23	0.27	0.29	0.34
Cell No. 2	0.21	0.30	0.32	0.34	0.35	0.41	0.19	0.29	0.32	0.43	0.52
IR Loss, Volts											
Cell No. 1	--	--	--	--	--	--	--	--	--	--	0.20
Cell No. 2	--	--	--	--	--	--	--	--	--	--	0.17
Oxidant	Air (dry)						Air (Sat. with H_2O at 23-40°C)				
Rate, cc/min (STP)	15,000						14,200	15,000+	15,000+	14,200	15,000+
Electrolyte, ml/hour	616						616				
Cathodes	CYW-41 and 42										
Anodes	FW-27 and 28 (Ru Mod. P-type)										

APPENDIX G-11

SIX CELL STACK PERFORMANCE WITH 9" x 5-3/4" ELECTRODES USING METHANOL AND AIR

Run Number	1511-45							
Cell Temp, °C	66	66	65	65	67	67	67	70
Electrolyte, M H_2SO_4	3.7							
CH_3OH in Electrolyte, M	1.0							
Current Density, ma/cm^2	0.0	10	20	40	50	70	100	100
Stack Current, amps	0.0	3.0	6.0	12.0	15.0	21.0	30.0	30
Terminal Voltages:								
Cell No. 1	0.74	0.51	0.48	0.39	0.32	0.24	0.13	IR
Cell No. 2	0.68	0.51	0.49	0.41	0.33	0.24	0.11	Losses
Cell No. 3	0.72	0.52	0.49	0.42	0.34	0.28	0.15	
Cell No. 4	0.63	0.49	0.43	0.38	0.32	0.26	0.15	
Cell No. 5	0.68	0.51	0.47	0.40	0.35	0.28	0.19	
Cell No. 6	0.60	0.51	0.50	0.46	0.42	0.34	0.26	
Total Stack Voltage	4.1	3.1	2.9	2.4	2.1	1.6	1.0	
Total Voltage Efficiency, %	54.3	41.1	38.4	31.8	26.5	21.2	13.2	
Terminal Power, mwatts/cm^2	0.0	5.2	9.7	16.0	16.6	18.7	16.6	
Terminal Power, watts	0.0	9.3	17.4	28.8	30.0	33.6	30.0	↓
Anode Polarization, Volts:								
Cell No. 1	0.16	0.31	0.35	0.35	0.34	0.39	0.42	0.194
Cell No. 2	0.26	0.37	0.35	0.37	0.39	0.41	0.47	0.220
Cell No. 3	0.17	0.31	0.35	0.36	0.37	0.41	0.45	0.172
Cell No. 4	0.27	0.38	0.35	0.37	0.42	0.43	0.47	0.154
Cell No. 5	0.16	0.29	0.34	0.36	0.36	0.41	0.43	0.176
Cell No. 6	0.26	0.34	0.35	0.37	0.40	0.42	0.47	0.150
Average	0.21	0.33	0.35	0.36	0.38	0.41	0.45	0.178
IR Loss, Volts (6 cells)	--	--	--	0.40	--	0.70	1.00	1.06
Oxidant	Air(Sat. with water at 42-60°C)							
Stoichiometric Ratio to Current	--	13.6	24.8	--	9.9	--	--	--
Rate, cc/min (STP)	4100	4100	14900	15000$^+$	14900	15000$^+$	15000$^+$	14,000
Electrolyte, ml/hour	616	616	616	616	--	--	--	--
CH_3OH, elec chem conv/pass, %	0.0	18.2	36.4	73.0	--	--	--	--
Cathodes	CYW-37, 38, 39, 40, 43, and 44)							
Anodes	FW-29, 30, 32, 33, 34, and 35(Ru mod. P-type)							

APPENDIX G-12

SIX CELL STACK AIR FLOW TESTS WITH 9" x 5-3/4" ELECTRODES USING METHANOL AND AIR

20-3/16" Dia. Inlet Ports and 14-3/16" Dia. Exit Ports in Each Air Frame

Run Number	1511-45										
Cell Temp, °C	65	65	65	66	66	65	65	65	65	65	65
Electrolyte, M H_2SO_4	3.7										
CH_3OH in Electrolyte, M	1.0										
Current Density, ma/cm^2	20	20	20	20	20	40	40	40	40	40	40
Stack Current, amps	6.0	6.0	6.0	6.0	6.0	12.0	12.0	12.0	12.0	12.0	12.0
Terminal Voltages:											
Cell No. 1	0.48	0.46	0.45	0.44	0.38	0.39	0.37	0.36	0.35	0.26	0.10
Cell No. 2	0.49	0.47	0.47	0.45	0.18	0.41	0.36	0.36	0.36	0.30	-0.20
Cell No. 3	0.49	0.47	0.46	0.44	0.14	0.42	0.39	0.39	0.38	0.35	-0.20
Cell No. 4	0.43	0.44	0.42	0.40	0.20	0.38	0.35	0.35	0.35	0.32	0.20
Cell No. 5	0.47	0.45	0.44	0.42	0.30	0.40	0.38	0.38	0.38	0.36	0.28
Cell No. 6	0.50	0.50	0.50	0.50	0.49	0.46	0.44	0.44	0.43	0.44	0.42
Total Stack Voltage	2.9	2.8	2.7	2.6	1.6	2.4	2.2	2.2	2.1	2.0	0.6
Total Voltage Efficiency, %	38.4	37.0	35.7	34.4	21.2	31.8	29.1	29.1	27.8	26.5	8.0
Terminal Power, mwatts/cm^2	9.7	9.3	9.0	8.7	5.3	16.0	14.6	14.6	14.0	13.3	4.0
Terminal Power, watts	17.4	16.8	16.2	15.6	9.6	28.8	26.4	26.4	25.2	24.0	7.2
Anode Polarization, Volts:											
Cell No. 1	0.35	0.35	0.34	0.33	0.25	0.35	0.37	0.35	0.35	0.31	--
Cell No. 2	0.35	0.36	0.37	0.39	0.26	0.37	0.42	0.39	0.39	0.41	--
Cell No. 3	0.35	0.35	0.35	0.36	0.19	0.36	0.38	0.37	0.37	0.37	--
Cell No. 4	0.35	0.35	0.35	0.35	0.20	0.37	0.45	0.41	0.42	0.40	--
Cell No. 5	0.34	0.34	0.33	0.31	0.17	0.36	0.37	0.37	0.36	0.35	--
Cell No. 6	0.35	0.35	0.33	0.33	0.29	0.37	0.43	0.40	0.40	0.39	--
Oxidant	Air (Sat. with water at 35-46°C)										
Stoichiometric Ratio to Current	18.6	10.9	8.0	6.1	4.0	--	9.3	8.0	6.0	4.0	3.0
Rate, cc/min (STP)	14,900	8700	6400	4900	3200	15,000+	14,900	12,900	9700	6450	4900
Electrolyte, ml/hour	616	616	616	616	616	616	616	616	616	616	616
CH_3OH, elec chem conv/pass %	36.4	36.4	36.4	36.4	36.4	73.0	73.0	73.0	73.0	73.0	73.0
Cathodes	CYW-37, 38, 39, 40, 43, and 44										
Anodes	FW-29, 30, 32, 33, 34, and 35 (Ru Mod. P-type)										

APPENDIX H-1

PERFORMANCE DATA FOR STATISICAL EVALUATION OF METHANOL CATALYSTS-BIASED REPLICATES

3.7 M H_2SO_4, 60°C, 1 M Methanol

Run No	Catalyst	Polarization from Methanol Theory at Indicated ma/cm² 1	10	50	100	Remarks
2269-46-1	Pt-40 Ru	.24	.30	.36	.40	Standard preparation,
2269-47-1	"	.25	.31	.36	.39	wet press
2465-11-1	Pt-40 Ru	.18	.25	.30	.33	Solution reduced,
2465-12-1	"	.21	.27	.34	.37	wet press
2465-50-1	Pt-40 Ru	--	.30	.34	.36	Reduced with formaldehyde,
2633-3-1	"	.27	.32	.35	.36	wet press
2623-14-2	Pt-40 Ru	.23	.29	.34	.36	Standard preparation,
2623-12-1	"	.23	.29	.34	.37	wet press
2623-25-1	Pt-40 Ru	.22	.28	.33	.36	Solution reduced,
2623-37-2	"	.22	.28	.33	.35	wet press
2624-14-2	Pt-40 Ru	--	.29	.34	.37	HNO_3, KOH treat,
2624-17-1	"	.23	.28	.33	.36	dry + 10% Teflon
2623-17-1	Pt-40 Ru	.22	.28	.32	.34	Standard preparation,
2623-21-1	"	.22	.28	.33	.36	dry + 10% Teflon
2623-18-1	Pt-40 Ru	.22	.28	.33	.35	50% NaOH treat,
2623-20-1	"	.23	.29	.32	.34	dry + 10% Teflon
2269-24-1	Pt-33 Ru	--	.29	.34	.36	Standard preparation,
2269-9-1	"	.24	.29	.34	.37	dry + 10% Teflon
2623-43-1	RuP-5	.20	.29	.34	.37	Before KOH treat,
2623-50-1	"	--	.26	.32	.34	wet press
2623-43-1	RuP-5	--	.27	.32	.35	After KOH treat,
2623-50-1	"	--	.25	.31	.33	wet press
2624-7-1	RuP-5	.14	.23	.28	.30	H_2 at 185°C,
2624-9-1	"	--	.24	.30	.33	wet press
2465-42-1	Ru-50 Ir	.25	.30	.33	.36	Standard preparation,
2465-49-1	"	--	.31	.34	.37	wet press

APPENDIX H-2

STATISTICAL EVALUATION OF METHANOL CATALYSTS, BIASED REPLICATES

It is important to assess, with some degree of certainty, whether differences in catalyst activity are due to changes in preparative technique or composition or simply to random error. Therefore, replications have been made for evaluating the variances inherent in the procedures used. Both selected (biased) and random (unbiased) replications, involving a variety of catalysts, have been employed.

Run No	Catalyst	Polarization from Methanol Theory, Volts, at 10 ma/cm^2 X_1	X_2	Pol Diff in mv/10 $(X_1-X_2)=X$	Polarization from Methanol Theory, Volts, at 10 ma/cm^2 X_1	X_2	Pol Diff in mv/10 $(X_1-X_2)=X$
2269, 46-1, 47-1	Pt-40 Ru	.30	.31	-1	.36	.36	0
2465, 11-1, 12-1	Pt-40 Ru	.25	.27	-2	.30	.34	-4
2465, 50-1, 3-1	Pt-40 Ru	.30	.32	-2	.34	.35	-1
2623, 14-2, 12-1	Pt-40 Ru	.29	.29	0	.34	.34	0
2623, 25-1, 37-2	Pt-40 Ru	.28	.28	0	.33	.33	0
2624, 14-2, 17-1	Pt-40 Ru	.29	.28	+1	.34	.33	+1
2623, 17-1, 21-1	Pt-40 Ru	.28	.28	0	.32	.33	-1
2623, 18-1, 20-1	Pt-40 Ru	.28	.29	-1	.33	.32	+1
2269, 24-1, 9-1	Pt-33 Ru	.29	.29	0	.34	.34	0
2633, 43-1, 50-1	RuP-5	.29	.26	+3	.34	.32	+2
" (KOH)	RuP-5	.27	.25	+2	.32	.31	+1
2624, 7-1, 9-1	RuP-5	.23	.24	+1	.28	.30	+2
2465, 42-1, 49-1	Ru-50 Ir	.30	.31	-1	.33	.34	-1

Biased Replicates

$\bar{X}'$ = absolute average of polarization differences in mv/10.

$$s = \sqrt{\frac{\sum (X_1-X_2)^2}{2N}}$$

Current Density, ma/cm^2	No of Paired Runs	$\bar{X}'$, mv/10	s, mv/10
10	13	1.1	1.0
50	13	1.1	1.1

Reproducibility of Pt-40 Ru Preparations, Irrespective of Method

$\bar{X}$ = average polarization in volts at indicated ma/cm^2, $s = \sqrt{\frac{\sum (X-\bar{X})^2}{N-1}}$

Current Density, ma/cm^2	No of Runs=N	$\bar{X}$, Volts	s, Volts
10	16	.287	.016
50	16	.335	.015
100	16	.361	.018

AD- Div.

Esso Research and Engineering Company,
Linden, New Jersey
HYDROCARBON-AIR FUEL CELL, by Carl E. Heath and others. First semi-annual report, 1 Jan. 1964 - 30 June 1964. 226 pages incl. illus. tables. (Rept. No. 5; Task No. 7900.21.903.01.00.) (Contract DA-36-039 AMC-03743(E)) Unclassified report

Studies were continued aimed toward the ultimate development of fuel cells using either hydrocarbons or methanol as fuels and air as the oxidant at moderate temperatures and pressures. Included are work carried out on the effects of the fuel, catalyst composition, and other major operating variables on the design and operation of the fuel electrodes, experiments performed to improve the over-all efficiency of the air electrodes, and tests designed to evaluate the operability of the fuel cell components in complete cells. These tests demonstrated

(over)

UNCLASSIFIED

1. Power supplies-Fuel cells
2. Hydrocarbons and Methanol
3. CO_2 Rejecting electrolyte
4. Electrodes

I. Heath, C. E.
II. U.S. Army Electronics Laboratories
III. Contract DA-36-039 AMC-03743(E)

UNCLASSIFIED

AD- Div.

Esso Research and Engineering Company,
Linden, New Jersey
HYDROCARBON-AIR FUEL CELL, by Carl E. Heath and others. First semi-annual report, 1 Jan. 1964 - 30 June 1964. 226 pages incl. illus. tables. (Rept. No. 5; Task No. 7900.21.903.01.00.) (Contract DA-36-039 AMC-03743(E)) Unclassified report

Studies were continued aimed toward the ultimate development of fuel cells using either hydrocarbons or methanol as fuels and air as the oxidant at moderate temperatures and pressures. Included are work carried out on the effects of the fuel, catalyst composition, and other major operating variables on the design and operation of the fuel electrodes, experiments performed to improve the over-all efficiency of the air electrodes, and tests designed to evaluate the operability of the fuel cell components in complete cells. These tests demonstrated

(over)

UNCLASSIFIED

1. Power supplies-Fuel cells
2. Hydrocarbons and Methanol
3. CO_2 Rejecting electrolyte
4. Electrodes

I. Heath, C. E.
II. U.S. Army Electronics Laboratories
III. Contract DA-36-039 AMC-03743(E)

UNCLASSIFIED

AD- Div.

Esso Research and Engineering Company,
Linden, New Jersey
HYDROCARBON-AIR FUEL CELL, by Carl E. Heath and others. First semi-annual report, 1 Jan. 1964 - 30 June 1964. 226 pages incl. illus. tables. (Rept. No. 5; Task No. 7900.21.903.01.00.) (Contract DA-36-039 AMC-03743(E)) Unclassified report

Studies were continued aimed toward the ultimate development of fuel cells using either hydrocarbons or methanol as fuels and air as the oxidant at moderate temperatures and pressures. Included are work carried out on the effects of the fuel, catalyst composition, and other major operating variables on the design and operation of the fuel electrodes, experiments performed to improve the over-all efficiency of the air electrodes, and tests designed to evaluate the operability of the fuel cell components in complete cells. These tests demonstrated

(over)

UNCLASSIFIED

1. Power supplies-Fuel cells
2. Hydrocarbons and Methanol
3. CO_2 Rejecting electrolyte
4. Electrodes

I. Heath, C. E.
II. U.S. Army Electronics
III. Contract DA-36-039 AMC-03743(E)

UNCLASSIFIED

AD- Div.

Esso Research and Engineering Company,
Linden, New Jersey
HYDROCARBON-AIR FUEL CELL, by Carl E. Heath and others. First semi-annual report, 1 Jan. 1964 - 30 June 1964. 226 pages incl. illus. tables. (Rept. No. 5; Task No. 7900.21.903.01.00.) (Contract DA-36-039 AMC-03743(E)) Unclassified report

Studies were continued aimed toward the ultimate development of fuel cells using either hydrocarbons or methanol as fuels and air as the oxidant at moderate temperatures and pressures. Included are work carried out on the effects of the fuel, catalyst composition, and other major operating variables on the design and operation of the fuel electrodes, experiments performed to improve the over-all efficiency of the air electrodes, and tests designed to evaluate the operability of the fuel cell components in complete cells. These tests demonstrated

(over)

UNCLASSIFIED

1. Power supplies-Fuel cells
2. Hydrocarbons and Methanol
3. CO_2 Rejecting electrolyte
4. Electrodes

I. Heath, C. E.
II. U.S. Army Electronics Laboratories
III. Contract DA-36-039 AMC-03743(E)

UNCLASSIFIED

AD-

UNCLASSIFIED

the operability of the hydrocarbon cell components at realistic operating conditions. They also showed the practicality of sustained performance of the methanol-air cell components in compact multicell systems without severe losses in efficiency due to the interactions within or between cells.

AD-

UNCLASSIFIED

the operability of the hydrocarbon cell components at realistic operating conditions. They also showed the practicality of sustained performance of the methanol-air cell components in compact multicell systems without severe losses in efficiency due to the interactions within or between cells.

AD-

UNCLASSIFIED

the operability of the hydrocarbon cell components at realistic operating conditions. They also showed the practicality of sustained performance of the methanol-air cell components in compact multicell systems without severe losses in efficiency due to the interactions within or between cells.

AD-

UNCLASSIFIED

the operability of the hydrocarbon cell components at realistic operating conditions. They also showed the practicality of sustained performance of the methanol-air cell components in compact multicell systems without severe losses in efficiency due to the interactions within or between cells.

AD- Div.

Esso Research and Engineering Company,
Linden, New Jersey
HYDROCARBON-AIR FUEL CELL, by Carl E. Heath and others. First semi-annual report, 1 Jan. 1964 - 30 June 1964. 226 pages incl. illus. tables. (Rept. No. 5; Task No. 7900.21.903.01.00.) (Contract DA-36-039 AMC-03743(E)) Unclassified report

Studies were continued aimed toward the ultimate development of fuel cells using either hydrocarbons or methanol as fuels and air as the oxidant at moderate temperatures and pressures. Included are work carried out on the effects of the fuel, catalyst composition, and other major operating variables on the design and operation of the fuel electrodes, experiments performed to improve the over-all efficiency of the air electrodes, and tests designed to evaluate the operability of the fuel cell components in complete cells. These tests demonstrated

(over)

UNCLASSIFIED

1. Power supplies-Fuel cells
2. Hydrocarbons and Methanol
3. CO_2 Rejecting electrolyte
4. Electrodes

I. Heath, C. E.
II. U.S. Army Electronics Laboratories
III. Contract DA-36-039 AMC-03743(E)

UNCLASSIFIED

AD- Div.

Esso Research and Engineering Company,
Linden, New Jersey
HYDROCARBON-AIR FUEL CELL, by Carl E. Heath and others. First semi-annual report, 1 Jan. 1964 - 30 June 1964. 226 pages incl. illus. tables. (Rept. No. 5; Task No. 7900.21.903.01.00.) (Contract DA-36-039 AMC-03743(E)) Unclassified report

Studies were continued aimed toward the ultimate development of fuel cells using either hydrocarbons or methanol as fuels and air as the oxidant at moderate temperatures and pressures. Included are work carried out on the effects of the fuel, catalyst composition, and other major operating variables on the design and operation of the fuel electrodes, experiments performed to improve the over-all efficiency of the air electrodes, and tests designed to evaluate the operability of the fuel cell components in complete cells. These tests demonstrated

(over)

UNCLASSIFIED

1. Power supplies-Fuel cells
2. Hydrocarbons and Methanol
3. CO_2 Rejecting electrolyte
4. Electrodes

I. Heath, C. E.
II. U.S. Army Electronics Laboratories
III. Contract DA-36-039 AMC-03743(E)

UNCLASSIFIED

AD- Div.

Esso Research and Engineering Company,
Linden, New Jersey
HYDROCARBON-AIR FUEL CELL, by Carl E. Heath and others. First semi-annual report, 1 Jan. 1964 - 30 June 1964. 226 pages incl. illus. tables. (Rept. No. 5; Task No. 7900.21.903.01.00.) (Contract DA-36-039 AMC-03743(E)) Unclassified report

Studies were continued aimed toward the ultimate development of fuel cells using either hydrocarbons or methanol as fuels and air as the oxidant at moderate temperatures and pressures. Included are work carried out on the effects of the fuel, catalyst composition, and other major operating variables on the design and operation of the fuel electrodes, experiments performed to improve the over-all efficiency of the air electrodes, and tests designed to evaluate the operability of the fuel cell components in complete cells. These tests demonstrated

(over)

UNCLASSIFIED

1. Power supplies-Fuel cells
2. Hydrocarbons and Methanol
3. CO_2 Rejecting electrolyte
4. Electrodes

I. Heath, C. E.
II. U.S. Army Electronics
III. Contract DA-36-039 AMC-03743(E)

UNCLASSIFIED

AD- Div.

Esso Research and Engineering Company,
Linden, New Jersey
HYDROCARBON-AIR FUEL CELL, by Carl E. Heath and others. First semi-annual report, 1 Jan. 1964 - 30 June 1964. 226 pages incl. illus. tables. (Rept. No. 5; Task No. 7900.21.903.01.00.) (Contract DA-36-039 AMC-03743(E)) Unclassified report

Studies were continued aimed toward the ultimate development of fuel cells using either hydrocarbons or methanol as fuels and air as the oxidant at moderate temperatures and pressures. Included are work carried out on the effects of the fuel, catalyst composition, and other major operating variables on the design and operation of the fuel electrodes, experiments performed to improve the over-all efficiency of the air electrodes, and tests designed to evaluate the operability of the fuel cell components in complete cells. These tests demonstrated

(over)

UNCLASSIFIED

1. Power supplies-Fuel cells
2. Hydrocarbons and Methanol
3. CO_2 Rejecting electrolyte
4. Electrodes

I. Heath, C. E.
II. U.S. Army Electronics Laboratories
III. Contract DA-36-039 AMC-03743(E)

UNCLASSIFIED

AD-

UNCLASSIFIED

the operability of the hydrocarbon cell components at realistic operating conditions. They also showed the practicality of sustained performance of the methanol-air cell components in compact multicell systems without severe losses in efficiency due to the interactions within or between cells.

AD-

UNCLASSIFIED

the operability of the hydrocarbon cell components at realistic operating conditions. They also showed the practicality of sustained performance of the methanol-air cell components in compact multicell systems without severe losses in efficiency due to the interactions within or between cells.

AD-

UNCLASSIFIED

the operability of the hydrocarbon cell components at realistic operating conditions. They also showed the practicality of sustained performance of the methanol-air cell components in compact multicell systems without severe losses in efficiency due to the interactions within or between cells.

AD-

UNCLASSIFIED

the operability of the hydrocarbon cell components at realistic operating conditions. They also showed the practicality of sustained performance of the methanol-air cell components in compact multicell systems without severe losses in efficiency due to the interactions within or between cells.

DISTRIBUTION LIST

FIRST SEMI-ANNUAL REPORT

CONTRACT NO. DA 36-039 AMC-03743(E)

Director
U.S.A. Electronics Laboratories
Fort Monmouth, N.J. 07703
ATTN: Logistics Division
(MARKED FOR PROJECT
ENGINEER) (2)
ATTN: AMSEL-RD-P (1)
ATTN: AMSEL-RD-DR (1)
ATTN: AMSEL-RD-ADO-RHA (1)
ATTN: Technical Documents Center (1)

OASD (Research & Engineering)
ATTN: Technical Library
Room 3E1065
The Pentagon
Washington 25, D.C. (1)

Chief of Research and Development
OCS, Department of the Army
Washington 25, D.C. (2)

Commanding General
U.S.A. Electronics Command
ATTN: AMSEL-TE
Fort Monmouth, N.J. 07703 (1)

Director
U.S. Naval Research Laboratory
ATTN: Code 2027
Washington, D.C. 20390 (1)

Commanding Office and Director
U.S. Naval Electronics Laboratory
ATTN: Library
San Diego 52, California (1)

Rome Air Development Center
ATTN: RAALD
Griffiss Air Force Base, N.Y. (1)

Commanding General
U.S.A. Electronics Research and
Development Activity
ATTN: Technical Library
Fort Huachuca, Arizona 85613 (1)

Commanding Officer
Harry Diamond Laboratories
Connecticut Ave. & Van Ness St., N.W.
Washington 25, D.C. (1)

Director
Proc. & Prod. Directorate
USAECOM
Fort Monmouth, N.J. 07703 (1)

Deputy President
U.S.A. Security Agency Board
Arlington Hall Station
Arlington 12, Virginia (1)

Commander
Defense Documentation Center
ATTN: TISIA
Cemeron Station, Building 5
Alexandria, Virginia 22314 (19)

Chief
U.S.A. Security Agency
ATTN: ACofS, G-4 (Tech. Library)
Arlington Hall Station
Arlington 12, Virginia (2)

Air Force Cambridge Research
Laboratories
ATTN: CRXL-R
L. G. Hanscom Field
Bedford, Massachusetts (1)

Headquarters
U.S.A. Material Command
Research and Development Directorate
ATTN: AMCRD-DE-MO
Washington, D.C. 20315 (1)

Commander
U.S. Army Research Office (Durham)
Box CM- Duke Station
Durham, North Carolina (1)

Commanding Officer
U.S.A. Combat Developments Command
ATTN: CDCMR-E
Fort Belvoir, Virginia 22060 (1)

Commanding General
U.S.A. Combat Development Command
Communications-Electronic Agency
Fort Huachuca, Arizona 85613 (1)

Air Force Systems Command
Scientific/Technical Liaison Office
U.S. Naval Air Development Center
Johnsville, Pennsylvania (1)

Director
U.S.A. Engineering Research and Development Laboratories
ATTN: Chief, Electric Power Branch
Fort Belvoir, Virginia 22060 (1)

Marine Corps Liaison Office
U.S.A. Electronics Laboratories
ATTN: AMSEL-RD-LNR
Fort Monmouth, N.J. 07703 (1)

AFSC Scientific/Technical Liaison Office
U.S.A. Electronics Laboratories
ATTN: AMSEL-RD-LNA
Fort Monmouth, N.J. 07703 (1)

USAEL Liaison Office
Rome Air Development Center
ATTN: RAOL
Griffiss Air Force Base, N.Y. 13442 (1)

Commanding Officer
U.S.A. Engineer Research and Development Laboratories
ATTN: STINFO Branch
Fort Belvoir, Virginia 22060 (2)

Commanding Officer
U.S.A. Electronics Research and Development Activity
ATTN: AMSEL-RD-WS-A
White Sands, New Mexico 88002 (1)

NASA Representative
Scientific and Technical Information Facility
P.O. Box 5700
Bethesda, Maryland 20014 (1)

Power Information Center
Moore School Building
200 South Thirty-Third Street
Philadelphia, Pennsylvania 19103 (1)

Commanding General
U.S. Army Material Command
ATTN: R&D Directorate
Washington, D.C. 20315 (2)

Systems Engineering Group (SEPIR)
Wright-Patterson Air Force Base
Ohio 45433 (1)

Electronic Systems Division (AFSC)
Scientific and Technical Information Div (ESTI)
L. G. Hanscom Field
Bedford, Massachusetts 01731 (1)

Director
Material Readiness Directorate
Hq, U.S. Army Electronics Command
ATTN: AMSEL-MR
Fort Monmouth, N.J. 07703 (1)

Dr. Bernard Stein
Physical Sciences Division
Army Research Office
3045 Columbia Pike
Arlington, Virginia (1)

Dr. Ralph Roberts
Head, Power Branch
Office of Naval Research (Code 429)
Department of the Navy
Washington, D.C. 20360 (1)

Mr. Bernard B. Rosenbaum
Bureau of Ships (Code 342B)
Department of the Navy
Washington 25, D.C. (1)

Mr. George W. Sherman
Aerospace Power Division
ATTN: APD
Wright-Patterson Air Force Base
Ohio 45433 (1)

Mr. M. Polk
Advanced Research Projects Agency
The Pentagon, Room 3E157
Washington 25, D.C. (1)

Lt. Col. John H. Anderson
SNAP-50/SPUR Office
U.S. Atomic Energy Commission
Division of Reactor Development
Washington, D. C. 20545 (1)

United Aircraft Corporation
Pratt & Whitney Aircraft Division
East Hartford 8, Connecticut
ATTN: Mr. W. H. Podolny (1)

Melpar, Inc.
3000 Arlington Boulevard
Falls Church, Virginia
ATTN: Mr. R. T. Foley (1)

General Electric Company
Direct Energy Conversion Operations
Lynn, Massachusetts
ATTN: Dr. E. Oster (1)

General Electric Company
Research Laboratory
Schenectady, New York
ATTN: Dr. H. Liebhafsky (1)

University of Pennsylvania
John Harrison Laboratory of Chemistry
Philadelphia 4, Pennsylvania
ATTN: Dr. J. Bockris (1)

Westinghouse Electric Corporation
43 West Front Street
Red Bank, New Jersey
ATTN: Mr. C. Arthur (1)

Magna Corporation
R&D Laboratories
1001 South East Street
Anaheim, California
ATTN: Dr. Silverman (1)

Douglas Aircraft Co., Inc.
Missile & Space Systems Division
Astropower Laboratory
ATTN: Mrs. Mac Daniel
2121 Paularino Avenue
Newport Beach, California (1)

American Oil Company
Research & Development Department
Whiting Laboratories
2500 New York Avenue
P.O. Box 431
Whiting, Indiana (1)

Engelhard Industries, Inc.
Military Service Department
113 Astor Street
Newark 2, New Jersey
ATTN: Mr. V. A. Forlenza (1)

University of California
Chemistry Department
Berkeley, California
ATTN: Dr. C. Tobias (1)

Union Carbide Corporation
Parma Research Center
P.O. Box 6116
Parma 30, Ohio
ATTN: Dr. C. E. Winters (1)

Electrochimica Corporation
1140 O'Brien Drive
Menlo Park, California
ATTN: Dr. M. Eisenberg (1)

Allis-Chalmers Manufacturing Company
Research Division
P.O. Box 512
Milwaukee, Wisconsin
ATTN: Dr. P. Joyner (1)

Texas Instruments, Incorporated
Energy Research Laboratory
P.O. Box 5474
Dallas 22, Texas
ATTN: Dr. C. G. Peattie (1)

Mr. Walter C. Scott
National Aeronautics & Space
Administration Headquarters
Code RNW
Washington, D.C. 20546 (1)

Institute for Defense Analysis
1666 Connecticut Avenue, N. W.
Washinton 25, D.C.
ATTN: Dr. Szego & Mr. Hamilton (1)

Mr. G. B. Wareham
Office of Assistant Director
Defense Research and Engineering
3D-1048 Pentagon
Washington 25, D.C. (1)

Director
Advanced Research Projects Agency
Washington 25, D.C. (6)

Director
U.S.A. Electronics Laboratories
Hq, USAECOM
ATTN: AMSEL-RD-DO, ARPA Coordinator
Fort Monmouth, N.J. 07703 (1)

UNCLASSIFIED